

INFORMATION TO USERS

This manuscript has been reproduced from the microfilm master. UMI films the text directly from the original or copy submitted. Thus, some thesis and dissertation copies are in typewriter face, while others may be from any type of computer printer.

The quality of this reproduction is dependent upon the quality of the copy submitted. Broken or indistinct print, colored or poor quality illustrations and photographs, print bleedthrough, substandard margins, and improper alignment can adversely affect reproduction.

In the unlikely event that the author did not send UMI a complete manuscript and there are missing pages, these will be noted. Also, if unauthorized copyright material had to be removed, a note will indicate the deletion.

Oversize materials (e.g., maps, drawings, charts) are reproduced by sectioning the original, beginning at the upper left-hand corner and continuing from left to right in equal sections with small overlaps. Each original is also photographed in one exposure and is included in reduced form at the back of the book.

Photographs included in the original manuscript have been reproduced xerographically in this copy. Higher quality 6" x 9" black and white photographic prints are available for any photographs or illustrations appearing in this copy for an additional charge. Contact UMI directly to order.

UMI

A Bell & Howell Information Company
300 North Zeeb Road, Ann Arbor, MI 48106-1346 USA
313/761-4700 800/521-0600

FLUVIAL AND HILLSLOPE GEOMORPHOLOGY

of

HOSEANNA CREEK WATERSHED,

CENTRAL ALASKA

A

THESIS

Presented to the Faculty of the University of Alaska

in Partial Fulfillment of the Requirements

for the Degree of

Doctor of Philosophy

By

Stephen C. Wilbur, B.A., M.S.

Fairbanks, Alaska

December, 1995

UMI Number: 9608769

UMI Microform 9608769

Copyright 1995, by UMI Company. All rights reserved.

This microform edition is protected against unauthorized
copying under Title 17, United States Code.

UMI

300 North Zeeb Road
Ann Arbor, MI 48103

FLUVIAL AND HILLSLOPE GEOMORPHOLOGY

of

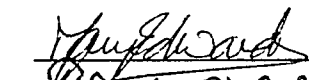
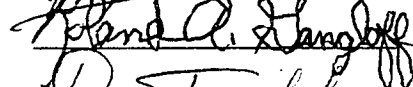
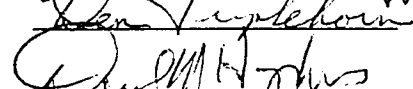
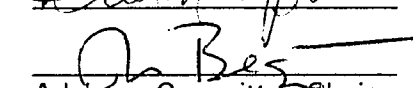

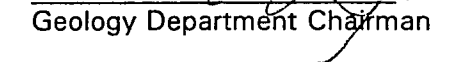
HOSEANNA CREEK WATERSHED,

CENTRAL ALASKA

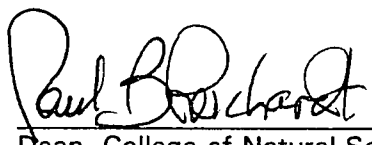
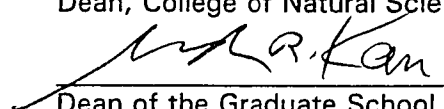
by

Stephen C. Wilbur

RECOMMENDED:






Advisory Committee Chair

Geology Department Chairman

APPROVED:


Dean, College of Natural Sciences

Dean of the Graduate School
Nov 17, 1995
Date

ABSTRACT

Hoseanna Creek Watershed is rapidly eroding and provides excellent opportunities to describe and quantify hillslope and fluvial processes in the subarctic and in discontinuous permafrost terrain. High landslide and badland densities occur due to asymmetric geologic structure and weakly consolidated lithologies. Late Quaternary regional glaciofluvial processes and tectonism have changed local base level at least 100 m, inducing headward incision through weak lithologies and yielding high rates of sediment production.

Earthflows, translational blocks, rotational blocks, lateral spreads or complex landslide types form in coal-bearing formations in response to lateral corrosion of toes by avulsing streams or to undermining of foot areas by headward incising streams. Slides undergo episodic resurgent activity when new lithostatic or hydrostatic thresholds are reached. Average horizontal displacement rates of seven slides monitored between 8/85 and 9/88 ranged from 0.2 m/yr in rotational blocks to 48 m/yr in the earthflows. Although unique sliding mechanisms are not apparent, permafrost and subarctic climate generate delays or catalysts for failure atypical of warmer climates. Freezing/thawing fronts affect soil strength and permeability; break-up/freeze-up processes affect the timing of water supply to the slide mass and affect development of aufeis-related ground-water pore pressures.

Aspectual and lithologic variations combine to yield three geohydrologic subbasin types which govern discharge ranges. Regressions were performed on multiple sets of sediment-discharge (Ts-Q) data. Regression variance (r^2) was found to have a maximum natural threshold indicative of intrinsic variability. Wide ranges in Q (0.001 to 2350 cfs) and Ts (0.005 to 1600 g/l) necessitated log-log scales and power functions. Each geohydrologic subbasin has a unique Ts-Q relationship termed here the mean sediment concentration potential C_p . Systematic differences in regression parameters indicate that variations in spatial conditions define C_p , while systematic changes in Ts-Q regression residuals R (termed here the maintenance rate R^*) describe the temporal variability of Ts through time with respect to C_p .

50-95% of the annual sediment load is transferred during less than 3% of the year.

Erosion rate indexes were established from peak load estimates; Nenana Gravel basins are eroding 260 times faster than schistose basins and ten times coal-bearing basins.

TABLE OF CONTENTS

ABSTRACT	iii
Table of Contents	v
List of Figures	ix
List of Tables	xv
PREFACE	xviii
DEDICATION	xx
 1.0 INTRODUCTION	
1.1 Objectives	1-1
1.2 Overview	1-1
1.3 Scope	1-3
1.4 Study Area and Physiography	1-4
 2.0 GEOLOGIC and CLIMATIC CONTROLS GOVERNING SURFACE PROCESSES	
2.1 Introduction	2-1
2.2 Climate	2-1
2.2.1 Regional Setting	2-1
2.2.2 Local Weather Stations	2-2
2.2.3 Temperature	2-2
2.2.4 Precipitation	2-5
2.2.5 Importance of Seasonal Patterns	2-8
2.3 Geology	2-9
2.3.1 Lithology and Stratigraphy	2-11
2.3.1.1 Basement Metamorphics	2-12
2.3.1.2 Usibelli Group	2-12
2.3.1.3 Nenana Gravel	2-17
2.3.1.4 Quaternary Deposits	2-17
2.3.1.5 Basin Lithology	2-32
2.3.1.6 Lithologic Control on Drainage	
Density	2-32
2.3.1.7 Lithologic Control on Stream	
Gradients	2-35
2.3.2 Structure	2-39

2.4	General Surface Processes - Geologic and Climatic	
	Interactions	2-40
2.4.1	North-South Valley Asymmetry and Permafrost	2-40
2.4.2	Weathering Processes	2-42
2.4.3	Significant Erosional or Depositional	
	Landforms	2-43
2.4.3.1	Badlands	2-43
2.4.3.2	Landslides	2-45
2.5	Geologic History	2-49
2.5.1	Tertiary	2-49
2.5.2	Pleistocene	2-49
3.0	LANDSLIDE MOVEMENT and EVOLUTION in DISCONTINUOUS PERMAFROST	
3.1	Introduction	3-1
3.1.1	Purpose	3-1
3.1.2	Background	3-1
3.1.3	Geologic Conditions Conducive to Landslide	
	Formation	3-5
3.2	Methods	3-5
3.3	Results	3-12
3.3.1	Descriptions and Summary of Movement Studies	3-12
3.3.1.1	Landslide I	3-12
3.3.1.2	Landslide II	3-17
3.3.1.3	Landslide III	3-20
3.3.1.4	Landslide IV	3-23
3.3.1.5	Landslide V	3-27
3.3.1.6	Landslide VI	3-31
3.3.1.7	Landslide VII	3-33
3.3.2	Summary of Change in Landslide Size (1949-1988)	3-36
3.3.3	Summary of Movement 1985-1988	3-40
3.3.4	Displacement Histories	3-42
3.3.5	Triggering Processes	3-57
3.3.5.1	Climatic Factors	3-57
3.3.5.2	Geologic Factors	3-63
3.4	Discussion	3-64

3.4.1	Sliding Mechanics	3-64
3.4.2	Temporal Processes	3-65
3.4.2.1	Earthflows	3-65
3.4.2.2	Block Slides	3-66
3.5	Summary of Motion and Development	3-67
3.6	Summary and Conclusions of Landslide Movement and Evolution	3-69
4.0	STREAMFLOW and SEDIMENT-DISCHARGE PROCESSES	
4.1	Introduction	4-1
4.1.1	Field Studies	4-1
4.1.2	Background	4-3
4.2	Methods	4-4
4.2.1	Hydrologic Stations	4-6
4.2.2	Discharge Measurements	4-13
4.2.2.1	Discharge Measurement Techniques	4-13
4.2.2.2	Indirect Discharge Measurements	4-14
4.2.2.3	Channel Roughness	4-15
4.2.3	Discharge Records	4-17
4.2.3.1	Nonstage Point Discharge Records	4-18
4.2.3.2	Continuous Stage Discharge Records	4-18
4.2.4	Sediment Sampling	4-21
4.2.4.1	Suspended Load Sampling Techniques	4-21
4.2.4.2	Bedload Sampling Techniques	4-22
4.2.5	Laboratory Analyses	4-23
4.2.5.1	Suspended Load	4-23
4.2.5.2	Comparison of Sampling Techniques	4-24
4.2.5.3	Comparison of Laboratory Techniques	4-27
4.2.5.4	Bedload	4-30
4.3	Results	4-31
4.3.1	Discharge Data	4-31
4.3.1.1	Base Flows	4-33
4.3.1.2	Peak Flows	4-34
4.3.1.3	Continuous Discharge Records	4-38
4.3.1.4	Controls on Discharge Variations	4-43
4.3.2	Sediment Concentration Data	4-44

4.3.2.1	Suspended Load	4-44
4.3.2.2	Bedload	4-50
4.3.2.3	Dissolved Load	4-57
4.4	Sediment-Discharge Relationships	4-60
4.4.1	Linear Regression Analyses of Sediment-Rating Curves	4-60
4.4.1.1	Theoretical Relationship	4-60
4.4.1.2	Operational Variances	4-66
4.4.1.3	Natural Variances	4-66
4.5	Sediment Supply and Transfer Processes	4-73
4.5.1	Sediment Rating Regression Residuals	4-73
4.5.2	Mean Sediment Concentration Potential and the Maintenance Rate	4-78
4.5.3	Changes in Supply and Runoff Rates	4-79
4.5.4	Geologic and Climatic Controls on Supply and Demand and Stream Maintenance	4-80
4.6	Sediment Load	4-82
4.6.1	Peak Sediment Loads	4-82
4.6.1.1	Observed	4-82
4.6.1.2	Predicted	4-84
4.6.2	Erosion Rates	4-87
4.6.2.1	Peak Erosion Rates	4-87
4.6.2.2	Estimated Long-Term Erosion Rates	4-87
4.7	Summary and Conclusions of Streamflow and Sediment-Discharge Processes	4-91
5.0	SUMMARY and CONCLUSIONS	
5.1	Climatic and Geologic Controls	5-1
5.2	Landslide Processes and Evolution	5-2
5.3	Streamflow and Sediment-Transfer Processes	5-3
REFERENCES		R-1
APPENDIX A	Geochronologic Data	A-1
APPENDIX B	Landslide Data	B-1
APPENDIX C	Streamflow/Sediment Data	C-1

LIST OF FIGURES

1.1-1. Location map of study area.	1-2
1.4-1. Basins within the Hoseanna Creek Watershed.	1-6
2.2-1. The Hoseanna Creek Watershed study area and vicinity.	2-3
2.2-2. Mean monthly temperatures for Poker Flats and McKinley Park.	2-4
2.2-3. Mean monthly precipitation for Poker Flats and McKinley Park.	2-7
2.3-1. Geologic map of Hoseanna Creek Watershed.	2-10
2.3-2. The late Cenozoic type section at Suntrana Creek.	2-13
2.3-3. Late Quaternary stream terrace and alluvial fan map of the western Hoseanna Creek Watershed.	2-21
2.3-4. Drainage changes on tributaries of Nenana River from the beginning of Dry Creek to the end of the Healy Glaciation.	2-23
2.3-5. Hoseanna Creek base level changes during the late Quaternary.	2-24
2.3-6. Schematic cross-section of the Hoseanna Creek fan.	2-27
2.3-7. Schematic cross-section of the Badlands Creek fan.	2-29
2.3-8. Schematic cross-section of the Popovitch Creek fan.	2-30
2.3-9. Schematic cross-section of the Hoseanna Creek bank near Popovitch Creek.	2-31

2.3-10. Plot of drainage density ($D - \text{km}/\text{km}^2$) versus area ($A - \text{km}^2$) for selected 3 rd order basins.	2-36
2.3-11. Representative stream profiles of creeks underlain by the three principal lithologies.	2-37
2.3-12. The actual and differential stream profiles of Hoseanna Creek.	2-38
2.4-1. Permafrost map of Hoseanna Creek Watershed.	2-41
2.4-2. Landslide map of Hoseanna Creek Watershed.	2-46
2.4-3. Lithologic control on the distribution of landslides.	2-47
2.4-4. Diagram depicting the predominant northward direction of landslide movement.	2-48
3.2-1. Location of surveyed slides.	3-6
3.3-1. Geologic cross section and plan view of LI.	3-13
3.3-2. Geologic cross section and plan view of LII.	3-18
3.3-3. Geologic cross section and plan view of LIII.	3-22
3.3-4. Geologic cross section and plan view of LIV.	3-25
3.3-5. Geologic cross section and plan view of LV.	3-29
3.3-6. Geologic cross section and plan view of LVI.	3-32
3.3-7. Geologic cross section and plan view of LVII.	3-35
3.3-8. Changes in the length ($L - \text{m}$) of each monitored slide from 1949-1984.	3-37

3.3-9. Changes in the area ($A - \text{km}^2$) of each monitored slide from 1949-1984.	3-38
3.3-10. The average CVD/CHD for the upper (1), middle (2), and foot (3) sections of each monitored slide.	3-43
3.3-11a. Plot of cumulative horizontal displacement rate of LI stakes from the west foot area during the monitoring period.	3-44
3.3-11b. Plot of cumulative horizontal displacement rate of LI stakes from the east foot area during the monitoring period.	3-45
3.3-11c. Plot of cumulative horizontal displacement rate of LI stakes from the center mid section during the monitoring period.	3-46
3.3-12a. The cumulative horizontal displacement rate of LII stakes from the east foot area during the monitoring period.	3-47
3.3-12b. The cumulative horizontal displacement rate of LII stakes from the west foot area during the monitoring period.	3-48
3.3-13. The cumulative horizontal displacement rate of all the LIII stakes during the monitoring period.	3-49
3.3-14a. The cumulative horizontal displacement rate of LIV stakes from the upper basin during the monitoring period.	3-50
3.3-14b. The cumulative horizontal displacement rate of LIV stakes from the mid section during the monitoring period.	3-51

3.3-14c. The cumulative horizontal displacement rate of LIV stakes from the lower section and foot area during the monitoring period.	3-52
3.3-15. The cumulative horizontal displacement rate of all the LV stakes during the monitoring period.	3-53
3.3-16. The cumulative horizontal displacement rate of all the LVI stakes during the monitoring period.	3-54
3.3-17. The cumulative horizontal displacement rate of all the LVII stakes during the monitoring period.	3-55
3.3-18. Percentage of Cumulative Horizontal Displacement (CHD) per year for slides LII, LIII, LV, LVI, and LVII.	3-56
3.3-19. Plot of 1985, 1986, 1987, and 1988 mean monthly temperature highs and lows for Poker Flats.	3-61
3.3-20. Plot of the number of freeze-thaw days during 1985, 1986, 1987, and 1988 for Poker Flats.	3-62
4.1-1. Locations of hydrologic stations.	4-2
4.2-1. Channel roughness as a function of channel geometry.	4-16
4.2-2. Comparison of grab sampling and Isco automated sampling techniques.	4-26
4.2-3. Comparison of filtered and unfiltered samples.	4-29
4.3-1. Plot of minimum discharge versus basin area.	4-35
4.3-2. Plot of maximum discharge versus basin area.	4-37

4.3-3. Composite 1987 summer hydrographs for Hoseanna Creek at bridge 3 (3M), Sanderson Creek above mining (10Sa), and Frances Creek (4N) (from Mack, 1988).	4-40
4.3-4. Composite 1988 summer hydrographs for Hoseanna Creek at bridge 3 (3M), Sanderson Creek above mining (10Sa), and Frances Creek (4N) (from Ray and Maurer, 1989).	4-41
4.3-5. Plot of base flow versus estimated 2-year peak flow.	4-42
4.3-6. Grain size distribution curves for bedload and channel bottom samples from Hoseanna Creek at bridge 1 (1M).	4-54
4.3-7. Grain size distribution curves for bedload and channel bottom samples from Frances Creek (4N).	4-55
4.3-8. Grain size distribution curves for bedload and channel bottom samples from Popovitch Creek (7N).	4-56
4.3-9. Plot of bedload percentage versus discharge.	4-58
4.3-10. Plot of bedload concentration versus discharge.	4-59
4.4-1. Plot of sediment-discharge regression goodness of fit (r^2) versus basin area (A - km^2).	4-64
4.4-2. Plot of sediment-discharge regression goodness of fit (r^2) versus the number of samples (n).	4-65
4.4-3. Nine examples of sediment-rating regression plots.	4-67
4.4-4. Plot of the sediment-discharge slope regression parameter (b) versus basin area (A - km^2).	4-68
4.4-5. Plot of the sediment-discharge y-intercept regression parameter (a) versus basin area (A - km^2).	4-69

4.4-6. Four examples of annual related shifts in the slope (b) and y-intercept (a) of sediment-discharge regression equations.	4-71
4.4-7. Theoretical changes to sediment-discharge regression lines due to spatial and temporal variability.	4-72
4.5-1. Plot of the regression residual (R - g/l) and discharge (Q - cfs) during 1988 storms for Frances Creek, Sanderson Creek and Hoseanna Creek at Bridge 3.	4-74
4.5-2a. Plot of the regression residual (R - g/l) and discharge (Q - cfs) during three 1989 storms for Hoseanna Creek at Bridge 6.	4-75
4.5-2b. Plot of the regression residual (R - g/l) and discharge (Q - cfs) during the June 24-26, 1989 storm for Hoseanna Creek at Bridge 6.	4-76
4.5-3. Plot of the regression residual (R - g/l) and discharge (Q - cfs) during the June 24-25, 1989 storm for Louise Creek.	4-77
4.5-4. Hypothetical relationships of discharge (Q), sediment concentration (Ts), sediment load (Qs), and the sediment concentration residual (R) over time.	4-80
4.6-1. Plot of peak sediment load versus basin area for a 2-year storm event.	4-88
4.6-2. Plot of peak sediment load versus basin area for a 5-year storm event.	4-89
4.6-3. Plot of peak sediment load versus basin area for a 50-year storm event.	4-90

LIST OF TABLES

2.2-1 Mean monthly temperature highs and lows for Poker Flats 1979-1989.	2-5
2.2-2 Mean monthly precipitation for Poker Flats, Gold Run Pass, and McKinley Park weather stations.	2-6
2.2-3 Eleven largest precipitation events at Poker Flats from 1979 to 1989.	2-8
2.3-1 Air photos used during study.	2-19
2.3-2 Radiocarbon and thermoluminescence dating results.	2-20
2.3-3 Ages of late Quaternary and Holocene stream terraces.	2-25
2.3-4 Exposed areas of different lithologies for selected subbasins.	2-33
2.3-5 Summary of drainage density analyses.	2-34
3.1-1 Classification of slope movements from Varnes (1978).	3-3
3.2-1 Descriptions of monitored slides.	3-9
3.3-1 Changes in average maximum slide lengths 1949 through 1987.	3-14
3.3-2 Changes in average maximum slide areas from 1949 through 1987.	3-14
3.3-3 Summary of movement for LI.	3-15
3.3-4 Summary of movement for LII.	3-20
3.3-5 Summary of movement for LIII.	3-23

3.3-6 Summary of movement for LIV.	3-26
3.3-7 Summary of movement for LV.	3-30
3.3-8 Summary of movement for LVI.	3-33
3.3-9 Summary of movement for LVII.	3-36
3.3-10 Summary of movement for LI through LVII.	3-41
3.3-11 Summary of significant rainfall events and movement of LI and LIV.	3-58
4.2-1 Summary of techniques/tools used to measure streamflow velocities.	4-4
4.2-2 Summary of sediment sampling methods.	4-6
4.2-3 Summary of hydrologic station records.	4-7
4.2-4 Quantity of various sample types taken during each year of study.	4-24
4.2-5 Comparison of grab sampling and Isco automated sampling techniques.	4-25
4.2-6 Results of lab analysis comparisons between ADGGS (filtered) and UCM (unfiltered) of duplicate suspended sediment samples taken during 1988.	4-28
4.3-1 Summary of point discharge records.	4-32
4.3-2 Summary of continuous stage discharge records.	4-33
4.3-3 Predicted discharges of Hoseanna Creek Watershed streams for the 2, 5, and 50 year recurrence intervals.	4-39

4.3-4. Summary of suspended sediment concentration records for nonstage point discharge record stations.	4-45
4.3-5 Summary of suspended sediment concentration records for continuous discharge record stations.	4-47
4.3-6 Exceptional sediment concentrations (greater than 50 g/L) sampled during storms from 1986-1992.	4-51
4.3-7 Summary of bedload samples collected at Hoseanna Creek Bridge 1 (1M), Frances Creek (4N), and Popovitch Creek (7N).	4-53
4.4-1 Summary of sediment-discharge regression parameters, where $\log T_s = \log a + b \log Q$.	4-62
4.6-1 Seasonal proportions of sediment load.	4-83
4.6-2 Predicted peak sediment concentrations (T_s), peak sediment loads (Q_s) and peak erosion rates (ER) for the predicted 2-year (Q_2), 5-year (Q_5), and 50-year (Q_{50}) flow events.	4-85

PREFACE

All steps in the building of knowledge require the seeds of yesterday's innovation and hard work. The late Dr. Clyde Wahrhaftig deserves an ovation for planting the seeds for the many geologists, biologists, scientists and engineers who have spent time in the north central Alaska Range. I am particularly thankful for the time I had with Clyde both in the field and back in the office learning from him the fundamentals and intricacies of Alaskan geology.

This opportunity to work with Clyde and this dissertation were made possible by the Usibelli Coal Mine (UCM), whom I wish to thank for their gracious logistical and financial support from 1985 through 1988. In the early spring of 1985, Charlie Boddy and Dan Renshaw of UCM approached Dr. Don Triplehorn and Dr. Jim Beget of the Geology Department, University of Alaska (UAF) with their desire to support a research project to document the natural geomorphic conditions in the Hoseanna Creek valley. The coal mine was operating in lands that had high landslide susceptibility and adjacent to creeks that had naturally occurring high sediment loads. Both of these geomorphic characteristics created potential problems with mining operations and with permitting. Thus, this dissertation is my effort to document these natural conditions and in some sense provide UCM with the data and information that they might need.

Because of the breadth of data and information that the mine was requiring they also solicited the help of the United States Geological Survey (USGS) Water Resources Division and the ADGGS (Alaska Division of Geological and Geophysical Surveys, now the Department of Water Resources of the State of Alaska). So in the early summer of 1985, I began to formulate my dissertation objectives and develop a study scope. At this time, the USGS established a streamflow monitoring station near the mouth of Hoseanna Creek. Also during 1985, I established a data baseline for landslides in the watershed and began reexamining Wahrhaftig's geologic maps on more detailed levels. In 1986, many hydrologic monitoring stations were established along the creeks of Hoseanna Creek Watershed by the ADGGS and/or myself.

Over the next four field seasons, much of the hydrologic and geologic field work was supported by UCM engineers and surveyors, and I had the pleasure of Ted Clarke's assistance (at the time a fellow graduate student at UAF and now a graduate student at the University of Wisconsin at Madison). In addition, I worked jointly with the ADGGS hydrologists, Steve Mack in 1986 and 1987, and Scott Ray in 1988 and also helped support the USGS effort. Many, many thanks go to Scott and Steve, and I owe an even greater debt of gratitude to Ted, for his unfailing assistance and friendship, and for the many enjoyable hours sloshing through the muddy waters and slippery hills of Hoseanna Creek Watershed. I completed my field work in April 1989, after which the USGS and ADGGS continued collecting hydrologic data.

I used the International System of Units (SI) throughout most of the text. However, because much of the hydrologic data was collected and reported by the USGS and the ADGGS, I have conformed to the their convention of using standard English units (e.g., discharge: cubic feet per second) when reporting hydrologic data. In some cases for clarity, I used both conventions.

No dissertation is accomplished without the help of many other affiliated workers, and in this light I would like to thank Robert Bates of IT Corporation for his drafting expertise; Robert Burrows of the Water Resources Division, USGS in Fairbanks for his help in understanding the rudiments of field hydrology; Alan Renshaw of UCM for his surveying expertise; and the engineering staff at UCM (Mitch Usibelli, Tim Venechuk, Dan Graham, Ernie Simoniet and Larry Jackson) for supplying needed data, information and logistical support. In addition, Joe Usibelli, Sr., Charlie Boddy of UCM, and Dan Renshaw deserve a special mention for their foresight in perceiving and following through with the studies, and to Joe Usibelli, Sr. and Joe Usibelli, Jr. for seeing that the project was funded. Lastly, I would like to thank Dr. Don Triplehorn, Dr. David Hopkins, and all those who participated as advisors and/or committee members since 1985, and in particular my chairman Dr. Jim Beget, for not losing faith in me these last few years.

DEDICATION

The untimely passing of Dr. Clyde Wahrhaftig has left a void in the culmination of this work, and so I would like to dedicate this dissertation in remembrance of him. I would also like to make a special dedication in remembrance of my mother, Barbara Crawford, who for many years planted in me the zest for knowledge and an able curiosity. Finally, I would like to honor my family (Winston, Chelsea, Brandon, Kimberly, Robert, Flynn and John) and especially my wife Kasey, from whom I have learned patience, which we all needed a lot of in order to let me do this.

1.0 INTRODUCTION

1.1 Objectives

Evaluating erosional and aggradational rates and processes is usually difficult due to the slow rates of geologic processes. Quantification can become practical where process rates are rapid and/or accelerated during our time. Hoseanna Creek Watershed of central Alaska (Figure 1.1-1) is geologically young with high topographic relief and is underlain by easily eroded lithologies; the basin therefore has the potential for rapid or accelerated erosional and aggradational processes. In addition to the geologic conditions of Hoseanna Creek Watershed, the subarctic environment provides a natural laboratory to investigate the effect of high latitude surface processes on the geologic setting. The subarctic setting is characterized by a pronounced cyclical pattern of seasonal processes. Dormant winters are followed by rapid changes during spring break-up and summer. As a result of the interaction of geology and climate, much of Hoseanna Creek Watershed displays landforms (e.g., landslides, badlands) that have high rates of sediment production, and many of the streams in this watershed are heavily laden with sediment. These fluvial and hillslope characteristics provide excellent opportunities to describe and quantify the short- and long-term effects of active fluvial and hillslope systems, and to describe and quantify erosional and aggradational processes.

1.2 Overview

The project was initiated during the summer of 1985 as an outgrowth of Usibelli Coal Mine's needs to better understand the impacts of their growing surface coal mine operations on the environment. The mine required extensive background characterization of slope stability, sediment load and sediment concentration data for areas adjacent to or within mining areas. More importantly, they needed to be able to predict the occurrences and provide explanations for the naturally occurring high sediment loads and intrinsic landslide susceptibility in many of the present and proposed mining areas.

To fulfill the objectives of this project, a thorough integration of data collection strategies was necessary. These included standard and new techniques such as:

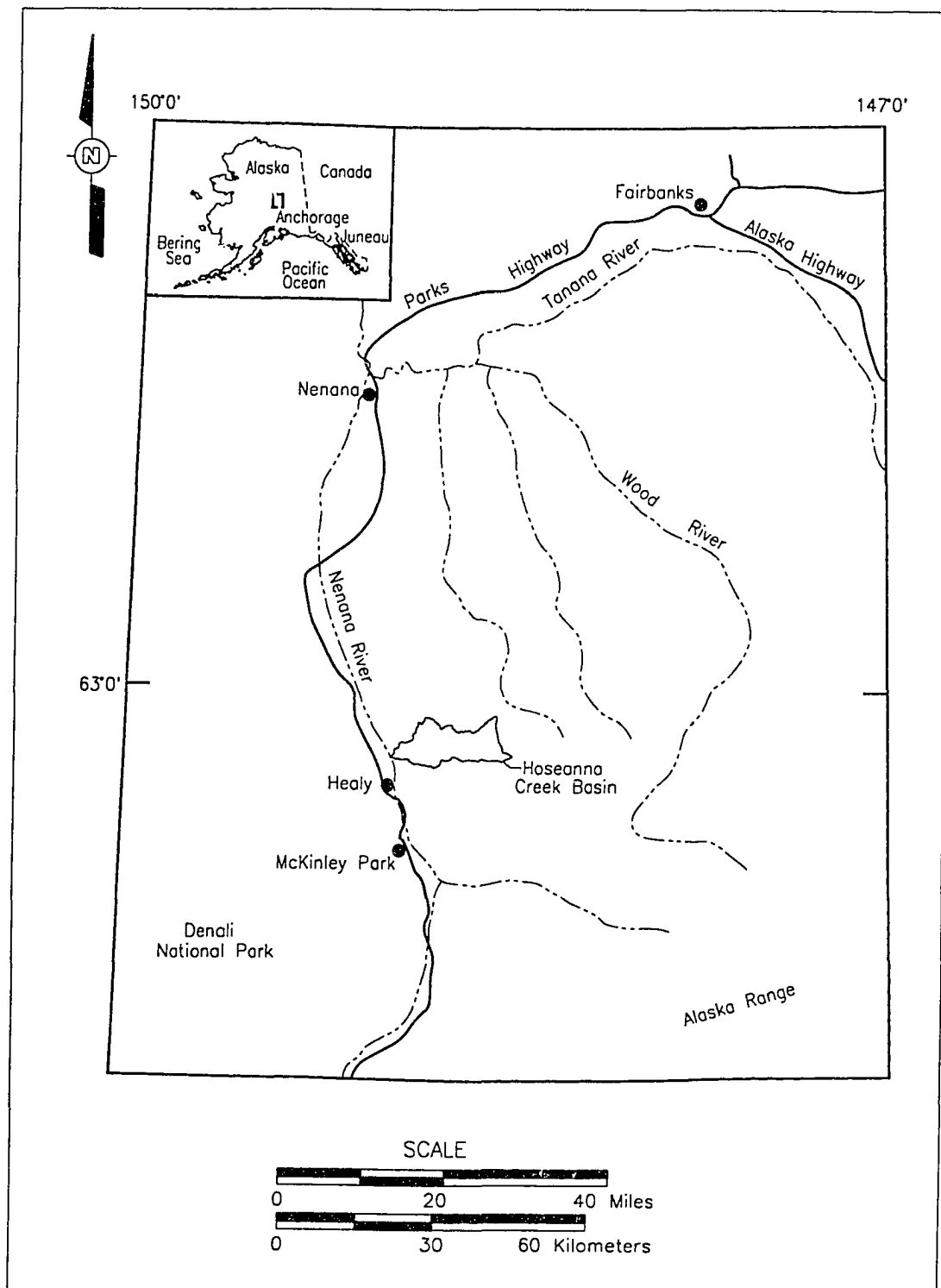


Figure 1.1-1. Location map of study area. The Hoseanna Creek Watershed is located approximately 160 km (road distance) southwest of Fairbanks in central Alaska on the north flank of the Alaska Range.

direct and indirect streamflow measurement techniques, various sediment sampling procedures and laboratory analyses for sediment samples, infrared electronic distance metering theodolite surveying, photo-geologic analyses, detailed and reconnaissance geologic mapping and relative and absolute dating techniques. In addition, supportive climatic and geologic data were compiled and then built upon from Usibelli Coal Mine records and earlier studies of the Nenana Valley area (Wahrhaftig and others, 1951; Wahrhaftig, 1958; Wahrhaftig and others, 1969; Wahrhaftig, 1970a-j; and Wahrhaftig, 1987).

1.3 Scope

This dissertation is composed of three parts in each of which a particular element or process related to landscape evolution in Hoseanna Creek Watershed is described and/or quantified. Section 2.0 (Geologic and Climatic Controls Governing Surface Processes), provides the foundation for understanding the next two parts: Section 3.0 (Landslide Movement in Discontinuous Permafrost), and Section 4.0 (Streamflow and Sediment-Discharge Processes), which are synthesized in Section 5.0 (Summary and Conclusions). In general, this study describes a model of landscape evolution in which short- and long-term sediment supply is dependent on the prevailing tectonic environment and the interaction between fluvial and hillslope processes.

Some of the data in this thesis have been presented in preliminary reports and short papers (Wilbur and Renshaw, 1987; Wilbur and Clarke, 1987; Wilbur and Clarke, 1988; Wilbur and Beget, 1988; and Wilbur, 1989). In addition, since much of the streamflow work was coordinated with the Alaska Division of Geological and Geophysical Surveys (ADGGS), some of the data collected for this study have been reported in Mack (1987 and 1988) and Ray and Mauer (1989). The ADGGS continued their studies after the completion of field work for this study, and these data are also referred to here (Ray, 1990; Ray and others, 1991; Ray and Vohden, 1992; and Ray and Vohden, 1993). The issues reported on here are not exhaustive of the data collected, but are efforts to focus on specific questions concerning the various aspects of landscape development that relate to specific geomorphic processes occurring in the subarctic Hoseanna Creek Watershed.

1.4 Study Area and Physiography

Hoseanna Creek Watershed lies within the Nenana coal field (Merritt, 1986), which is located on the north flank of the Alaska Range about 120 km southwest of Fairbanks. The watershed is 125 km², trends east-west parallel to the main structural grain in the region, and is drained by a small tributary to the northward-flowing Nenana River (Figure 1.1-1). The mouth of Hoseanna Creek (also known as Lignite Creek) meets the Nenana River about 8 km north of the old Healy townsite. Usibelli Peak, at the southeastern edge of the watershed, is the highest point (1610 m). Most of the watershed is at much lower elevations ranging from 360 m at the mouth to 1060 m on much of the southern divide, and in general the southern drainage basins have a higher average elevation, and thus higher average stream gradients, than the northern drainage basins.

Hoseanna Creek Watershed is comprised of 19 major basins and 14 minor basins (Figure 1.4-1). For the purposes of this study, a major basin is referred as a drainage basin (greater than 0.9 mi²) that heads at the Hoseanna Creek Watershed boundary and discharges to the main channel of Hoseanna Creek (e.g., Popovitch Creek - basin 7N on Figure 1.4-1). A minor basin is any other drainage basin that has a recognizable streamcourse that discharges to the main channel of Hoseanna Creek but does not head at the Hoseanna Creek watershed boundary (e.g. basin DN on Figure 1.4-1). For identification purposes each basin was assigned a number according to its order going upstream and whether it was on the north or south side of the main channel (i.e., major basins: 1N, 2N, 3N..., 1S, 2S, 3S..., and minor basins: AN, BN, CN..., AS, BS, CS...). This basin classification was used for identifying hydrologic stations, and for giving identity to basin types that have similar lithologic, erosion, and vegetational characteristics. This way various geomorphologic characteristics could be readily compared among basins.

Currently, the Usibelli Coal Mine has two surface mines in the Hoseanna Creek Watershed (Figure 1.1-1). The main pit is located at Poker Flats, which is on the south side of the basin near the mouth of Hoseanna Creek. A smaller pit is located in the upper basin at Gold Run Pass which is on the south side of a major tributary called Sanderson Creek. From 1985 through 1987 access throughout the watershed was provided by only a few roads. In 1988, Usibelli Coal Mine completed a haul road to the Gold Run Pass Mine. The haul road traverses up the

basin on Holocene stream terraces for about two-thirds up the axes of the main valley. As a result of this haul road, accessibility within the watershed became far easier in 1988 and therefore the 1988 data set is more comprehensive than that for the three previous years.

1-6

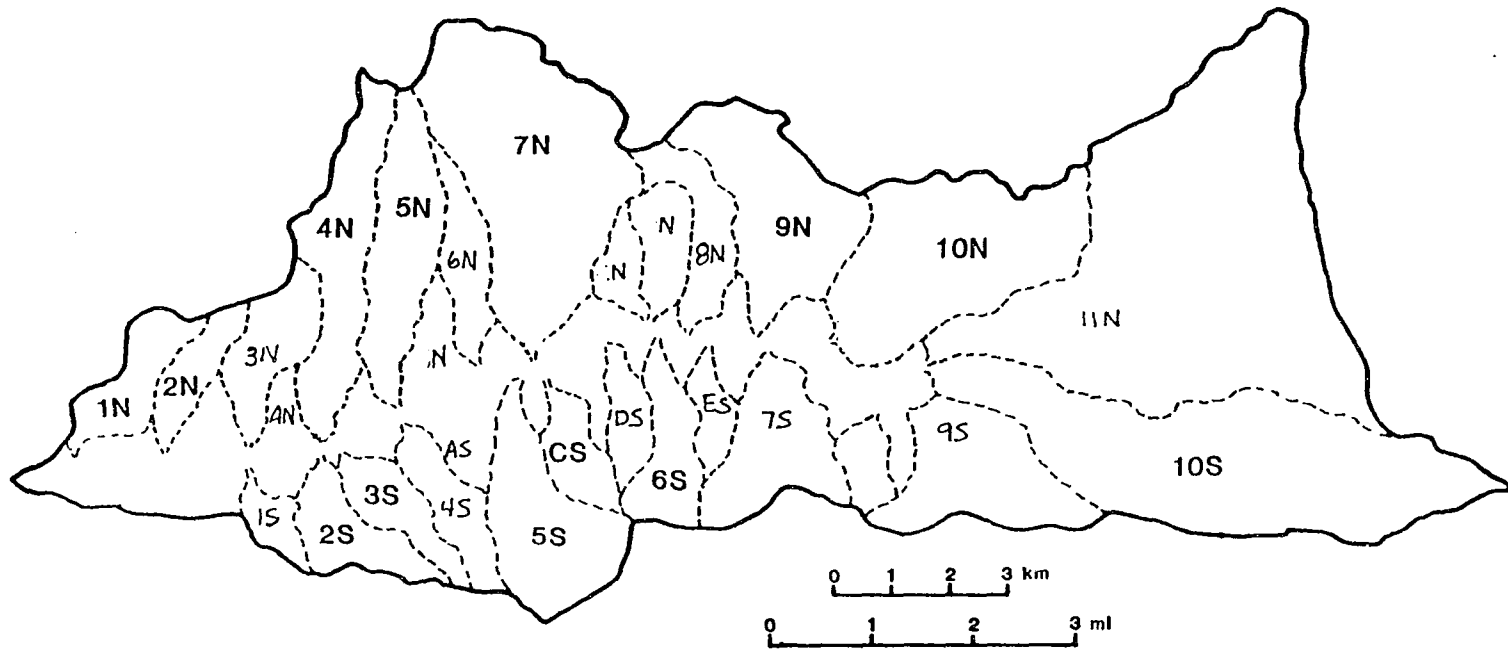


Figure 1.4-1. Basins within the Hoseanna Creek Watershed. The watershed is comprised of 19 major basins denoted as 1N, 2N, etc., and 14 minor basins denoted as AS, BS, etc.

2.0 GEOLOGIC and CLIMATIC CONTROLS GOVERNING SURFACE PROCESSES

2.1 Introduction

Hoseanna Creek Watershed is a geologically very recent and currently eroding very rapidly. Processes or landforms that commonly occur within the watershed include but are not limited to mudflows, debris flows, mudslides, badlands, landslides, earthflows, skin failures, highly concentrated flows during flooding, spring break-up and fall freeze-up phenomena (e.g., aufeis, freeze-thaw induced sloughing).

Continued Late Cenozoic uplift of the Alaska Range accompanied by broad folding and high-angle normal and reverse faulting have provided the impetus for significant downcutting of the northward flowing Nenana River and subsequently pronounced changes in the local base level for Hoseanna Creek. Tectonic activity has been accompanied by Pleistocene glaciation within the Alaska Range. The tectonics and glaciation have had profound effects on the fluvial dynamics of the Nenana River System which encompasses the Hoseanna Creek Watershed.

Hoseanna Creek Watershed has a subarctic interior climate regime, which includes short warm summers and long cold winters that provide for the maintenance of discontinuous permafrost terrain and cryogenic processes. Active spring break-up and summer processes follow essentially dormant wintertime fluvial and hillslope processes to produce significant changes that exceed micro and meso-scale fluvial and hillslope thresholds. These combine to influence sediment supply, transfer and storage on both large and small temporal and spatial scales.

2.2 Climate

2.2.1 Regional Setting

The semi-arid climate of the Nenana Valley region follows typical interior Alaskan subarctic patterns, in which short warm summers with high intensity cyclonic storms follow long cold winters of low precipitation. In addition, because of the area's proximity to the Nenana River gorge which transects the Alaska Range, warm moist winds (chinooks) from coastal Alaska occasionally cross into the Nenana Valley area during wintertime. The chinooks invigorate the dormant winter

patterns by producing warmer periods which may yield snow melt and/or rain.

2.2.2 Local Weather Stations

The United States Weather Service does not have an official weather station in the area. The closest weather station is at McKinley Park, 26 km south of Hoseanna Creek and just south of the Nenana Gorge within the heart of the Alaska Range (Figure 2.2-1). Temperature and precipitation records have been kept at McKinley Park since 1925. Temperature and precipitation records have been kept by the mine at Poker Flats within the Hoseanna Creek Watershed since 1979, but not until 1985 were records kept for the entire year (Tables 2.2-1 and 2.2-2). In September 1986 the State of Alaska Division of Geological and Geophysical Surveys (ADGGS) installed a continuous recording precipitation and temperature gage at Gold Run Pass (Mack 1987). The Gold Run Pass site is at a higher elevation (762 m above m.s.l.) and is approximately 15 km east of the Poker Flats site (530 m above m.s.l.) and the Nenana Valley. The Gold Run Pass gage has a "Wyoming" shield around it to protect the gage orifice from the wind, while the Poker Flats gage has not been shielded. In addition, the Poker Flats gage has been moved a couple times since 1979, and some of the locations are better protected than others.

2.2.3 Temperature

The short-term temperature record at Poker Flats (1979-1989) is quite similar to the short- (1979-1989) and the long-term (1925-1989) records at McKinley Park (Figure 2.2-2); therefore, the climate patterns over the last 90 years at Poker Flats (and more generally for the Hoseanna Creek Watershed) can likely be estimated from the McKinley Park data. The mean annual temperature at McKinley Park since 1925 is -3.1°C , with a mean January temperature of -18.3°C , and an annual average of 209 days with temperatures below freezing. Much of the year (early September to late May) is susceptible to frost activity, with about 165 days of below freezing temperatures, and about 80 days of freezing and thawing (USWBR). For Poker Flats between 1979-1989, mean monthly January and July temperatures ranged from -14.4 to -6.7°C and 8.3 to 18.9°C respectively (Table 2.2-1),

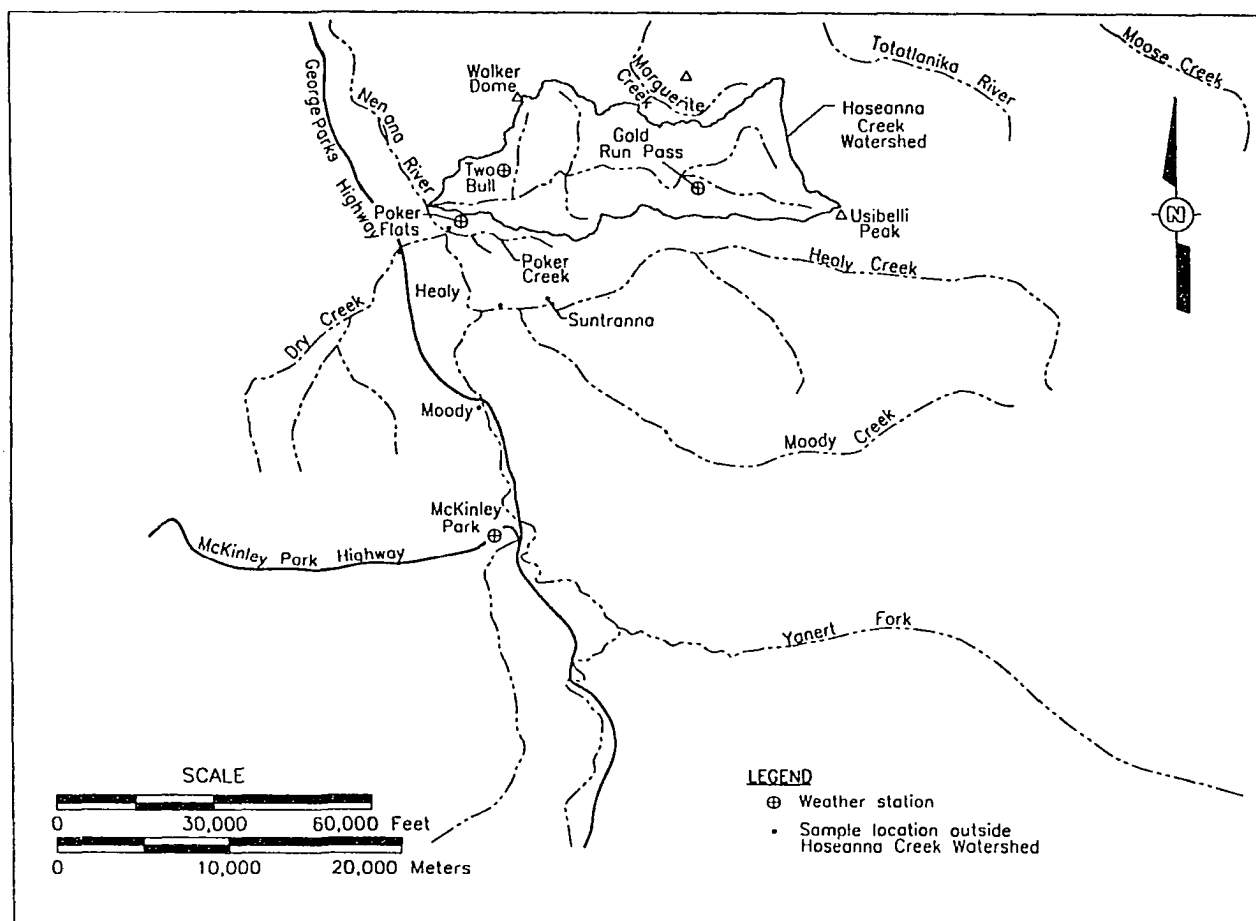


Figure 2.2-1. The Hoseanna Creek Watershed study area and vicinity. The map shows the locations of: weather stations at McKinley Park, Poker Flats, Two Bull Ridge, and Gold Run Pass; the Moody Lake silt sample; the water samples collected at Dry Creek, Suntrana Creek and Healy Creek; the late Cenozoic type section at Suntrana Creek; and other geographic points of interest.

2-4

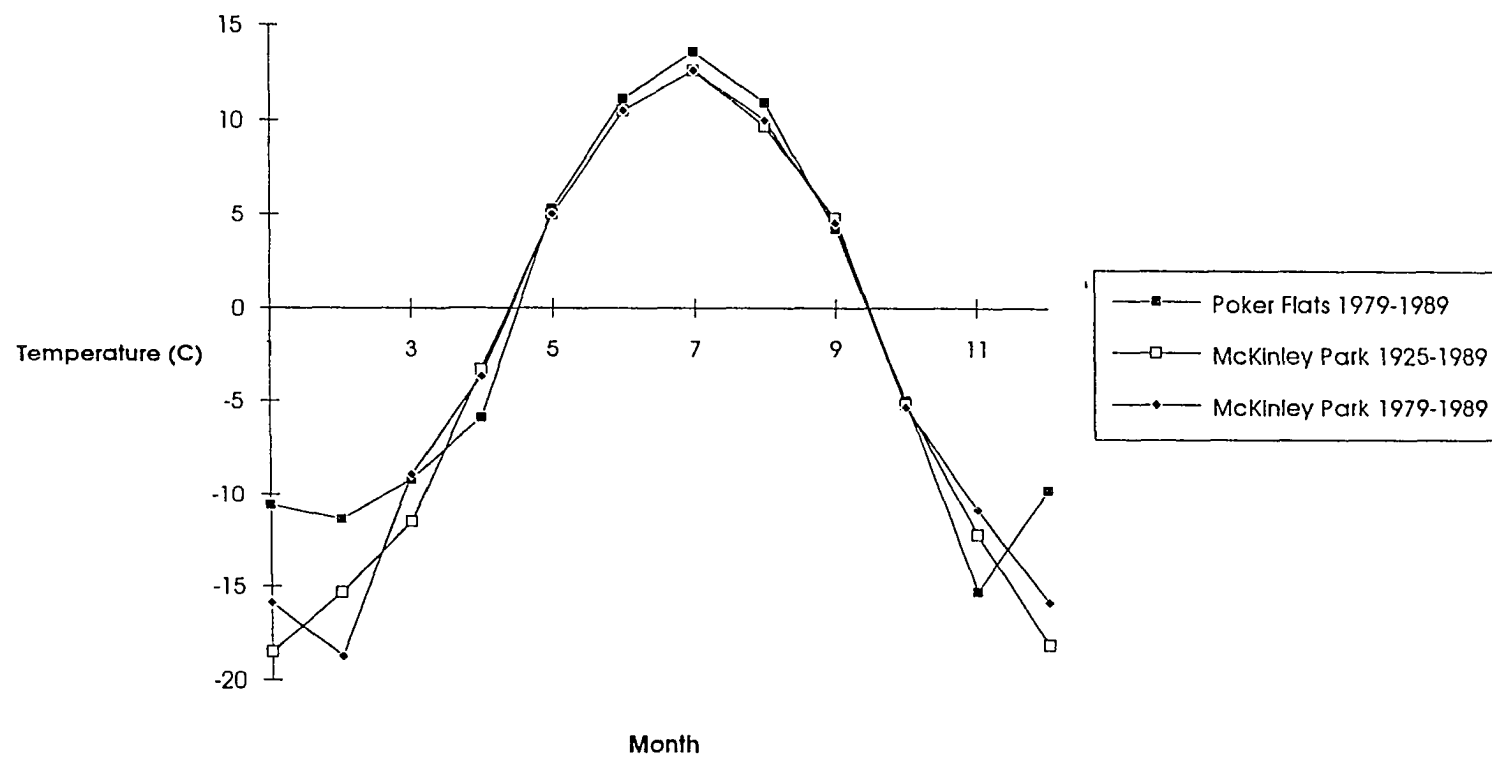


Figure 2.2-2. Mean monthly temperatures for Poker Flats and McKinley Park.

Table 2.2-1. Mean monthly temperature highs and lows for Poker Flats 1979-1989.

Month	Year Began	High (C)	Low (C)
January	1985	-6.7	-14.4
February	1985	-8.3	-14.4
March	1985	-5.6	-12.8
April	1984	-1.1	-10.6
May	1980	10.0	0.6
June	1979	16.1	6.1
July	1979	18.9	8.3
August	1979	15.6	6.1
September	1980	7.8	0.6
October	1980	-1.7	-8.3
November	1985	-11.7	-18.9
December	1986	-5.6	-13.9

2.2.4 Precipitation

Precipitation records for McKinley Park, Poker Flats and Gold Run Pass are summarized in Table 2.2-2. In general, average annual precipitation is about 20 to 25% higher at Gold Run Pass than at Poker Flats (Ray, 1990), although for any given summer storm, rainfall at Poker Flats can exceed the rainfall at Gold Run Pass. In addition, the summer months at Poker Flats during the years 1979-1989 show a consistently higher average precipitation than the 1979-89 and the 1925-89 McKinley Park averages (Figure 2.2-3). The Gold Run Pass and Poker Flats short-term rainfall records suggest that Hoseanna Creek Watershed receives about 30 to 45% more rainfall than McKinley Park station during the summer and annually. This is likely a reflection of different summertime moisture sources operating within and outside of the Alaska Range and the lower elevation of the McKinley Park station (see summary in Ray and Maurer 1990).

The 1979-1988 average annual precipitation at Poker Flats was 38.6 cm (15.2 in), of which 67% fell as rain from June through August, and another 23% fell as rain and/or snow during May, September and October. A major portion of the summer precipitation is produced by only a few major cyclonic storms which typically

produce three to eight cm during a single event. Thus 5-20% of the annual precipitation may fall during a very short period (e.g.: 48 hours). More than one of these events commonly occurs in a single year. In addition, the majority of the relatively small volume of winter precipitation that falls as snow is held in storage until late April or early May when spring break-up occurs. Both spring break-up and summer storms are major causes of high runoff events. Thus, precipitation in Hoseanna Creek Watershed typically arrives in short spurts which provide the impetus and energy for hillslope and fluvial dynamics.

Table 2.2-2. Mean monthly precipitation for Poker Flats, Gold Run Pass, and McKinley Park weather stations. All precipitation data are in cm.

Month	Poker Flats (1979- 1989) ¹	Poker Flats (1987- 1989) ¹	Gold Run Pass (1987- 1989) ²	McKinley Park (1925- 1989) ³	McKinley Park (1979- 1989) ³
January	1.14			1.83	2.29
February	0.51			1.50	1.27
March	0.84			1.44	1.09
April	0.86			1.02	1.02
May	2.13	2.44	2.74	2.06	1.32
June	8.23	8.74	11.15	6.27	6.48
July	9.58	7.77	7.42	7.74	6.58
August	7.70	5.99	9.04	6.07	5.38
September	3.94	3.30	5.69	3.69	3.28
October	2.67			2.36	1.91
November	1.68			2.24	1.78
December	1.12			2.11	2.26

1: Usibelli Coal Mine Records, 2: Ray (1990), 3: United States Weather Bureau Records

The largest 24 hour storm recorded at Poker Flats between 1979 and 1989 occurred on July 20, 1986 and produced 6.65 cm. The largest 48 hour storm occurred on June 17 and June 18, 1980 and produced 8.56 cm. Over the same eleven year period all the large storms (greater than 3.30 cm) occurred from late May to late August (Table 2.2-3). Commonly, when the storms occur in late May a significant snowpack still exists; the high rainfall volume coupled with snowmelt can produce profound channel changes (i.e., avulsions and/or migrations accompanied by lateral corrasion of saturated hillslopes) that result in extreme

2-7

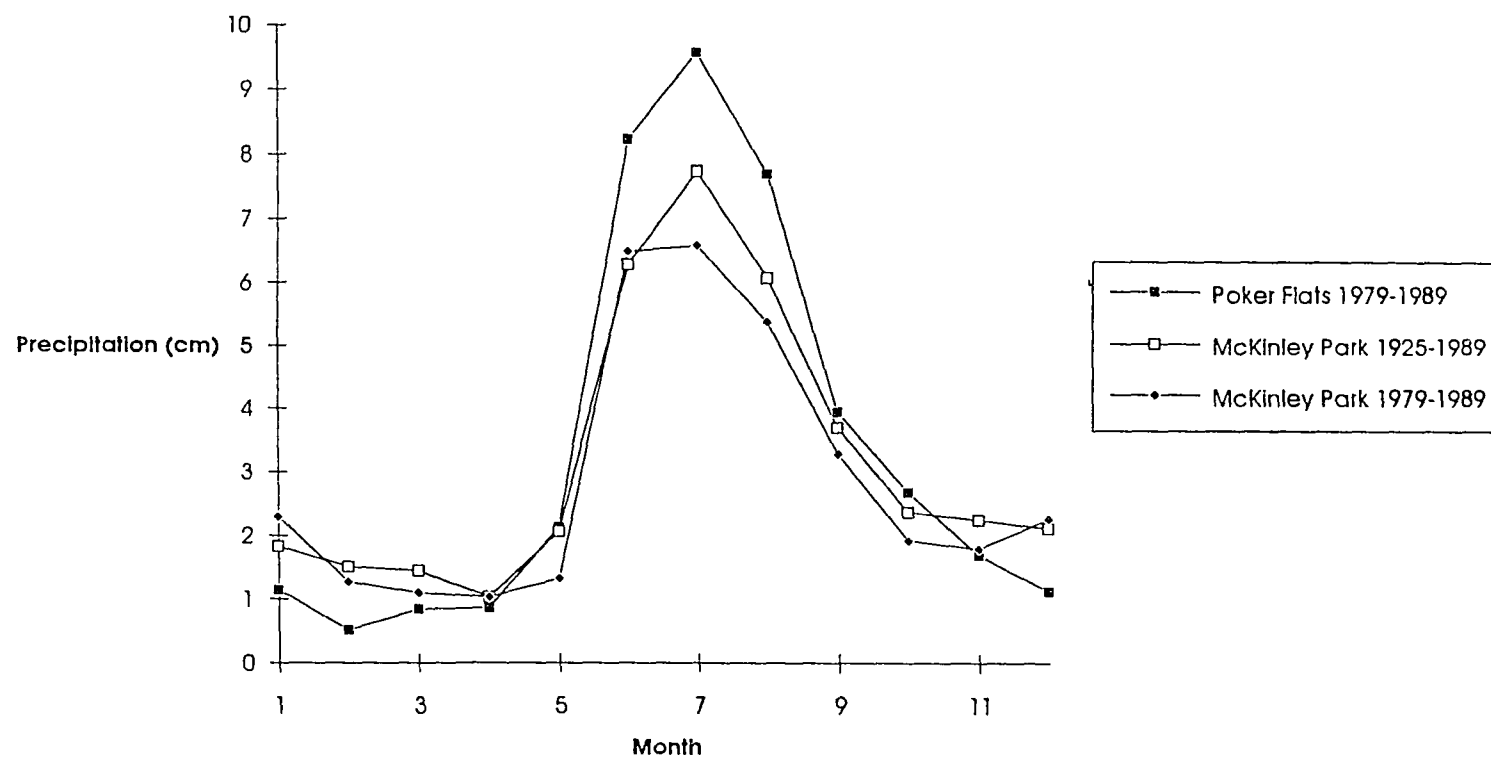


Figure 2.2-3. Mean monthly precipitation for Poker Flats and McKinley Park.

sediment burdens to the streams and sediment transport processes of Hoseanna Creek Watershed.

Table 2.2-3. Eleven largest precipitation events at Poker Flats from 1979 to 1989.

Date	1 Day Storm (cm)	Date	2 Day Storm (cm)
07/20/86	6.65	06/17-18/80	8.56
06/17/80	5.38	07/20-21/80	6.91
07/25/84	5.05	06/28-29/79	6.35
06/16/82	4.83	07/24-25/84	5.99
06/02/86	3.78	08/28-29/79	5.84
06/06/89	3.73	06/16-17/82	5.59
08/21/86	3.56	08/20-21/86	5.49
07/29/87	3.51	06/05-06/89	4.60
05/30/88	3.51	07/29-30/87	4.17
06/18/88	3.33	07/10-11/83	4.09
06/29/79	3.30	06/02-03/86	3.78

2.2.5 Importance of Seasonal Patterns

Many of the surface processes in Hoseanna Creek Watershed are characterized by a cyclical pattern of wintertime dormancy and summertime activity. The transition between winters and springs are marked by major dynamic changes (freeze-up and break-up) in both surface and near-surface hydrologic processes (Michel, 1971). Short, warm moderately dry summers are interrupted by major and minor cyclonic storms which can yield high intensity basin-wide or smaller rain events. The long cold and dry winters maintain discontinuous permafrost and a variably thick frozen active layer over most of the hillslopes. In addition, thick stream aufeis builds during the winter in Hoseanna Creek and its tributaries.

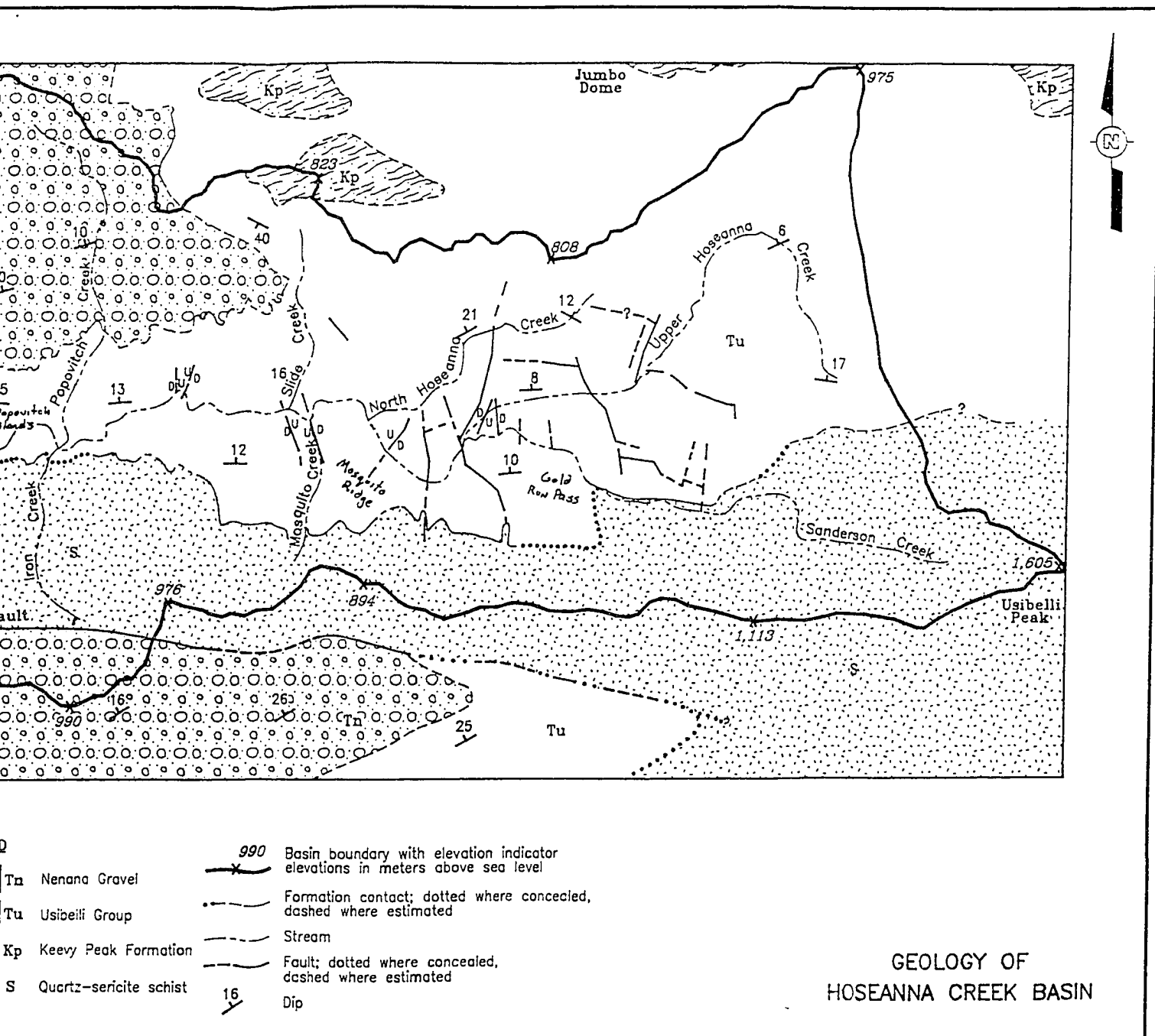
Two weather characteristics are relevant to mass wasting and sediment-transfer. First, subarctic creeks experience major changes in both surface (Michel, 1971) and

subsurface (Kane, 1981) flow during break-up, summer and freeze-up seasons. Second, because 90% of the precipitation occurs during May-October and commonly falls during large cyclonic storms, rapid and large influxes of liquid water yield peaked hydrographs of short duration, high stream power, and maximum potential for sediment transport and erosion. In addition, sediment supply is seasonally dependent on weather patterns such as mass wasting triggered by spring break-up or major storms.

2.3 Geology

The Hoseanna Creek Watershed and vicinity was first mapped by the USGS in 1910 (Capps, 1912) and 1918 (Martin, 1919), and summarized by Capps (1940). The USGS was intent on surveying the mineral and coal resources of interior Alaska at the time and identified a major coal resource in the Nenana coal field. Both Capps and Martin traversed up Hoseanna Creek, Healy Creek and a number of other streams in the area. Capps' study was reconnaissance geologic mapping covering most of the northern flank of the Alaska Range between the Nenana River and the Wood River (known then as the Bonnifield Region - Capps, 1940). Martin concentrated on estimating coal reserves in both the Healy and Hoseanna Creek Watershed and in doing so described a number of stratigraphic sections along Hoseanna Creek. Both Martin and Capps took photographs and described for the first time various "badland" outcrops seen throughout Hoseanna Creek Watershed.

During the 1940's, the USGS supported the war effort by defining in detail the coal reserves of the Nenana coal field (Barnes and others, 1951). Several important studies were produced including Wahrhaftig and others (1951) and Wahrhaftig and Birman (1954); eventually more detailed and farther ranging projects grew out of this work. The results of the coal resource studies produced several other important documents describing the coal geology (Wahrhaftig, 1973), descriptions and paleontology of the Tertiary sedimentary sequences (Wahrhaftig and others, 1969; Wolfe and Tanai, 1980) and the metamorphic basement rocks (Wahrhaftig, 1968). The Late Pleistocene framework for this area was established in Wahrhaftig's Quaternary history of the Nenana Valley (1958). In 1970, a 1:63,360 series of geologic maps of eight quadrangles was published (Wahrhaftig, 1970a through 1970h). In addition, Wahrhaftig wrote a few unpublished manuscripts regarding other geologic and geomorphic studies (e.g., Wahrhaftig [1973] on the



The prevailing attitudes high angle reverse fault the Tertiary strata in south trending faults. its see Figure 2.3-3.

Although seven formations are recognized in Wahrhaftig 1970c, only three distinctions are important to describe the principal controls on erosion. The three important lithologies are the late Tertiary Nenana Gravel, the mid Tertiary Usibelli Group, and the precambrian quartz-sericite schist (modified from Wahrhaftig, 1970c).

Nenana Gravel, a compilation of more than 70 years of badland photography, and Wahrhaftig [1959] which describes the coal depositional environments), that are important to this study. Wahrhaftig (1987) reexamined the coal-bearing sequence, officially defining the Usibelli Group and summarized some of his findings regarding badland erosion and development.

At the inception of this study during the summer of 1985, I had the honor of assisting Dr. Wahrhaftig for six weeks in his on-going study of badlands development throughout the Nenana coal field. We visited over 50 of his badland sites from the Toklat River to the Wood River, including a number of sites in the Hoseanna Creek Watershed. From this beginning, I reexamined the geology of Hoseanna Creek Watershed for the purposes of revising the coal reserve estimates for Usibelli Coal Mine and to outline the framework for this study. Wahrhaftig's base map (1970c) was revised to incorporate more detail in the nature of geologic contacts and the distribution of Precambrian, Tertiary and Quaternary formations which are important to discerning the causes for specific surface processes.

2.3.1 Lithology and Stratigraphy

Lithologic differences among rock-types in the Hoseanna Creek Watershed are significant because each rock-type is associated with specific landscape features and processes which result in different surface features and processes. Seven formations are recognized in the basin, but these can be grouped into three lithologic groups with differences that are important to surface processes (Figure 2.3-1 modified after Wahrhaftig, 1970c). The three principle rock-types are, from oldest to youngest, the highly deformed and relatively resistant basement metamorphics including pelitic and quartzose schists of Precambrian and early Paleozoic age (Wahrhaftig, 1968; Csejtey and others, 1986), the mildly deformed and weakly consolidated coal-bearing mid to late Tertiary Usibelli Group (Wahrhaftig and others, 1951; Wahrhaftig and others, 1969; Wahrhaftig, 1987), and the gently tilted gravel-conglomerate sandstone beds of the late Tertiary Nenana Gravel (Wahrhaftig, 1987). In addition, significant deposits of late Pleistocene glaciofluvial terraces (Wahrhaftig, 1958; Thorson, 1983) and younger alluvial, fluvial and landslide deposits occur within Hoseanna Creek Watershed.

2.3.1.1 Basement Metamorphics

Most of the basement metamorphics within Hoseanna Creek Watershed have not been formally assigned to units described in Csejtey and others (1986). The predominant basement rock is a quartz-sericite schist previously informally but incorrectly referred to as the Birch Creek Schist known from central Alaska northeast of Fairbanks (Wahrhaftig, 1968; Wahrhaftig, 1987). The quartz-sericite schist is the most resistant rock type in the basin and is the core of the major anticlinal feature that forms the highest parts of Hoseanna Creek Watershed along the southern drainage divide; however, the schist is exposed only on the south side of the basin (with very minor exceptions) and therefore the schist terrain has a pronounced north facing aspect (Figure 2.3-1). This predominately north-facing aspect is important for certain cryogenic surface processes in the schist terrain.

An approximately 550 million year unconformity occurs between the basement metamorphics and the overlying Tertiary sedimentary sequences (Wahrhaftig, 1970a). The metamorphic contact represents the proto-topographic surface that the Tertiary coal-bearing sequences were deposited on. Typical relief of the proto-topographic surface has been estimated by Wahrhaftig (personal communication, 1985) to be on the order of 300 to 600 m. The metamorphic contact with the Tertiary coal-bearing rocks is characterized by a deeply weathered clayey horizon in the proto-topographic lows that grades to fresh rock at the proto-topographic highs. Where present, the clay horizon is conducive to landslide formation, gelifluction and other near-surface mass wasting.

2.3.1.2 Usibelli Group

The metamorphics are unconformably overlain by the coal-bearing mid-late Tertiary Usibelli Group (Wahrhaftig and others, 1969; Wahrhaftig, 1987) which is comprised of poorly to moderately consolidated conglomerate, sandstone, siltstone, claystone and coal sequences. Five formations are distinguished on the basis of thickness and lateral continuity of coal beds, and the thickness, color, pebble lithology and texture of the sedimentary beds. These include from oldest to youngest the Healy Creek, Sanctuary, Suntrana, Lignite Creek and Grubstake Formations (Figure 2.3-2).

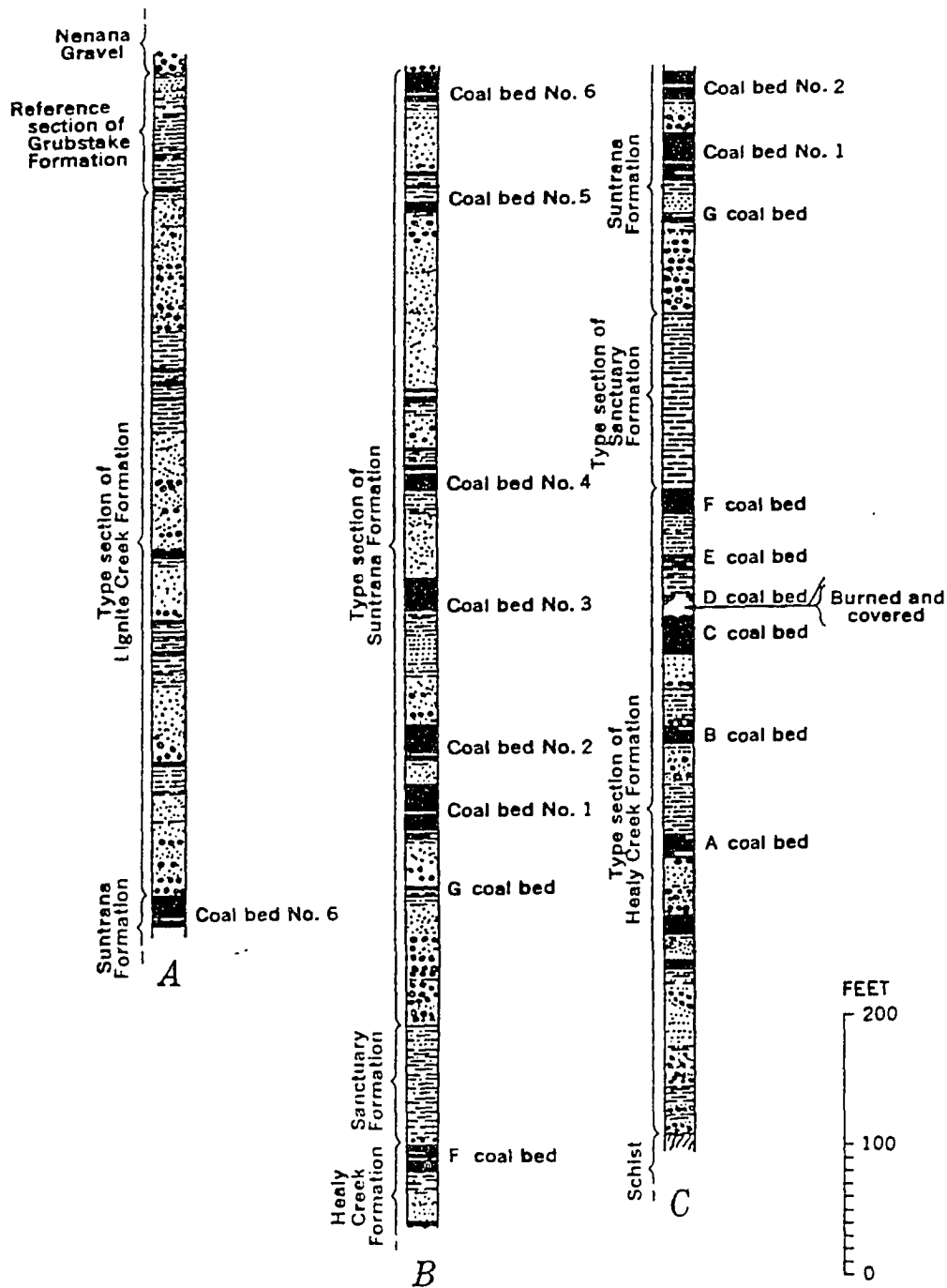


Figure 2.3-2. The late Cenozoic type section at Suntrana Creek. See Figure 2.2-1 for location of Suntrana Creek (from Wahrhaftig, 1987).

Healy Creek Formation

The oldest unit is the locally very thin (< 30 m) to 335 m thick Healy Creek Formation of early and middle Miocene age (Wolfe and Tanai, 1980). It has lenticular subbituminous coal beds (from 1-14 m thick), and thick lenticular sequences of moderately consolidated poorly sorted pebbly to coarse-grained sandstone, conglomerate, and minor thin claystone horizons (Figure 2.3-2). In general, the lower part is comprised of poorly sorted gravelly sands comprised of debris flow-type deposits with chert and abundant schist clasts, while the middle and upper parts are comprised of fining-upward sequences of poorly to moderately sorted sands and gravels comprised of subrounded clasts of chert with minor amounts of schist. The characteristic short lenticular sequences of the lower section become more uniformly thick and more widespread in the upper section. These qualities are indicative of high energy braided river deposits that grade upward into point-bar deposits (Buffler and Triplehorn, 1976). Clays in the Healy Creek Formation consist of 50-70% kaolinite-chlorite, 20-45% illite, and less than 15% montmorillonite (Triplehorn, 1976).

Because the nature and condition of the contact with the underlying schist is highly variable (0 to 600 m of relief), large ranges in thickness of the Healy Creek Formation occur within Hoseanna Creek Watershed. The proto-topographic lows have retained the clays derived from weathering and soil creep and have the thickest Healy Creek Formation sequences, while the proto-topographic highs have no weathered material remaining and have the thinnest Healy Creek Formation sequences. The Healy Creek Formation crops out primarily in the valley bottom or on the south side of the valley conspicuously draped on the schist from just east of Iron Creek to just east of Gold Run Pass and covers approximately 7.5% of the Hoseanna Creek Watershed.

Sanctuary Formation

Overlying the Healy Creek Formation is the locally absent to 60 m thick middle Miocene (Wolfe and Tanai, 1980) Sanctuary Shale (Tsc), which is a moderately consolidated gray claystone when fresh that rapidly weathers to a friable chocolate or yellowish brown (Figure 2.3-2). These colors and clayey texture make the Sanctuary Formation readily identified in the field. It has alternating pale-

weathering and dark-weathering laminae a fraction of a cm to 3 cm thick. The laminated character and the variable distribution of thickness from 0 in the west to more than 60 m in the east, indicate that the Sanctuary Shale was likely to have been deposited in a large shallow lake with the center of the lake (depocenter) in the eastern part of what is now Hoseanna Creek Watershed. The lake extended to the west to a prominent topographic high formed by the schist in the vicinity of what is now just west of Louise Creek (Figure 2.3-1).

The Sanctuary clays consist of 50% kaolinite-chlorite, approximately 35% illite, and about 15% montmorillonite (Triplehorn, 1976). Because the Sanctuary Shale is easily weathered in this climate, it is very conducive to mass wasting, so that the distribution and thickness of this formation is very important to the spatial distribution of hillslope processes.

Because the Sanctuary Shale is relatively thin and non-resistant, the formation occurs in a narrow east-west band in the center of the valley. The Sanctuary Shale is most prominent on the south-facing flank of the major homoclinal ridge in the DS subbasin, and on the north flank of Mosquito Ridge, where the formation covers essentially the entire flank (Figure 2.3-1). The stratigraphic position under the Suntrana Formation provides an important failure zone for the overlying Suntrana Formation throughout the south side of the watershed.

Suntrana Formation

Conformably overlying the Sanctuary Formation is the 180 m to 275 m thick middle Miocene (Wolfe and Tanai, 1980) Suntrana Formation (Tsn). The Suntrana Formation has very continuous (i.e., the #6 coal seam is continuous for over 50 radial miles from the depocenter, [Wahrhaftig, 1973]) and relatively thick coal beds (6 to 15 m thick), with fining upward sequences of clay horizons (up to 3 m thick) and thick sequences of poorly consolidated but moderately sorted to well sorted, fine- to coarse-grained, cross-bedded, quartz-rich sandstone (Figure 2.3-2). The Suntrana Formation is commonly exposed in the large and small "badlands" where creeks have laterally corraded and undercut sedimentary strata dipping away from the creek. Clay below the # 1 coal seam is nearly pure kaolinite; above the seam, it is 35 to 60% montmorillonite, 25-50% kaolinite-chlorite, and 15% illite (Triplehorn, 1976). Most sequences are interpreted as sandy braided-stream deposits (Buffler

and Triplehorn, 1976).

The Suntrana Formation contains the major coal resources of the Nenana coal field. Commonly, the thick coal seams act as major aquifers overlying thick clay aquitards. This combination of coal aquifer and clay aquitard promotes high local pore pressures and is also conducive to landslide development. The Suntrana Formation crops out throughout the basin and is the major geologic unit through which Hoseanna Creek and its tributaries flow.

Lignite Creek

The youngest coal-bearing formation is the 120 m to 225 m thick middle to late Miocene (Wolfe and Tanai, 1980) Lignite Creek Formation (Tlc) (Figure 2.3-2). The Lignite Creek Formation is comprised of fining-upward cross-bedded sequences of thick (> 10 m) moderately sorted to well sorted but weakly consolidated fine-grained sandstone interbedded with moderately thick silt-clay zones (many greater than 3 m), many thin beds of coal or lignite (0.2 to 2 m thick) and a fundamental change in sand mineralogy from the underlying Suntrana Formation (from predominantly quartz to up to 25% feldspar). The Lignite Creek Formation is interpreted to have been deposited by southward-flowing low-gradient meandering streams (Buffler and Triplehorn, 1976). The Lignite Creek Formation is exposed in large badlands and occurs primarily in the headwaters and mid-sections of the northern drainages and in the lower valley of Hoseanna Creek.

Grubstake Formation

The youngest formation within the Usibelli Group is the locally very thin (<10m) late Miocene (Wolfe and Tanai, 1980) Grubstake Formation (Tg). The Grubstake Formation exposed in Hoseanna Creek Watershed is a thinly laminated claystone that crops out in only a few places. The Grubstake Formation was deposited in a large shallow lake that formed during the cessation of southward flowing drainages during the initial rise of the Alaska Range (Wahrhaftig, 1987). The depocenter is located to the northeast, and most of present day Hoseanna Creek Watershed is situated at the southwest edge of the former shallow lake.

The overall thickness of the coal-bearing strata ranges from about 390 m in the

western part of the basin to more than 900 m in the east. Analyses of clay mineralogies within the Usibelli Group indicate that three different clay mineral associations exist: a lower interval in the Healy Creek Formation with little or no montmorillonite, an upper interval in the Lignite Creek Formation and Suntrana Formation with abundant montmorillonite, and a relatively thin intermediate layer with predominant kaolinite (Triplehorn, 1976). These mineralogic associations may account for some of the observed variability in landslide susceptibility due to the intrinsic freezing properties of the different clay minerals. (see geologic factors in Section 3.3.5.2)

2.3.1.3 Nenana Gravel

Overlying the Usibelli Group is the very thick (greater than 1000 m in Hoseanna Creek Watershed) massive to thick bedded, poorly consolidated late Miocene to middle Pliocene (Wahrhaftig, 1987) Nenana Gravel (Figure 2.3-2). This formation has a distinct orange-brown outcrop color, and is composed mainly of large cross-bedded, poorly sorted to moderately sorted intercalated coarse sand lenses and gravel sequences. Much of this lithology is exposed in large basin-wide rapidly eroding badlands in the headwaters of Popovitch (7N), Louise (5N) and Frances (4N) Creeks, and in the headwaters of Iron Creek (5S) (Figure 2.3-1). The Nenana Gravel is either deposited on the Grubstake Formation or on the Lignite Creek Formation. Pebble mineralogy, pebble imbrication and cross-bedding indicate an Alaska Range source for northward flowing streams. The Nenana Gravel was deposited by high-gradient, north-flowing, braided streams and alluvial fans during significant growth and rise of the Alaska Range (Wahrhaftig, 1987).

2.3.1.4 Quaternary Deposits

Chronologic control for landscape development of the mid to late Quaternary deposits in Hosenanna Creek Watershed is dependent on the Quaternary chronology established for the Nenana River Valley, which was initially described by Wahrhaftig (1958) and later revised by Thorson (1975, 1983, and 1986). Several related studies in the Nenana Valley were completed by Ten Brink (1982), Ritter (1982), and Beget and Keskinen (1991). Wahrhaftig mapped a four-fold Quaternary glacial sequence from oldest to youngest as Browne, Dry Creek, Healy, and Riley Creek, corresponding to the well known four-fold sequence established for North America

at the time. In addition, he recognized several advances (i.e., stadials) within the Healy (Healy I and II) and Riley Creek (I, II, III, IV) Glaciations.

Since then, Thorson (1975, 1983 and 1986) has argued against the supposed evidence for the limits of the Dry Creek glaciation, and described a younger drift which he termed Lignite Creek. In addition, he described evidence for much older early Quaternary glaciations down valley from the Browne limits (i.e., Teklanika) and between Lignite Creek and Browne limits which Thorson (1983 and 1986) referred to as Bear Creek. Thus evidence for up to seven Quaternary glacial drift sequences have been described (i.e., Teklanika, Browne, Bear, Dry Creek, Lignite Creek, Healy and Riley Creek. Although, concurrence as to the relative chronology and existence of a least four glacial events exist, little absolute dating control has been accomplished. Beget and Keskinin (1991) describe a section of Lignite Creek (?) till that incorporates the Stampede tephra, which is believed to be older than 140,000 yrs BP. In addition, tentative correlations of late Wisconsin glacial deposits in the Nenana River valley (i.e., Riley Creek stratigraphy) with the McKinley River stratigraphy (Ten Brink and others, 1983) provide chronologic constraints on the timing of the late Wisconsin glaciations.

Late Quaternary Studies in Hoseanna Creek Watershed and Vicinity

Localities in Hoseanna Creek Watershed and vicinity that could supply relative or absolute dating of Late Quaternary deposits were investigated as part of this study. A number of air photo surveys of the area were made since 1949 that cover some or all of the Hoseanna Creek Watershed (Table 2.3-1). These photos were used in conjunction with basin-wide and detailed field surveys to identify the late Quaternary glaciofluvial units identified in Wahrhaftig (1958) and Thorson (1983), and late Holocene stream terraces, and alluvial fans. Stratigraphic descriptions and relationships were used in conjunction with radiocarbon and thermoluminescence dating techniques (Table 2.3-2) to date some of the late Quaternary deposits, while dendrometric techniques were used to date some of the more recent Holocene surfaces (Figure 2.3-3). In addition, relative age control was provided by alluvial and fluvial process knowledge when relating the timing of events between deposits in the Hoseanna Creek Watershed and the established Nenana River stratigraphic units.

I attempted to date the older Healy outwash by utilizing thermoluminescence dating of sediments collected from the Healy II Moody Lake deposits and of alluvial silts mapped as Healy I alluvium by Wahrhaftig (1970c). Moody Lake was a proglacial lake that formed behind the Healy II moraine which was located just south of Healy. Healy I alluvium was shed from proto-Walker Dome to southwest and presumably graded to Healy I outwash in the Nenana River located along the eastern Nenana River Valley. The proto-Frances Creek of Hoseanna Creek Watershed incised into the Healy I alluvium. Sample locations for the Moody Lake silt and the Healy I alluvium are shown on Figure 2.2-1.

Table 2.3-1. Air photos used during study.

Year of Aerial Photography	Approximate Scale	Hoseanna Creek Watershed Coverage
1949	1:43,000	Entire Basin
1968	1:43,000	Upper Basin
1974	1:12,000	Entire Basin
1978	1:12,000	Entire Basin
1981	1:63,000	Entire Basin
1984	1:12,000	Valley bottom from mouth to 10S
1985	1:12,000	Valley bottom from mouth to 10S

Table 2.3-2. Radiocarbon and thermoluminescence dating results. Sample locations were as follows: Hoseanna Creek fan (HCF), Popovitch Creek fan (PCF), Hoseanna Creek bank (HCB), Badlands Creek fan (BCF), Nenana River gorge (NRG), and Frances Creek terrace (FCT). All radiocarbon age dates are C-13 corrected.

Sample ID	Sample Site	Sample in Lithologic Unit	Sample Description	Lab ID	Sample Type	Lab	Age (yrs BP)
86C0t:1	HCF	Qa ₇	wood	GX-12495	C-14	Krueger	1000 ± 190
86C0t:2	HCF	Qa ₇	wood	GX-12496	C-14	Krueger	1045 ± 70
86CVt:1	HCB	Qa ₉	wood	GX-13066	C-14	Krueger	2465 ± 80
86CVt:2	PCF	Qa ₅	wood	GX-13067	C-14	Krueger	395 ± 75
87CLf:1	HCF	Qa ₈	wood	GX-13393	C-14	Krueger	1425 ± 135
87CLf:2	HCF	Qa ₈	wood	GX-13394	C-14	Krueger	2170 ± 140
87CB2:1	BCF	Qa ₆	wood	GX-13396	C-14	Krueger	620 ± 95
86TML:1	NRG	Qh ₁₁	Moody Lake silts	Alpha-3041	TL	Alpha	> 63,800 ± 10,500
86TFR:10	FCT	Qh ₁	Healy alluvium	Alpha-3071	TL	Alpha	< 205,000 ± 28,000

Figure 2.3-3. See back cover map insert.

Quaternary Outwash, Stream Terrace Deposits and Alluvium

The east and west ends of the watershed are thinly to thickly mantled by Quaternary glaciofluvial and alluvial deposits (Wahrhaftig, 1958). The older and higher elevation stream gravels grade to mid and late Pleistocene glacial outwash from the Nenana Valley glaciers (Wahrhaftig, 1958). The oldest Quaternary alluvium in Hoseanna Creek Watershed mapped by Wahrhaftig (1958) were correlated with the Dry Creek outwash deposits; these may be, according to Thorson (1983) associated with Lignite Creek drift which he indicates as pre-Wisconsin in age). The Dry Creek deposits, nonetheless, form the eastern drainage divide of Hoseanna Creek Watershed and indicate northward flowing drainage towards Marguerite Creek of the Totatlanika River drainage basin (Figure 2.1-1).

Continued downcutting of the north-flowing Nenana River led to headward incision of the east-west trending proto-Hoseanna Creek and piracy of the northward flowing streams (Figure 2.3-4). The later and lower elevation gravels (mapped as pre?-Wisconsin and early Wisconsin Healy outwash and late Wisconsin Riley Creek outwash) occur within the basin and indicate drainage towards the Nenana River relatively parallel to current drainage paths. The youngest Holocene age gravels occur at 1.6 to 9 m above the present main channel of Hoseanna Creek west of 7S and are much more pronounced in the lower Hoseanna Creek valley (Figure 2.3-3). The recent terrace sequence indicates recent cutting and filling episodes in the lower valley concurrent with east and west migration of the Nenana River and mainly filling in the upper valley between 7S and 10S. The spatial distribution of cutting and/or filling likely reflects local neotectonics (Thorson 1978).

Assuming the geochronology is reliable and correlations are correct, the late Quaternary terrace deposits appear to record a dramatic lowering of local base level that has affected Hoseanna Creek for the last approximately 200,000 years (Figure 2.3-5, and Table 2.3-3). The entire sequence of late Pleistocene terraces is displayed in the lower Hoseanna Creek Watershed and at the confluence of Hoseanna Creek and the Nenana River. Figure 2.3-5 illustrates the apparent amount and rate of cutting and/or filling during the last 200,000 years.

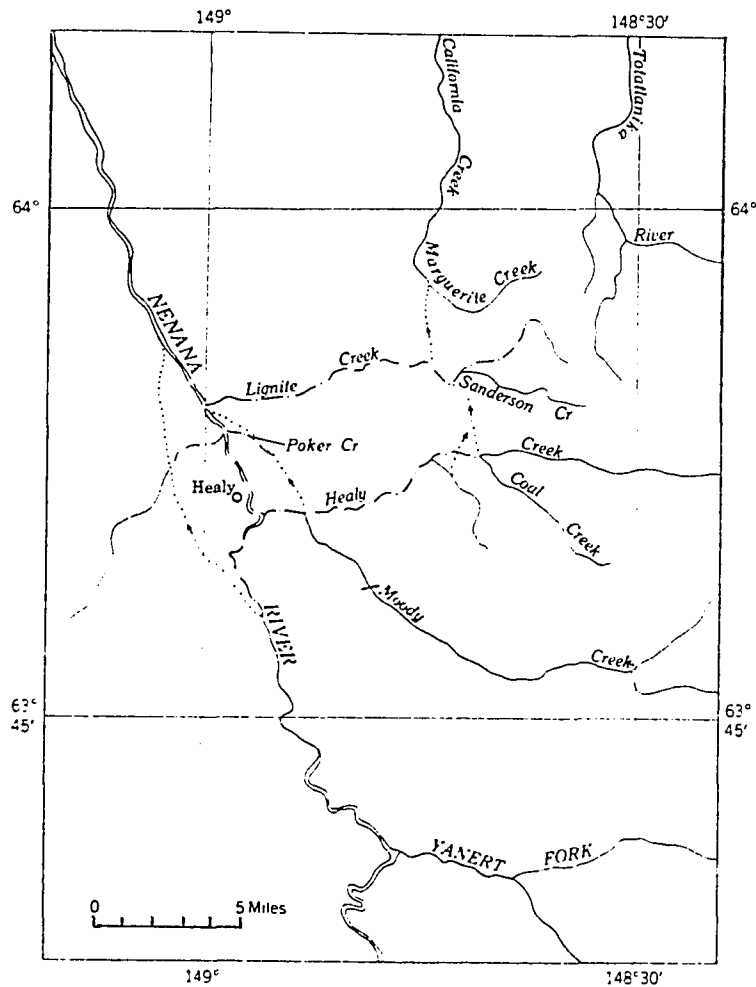


Figure 2.3-4. Drainage changes on tributaries of the Nenana River from the beginning of the Dry Creek to the end of the Healy glaciation. Solid lines indicate stream courses relatively unchanged from the beginning of the Dry Creek glaciation to the present; dash-dot lines, stream courses developed since the Dry Creek; dotted lines, stream courses abandoned since the Dry Creek glaciation (from Wahrhaftig, 1958).

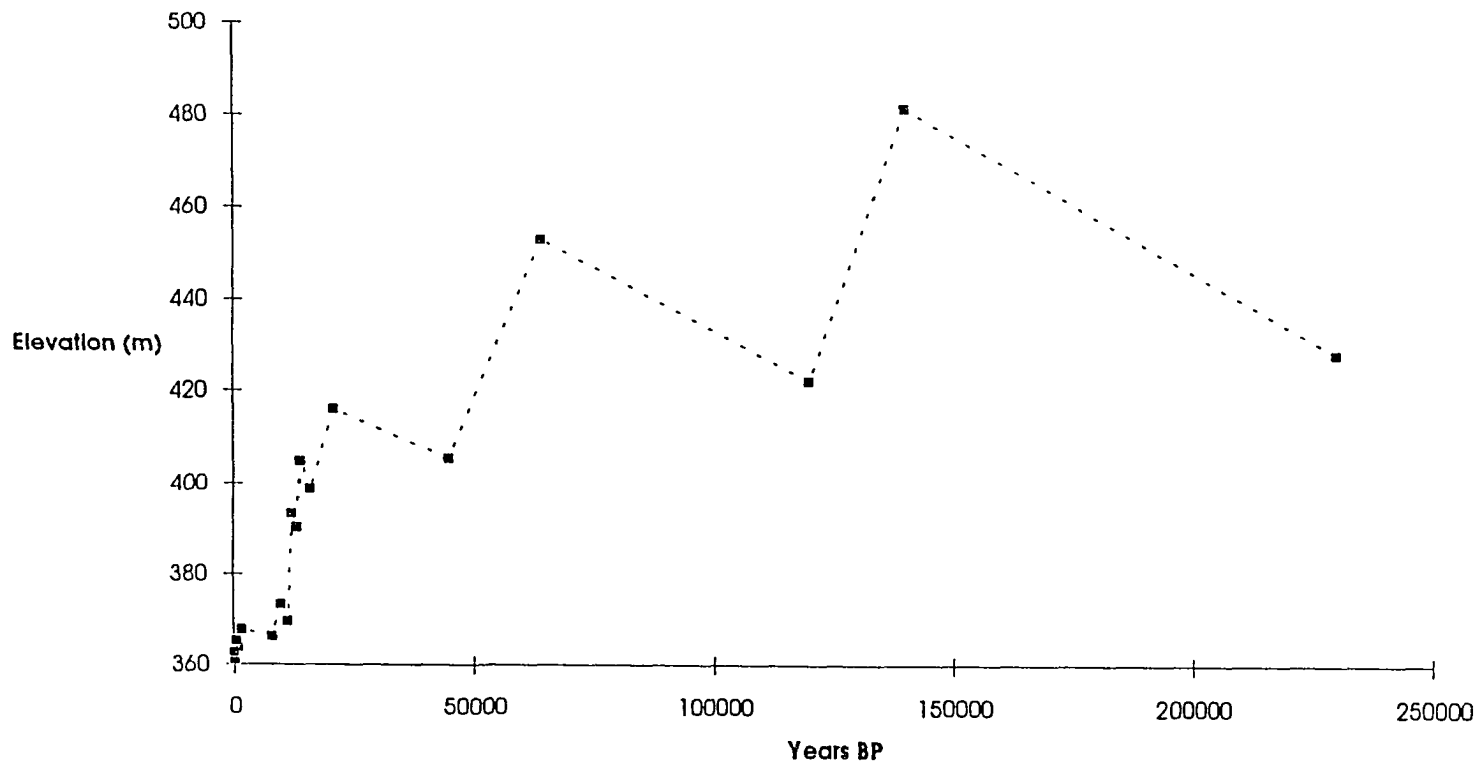


Figure 2.3-5. Hoseanna Creek base level changes during the late Quaternary. Peaks correspond to maximum glacial advances in the Nenana Valley. Aggradation rates of fluvial terraces are slower than the erosion rates because glacial advances are believed to take longer than retreats. The rate of bedrock incision (connect troughs of curve) has not been constant and reflects changes in the local uplift rate (and faulting). Refer to Table 2.3-3 for references to the terrace tops.

Table 2.3-3. Ages of late Quaternary and Holocene stream terraces.

Quaternary Terrace/ Alluvial Fan	Strat Unit	Projected Elevation Top (m)	Projected Elevation Bottom (m)	Age (yrs BP)	Source
Dry Creek	Qda	>520	>460	>230,000	Thorson (1983)
Healy I	Qh1	482	428	<200,000	86TFR:1
Healy II	Qh2	453	422	>64,000	86TML:1
Riley Creek I	Qr1	416	405	17,000 - 25,000	Ten Brink (1983)
Riley Creek II	Qr2	405	399	13,500 - 15,000	Ten Brink (1983)
Riley Creek III	Qr3	393	390	11,800 - 12,800	Ten Brink (1983)
Riley Creek IV	Qr4	373	370	9,500 - 10,500	Ten Brink (1983)
Holocene I	Q7 - Q9	368	366	800 - 2,500	Table 2.3-1
Holocene II	Q4 - Q6	365	364	150 - 800	Table 2.3-1 and tree rings
Holocene III	Q1 - Q3	363	361	0 - 150	tree rings

The age control described above provided a framework for understanding the relationships between the interaction of landslide development and creek avulsions and migrations. In addition, the relative youthfulness of the drainage basin network seems to demonstrate highly accelerated erosional processes. What we observe in the basin today is clearly a product of significant landscape evolution that has occurred in Hoseanna Creek Watershed for much of the late Quaternary, and particularly since the last major interglacial.

Alluvial Fans

Alluvial fans at the mouth of Hoseanna Creek, Badlands Creek (2N), Two Bull Creek (3N), Louise Creek (5N), Popovitch Creek (7N) and 8N are significant depositional landforms in the Hoseanna Creek Watershed (Figure 2.3-3). These fans have formed from only the northern basins which have sufficient sediment production to sustain growth into Hoseanna Creek. The age of each fan reflects part of the recent history of the Hoseanna Creek channel. The three largest fans (Popovitch, Badlands and Hoseanna Creek) were investigated in some detail to help discern the timing and spatial relationships between the hillslope responses along Hoseanna Creek and fluvial perturbations catalyzed by changing the creek grade.

The timing and magnitude of alluvial fan growth records the responses of individual basins to vigorous headward erosion. Thus alluvial fan growth at the mouth of a basin succeeds incision at the mouth and occurs during headward incision into its basin.

The Hoseanna Creek fan is situated at the confluence with the Nenana River (mapped as Qa₇, Qa₈ and Qa₉ on Figure 2.3-3). Prior to mine development (indicated in the 1974 air photos and by detailed topographic mapping), Hoseanna Creek was actively contributing to a very small fan that was incised approximately 7 to 10 m into the south side of the older, much larger fan surface. Stratigraphy of the older fan is exposed along a broad cliff cut just north of the Usibelli Coal Mine office. This approximately 11 m high cut was made by the eastward corradng and downcutting Nenana River. The Lignite Creek Formation is exposed at the base of the cut and is overlain by a 1 to 3 m thick layer of Nenana River gravels. A 3 m sequence of Hoseanna Creek fan deposits (i.e., Qa₇ and Qa₈) overlie the Nenana River gravels to the cliff top.

Exposed within the section are two paleo channels of Hoseanna Creek that were incised into the Nenana River gravels. The base of a southern channel, and likely the oldest Hoseanna Creek fan deposits in the section, is dated by a branch (87CLf:2) at 2170 ± 140 yrs BP (Figure 2.3-6 and Table 2.3-2). The top of the fan is dated by wood detritus (86COt:1) within the highest horizon of alluvial deposits below soil development at 1000 ± 190 yrs BP. Two other dates from wood samples provide supporting evidence for age control, and thus bracket the

2-27

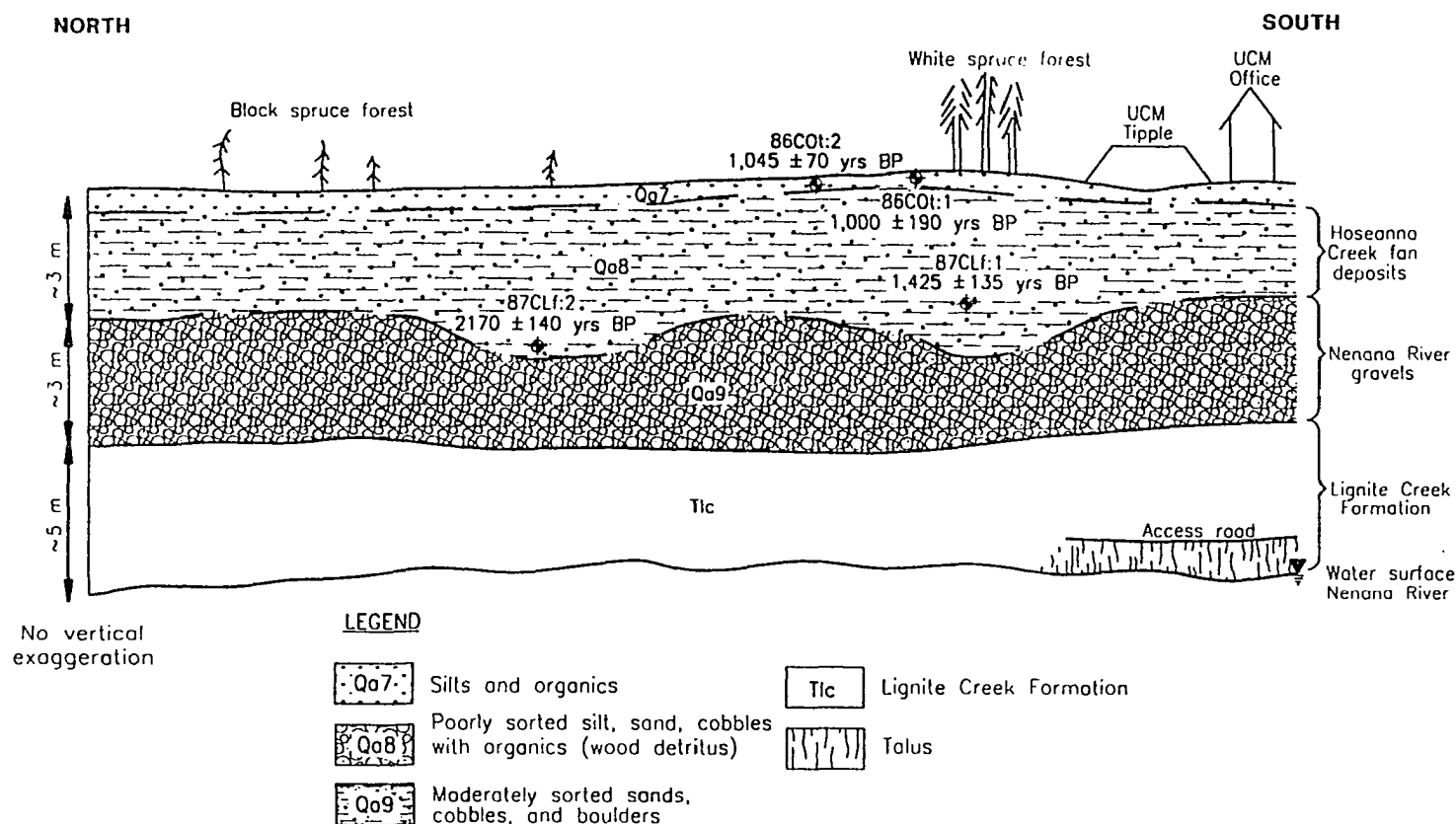


Figure 2.3-6. Schematic cross-section of the Hoseanna Creek fan. The section is located on the west bank of the Nenana River just north of the mine tipple (see Figure 2.3-3 for location). Radiocarbon samples 87CLf:1 and 87CLf:2 were collected from the river bank in organic alluvial sediments. Samples 86Cot:1 and 86Cot:2 are projected to the section from a stratigraphically equivalent horizon and 600 m to the east in organic detritus from a trench wall.

growth of the fan from approximately 2170 to 1000 yrs BP. Since 1979, mining activities on the older fan surface and across the Nenana River have controlled the migration of the Nenana River and the location of the Hoseanna Creek channel.

The Badlands Creek fan is located directly across from the Poker Flats mine and is supplied primarily with material from a large badland upstream in Badlands Creek (Figure 2.3-3) that exposes a thick section of the Lignite Creek Formation. Badlands Creek is deeply incised into the fan; the incision has exposed buried trees in growth position, and the contact of Badland Creek fan deposits overlying Hoseanna Creek stream deposits (Figure 2.3-7). Wood detritus (87CB2:1) in the stream deposits was dated at 620 ± 95 yrs BP (Table 2.3-2) and gives a maximum age for the initiation of fan growth. Prior to 1981 (before the haul road was built), Hoseanna Creek meandered up against the south wall of the valley undermining slopes and causing the hillslope to be unstable. At this time, the Badlands Creek fan was almost across the valley. In 1981, Hoseanna Creek was moved northward and straightened to accommodate the haul road and resulted in shortening and oversteepening the lower reaches of Badlands Creek. This initiated the incision of the fan that is present today.

The Popovitch Creek fan is located midway in the Hoseanna Creek Watershed, and emanates from the fairly large Popovitch Creek Basin (Figure 2.3-3), which is supplied largely with material from the Nenana Gravel. The fan deposits are exposed in a 6 m high cliff cut made by the northwestward laterally corradng Hoseanna Creek (Figure 2.3-8). Hoseanna Creek stream deposits covered by buried plant matter (87CVt:2) and trees in growth position are exposed at the base of the cut. The organic horizon was dated at 395 ± 75 yrs BP (Table 2.3-2). Thus, approximately 400 years ago, the fan began building southward across the Hoseanna Creek channel, forcing the creek up against the southern hillslope and invigorating hillslope failures.

About 300 m downstream of the Popovitch fan is an approximately 10 m high cut into the right (northeast) bank of Hoseanna Creek. Suntrana Formation sandstone and silt are exposed at the based of the cut. About 3.0 m of Hoseanna Creek stream deposits overlie and are cut into the Suntrana Formation about 4 m above the low water surface (Figure 2.3-9). These stream deposits are dominated by sands and cobbles from Popovitch Creek, but they also comprise coal detritus and

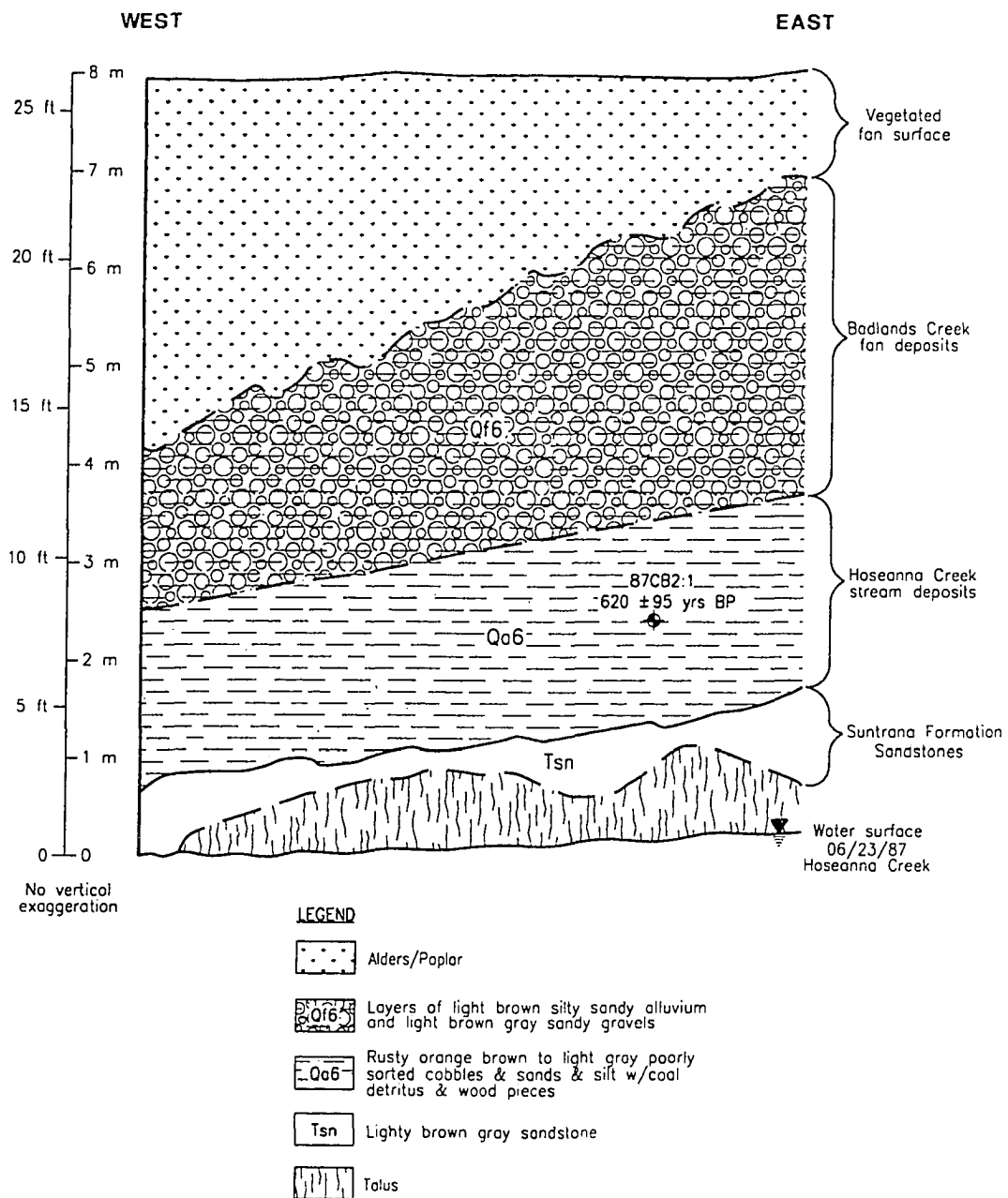


Figure 2.3-7. Schematic cross-section of the Badlands Creek fan. This section is located on a river bank cut into the south-facing west wall of the Badlands Creek fan at the confluence of Badlands and Hoseanna Creeks (see Figure 2.3-3 for location).

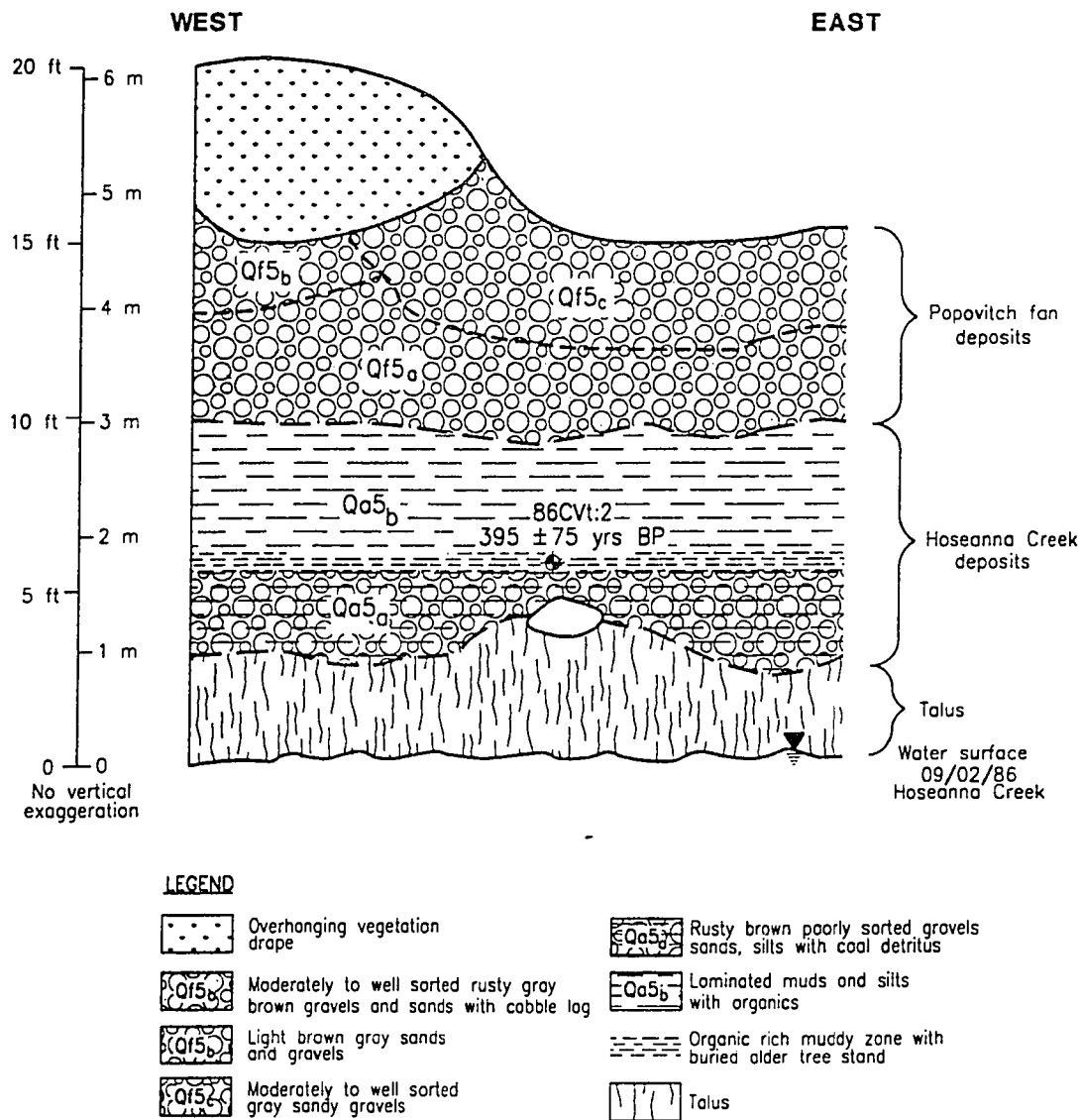


Figure 2.3-8. Schematic cross-section of the Popovitch Creek fan. This section is located on a southeast-facing river bank cut into the Popovitch fan, approximately 150 m upstream from the confluence of Popovitch and Hoseanna Creeks (see Figure 2.3-3 for location).

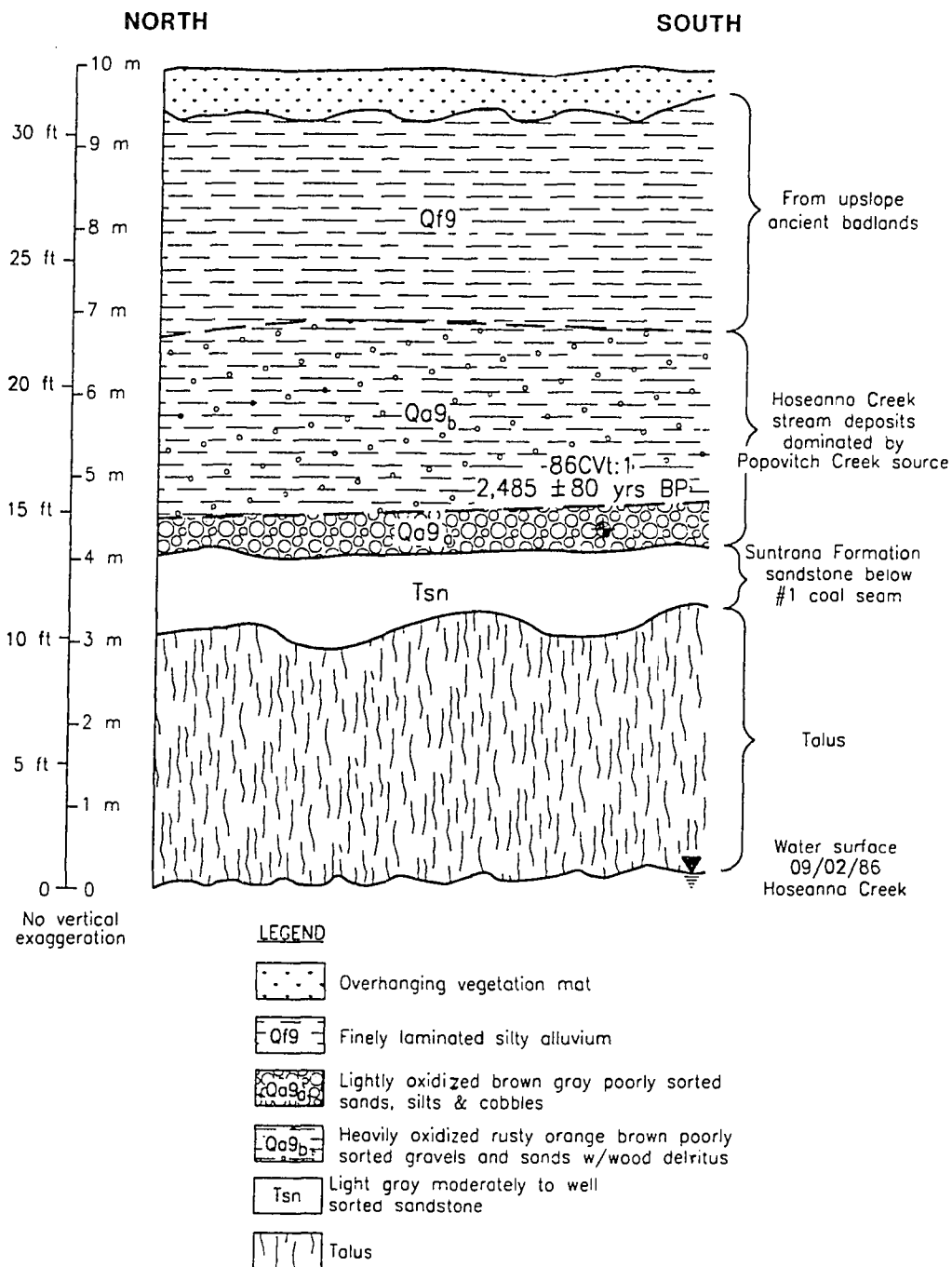


Figure 2.3-9. Schematic cross-section of the Hoseanna Creek bank near Popovitch Creek. This section is located along Hoseanna Creek on a river bank cut into a west-facing hill approximately 300 m downstream of the confluence of Hoseanna and Popovitch Creeks (see Figure 2.3-3 for location).

schist indicative of a multiple source (i.e., Hoseanna Creek rather than Popovitch Creek), and thus indicate an earlier incision of the main channel. At the base of the stream deposit a few pieces of tree remains are mixed with the predominantly coarser detritus. A wood piece was dated at $2,485 \pm 80$ yrs B.P (Table 2.3-1). This datum references the level of the creek approximately 2405 to 2565 yrs BP, and indicates that at least 4 m of incision have occurred at this location (or 1.6 mm/yr).

2.3.1.5 Basin Lithology

The areal percentage covered by each major lithologic category in each major basin was computed and is shown in Table 2.3-4. Of the 18 major basins in Hoseanna Creek Watershed, all but one are underlain by more than one lithology. However, due to the prevalence and distribution (i.e., headwaters versus mouth) of outcrops, many of the creek hillslope processes are dominated by only one lithology. Five are dominated primarily by metamorphics (CS, 4S, 5S, 9S and 10S), five are dominated primarily by the coal-bearing group (2N, 3N, 9N, 10N and UH), three are dominated by the Nenana Gravel (4N, 5N, and 7N), and one (1N) is dominated by the late Quaternary stream gravels. The remaining basins (2S, 3S, 6S and 7S) are underlain and influenced by more than one lithology. The different lithologic basin groups provide a natural laboratory to compare and contrast the influence of lithologic properties on surface processes.

2.3.1.6 Lithologic Control on Drainage Density

Drainage densities were determined for basins within one lithologic category. Since most of the basins are underlain by more than one lithology, smaller third order basins that contained only one lithology were chosen as representative for a given lithology. Drainage density (Bates and Jackson, 1987) is defined as the total length of all mappable stream channels in a basin divided by the total area of the basin (km/km^2). Differences in drainage densities are taken as an indication of differences in long term erosion rates. Since the valley is relatively young, the mechanisms observed today are likely represented by the existing landform characteristics (such as drainage density). For example, well vegetated stable slopes commonly have fewer drainage paths than a highly incised badland.

Table 2.3-4. Exposed area of different lithologies for selected basins.

Basin ID	Area (km ²)	Quaternary Gravels	Nenana Gravel	Usibelli Group	Quartz-sericite Schist
1N	1.79	46.8	1.7	51.5	0.0
2N	1.58	57.1	6.5	36.3	0.0
3N	2.33	33.2	27.8	39.0	0.0
4N	4.41	24.3	55.1	20.2	0.4
5N	4.04	23.1	56.4	19.4	1.1
7N	10.73	16.1	71.7	12.2	0.0
9N	5.39	0.0	2.7	92.4	4.9
10N	8.11	0.0	0.0	100.0	0.0
2S	2.07	8.5	32.8	30.8	27.9
3S	1.79	3.3	18.8	2.3	75.6
4S	1.92	0.0	0.0	0.0	100.0
5S	4.64	3.4	33.2	0.4	63.0
CS	1.63	1.0	0.0	0.0	99.0
6S	2.18	0.2	0.0	27.1	72.7
7S	2.20	0.5	0.0	48.9	50.6
9S	4.45	28.9	0.0	23.6	47.5
10S	13.63	3.2	0.0	16.1	80.7
11N	22.37	10.2	0.0	82.5	7.3

The drainage density for each lithology was calculated using areal and stream data measured from enlargements of the USGS 1:63,360 scale topographic maps to a 1:24,000 scale. Enlargements were utilized because they were easier to work with and the relative sizes of basins were on a scale with which the entire basin could be analyzed. However, drainage density is a function of mappable stream segments and these will vary with map scale. Therefore, the same scale needs to be used throughout an analysis, and the quantitative results cannot be directly compared to numbers generated from maps with other scales.

The results of the drainage density analysis are summarized in Table 2.3-5. Basins underlain by the resistant metamorphics generally have the lowest densities (average 8.1 km/km² and range from 6.1 to 9.9); basins in the coal bearing group have higher densities (average 9.9 km/km², and range from 6.6-12.6), while the Nenana Gravel basins have the highest overall densities (average 12.2 km/km², and range from 10.4 to 14.8). In general, the size of the basin affects measured

Table 2.3-5. Summary of drainage density analyses. Drainage density analyses were performed on 37 representative third order streams draining areas within only one of the three principle lithologies. See map in appendix for locations of each third order stream. Abbreviations are as follows: L1 - first order stream, L2 - second order stream, L3 - third order stream, 10N-A - a third order stream from basin 10N, Avg L1 - the total length of all first order streams in a third order basin divided by the total number of first order streams, Density - the total length of all L1 + L2 + L3 divided by the total area of the third order basin, and L1/L3 - the ratio of the total length of L1 divided by the total length of L3.

Lithology	Basin	Number of L1	Total of L1 (km)	Avg L1 (km)	Number of L2	Total of L2 (km)	Avg L2 (km)	L3 (km)	Area (m ²)	Area (km ²)	Density (km/km ²)	L1/L3
Schist	CS-W	34	10.10	0.30	3	1.42	0.47	1.03	0.12	1.81	7.82	0.29
	6S-E	12	3.36	0.28	2	0.60	0.30	0.41	0.21	0.54	8.04	0.68
	6S-W	12	2.02	0.17	2	0.24	0.12	0.94	0.20	0.52	6.18	0.18
	10S-A	13	3.58	0.28	2	1.70	0.85	0.31	0.29	0.75	7.45	0.69
	10S-B	8	1.44	0.18	3	0.94	0.31	0.17	0.10	0.26	9.85	1.06
	10S-C	6	1.42	0.24	2	0.46	0.23	0.29	0.09	0.23	9.31	0.82
	10S-D	11	3.31	0.30	2	0.48	0.24	0.29	0.20	0.52	7.88	1.04
	10S-E	12	4.32	0.36	3	1.30	0.43	0.36	0.25	0.65	9.24	1.00
	10S-F	10	3.64	0.36	2	0.74	0.37	0.24	0.21	0.54	8.50	1.52
	10S-G	10	3.36	0.34	3	0.67	0.22	0.43	0.19	0.49	9.07	0.78
	SS-B	8	2.09	0.26	2	0.36	0.18	0.53	0.19	0.49	6.06	0.49
	Averages	12.4	3.51	0.28	2.4	0.61	0.34	0.45	0.23	0.60	8.13	0.79
Usbell Group	10N-A	15	2.35	0.16	2	0.24	0.12	0.82	0.20	0.52	6.59	0.19
	10N-B	11	1.90	0.17	3	0.58	0.19	0.36	0.13	0.34	6.44	0.48
	10N-C	12	1.44	0.12	2	0.24	0.12	0.60	0.09	0.23	9.79	0.20
	10N-D	18	3.36	0.19	5	0.58	0.12	0.77	0.17	0.44	10.70	0.24
	10N-E	44	7.32	0.17	6	2.57	0.43	0.94	0.48	1.24	8.72	0.18
	10N-F	33	5.38	0.16	8	1.70	0.21	0.94	0.33	0.85	9.39	0.17
	10N-G	31	4.54	0.15	6	1.68	0.28	0.82	0.26	0.67	10.46	0.18
	10N-H	29	4.34	0.15	5	0.82	0.16	1.03	0.19	0.49	12.58	0.15
	10N-I	26	3.84	0.15	3	0.96	0.32	0.72	0.18	0.47	11.85	0.21
	9N-A	34	5.11	0.15	8	1.51	0.19	0.90	0.27	0.70	10.78	0.17
	9N-B	10	1.98	0.20	4	0.70	0.18	0.26	0.10	0.26	11.36	0.76
	9N-C	27	3.96	0.15	5	1.53	0.31	0.74	0.24	0.62	10.03	0.20
	9N-D	12	2.16	0.18	2	0.45	0.23	0.44	0.10	0.26	11.78	0.41
	9N-E	9	2.12	0.24	3	0.92	0.31	0.17	0.12	0.31	10.33	1.39
	9N-F	11	2.09	0.19	2	0.82	0.41	0.34	0.12	0.31	10.46	0.56
	Averages	21.5	3.46	0.17	4.3	1.02	0.24	0.66	0.20	0.51	10.21	0.36
Nenana Gravel	5N-A	20	2.38	0.12	3	1.18	0.39	0.26	0.10	0.26	14.76	0.46
	5N-B	11	1.15	0.10	3	0.62	0.21	0.38	0.08	0.21	10.38	0.28
	7N-A	14	1.70	0.12	2	0.36	0.18	0.43	0.07	0.18	13.74	0.28
	7N-B	23	3.89	0.17	4	1.92	0.48	0.46	0.17	0.44	14.25	0.37
	7N-C	6	1.42	0.24	2	0.67	0.34	0.24	0.08	0.21	11.25	0.99
	7N-D	23	2.66	0.12	7	1.03	0.15	0.72	0.13	0.34	13.10	0.16
	7N-E	26	5.64	0.22	5	1.75	0.35	0.72	0.30	0.78	10.44	0.30
	7N-F	19	2.83	0.15	3	0.89	0.30	0.46	0.15	0.39	10.76	0.32
	EN-A	14	2.40	0.17	2	0.72	0.36	0.24	0.12	0.31	10.82	0.71
	EN-B	36	5.47	0.15	5	1.20	0.24	1.15	0.24	0.62	12.59	0.13
	SS-A	28	5.28	0.19	3	1.20	0.40	0.53	0.22	0.57	12.31	0.36
	Averages	20.0	3.17	0.16	3.5	1.06	0.31	0.51	0.15	0.39	12.22	0.40

drainage density, the larger the basin, the lower the drainage density, other variables being held constant. One consequence is that lithologic control of drainage density is more evident, if basin area can be held constant. Figure 2.3-10 demonstrates that 3rd order basins underlain by the schist have a maximum density per area threshold, while the basins underlain by the Nenana Gravel have a minimum density per area threshold. In addition, the metamorphic rocks have 1st order streams which are relatively twice the length of those in the Tertiary formations (Table 2.3-5). This indicates that the headwaters of basins underlain by the sedimentary units are much more dissected and thus able to provide more sediment to trunk streams for any given storm.

2.3.1.7 Lithologic Control on Stream Gradients

Hoseanna Creek and all its tributaries are high gradient subarctic streams with the potential for high stream velocities and sediment transport. However, the lithologies exert a significant control on the stream gradients of each basin, as is common for streams elsewhere (Schumm, 1977). The more resistant metamorphic basement rock in the southern basins are less incised but begin at higher elevations, so that overall relief is greater and stream profiles are steeper (Figure 2.3-11). In contrast, the weaker Tertiary formations are more incised and have less overall relief so that stream profiles are relatively lower.

Overall, Hoseanna Creek has an average gradient of 10m/1000m (Figure 2.3-12A). Variations of gradient along the streamcourse are indicated by the differential gradient plot of Figure 2.3-12B, which shows the average gradient over approximately 300 m (1000 ft) sections along the main channel. Differences greater than the average gradient are indicators of relatively higher gradients due to channel control nick points or points of relatively higher discharge influx, while differences less than the average gradient are indicators of points of relatively high sediment influx and stream aggradation. Thus, downstream of 25,000 ft the main channel has significantly more variation in average gradient and indicates the relative effects from sediment input from the north and channel control provided by resistant coal or schist.

2-36

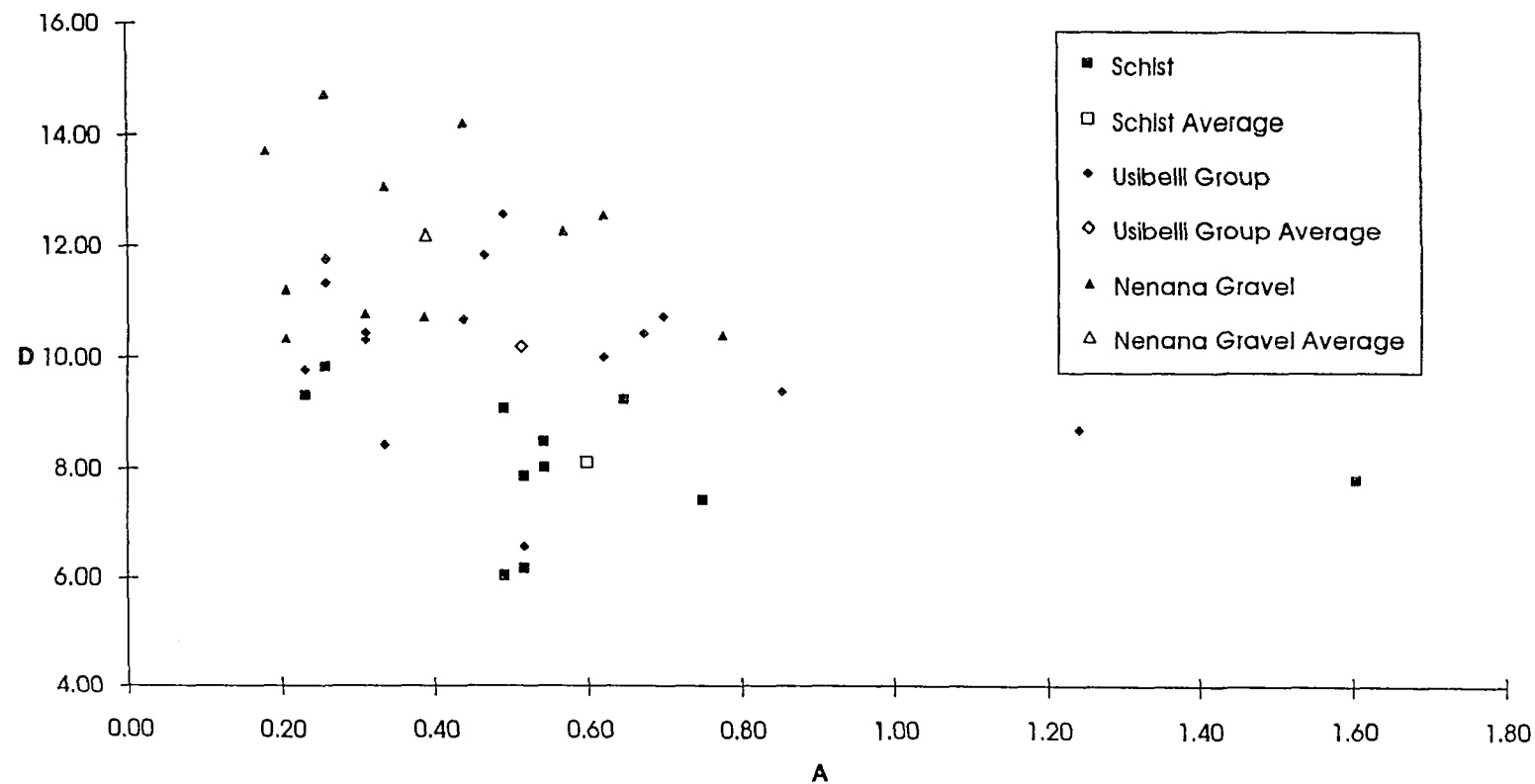


Figure 2-3-10. Plot of drainage density (D - km/km²) versus area (A - km²) for selected 3rd order basins. The basins are underlain by either schist, coal-bearing rocks, or the Nenana Gravel. The line separates two fields of basin-types. Below the line are basins underlain by schist which have a maximum density per area threshold. Basins above the line are underlain by Nenana Gravel which have a minimum density per area threshold. Coal-bearing rocks have intermediate densities.

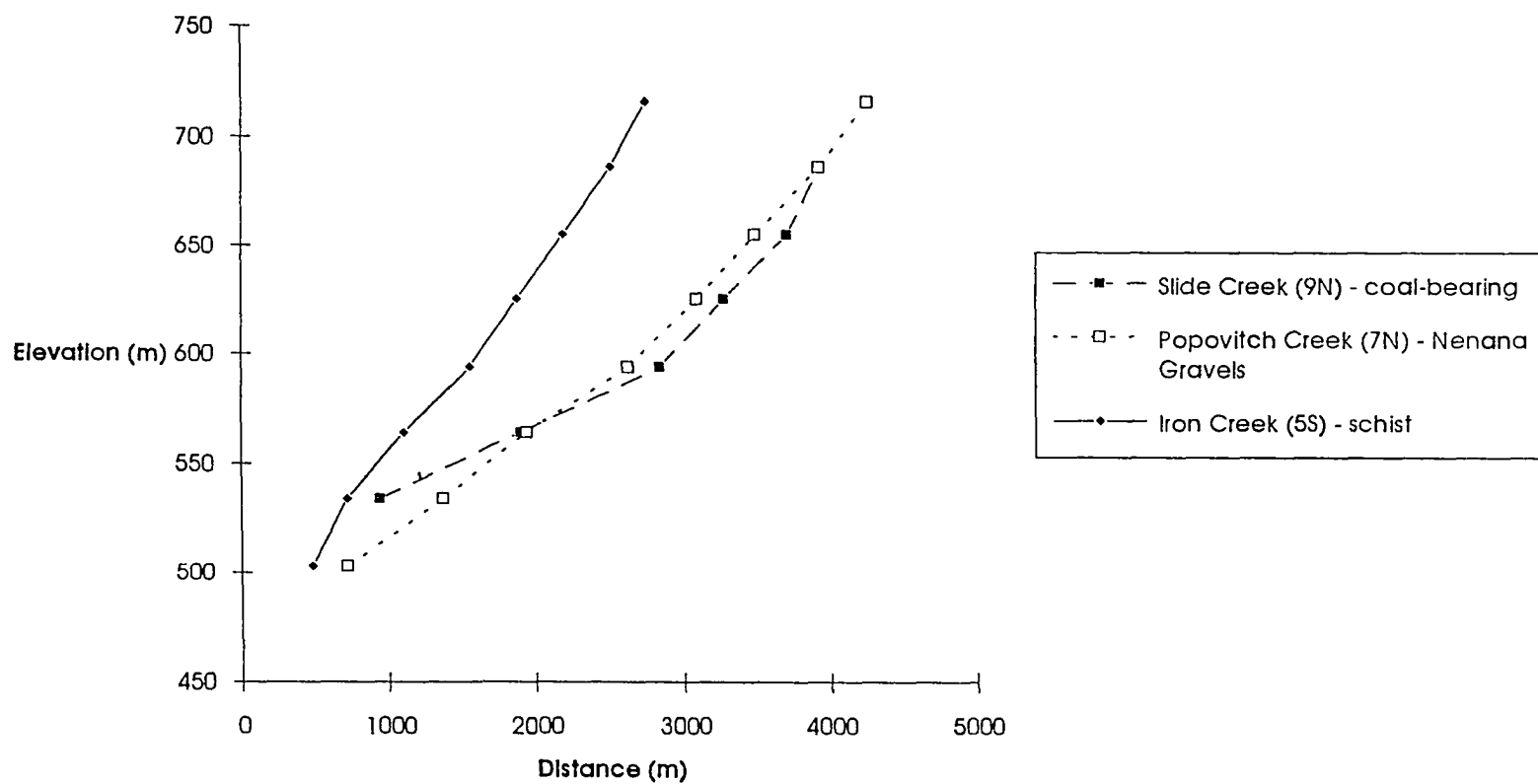


Figure 2.3-11. Representative stream profiles of creeks underlain by the three principal lithologies. Schist basins generally have steeper gradients than coal-bearing or gravel basins.

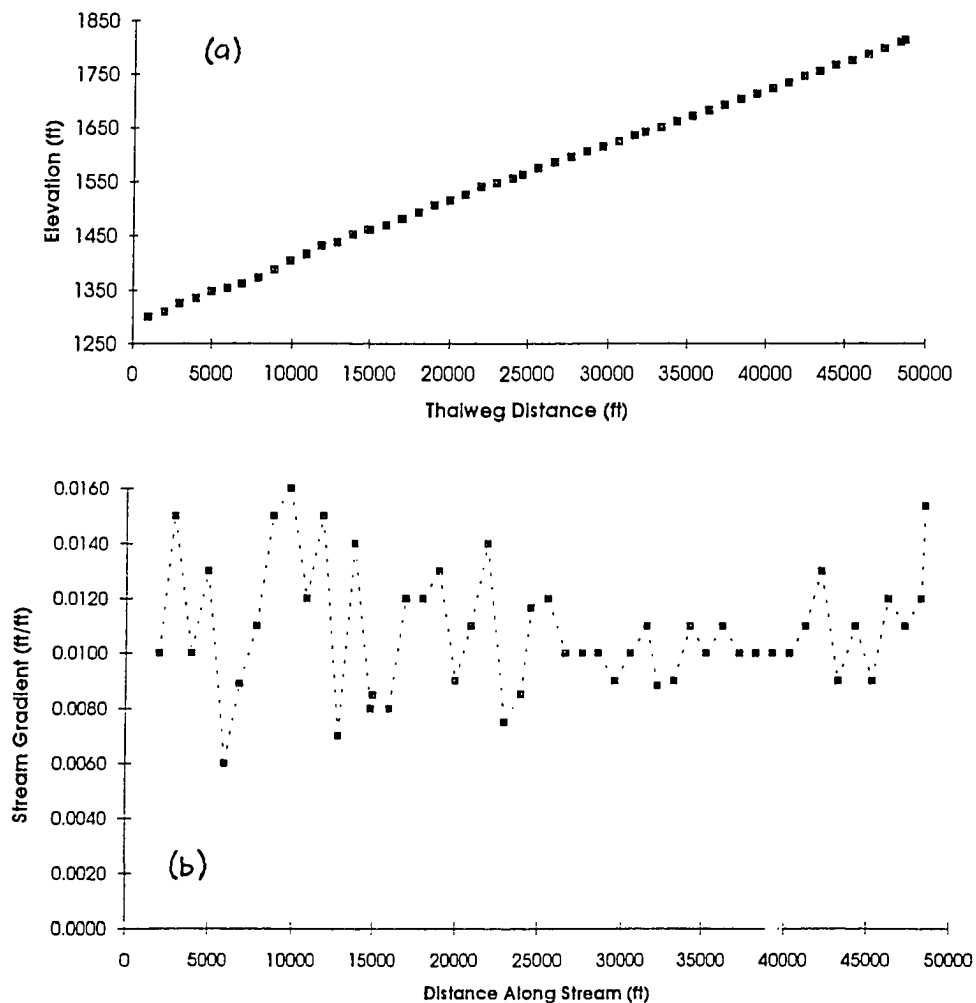


Figure 2.3-12. The actual and differential stream profiles of Hoseanna Creek. The actual (Figure 2.3-12a) and differential (Figure 2.3-12b) gradients are plotted with distance from the mouth of Hoseanna Creek. The average gradient for the main channel below approximately 25,000 ft from the mouth ranges from 6 to 16 ft per 1,000 ft, and the range is significantly greater than the range above 25,000 ft. The variations in average gradient are attributed to differences in erosion resistance and/or sediment production between north and south tributaries.

2.3.2 Structure

Three important structural elements in Hoseanna Creek Watershed control landscape development. The resistant but intensely deformed isoclinally folded metamorphic rocks provide the basement upon which at least two younger Late Tertiary fold and fault patterns have occurred. The regional structural grain of the Alaska Range and thus of the Nenana coal field trends predominantly east-west (Csejtsy and others, 1986; Wahrhaftig, 1970a-i).

Beginning about 8 to 10 million years ago and ending well before 2.8 million years ago (Wahrhaftig, 1987), the Tertiary formations were deformed into irregular box folds (including the westward-plunging Hoseanna Creek syncline in the lower valley, Figure 2.3-1) with 600 to 1800 m amplitudes and 8 to 16 km wavelengths, and steep locally faulted limbs (Wahrhaftig, 1970c). Approximately 2.8 million years ago (Wahrhaftig, 1987), the emplacement of Jumbo Dome to the north of the upper basin locally deformed the Tertiary strata into relatively tighter and steeper box folds and a number of short (< 2km) high angle horst-graben-type faults. Since then, faulting probably due to the continued rise of the Alaska Range has continued through the late Quaternary.

Thus, there are faults associated with the Hoseanna Creek syncline in the lower valley; there are faults related to the emplacement of Jumbo Dome 2.8 million years ago; and there is possibly a third set associated with late Quaternary deformation (i.e., the Poker Flats fault, Figure 2.3-1).

The Poker Flats fault is the large scissor-like high angle reverse fault with a maximum offset of more than 1000 m (south side down) that runs east-west closely parallel to the southern drainage divide in the southwest part of the basin (Figure 2.3-1). This fault has offset the Late Wisconsin Healy Glaciation terraces and has offset channels in the headwaters of Iron Creek (5S). The fault has uplifted Hoseanna Creek Watershed at its mouth causing incision, and has been accompanied by relative downdropping in upper basin causing filling in the main channel. An apparent hinge point of the scissor fault occurs in the vicinity of the fault along Mosquito Creek (Figure 2.3-1).

This east-west trending, north-dipping beds are conducive to landslide formation,

badland development and have enabled rapid erosion of the basin. Areas underlain by the coal-bearing formations are the lowest in elevation and form the axes of the basin. In the mid and upper valley, the Usibelli Group beds strike predominantly N70W and dip to the north 5-25° (Figure 2.3-1). West and downstream of a schist bedrock topographic high in the vicinity at 4S, Hoseanna Creek flows down the axis of a gently plunging syncline, so that from east to west the creek cuts through first the metamorphics, then Suntrana Formation and into Lignite Creek Formation before flowing out into the Nenana River Valley.

2.4 General Surface Processes - Geologic and Climatic Interactions

The east-west structural trend of the basin, the north-south distribution of geologic units, and the high latitude predisposed the proto-Hoseanna Creek Watershed to erosional processes unique to northern or southern aspects that eventually promoted the growth and development of valley asymmetry. The resultant north versus south differences between climatic and geomorphic processes, vegetation-types, cryogenic activity (Washburn, 1970), and hydrologic processes produced different north and south surface and subsurface fluvial and hillslope regimes.

2.4.1 North-South Valley Asymmetry and Permafrost

Photo-geologic analyses using the photos listed in Table 2.3-1 and field mapping conducted from 1985 through 1988, indicate that discontinuous patches of permafrost cover about 33% of the basin area (Figure 2.4-1). Almost all of the permafrost occurs on north-facing slopes in areas underlain by the metamorphics, with smaller areas of permafrost in sedimentary terrain. Road cuts and drill holes indicate that in most places the permafrost is relatively thin (< 20 m thick), but in a few places it may be as great as 40 m thick. From the few available temperature profiles (Golder 1985; field studies, 1987), most of the permafrost appears to be isothermal or nearly isothermal at around -1.0 to 0.0°C. Because it is thin and warm, some of the permafrost in the finer-grained materials may be readily susceptible to thermal erosion if disturbed.

Most of the north-facing schist terrain is in permafrost and is covered by stunted black spruce forest or a thin tundra mat susceptible to solifluction, frost heaving, frost boils and frost scarring. At higher elevations patterned ground, frost-heaved

2-41

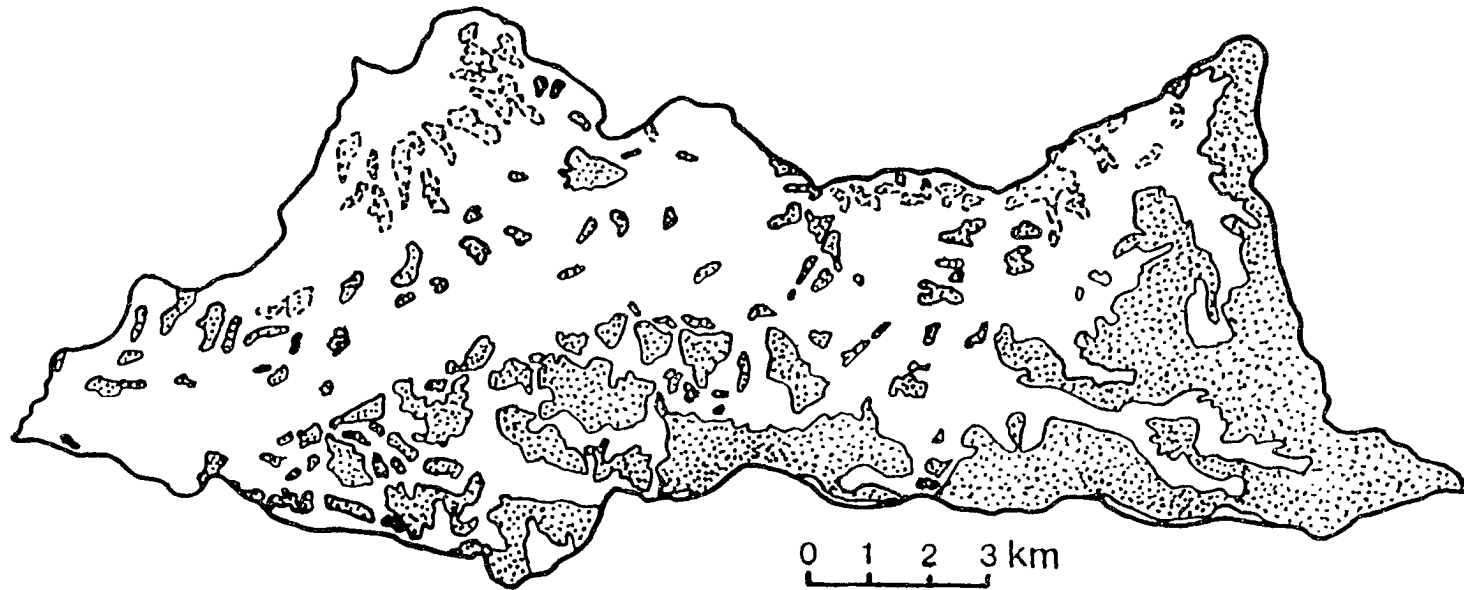


Figure 2.4-1. Permafrost map of Hoseanna Creek Watershed. Areas encircled by dashed lines indicate areas less certain of permafrost.

boulder fields, and frost shattered rubble is common. Field work indicates that storm infiltration capacity is low, supra-permafrost groundwater storage is minimal and interception and evapotranspiration are low (see Section 4.0). As a consequence, many of the basins draining the schist terrain exhibit very peaked hydrographs.

In contrast, south-facing slopes are underlain by weakly consolidated Tertiary sedimentary formations ranging from thick gravel Nenana Gravel to layered sand-silt-clay-coal of the Usibelli Group. Very little permafrost is evident, and the north-dipping sands and gravels are readily infiltrated. Perched groundwater in coal seams overlying clay aquitards may locally flow down dip to the north (and perhaps out of the basin and into the Marguerite Creek Watershed). In addition, the vegetation is more lush, allowing for more evapotranspiration and higher amounts of interception. These factors result in lower base flows and smaller peak discharges than those in the north flowing creeks.

2.4.2 Weathering Processes

The valley asymmetry has pronounced effects on physical weathering processes. The Usibelli Group is comprised of weakly consolidated sand-silt, clay and coal sequences that rapidly disaggregate in the cold climate. Due to the northern latitude, south-facing badlands experience many days of heightened freeze-thaw processes. Daily freeze-thaw cycles during fall, winter and spring cause grain-to-grain breakdown of the weakly consolidated sediments which then fall grain by grain or as large sloughed blocks and form poorly packed talus cones at the badland's base. The talus is readily saturated during spring break-up which leads to mudflows, debris flows, and super-concentrated transitional flows that are injected into the swollen high energy creeks.

In addition to freeze-thaw processes, the subarctic regime of Hoseanna Creek Watershed is characterized by typical cryogenic processes. In particular, the thermal erosion of permafrost appears to be critical. That is, the undercutting by streams, erodes the vegetative mat, and exposes the permafrost to thermal degradation; the thermal degradation works in an upslope and sideslope direction and allows the previously frozen substrate to erode. In addition, hydrologic processes undergo cyclical (seasonal) patterns of long winter dormancy and short

summertime activity, that separated by even quicker break-up and freeze-up transitions.

Although physical weathering processes appear dominant, some chemical weathering does occur. During freeze-up, some of the north-flowing creeks (in particular Iron Creek (5S) and Clinker Creek (9S) have been observed to increase their dissolved solids concentrations (predominantly an iron precipitate coloring the water very orange). This change in the chemical make-up of the water suggests that when the creek water temperature declines and concentrations of physical weathered material have been depleted, the role of chemical weathering may dominate in the schistose creeks.

2.4.3 Significant Erosional or Depositional Landforms

The interaction of climate and geology in the Hoseanna Creek Watershed has produced distinct landscape features that are closely associated with specific erosion processes. Such features are common throughout the Nenana coal field. The two landforms that are considerable sources of sediment (i.e., erode most rapidly) are the badlands and the landslides.

Landslides commonly form if strata dip toward a stream cut; Steep unvegetated cliffs or badlands may form where strata dip away from the stream cut. Both landforms are prolific sediment producers. About 5% of the area underlain by the Usibelli Group is exposed by these distinctive badlands, and over 9% is covered by landslide deposits.

2.4.3.1 Badlands

The badlands are intricately dissected gullies that occur in the Tertiary formations throughout the Nenana coal field. While each Tertiary lithology produces a distinctive badland form (i.e., textural properties reflected in density of spires, etc), all of the badlands can be described as very steep vegetationless cliffs with characteristic spires, re-entrants, and vertical walls.

Badlands are present throughout the basin in the Tertiary rocks, are most common along streamcourses, and total 3-6% of the Hoseanna Creek Watershed area.

Individual badlands can be very picturesque as they expose much of the layered sequences of the coal-bearing rocks (e.g., Popovitch Badlands - Figure 2.3-1), are up to 225 m in relief, and cover from a few square meters to as much as one square kilometer. Based on repeated photography over periods of 10 to 70 years (Wahrhaftig, 1987), and on measurements of the volume and frequency of debris flows (Wahrhaftig and Birman, 1954), the badlands have been estimated to erode at an average rate exceeding 1 cm/a.

The badlands are persistent landforms evidencing long-term high erosion rates. Because the Tertiary rocks are poorly consolidated they easily disintegrate in this climate. The badlands are initiated as (1) meander scars on the banks of streams, (2) as the headwalls of landslides, and (3) as nickpoints of rejuvenation in minor tributaries (Wahrhaftig, 1987). Vegetation is unable to stabilize the cliffs because erosion is too rapid. Once initiated, badlands erosion eats headward and laterally into cliffs progressively exposing more rock to breakdown and erosion.

Badlands erosion has an annual cycle, beginning in the late fall and winter with the ravelling of coarse clasts and detachment of sandstone slabs. The ravelling is due to the accumulation of ice veins behind the clasts and slabs during freezing followed by the thawing during warm sunny days. The clasts or slabs tumble to the base of the badlands, knocking others loose on their way, and accumulate in a single winter as thick talus cones, sometimes completely covering the floors of gullies or minor tributaries. Spring break-up or early summer high runoff events mobilize the talus, producing catastrophic debris flows that choke the minor tributary channels and are deposited as alluvial fans across larger tributaries or the main channel of Hoseanna Creek. The fans are cleared during highwater stages of the tributaries and Hoseanna Creek (Wahrhaftig, 1987).

The badlands are dynamically evolving landforms, with slopes steeper than the angle of repose. As the head of the badland erodes, it migrates uphill parallel to the slope. Eventually, the badland talus stabilizes when the gully or creek channel floors grow so wide that debris flows and high runoff events cannot remove all the talus. The stabilized talus begins to vegetate from the base in an upslope direction. Badlands in Hoseanna Creek Watershed have been persistent landforms throughout the Late Quaternary; many of the badlands have been rejuvenated by newly invigorated headward incision and/or lateral corrasion.

2.4.3.2 Landslides

Landslides are common in all parts of the watershed. Over 9% of the watershed is covered by landslide deposits which range in area from 0.002 to 0.6 km² (Figure 2.4-2). Much more of the watershed is covered by smaller sized deposits resulting from mass wasting. Over 76 slides (active and inactive) have been identified during field mapping and photogeologic studies. Almost all occur in the coal-bearing rocks. The schist comprises 26% of the watershed area, but only 1% of the schist area (or 0.3% of the total watershed area) is in slides (Figure 2.4-3). Similarly, the Nenana Gravel comprises 21% of the watershed's area, but only 0.8% of the Nenana Gravel area (0.2% of the total watershed area) is in slides. In contrast, the coal-bearing formations produce 98% of all the sliding. The Sanctuary Formation has 20% of its area in slide, the Suntrana Formation 10%, the Lignite Creek Formation 8%, and the Healy Creek Formation 5%. Because the Lignite Creek Formation and the Suntrana Formation cover the largest areas, they contribute to more than 69% of the sliding in the watershed. The strong lithologic control on sliding reflects the ubiquitous presence of clay-rich horizons in the Tertiary strata.

The tendency to failure in the coal-bearing strata is intrinsically related to the prevailing structure, and is catalyzed by undercutting streams and vigorous basin-wide headward incision. Many of the landslides slip or flow down bedding planes in the gently folded beds. The predominant north to northwest direction of landsliding is perpendicular to the regional strike of all the Tertiary beds, indicating the slides mainly move down dip (Figure 2.4-4). Landsliding is also facilitated by the presence of frozen bedrock in almost all of the slides that face north to northwest. Slide activity exposes the frozen ground to thermal erosion, which further increases the rate of sliding and sediment production.

Different clay mineralogic compositions within the Tertiary sequences (Triplehorn, 1976) may account for some of the variability in landslide susceptibility because the different the different clay minerals vary in plasticity, moisture content, swellability, and freezing point depression.

2-46

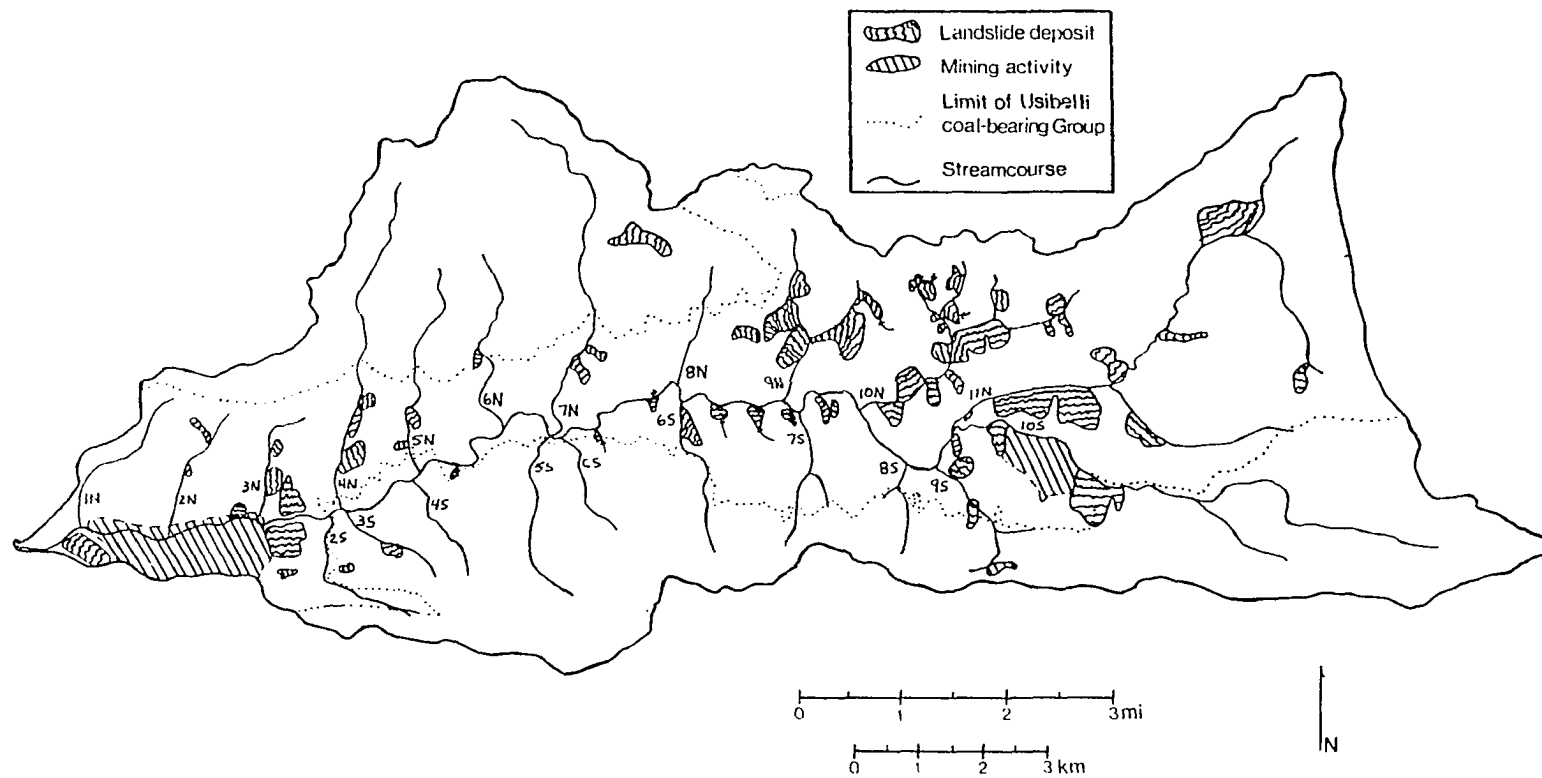


Figure 2.4-2. Landslide map of Hoseanna Creek Watershed.

2-47

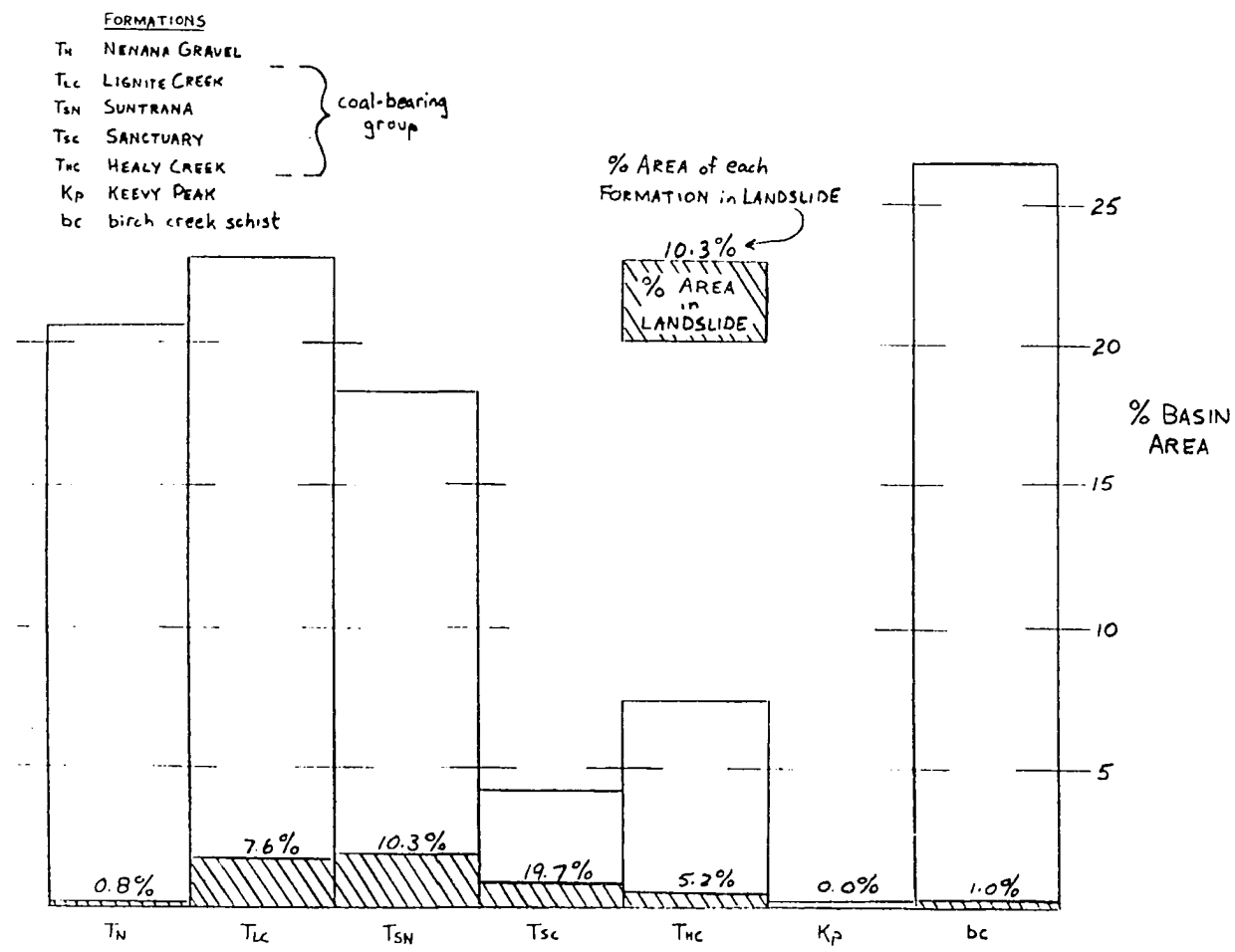


Figure 2.4-3. Lithologic control on the distribution of landslides.

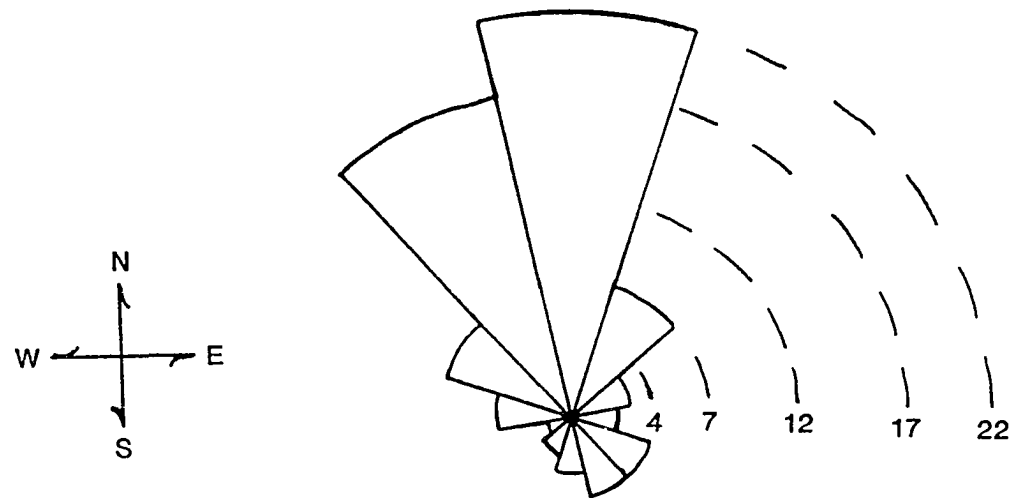


Figure 2.4-4. Diagram depicting the predominant northward direction of landslide movement.

2.5 Geologic History

Hoseanna Creek did not exist until after the Dry Creek or Lignite Creek Glaciation, and so all the surface morphology in the Hoseanna Creek Watershed is late Pleistocene or younger. However, several important events prior to the late Pleistocene and up through the late Wisconsin have influenced the way surface processes operate today: a) uplift of the Alaska Range to the south and of the proto-Hoseanna Creek Watershed accompanied with downcutting by the Nenana River, b) emplacement of Jumbo Dome to the north of the upper basin complicated the prevailing mildly folded structure, c) repeated glaciations within the Nenana River system, and d) continued late Quaternary tectonism. In general, tectonic episodes folded and faulted the strata, pre-disposing them to oversteepening and failure, while the tectonics and glaciations caused major changes in river and creek gradient.

2.5.1 Tertiary

The regional structure is a result of the late Cenozoic uplift of the Alaska Range. The late Miocene Grubstake Formation records the end of the early to mid Tertiary history of southward flowing streams that deposited the coal-bearing sedimentary sequences. The late Miocene to late Pliocene Nenana Gravel record the initiation of northward flowing drainages and the growth of the Alaska Range to the south. During this rise, the sedimentary formations in the proto-Hoseanna Creek Watershed and surrounding area were mildly deformed into east-west trending broad folds offset by short north-south trending high-angle normal and reverse faults (Wahrhaftig, 1970c,d).

Approximately 5.6 km north of the center of the upper watershed, the hornblende andesitic Jumbo Dome was emplaced approximately 2.7 million years ago (Wahrhaftig, 1987) and locally folded the Usibelli Group beds into shorter wavelength east-west folds with small amplitudes and produced a number of north-south trending normal faults.

2.5.2 Pleistocene

Pleistocene tectonism in the Nenana Valley and vicinity continued as evidenced by

offset drainages, and displaced and warped late Quaternary stream terraces (Thorson 1978), although the style of deformation appears to have changed from the broader folding in the late Tertiary and the emplacement tectonics associated with Jumbo Dome (Wahrhaftig, 1970j).

The Pleistocene uplift caused significant downcutting by the Nenana River and thus lowering in the relative elevation of the confluence of the Nenana River and Hoseanna Creek. This lowered local base level provided impetus for hillslope and fluvial dynamics. Superimposed on the tectonically induced downward trend were periods of river aggradation accompanying glaciation in the Nenana River Valley. Thus, Hoseanna Creek aggraded during glaciations and cut during interglaciations. Figure 2.3-5 and Table 2.3-2 summarize the more than 100 m of elevation change at the confluence of Hoseanna Creek and the Nenana River during the last approximately 200,000 years.

The rate of downcutting has not been constant (Thorson, 1978). Much of the more recent downcutting can be attributed to activity on the Poker Flats fault (Figure 2.3-1) which offsets early Wisconsin (Healy) outwash, and can be inferred to have moved between 25,000 and 10,000 years BP, based on the very rapid rate of downcutting during this time (Figure 2.3-5). Furthermore, downcutting of fluvial terraces was most rapid following deglaciation, and may have slowed during bedrock incision. In addition, because the onsets of glaciations are believed to be slower than retreat, the long-term aggradation rates of fluvial terraces are thought to be slower than the long-term local erosion rates (Ritter and Ten Brink, 1986).

The effect of the rising and falling Nenana River on local base levels throughout the late Quaternary has resulted in episodic cutting and filling of Hoseanna Creek to meet the changing grade. Filling episodes are recorded by stream terrace aggradation and alluvial fan growth (Figure 2.3-3). Creek grade responses occur first at the mouth where the changes occurred and then migrate headward. The rate of headward migration of cutting or filling is dependent on the amount of base level change and on rock/sediment resistance to incision. The response time in a given part of the basin is related to the distance downstream from the mouth (or the location of grade change).

Growth of alluvial fans records responses of upstream drainages to vigorous

headward erosion. Thus alluvial fan growth succeeds incision at the mouth and occurs during incision in the headwaters. This process of fan growth following incision has had several cycles within the Holocene; fan growth has occurred after aggradation associated with late Wisconsin glaciation and after the latest faulting at Poker Flat fault. In addition, there were no early Holocene deposits found in the watershed.

Prior to approximately 2170 years BP, the Nenana River had migrated eastward at the mouth of Hoseanna Creek and had incised the Usibelli Group; Hoseanna Creek was shortened and adjusted its grade by incising through its fan and also into bedrock. The increased gradient at the mouth increased the carrying capacity of Hoseanna Creek and caused the creek to rejuvenate eastward stepping incision into the upper part of the watershed. Hoseanna Creek incised rapidly headward through stream deposits, less rapidly through the coal bearing group, and relatively slowly through the metamorphic rocks. As the incision worked its way headward, gradients of tributary streams (i.e., Badlands Creek and Popovitch Creek) were also increased, and they incised headward. The headward incision intensified hillslope failures and landslide formation and increased erosion and sediment delivery to the mouths of the tributaries and to the mouth of Hoseanna Creek. The increased sediment production supplied enough material to build the Hoseanna Creek fan and possibly force the Nenana River westward. Growth of the Hoseanna Creek fan lasted until about 1000 years ago. Shortly before 1000 years ago, the Nenana River began migrating eastward into the Hoseanna Creek fan and Hoseanna Creek began cutting through its fan.

When the Hoseanna Creek fan first prograded westward, the lower reaches of Hoseanna Creek adjusted first by aggrading thus reducing the gradient of the main channel. The reduced gradient caused by the 1000-2000 year old westward fan progradation caused tributary fans to build into the main channel. This took place at Badlands Creek about 600 yrs ago and at Popovitch Creek about 400 years ago. Later, the incision initiated at the mouth of Hoseanna Creek 1000 years ago migrated headward causing dissection of both fans within the last hundred years.

3.0 LANDSLIDE MOVEMENT and EVOLUTION in DISCONTINUOUS PERMAFROST

3.1 Introduction

3.1.1 Purpose

The purpose of this section is to present the results of a 4-year study of landslide movement from seven different landslides within Hoseanna Creek Watershed. The short-term movement histories are related to landslide geomorphology, geologic controls and climatic processes. The timing and magnitude of displacement processes determined from survey data are related to the mechanics of sliding and provide the basis for quantifying process rates. From these observations and measurements a general picture of landslide evolution is described, which is then used to link landslide processes and their contribution to the sediment transfer processes described in Section 4.0.

3.1.2 Background

Terzaghi (1950) compiled a comprehensive treatise on landslide types and mechanisms; his work is still a fundamental resource for both engineers and earth scientists. Probably the most useful and complete classification of mass movements was compiled by Varnes (1978), who describes translational slides, block slides, rotational slides, lateral spreads, and earthflows. Similar classification schemes but emphasizing either mechanism or material are presented by Nemcok and others (1972), Zaruba (1969), Coates (1977) and Campbell and others (1985). An earlier general summary of mass movements was written by Sharpe (1938) for landslides in soil and rock. Studies of particular forms of mass movements have been provided by Keefer and Johnson (1983) for earthflows, Hutchinson and Bhandari (1971) and Brunsden (1984) for mudslides, Campbell (1975) on soil slips and debris flows, Johnson and Radine (1984) on debris flows, Fisher (1971) and Middleton and Hampton (1973) for sediment gravity flows. In addition, Zaruba (1952) and Nemcok (1972) have published comprehensive studies of mass movements in subarctic or arctic environments.

The nomenclature for the description of landslide terrain and processes used here follows that of Cruden (1990), "Suggested Nomenclature for Landslides," while the

technical terms for landslide names referred to here follow the classification scheme described by Varnes (1978). His classification and nomenclature are presented in Table 3.3-1. The classes of slope movements give primary consideration to the type of movement and secondary consideration to the type of material. The nomenclature uses compound names referenced to a mechanism for downslope movement and the kind of material that the moving mass comprises (e.g., translational earth block slide).

Because of the predominance of fine-grained materials in the Usibelli Group, and for the slides studied in detail for this report generally only earth slumps, earth slides, earth spreads, earthflows and complex forms are relevant. Earth slides are either rotational or translational. In the case of translational earth movements, a detached mass remains in constant sliding contact with underlying stable slope materials; shearing movement takes place along this surface. The detached moving mass may break up into a few or many discrete subunits depending on the rate of motion, the characteristics of the basal slip surface, the shearing material, and the moving mass (Varnes, 1978).

Rotational slides within Hoseanna Creek Watershed occur along concave upward, curved, ruptured surfaces which impart a backward tilt to the moving mass. Typically the rupture surfaces are oblique or perpendicular to the strike of competent sandstone and coal beds and may follow pre-existing faults or fracture patterns (Varnes, 1978). Translational slides in Hoseanna Creek Watershed occur along planar or undulatory surfaces and most commonly follow pre-existing discontinuities such as coal-clay interfaces, silt-clay interfaces, bedding planes within thick clay units or the bedrock-regolith interface. The amount of disruption of the moving mass is a function of the degree by which the rupture surface departs from planarity (e.g., a wide shear zone within a thick clay horizon) and the distance the mass has moved (Campbell and others, 1985).

Lateral earth spreads within Hoseanna Creek Watershed are gently dipping translational displacements that result in the overall extension (or spreading) of detached, coherent masses, which move divergently toward a free face on a basal shear surface or on subjacent material that deforms by plastic flow (Campbell and others, 1985).

Table 3.1-1. Classification of slope movements from Varnes (1978).

Type of Movement			Type of Material		
			Bedrock	Engineering Soils	
				Predominantly Coarse	Predominantly Fine
Falls			Rock fall	Debris fall	Earth fall
Topples			Rock topple	Debris topple	Earth topple
Slides	Rotational	Few Units	Rock slump	Debris slump	Earth slump
	Translational	----- Many Units	Rock block slide	Debris block slide	Earth block slide
			Rock slide	Debris slide	Earth slide
Lateral Spreads			Rock spread	Debris spread	Earth spread
Flows			Rock flow (deep creep)	Debris flow (soil creep)	Earth flow (soil creep)
Complex			combination of two or more principal types of movement		

Earthflows in Hoseanna Creek Watershed are moving masses of jumbled fine sands, silt and clay that have internal differential movements distributed throughout the mass of the slide. The differential movements can be intergranular or may take place on closely-spaced shear surfaces, some of which may be short-lived and heal without leaving evidence of movement (Keefer and Johnson, 1983). Observational evidence from earthflows in Hoseanna Creek Watershed indicate that immediately after significant horizontal displacement, the upper reaches of the landslides just below the headwall are covered by a field of extension cracks, the foot areas are compressed into furrows and ridges, and the moving masses are usually bounded by visible shear surfaces.

Complex slides exhibit more than one major mode of movement. Nearly all landslides are complex to some degree, so the term complex is not often used to

name a slide class (Campbell and others, 1985). Different parts of the landslide will move by flowing and sliding, or a single mass may move by toppling, sliding and flowing in sequence. The class used here reflects the dominant material and mechanism.

Typical displacement rates quoted for landslides (after Campbell and others, 1985) are as follows:

Extremely rapid	> 3 m/sec
Very rapid	0.3 m/min to 3 m/sec
Rapid	1.5 m/day to 0.3 m/min
Moderate	1.5 m/mo to 1.5 m/day
Slow	1.5 m/yr to 1.5 m/mo
Very slow	0.06 m/yr to 1.5 m/yr
Extremely slow	< 0.06 m/yr

However, the rates cited here cannot be used to estimate longer term averages. The displacement rates of landslides with non-steady motion cited by Campbell and others (1985) (e.g., earthflow displacements) are maximum rates achieved (during the slide history) and require continued observation before, during, and after the event, and therefore cannot be directly compared to the slower rates for landslides with more steady motion (e.g., block slides). The survey data collected for this study was used to discern annual movement histories and estimate long-term rates from cumulative horizontal displacements. In this section, all the landslide displacement rates are measured over a similar time scale, and therefore displacement rates for all types are readily compared.

Active landslides are defined as those with known current movement with defined limits such as a headscarp, and lateral and toe boundaries. Active landslides are typically non-vegetated over some or most of the landslide area, and have younger and early ecensis trees such as willows and alders, and spruce saplings; many of the trees are tilted. Inactive landslides are defined as those with lateral, toe and head boundaries that are covered with stable mature trees (forest) and with no known historical record of movement.

Landslides are very widespread in Hoseanna Creek Watershed (Figure 2.4-2) and

occurs as four different types (after Varnes, 1978): a) translational slides (from block to disrupted) which creep parallel to sedimentary bedding planes, normally on clay horizons; b) earthflows, which may flow down dip or directly downhill across bedding; c) rotational slump blocks, which occur where sedimentary bedding planes and topography do not favor translational slide development; and d) spreads. All of the larger landslides are complex and exhibit characteristics of more than one type. Many other forms of mass wasting occur within Hoseanna Creek Watershed, including mudflows, debris flows, smaller skin failures (soil slips), solifluction, rock avalanching, cliff toppling, and frost (mud) boils. These landforms and processes are not directly addressed in this report.

3.1.3 Geologic Conditions Conducive to Landslide Formation

Significant hillslope failures are almost entirely confined to terrain underlain by the Tertiary Usibelli Group. In general, gently to moderately dipping, weakly consolidated sand, silt, clay and coal sequences have been undermined by rapid headward incision of the drainage network. Typically, bedding planes dip 5-25 degrees to the north so that there are many north-facing slopes which are conducive to permafrost formation in the subarctic climate. Once exposed or disturbed the permafrost terrain is susceptible to accelerated degradation (e.g., thermal erosion) which can initiate hillslope failures. Most of the landslides move downhill on north-facing oversteepened slopes parallel to bedding planes (Figure 2.4-4), and commonly on clay horizons.

3.2 Methods

A photo-geologic reconnaissance for landslides within the Hoseanna Creek Watershed was performed using Usibelli Coal Mine photos from 1974 and 1984 of a scale of 1:12,000 (see Table 2.3-1). Seven different landslides (Figure 3.2-1 and Table 3.2-1) of varying type and size and apparently different stages of activity were chosen for monitoring of movement beginning in August 1985. On each slide, 1.2 m wooden laths were staked in representative portions of the slide and then surveyed in with a precision of ± 0.03 meters using an infrared electronic distance metering (EDM) theodolite. All survey points were re-measured (if they still existed) during the summers of 1986, 1987, and 1988. Additional locations were established on some slides to increase spatial coverage on the more active

3-6

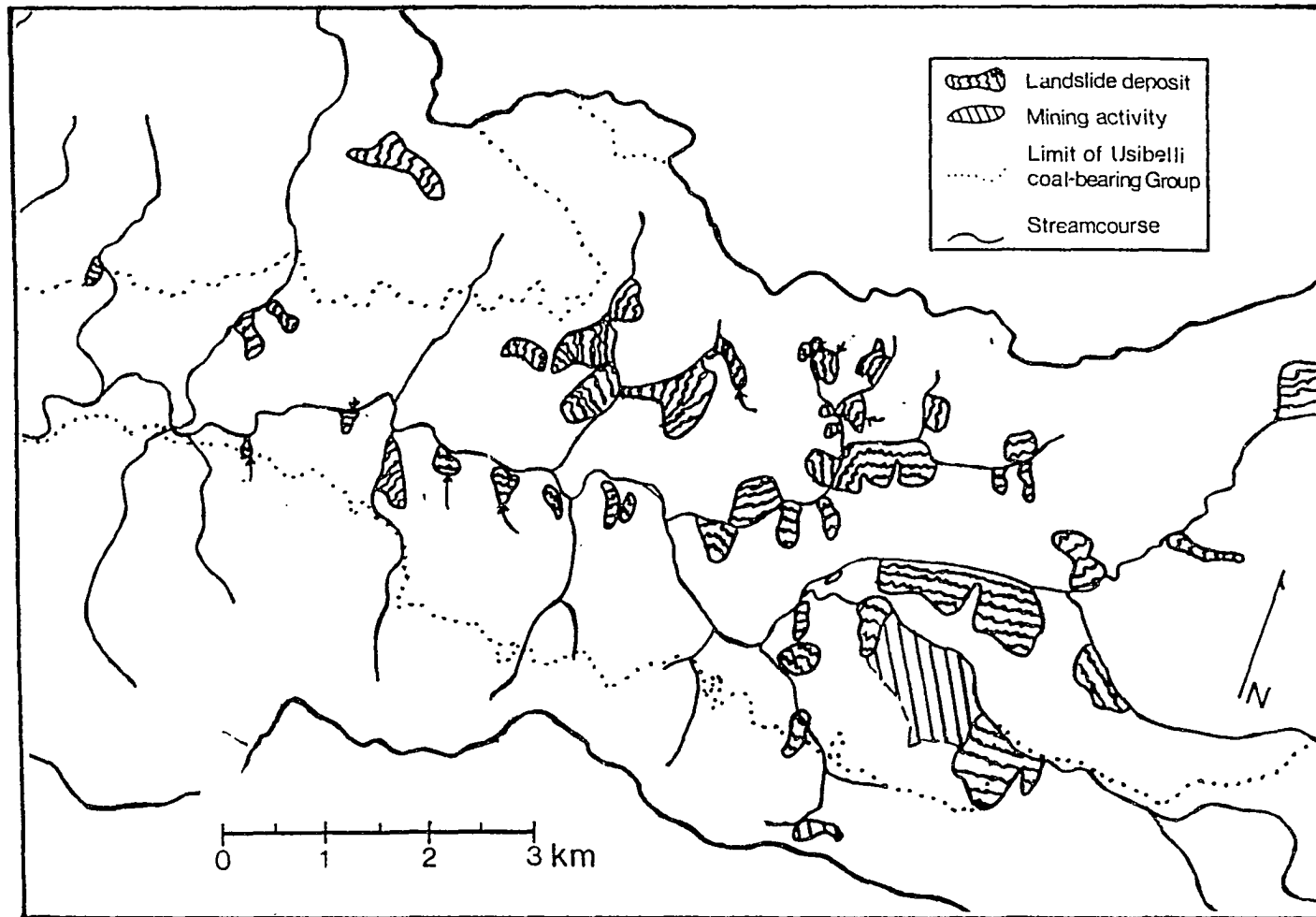


Figure 3.2-1. Location of surveyed slides. The seven surveyed slides are shown with respect to the Hoseanna Creek Watershed drainage network and other important geographic locations.

slides. Some slides were visited several times throughout the year to determine the time of year when most or all of the movement was occurring.

Terms used to describe landslide movement are defined as follows:

horizontal displacement (HD): the difference in horizontal distance between successive measurements

$$HD = (\Delta N^2 + \Delta E^2)^{1/2},$$

where N and E are the surveyed coordinates for northing and easting;

vertical displacement (VD): the difference in vertical distance (elevation) between successive measurements

$$VD = \Delta Z,$$

where Z is the surveyed elevation;

horizontal displacement rate (HDR) = HD/t, where t is the time interval (in years) between successive measurements;

vertical displacement rate (VDR) = VD/t.

cumulative horizontal displacement (CHD) = $[(N_i - N_f)^2 + (E_i - E_f)^2]^{1/2}$

where i = the initial survey coordinate, and f = the final survey coordinate.

cumulative vertical displacement (CVD) = $Z_i - Z_f$

cumulative horizontal displacement rate (CHDR) = CHD/T, where $T = \Sigma (t_1 + t_2 + \dots t_n)$

cumulative vertical displacement rate (CVDR) = CVD/T.

average CHDR (average displacements across a slide section) = $1/n(CHDR_{s_1} + CHDR_{s_2} + \dots CHDR_{s_n})$,

where s_1 , s_2 and s_n are stake numbers, and n is the number of stakes in a slide section.

$$\text{average CVDR} = 1/n(\text{CVDR}_{s1} + \text{CVDR}_{s2} + \dots \text{CVDR}_{sn})$$

In general, the error in HD and VD is a function of the slope distance between the theodolite and the prism (survey stake) and is affected by natural variance and operational errors. Natural variance might be a poorly defined ground surface such as tundra with an expandable soft mat or a surface that has experienced erosion or deposition at the stake. Operational errors occur in leveling the prism with a handheld bubble level, not setting the prism in the exact same location every time, and destruction or repositioning of the stake by natural forces (animals, snowpack, freeze-thaw, and erosion and deposition). The most accurate values were obtained in slides with a closer (smaller) survey network (LI and LV), and the least accurate for slides with the long distance survey network (LVI and LVII). In general, error for all the slides is estimated at $< \pm 0.05$ m for HD, and $< \pm 0.03$ m for VD. Data from the EDM theodolite are very accurate and precise for point (stake) data. However, the point data are assumed to represent the near vicinity of the slide mass in depth and breadth, and thus the stake displacements are extrapolated into areas without survey data. This assumption is generally supported by observation; nevertheless, in some cases, skin failures occurred, so that the stake data does not always reflect the slide mass in terms of depth, but does reflect the process of erosion of the slide mass.

A detailed photo-geologic analysis of each slide was done to determine historic changes. Vertical air photos of the Hoseanna Creek Watershed area are available at three scales (1:65,500, 1:43,800 and 1:12,000) for the following years: 1949, 1968, 1974, 1978, 1981, and 1984 (Table 2.3-1). In addition, 1:2,400 scale topographic maps with 5 ft contour intervals were made from the 1974 photography. From each photo year, area and length were determined for each slide and surface conditions were described that indicated slide activity.

Table 3.2-1. Descriptions of Monitored Slides

Slide	Type (after Varnes, 1978)	Area (X 10 ³ m ²)	Geology (after Wahrhaftig 1970)	Composition (in order of predominance)	Attitude of Bedrock	General Flow- Slide Direction	Avg. Pre- slide Slope ^c	Permafrost Present?	Surficial conditions
LI	slump/earthflow	7.5 ^a	Suntrana	fine sands, silts, clay, coal fragments	N70E 12-15N	N20W	17	at scarp	young tilted trees at toe only, mostly unvegetated
LII	disrupted translational	40.5 ^a	Suntrana/ Sanctuary	clay, silt	E-W 12-14N	N	16	at scarp	old tilted stand mixed with saplings, mostly
LIII	disrupted translational	40.0 ^a	Suntrana/ Sanctuary	clay, silt	E-W 12-15N	N10E	14	at scarp	old tilted stand mixed with saplings, mostly
LIV	earthflow	59.5 ^b	Lignite Creek	silts, clay, fine sands, coal fragments	N70E 6-10N	N35W	10	possibly along east scarp wall	almost all exposed, grassy in toe areas

LV	translational earth block slide	9.9 ^a	Healy Creek/ schist	coarse-medium sands, clay	N80E 10-15N	N20W	20	at scarp	all exposed except for tilted young trees at toe
LVI	rotational block slide with mudflows	70.0 ^b	Lignite Creek	fine sands, silt, coal fragments	N70E 6-7N	W	27	not observed	mixed forest with open unvegetated areas
LVII	disrupted block slide/lateral earth spread	52.5 ^b	Lignite Creek	sands, clay, coal fragments	N70E 6-10N	N40W	16	not observed	scattered young and old stands throughout mid portions, grass and tilted willows at toe

a) area based on 1984 air photos

b) area based on 1981 air photos

c) slope estimated from base map made from 1974 air photos

In addition to the survey program, an on-site geologic and geomorphologic description of each slide's terrain was made. The field studies documented principle lithologies, attitudes of sedimentary bedding planes, surface features such as shear zones, crevasses, compressional ridges and furrows, scarp heights, and characterized permafrost, if present. The relationship with other dated geomorphic surfaces (Section 2.3.1.4) such as adjacent stream terraces, was also described.

One of the primary objectives of this study was to quantify the annual displacement rates among the different types of slides within Hoseanna Creek Watershed to provide an analog for slides in other subarctic terrains, in particular the Nenana coal field. Thus, the frequency of surveying at each slide was designed to investigate processes that might be observable in other areas on an annual time scale; thus, short term mechanisms (i.e., during maximum displacements lasting hours to days) were not directly investigated.

Observational and process descriptions were combined. The survey data are enhanced with field descriptions, and thus give meaning to the vector data, while air-photo analyses put the short-term survey data into a longer-term perspective. Even though a variety of slides over a broad area of Hoseanna Creek Watershed was studied, there were limitations to the use of surveying techniques employed here: 1) the temporal and spatial coverage per slide was limited, 2) most of the slides are very large and detailed surveying requires a long time to cover large areas, 3) since all of a given slide could not be covered, only a representative location for survey stakes could be established.

3.3 Results

3.3.1 Descriptions and Summary of Movement Studies

3.3.1.1 Landslide I

Landslide I (LI) is a relatively narrow and long (160 m along the direction of movement) earthflow covering an area of approximately 7,500 m² (Table 3.2-1); it is located at an elevation range of 503 m (1649 ft) to 549 m (1797 ft) above mean sea level (m.s.l.) in mid valley on the south side of Hoseanna Creek between creeks 6S and CS (Figure 3.2-1). Hoseanna Creek flows through a narrow channel as it corrades the toe of the slide.

The slide occurs within the Suntrana Formation below the #1 coal seam just above the contact with the Sanctuary Formation (Figure 3.3-1). Sand, coal and clay form a dipslope, with dips approximately 12-15° N and strikes N70E. The pre-slide topographic slope is estimated to have been 17°, which is greater than the dip, and presents an unstable configuration. The surrounding undisturbed surface is poorly drained and vegetated with a stunted black spruce-*Sphagnum* community, suggesting the presence of permafrost. At the headscarp, characteristics such as thawing clay that releases water, ice lenses and ice blebs contained in the fine-grained material indicate the presence of permafrost. Vegetation on the slide is absent, except in the foot area, which is covered by young (less than 25 years old) willows and alders and some tilted black spruce remnant stands. The surface of the upper and mid sections of the slide are strewn with aggregate blocks of fine sand, silt, clay and coal fragments. In addition, the surface of the unvegetated mid section is covered by small undulating furrows and ridges.

Sometime prior to 1949 (but after formation of the 70 to 170 year-old terrace across the creek), Hoseanna Creek migrated southward against the base of the slope; lateral corrasion oversteepened the slope and exposed the clayey permafrost to thermal degradation resulting in incipient translational block failure. By 1949, continued headward enlargement, possibly due to thermal erosion, accompanied by toe extension into Hoseanna Creek produced a relatively small slide of approximately 4,000 m² and 80 m long (Tables 3.3-1 and 3.3-2). By 1968 the slide had not grown significantly larger, but extended another 40 m into the valley

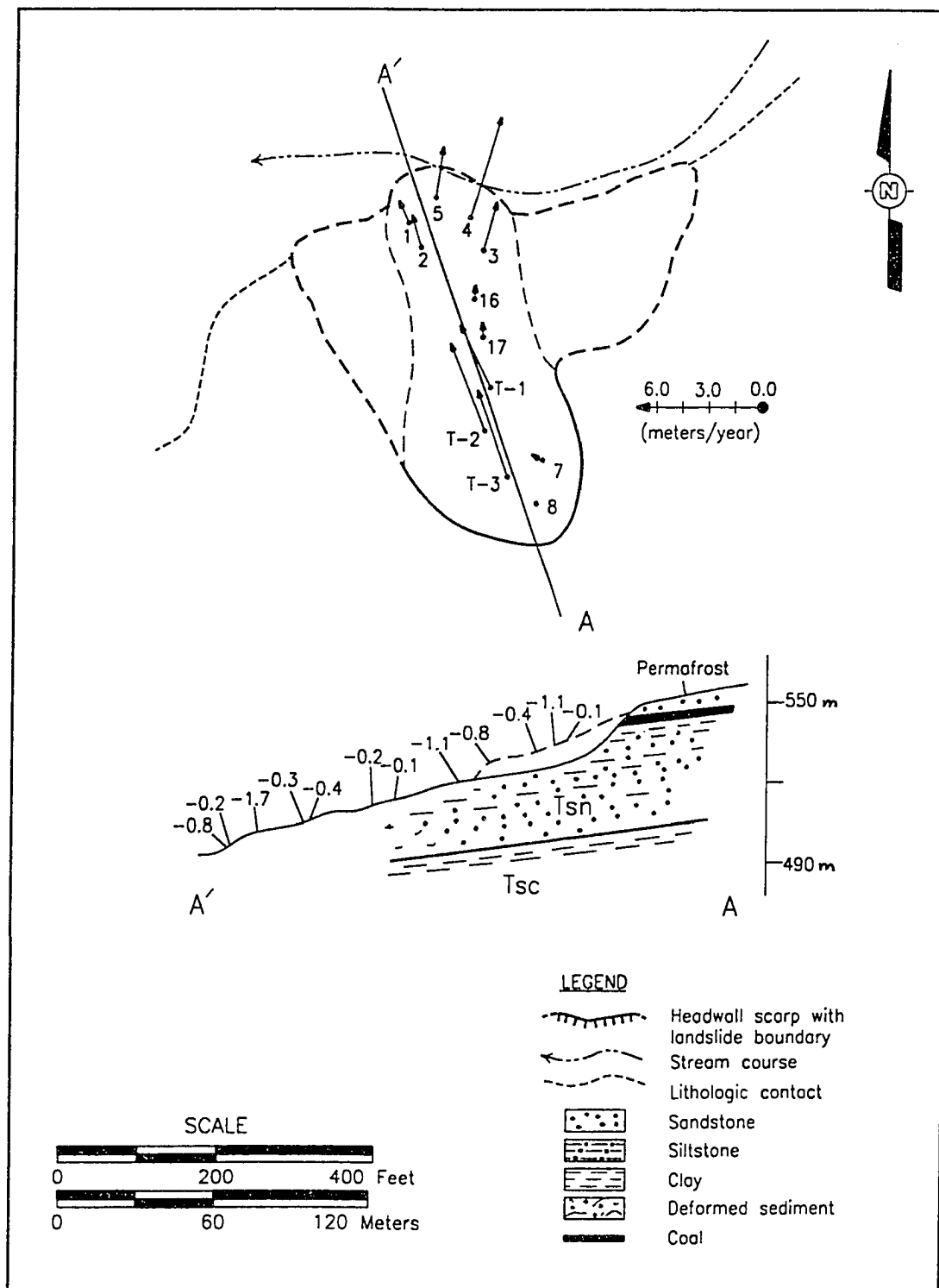


Figure 3.3-1. Geologic cross section and plan view of LI.

Table 3.3-1. Changes in average maximum slide lengths 1949 through 1987. Measured lengths (meters) are based on air photo analyses and field surveys.

Slide	1949	1968	1974	1981	1984	1987
I	80	120	140		160	160?
II	120	140	170		190	205
III	230	250	280		280	280
IV	240	300	370	455		500
V	100	140	165		150	150
VI	120	150	180	180		180?
VII	240	240	360	360		?

Table 3.3-2. Changes in average maximum slide areas from 1949 through 1984. Measured areas ($\times 10^3 \text{ m}^2$) are based on air photo analyses and field surveys.

Slide	1949	1968	1974	1981	1984
I	4.0	3.8	5.1		7.5
II	24.8	30.5	34.5		40.5
III	17.2	30.7	39.8		40.0
IV	14.0	24.5	30.5	59.5	
V	3.0	8.9	9.0		9.9
VI	27.5	67.3	72.5	70.0	
VII	23.5	37.5	52.5	52.5	

Table 3.3-3. Summary of Movement for LI.

Slide Section	Period of Record		Stake	CHD (m)	CHDR (m/yr)	Direction	CVD (m)	CVDR (m/yr)	CVD/C HD
Foot	8/19/85	10/8/88	1	4.11	1.31	N26W	-0.52	-0.17	-0.13
	8/19/85	10/8/88	2	5.73	1.82	N17W	-1.01	-0.32	-0.18
	8/19/85	10/8/88	3	8.49	2.70	N16E	-1.40	-0.44	-0.16
	8/19/85	4/5/87	4A	6.12	3.76	N14E	-0.60	-0.37	-0.10
	8/31/87	10/8/88	4B	6.33	2.02	N21E	-4.23	-1.34	-0.67*
	8/31/87	10/8/88	4C	0.61	0.19	N15E	-0.13	-0.04	-0.22
	8/19/85	4/5/87	5A	3.66	2.24	N4E	-0.54	-0.34	-0.15
	8/31/87	10/8/88	5B	1.89	0.60	N12E	-1.41	-0.45	-0.75*
	8/31/87	10/8/88	5C	0.42	0.13	N5E	-0.06	-0.02	-0.14
Upper Block	7/18/86	5/1/88	7	1.04	0.38	N69W	-1.20	-0.44	-1.15
	7/18/86	5/1/88	8	0.38	0.14	N13W	-0.19	-0.07	-0.50
Mid Section	7/18/86	10/8/88	6	0.96	0.30	N1E	-0.36	-0.12	-0.38
	7/18/86	10/8/88	16	2.22	0.71	N5E	-0.72	-0.23	-0.32
	7/18/86	10/8/88	17	2.52	0.80	N4W	-0.41	-0.13	-0.16
	7/18/86	10/8/88	18	1.32	0.42	N9W	-0.23	-0.07	-0.17
LI Upper Basin	5/1/88	10/8/88	T1	1.69	3.84	N26W	-0.50	-1.14	-0.297
	5/1/88	10/8/88	T2	2.27	5.17	N22W	-0.36	-0.82	-0.159
	5/1/88	10/8/88	T3	2.21	5.04	N20W	-0.47	-1.08	-0.214

*Skin Failure

bottom, forcing the creek into a much narrower channel. By 1974, the slide had grown to 5,100 m² and 140 m long, and exhibited both disrupted translational block slide (e.g., detached vegetated coherent blocks) and earthflow characteristics (e.g., bulbous nose). The continued northward movement into the mainchannel of Hoseanna Creek forced the creek to corrade to the north into the late Holocene stream terrace. From 1974 to 1984, the slide continued to expand headward and toward and had reached a size of 7,500 m² and 160 m long.

When the slide was first visited in August 1985, Hoseanna Creek flowed through a narrow channel approximately 12 m (40 ft) meters wide, which during the time of the monitoring period, was the narrowest part of the main creek downstream of the

confluence of Sanderson (10S) and Upper Hoseanna Creeks (11N). Survey stakes were placed across the foot and mid section of the slide and their positions recorded. In the following years 13 more stakes were added to an upper block, and upper, mid and foot sections (Table 3.3-3 and Figure 3-3.1), as the slide continued moving farther into the main channel of Hoseanna Creek. Two of the foot stakes were lost to the creek (LI-4A and LI-5A) as continued lateral corrosion removed toe material including the stakes.

The foot section had the most extensive survey coverage, both in time (8/19/85 to 10/8/88) and space (10 stakes), while the upper basin was staked and surveyed only during the last year. All sections of the slide experienced significant movement. The upper basin area and foot areas had the highest CHDR's and CVDR's, while the upper block had the lowest CHDR's and CVDR's. CHDR's in the foot area ranged from 0.13 to 3.76 m/yr, but the stakes were not all in place for the same duration; stakes surveyed for the entire period averaged 1.3 to 2.7 m/yr. CHDR's in the upper basin were relatively high (3.8 to 5.2 m/yr), but these rates do not include a winter; if winter time was included in the rate calculations, then the rates would drop off to 1.5-2.1 m/yr; therefore, estimates of average CHDR for the upper basin, mid section, and foot areas are 1.8, 0.6 and 1.5 m/yr, respectively. These rates indicate extension in the upper basin and foot areas and compression in the mid section.

The predominant direction of movement in the upper block, upper basin and mid section was to the NW and fairly uniform, while movement in the foot area was to the NE and divergent (Figure 3.3-1). CVD/CHD's (excluding skin failures) were greatest in the upper block and ranged from -0.5 to -1.2, indicating predominantly downward movement. CVD/CHD's were lowest in the foot area and ranged from -0.1 to -0.2; these values indicate fairly low-angle deformation (basal shearing) typical of earthflows.

Due to the intrusion of the slide into the main creek channel, the geohydrologic and regimes of the creek, landslide and displacement mechanisms are closely linked. Aufeis build-up during the winter dams the slide toe and stabilizes foot activity; movement cannot resume until the ice dam has been removed. Depending on the amount of snowmelt, the slide may store water, and the piezometric surface may rise within the slide to meet the aufeis level. If break-up is rapid and water

production from snow melt is high, pronounced movement during spring can occur.

3.3.1.2 Landslide II

Landslide II (LII) is a wide parabolically-shaped disrupted translational slide approximately 40,500 m² in area and 205 m long (Table 3.2-1); it is located at an elevation range of 515 m (1689 ft) to 565 m (1855 ft) above m.s.l. in mid valley on the south side of Hoseanna Creek between creeks 6S and ES (Figure 3.1-1). The main Hoseanna Creek channel lies just to the north of the slide toe. During the monitoring period, only the east portion of the slide toe appeared to be corraded by streamflows. The slide appears to have been recently activated, just prior to 1949, based on the study of 1949 photos.

The slide occurs in the vicinity of the contact with the base of the Suntrana Formation and the upper part of the Sanctuary Formation (Figure 3.3-2). Dipslope sand and clay bedding dips approximately 12-14° N, with an E-W strike. The pre-slide topographic slope is estimated at approximately 16°, which is greater than the dip and thus presents an unstable configuration. The surrounding undisturbed surface is vegetated with a stunted black spruce-*Sphagnum* community, suggesting the presence of permafrost; during the summer surveys, small ice lenses and ice blebs were observed within the fine-grained sedimentary material exposed at the headscarp. Vegetation was absent on the slide in the upper section at the base of the headscarp, indicating renewed headscarp enlargement or recent mid slide movement. Most of the slide surface was covered with tilted willows, alders and some spruce. The distribution and orientation of the willows and alders indicate recent disturbances; tilted spruce occur on remnants of coherent blocks of the former stable slope.

Prior to 1949 (and most likely after the formation of the ≤ 150-year old stream terrace opposite the slide), Hoseanna Creek migrated southward against the base of the slope; lateral corrasion oversteepened the slope and exposed the clayey permafrost to thermal degradation, producing incipient translational block failure. By 1949, the slide mass was approximately 24,800 m² and 120 m long (Tables 3.3-1 and 3.3-2) and appeared somewhat stable as indicated by significant growth of vegetation. However, during the next 35 years translational slide movement had resumed, and the slide experienced continued steady growth in area and length. By

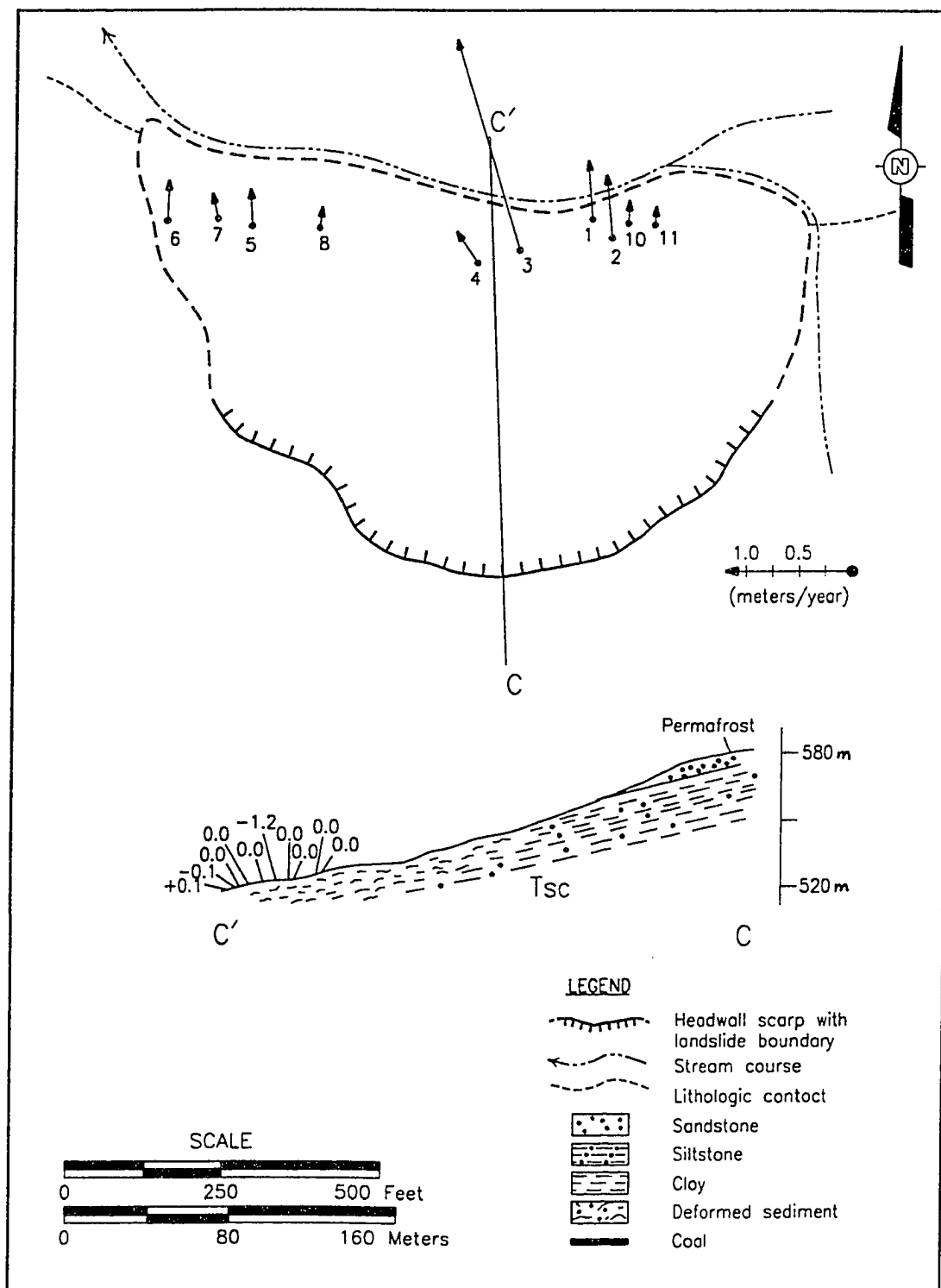


Figure 3.3-2. Geologic cross section and plan view of LII.

1968, the slide mass had grown to 35,000 m² and 140 m long, and by 1984, 40,500 m² and 190 m long. Size increase occurred primarily by headscarp retreat (retrogressive failure) and was accompanied secondarily by foot movement into the creek.

When the slide was first visited in August 1985, only the highest stream discharges could reach the slide toe; however, the slide toe had a muddy vegetationless front steeper than 60 degrees, which was backed by furrows and ridges that were mantled by vegetation across the foot area. Six survey stakes were surveyed on the slide approximately 10-20 meters upslope from the toe edge. In the following years five more stakes were added (Table 3.3-4). The survey data from one stake (LII-9) is unreliable, and is not included. No stakes were lost during the four years of surveying.

For five of the six original stakes, CHD ranged from 0.94 to 1.74 m (or 0.3 to 0.6 m/yr), while CVD ranged from -0.22 to +0.44 m (or -0.07 to +0.14 m/yr). Positive CVD's occurred with three of the stakes and are indicative of slide mass thickening in the toe area due to compressive stresses. One stake (LII-3) had an anomalously high CHD of 6.2 m (or 2.0 m/yr), and a CVD of -3.71 m (or -1.22 m/yr). These high values were caused by the rapid movement of the stake while riding downslope towards the creek channel on a surficial skin failure and are not indicative of movement of the slide mass. The CVD/CHD ratios ranged from -0.60 to +0.27, indicating that there were both significant upward and downward components of movement across the slide foot. In addition, for some stakes, the ratios in successive years were first positive and then negative. Direction of movement in the toe and foot areas was from N8E to N34W, with the primary direction of movement indicated by eight of eleven stakes which had movements that ranged between N8E and N5W.

Table 3.3-4. Summary of Movement for LII.

Slide Section	Period of Record		Stake	CHD (m)	CHDR (m/yr)	Direction	CVD (m)	CVDR (m/yr)	CVD/CH D
Foot	8/19/85	9/4/88	1	1.63	0.54	N5W	+0.44	+0.14	+0.267
	8/19/85	9/4/88	2	1.74	0.57	N5W	+0.01	+0.002	+0.004
	8/19/85	9/4/88	3	6.18	2.03	N17W	-3.71	-1.22	-0.600
	8/19/85	9/4/88	4	1.03	0.34	N34W	+0.06	+0.02	+0.171
	8/19/85	9/4/88	5	0.94	0.31	N3W	-0.12	-0.04	-0.129
	8/19/85	9/4/88	6	1.11	0.36	N2E	-0.22	-0.07	-0.198
	8/6/86	9/4/88	7	0.68	0.22	N13W	-0.09	-0.03	-0.138
	8/6/86	10/12/87	8	0.36	0.17	N8E	-0.02	-0.01	-0.067
	6/28/87	9/4/88	10	0.59	0.19	N3E	-0.13	-0.04	-0.211
	6/28/87	9/4/88	11	0.44	0.15	N4E	-0.11	-0.04	-0.253

The general uniformity in horizontal direction and magnitude of the motion vectors (with minor variations) indicate the presence of a singular but probably wide disconformity probably clay bedding within the Sanctuary Formation at the slide base that accommodates shear deformation. On the other hand, the minor variations in direction and magnitude, and the upward and downward components suggest that the slide mass may be decoupling to a degree over an uneven surface perhaps involving shearing throughout a thick portion of the Sanctuary clay into individual blocks. The apparent spatial distribution of movement is also suggested by the distribution of tilted willows, alders and spruce described above.

The interaction between Hoseanna Creek and LII is similar to that for LI. However, because the creek is relatively wider and the toe is somewhat removed from the main channel highwater, the magnitude and timing of movement of LII is likely not as sensitive to the timing of aufeis break-up in the main channel and the availability of water from snowmelt.

3.3.1.3 Landslide III

Landslide III (LIII) is asymmetric, relatively long, narrow and parabolic in plan view; it is a disrupted translational slide approximately 40,000 m² and 280 m long (Table 3.2-1), and is located at an elevation range of 521 m (1709 ft) to 591 m (1940 ft) above m.s.l. in mid valley on the south side of Hoseanna Creek just upstream of Landslide II (Figure 3.1-1). The main channel of Hoseanna Creek lies just to the north of the slide toe. The toe is corraded during break-up and summer storm

highwater events. The slide appears to have been initiated recently, just prior to 1949; in the 1949 photos, the slide crown and lateral borders are poorly defined and the surface vegetation is predominantly black spruce with minor willows and alders. In 1949, the slide was approximately 17,200 m² and 230 m long (Tables 3.3-1 and 3.3-2). By 1968 the slide area had almost doubled to 30,700 m² but did not increase much in the direction of movement, as most of the new slide area was added from lateral crown enlargement. This retrogressive enlargement continued up to 1974 by which time the slide increased to 39,800 m² and 280 m long. From 1974 to 1988, the size did not change significantly, thus remained about the same during the monitoring period (1985-1988).

The slide mass occurs across the contact between the base of the Suntrana Formation and the upper part of the Sanctuary Formation (Figure 3.3-3). Dipslope sand and clay bedding dips approximately 12-14°N and strikes approximately E-W. The pre-slide topography sloped to the north at 14°. The topographic slope was greater than the dip of the Sanctuary Formation bedding, which presents an unstable configuration. The surrounding undisturbed surface is vegetated with a stunted black spruce-*Sphagnum* community, suggesting the presence of permafrost. Like LII, vegetation on LIII is absent only in the headscarp area, and much of the slide surface is covered by tilted willows, alders and spruce.

When the slide was first visited in August 1985, six survey stakes were placed on the slide approximately 10-20 meters upslope from the toe edge. No additional stakes were added and no stakes were lost over the four years of surveying. Between 8/19/85 and 10/10/88 the six stakes had a CHD ranging from 0.5 to 1.0 m (or 0.2 to 0.3 m/yr), while the CVD ranged from -0.15 to -0.30 m (or -0.05 to -0.10 m/yr). The direction of movement of the six stakes in the foot area ranged between N9E and N28E (Table 3.3-5), while their CVD/CHD ratios ranged from -0.16 to -0.53. The vectors indicate an overall downward displacement to the NNE either parallel to or at a slope greater than bedding. The general uniformity in horizontal direction and magnitude of the motion vectors indicate the presence of a singular discontinuity for accommodating shear deformation (most likely clay bedding within the Sanctuary Formation). Minor variations in direction and magnitude suggest that the slide mass has decoupled somewhat. However, all the motion has been downward in the foot area, in contrast to the more typical upward component due to thickening by compression. This is likely due to the continued

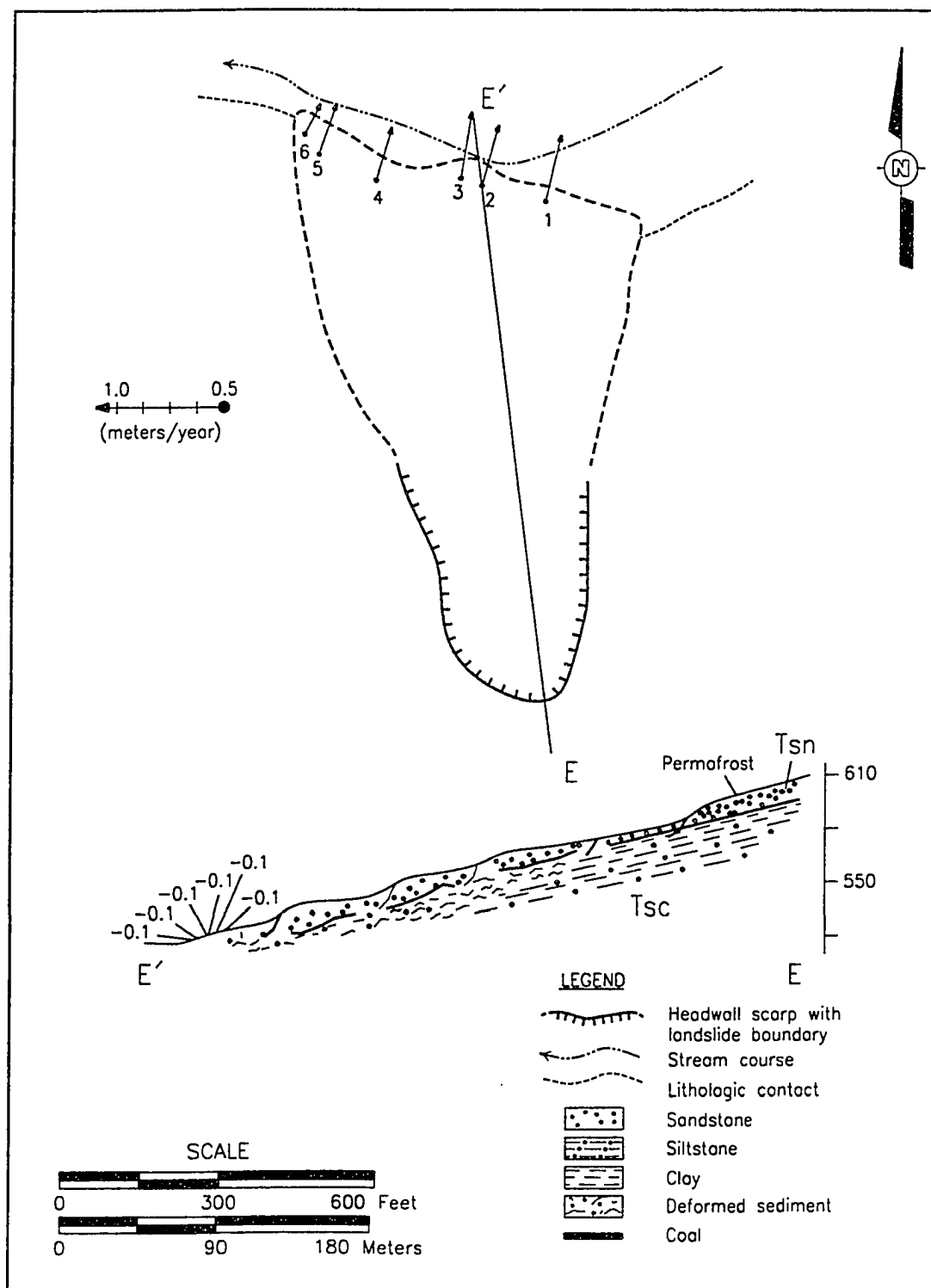


Figure 3.3-3. Geologic cross section and plan view of LIII.

loss of toe material by lateral corrosion of Hoseanna Creek.

As with LII, the interaction between Hoseanna Creek and LIII is similar to that of LI as on LI, but here the Hoseanna Creek channel is relatively wider and the toe is somewhat removed from the main channel. Consequently, the magnitude and timing of movement of LIII are likely not as sensitive to the timing of aufeis break-up and the availability of water from snowmelt.

Table 3.3-5. Summary of Movement for LIII

Slide Section	Period of Record	Stake	CHD (m)	CHDR (m/yr)	Direction	CVD (m)	CVDR (m/yr)	CVD/HVD
Foot	8/19/85-10/10/88	1	0.97	0.31	N13E	-0.22	-0.07	-0.23
		2	0.91	0.29	N16E	-0.24	-0.08	-0.27
		3	0.95	0.30	N9E	-0.15	-0.05	-0.16
		4	0.78	0.25	N17E	-0.30	-0.10	-0.39
		5	0.73	0.23	N19E	-0.26	-0.08	-0.36
		6	0.50	0.16	N28E	-0.27	-0.08	-0.53

3.3.1.4 Landslide IV

Landslide IV (LIV) is a relatively long and narrow earthflow approximately 59,500 m² and 500 m long (Table 3.2-1), located at an elevation range of 628 m (2060 ft) to 747 m (2450 ft) above m.s.l. in the northeast part of Slide Creek Basin (9N) on a northwest-facing slope (Figure 3.1-1). A small northeast tributary to Slide Creek begins just upslope of the foot of the slide and then incises a small channel along the north flank of the foot. At the junction of the slide with the tributary the slide turns abruptly (at right angles) westward into the tributary and is directed downstream. This slide is one of the most active in the Hoseanna Creek Watershed, and appears to have been initiated recently, just prior to 1949, based on the 1949 photos. Since 1949 continued headscarp retreat and toe advancement have occurred.

The slide occurs wholly within the Lignite Creek Formation. Dipslope sand, silt,

lignite and clay bedding dip approximately 6-10°N and strike N70E (Figure 3.3-4). The pre-slide topographic slope is estimated at 10° to the northwest, which is greater than the bedrock dip presenting an unstable configuration. Only the lowermost tongue area of the slide surface is vegetated with grasses and an occasional tree.

In 1949, LIV was relatively small, only 14,000 m² and 240 m long (Tables 3.3-1 and 3.3-2). By 1968, the slide had grown to 24,500 m² and 300 m long. It continued to grow and increased considerably during the next six years as both the headscarp retreated and the tongue advanced, so that by 1974 the slide was 30,500 m² and 370 m long. Rapid lengthening continued through the monitoring period, and by 1988 the length had more than doubled to 500 m, and the area had increased more than four-fold to over 60,000 m².

When the slide was first surveyed in August 1985, eight stakes were placed in the upper, mid and lower sections. I suspected that this slide might be active several times a year, so by October 1988, the slide had been visited another ten times and 18 more stakes were placed across the slide mass to detect the magnitude, frequency and locations of movement within the earthflow (Table 3.3-6 and Figure 3.3-4). In fact, headscarp retreat was so vigorous (> 3 m between 1985 and 1986) that several control stakes were lost by 1988.

Several times during the monitoring period, lateral shear zones and lateral ridges extended up to one-half the slide length. On five separate occasions (June 1985, May 1986, May 1987, September 1987, and September 1988), the upper slide area was covered by a large region of open cracks or crevasses which were perpendicular to movement in the center of the slide but became curved and concave downhill, finally intersecting the lateral shear zones at angles as high as 45 degrees. This morphology is predicted by the shear-stress relationship at boundary conditions for ice (Nye, 1951). In addition, "bergschrunds" had developed at the base of the headscarp as the upper basin material moved away from headscarp talus. Such patterns of cracks indicate that the upper part of the earthflow was subject to extensional stresses to which it responded by flowing rather than by moving as a single coherent block similar to that of deforming ice. In the lower slide, furrows and ridges as much as 5 m in relief stood perpendicular to slope movement and reflect a zone of compression and thickening.

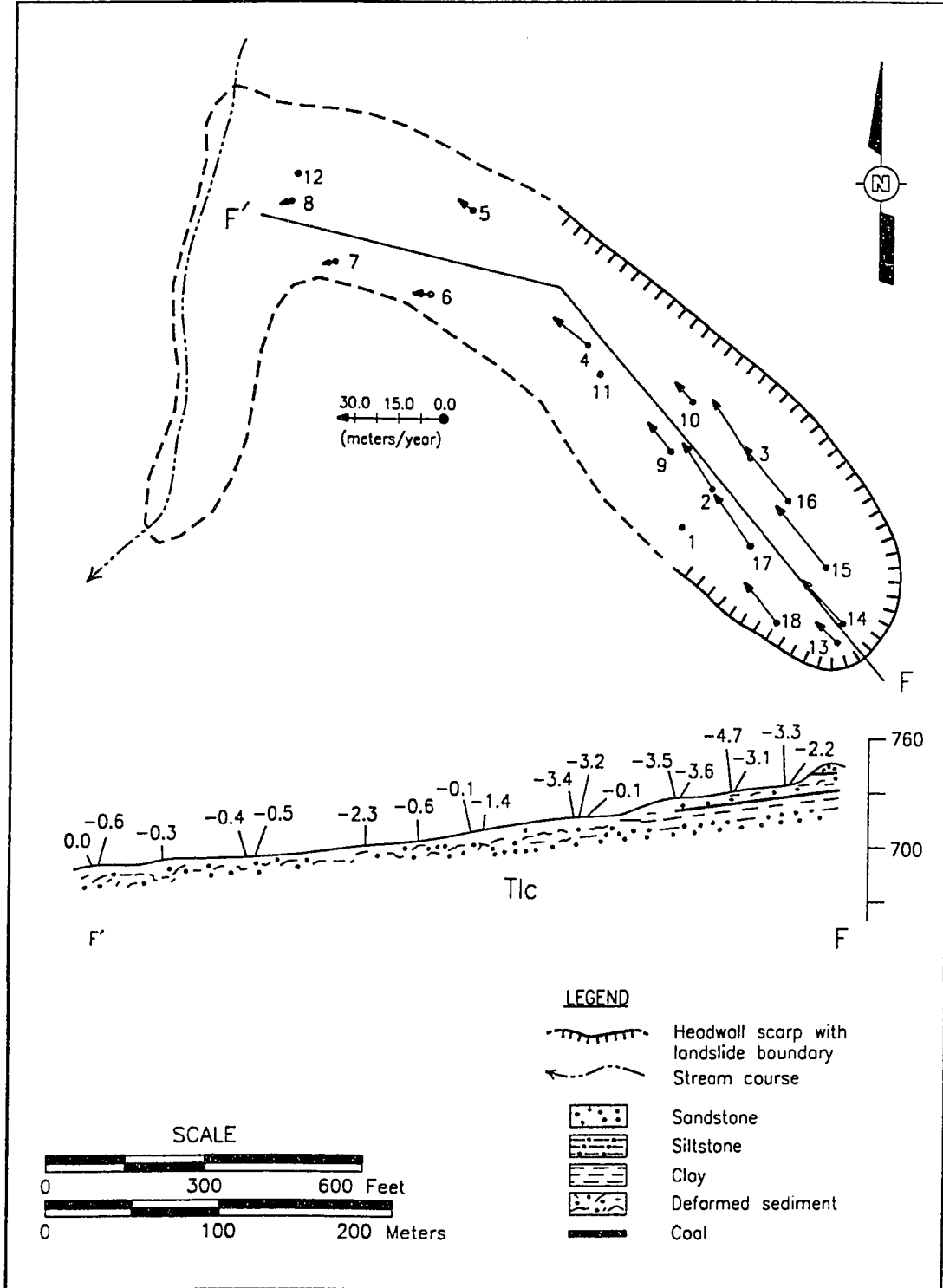


Figure 3.3-4. Geologic cross section and plan view of LIV.

Table 3.3-6. Summary of Movement for LIV.

Slide Section	Period of Record		Stake	CHD (m)	CHDR (m/yr)	Direction	CVD (m)	CVDR (m/yr)	CVD/HVD
LIV Upper Section	7/31/86	10/9/88	13	21.71	9.89	N48W	-4.91	-2.24	-0.23
	7/31/86		14	43.42	19.78	N44W	-7.25	-3.30	-0.17
	7/31/86		15	57.96	26.41	N40W	-10.22	-4.66	-0.18
	7/31/86		16	51.01	23.24	N41W	-7.99	-3.64	-0.16
	7/31/86		17	45.67	20.81	N36W	-7.65	-3.49	-0.17
	7/31/86		18	37.48	17.08	N40W	-6.83	-3.11	-0.18
	9/1/87		20	18.03	16.29	N48W	-8.04	-2.75	-0.17
	9/1/87		21	17.08	15.43	N48W	-2.69	-2.43	-0.16
	9/1/88		26	2.68	25.78	N49W	-0.45	-4.33	-0.17
LIV Mid Section	8/20/85	10/9/88	1	2.23	0.71	N34W	-0.30	-0.10	-0.14
	8/20/85	10/9/88	2	57.29	18.25	N34W	-10.05	-3.20	-0.18
	8/20/85	10/9/88	3	72.20	23.00	N34W	-10.82	-3.45	-0.15
	8/20/85	9/1/88	4	44.88	14.78	N53W	-6.85	-2.26	-0.15
	7/31/86	10/9/88	9	26.10	11.89	N39W	-3.16	-1.44	-0.12
	7/31/86	10/9/88	10	18.39	8.38	N42W	-1.80	-0.82	-0.10
	7/31/86	10/9/88	11	4.56	2.08	N63W	-0.59	-0.27	-0.13
LIV Lower Section and Foot Area	8/20/85	10/9/88	5	16.35	5.21	N57W	-1.14	-0.36	-0.07
	8/20/85		6	15.06	4.80	N88W	-1.65	-0.52	-0.11
	8/20/85		7	8.94	2.85	S84W	-1.07	-0.34	-0.12
	8/20/85		8	8.88	2.83	S72W	-1.94	-0.62	-0.21
	7/31/86		12	1.00	0.46	S40W	+0.003	0.00	+0.003
	4/4/88		23	0.17	0.33	S55W	+0.09	+0.18	+0.55
	4/4/88		24	0.64	1.25	S88W	+0.02	+0.04	+0.03

The upper slide area surface features indicated very recent and substantial movement. After rainstorms and within a month of some of these survey dates, the extensional features had mostly disappeared (i.e., erosion but not movement). Indeed, some of the summer rainstorms eroded the fresh flow features rather than initiating movement. In May 1987, the substrate was probed by a metal rod and several pits were dug across the slide mass; it was found that the sediment was

frozen about 30-60 cm below the surface even though a large crevasse field covered the entire upper slide area.

The upper slide area had the most extensive spatial coverage (9 stakes); while the mid section, and foot area were staked and surveyed the longest, from 8/20/85 to 9/1/88. All sections of LIV experienced significant movement, although the upper section had by far the greatest CHDR's and VHDR's. The maximum CHDR (and CVDR) measured for any one stake, LIV-15, was 26.4 m/yr (and -4.7 m/yr).

The predominant direction of movement for the entire slide except the foot area ranged from N34W and N53W. The movement of stakes in the foot area (N57W to S40W) reflect the change in direction of the foot as it turns at right angles and heads down the southwest flowing tributary (Figure 3-5). In addition, the CVD/CHD ratios had a smaller range of values (-0.098 to -0.226) in the upper sections, equal to or greater than the dip of the sedimentary beds. In the foot area these ratios were both positive and negative, ranging from -0.214 to +0.554.

The foot of the slide completely obliterates the small tributary. Slide motion is likely not linked to the ability of the tributary to remove toe material, but rather to upslope processes within the slide mass, and therefore the slide dominates geomorphic processes at the creek. This differs from the temporal connection of lateral corrasion and toe movement for slides along the main channel of Hoseanna Creek.

3.3.1.5 Landslide V

Landslide V (LV) is a relatively long and narrow block slide approximately 9,900 m² and 150 m long (Table 3.2-1), and is located at an elevation range of 491 m (1611 ft) to 549 m (1791 ft) above m.s.l. in mid valley on the south side of Hoseanna Creek just upstream of the confluences with Clear Creek (CS) and Popovitch Creek (7N) (Figure 3.1-1). Hoseanna Creek flows westward to the north of the slide toe. Due to the wide channel area and the greater distance from Hoseanna Creek to the slide, it is likely that the creek will corrade near the slide toe only during very high runoff events. In addition, an alluvial fan emanates from the slide mass into Hoseanna Creek channel and has forced the creek away from the slide toe;

continued sediment production from the slide to the fan maintains the fan size and prevents the creek from migrating up against the slide toe.

This slide is apparently much older than most of the other slides and its movement history is most likely linked to the growth and incision of the Popovitch Creek fan (which began growing about 400 yrs BP, see Section 2.3) which lies directly across Hoseanna Creek from the slide. The slide grew approximately 3X in area and 1.6X in length between 1949 and 1974, but except for vegetation and the alluvial fan size, the slide does not appear to have grown much since 1974, and in fact appears to have been shortened 15 m due to removal of slide material from the toe during high flows prior to 1984 (Tables 3.3-1 and 3.3-2).

The slide occurs at the contact of the base between the Healy Creek Formation and the metamorphic basement (Figure 3.3-5). The contact is marked by the extensive weathered schist/clay horizon. It is likely that most or all of the deformation to sustain movement occurs within this zone. Dipslope sand, coal and clay bedding dip approximately 10-15°N and strike N80E. The pre-slide topographic slope is estimated at 27° and slopes generally northward. These geologic and topographic conditions present an unstable configuration. The surrounding undisturbed surface is vegetated with a stunted black spruce-*Sphagnum* community, suggesting the presence of permafrost. At the headscarp some characteristics of permafrost were present including small ice lenses or ice blebs that occurred within lenses of fine-grained material within the sandstone. Vegetation is absent on the slide, except for the toe area, which has tilted willows, alders and some spruce community remnants.

Approximately 400 years ago, the Popovitch Creek fan began to growth southward and force Hoseanna Creek to the south side of the valley and up against the slope. Lateral corrasion of the valley wall in the vicinity of the slide resulted in failure of several sections of the hillslope, including portions of the hillslope just to the northeast. However, LV is the only remaining slide still active on the north-facing slope. The other slide areas have since stabilized judging by the stable forest covering the slide areas. Sometime prior to 1949, Hoseanna Creek migrated northward back into the Popovitch fan, presumably as a result of high sediment production from the adjacent landslides. This corrasion has continued to cut into Popovitch fan and left the slide area relatively free to stabilize.

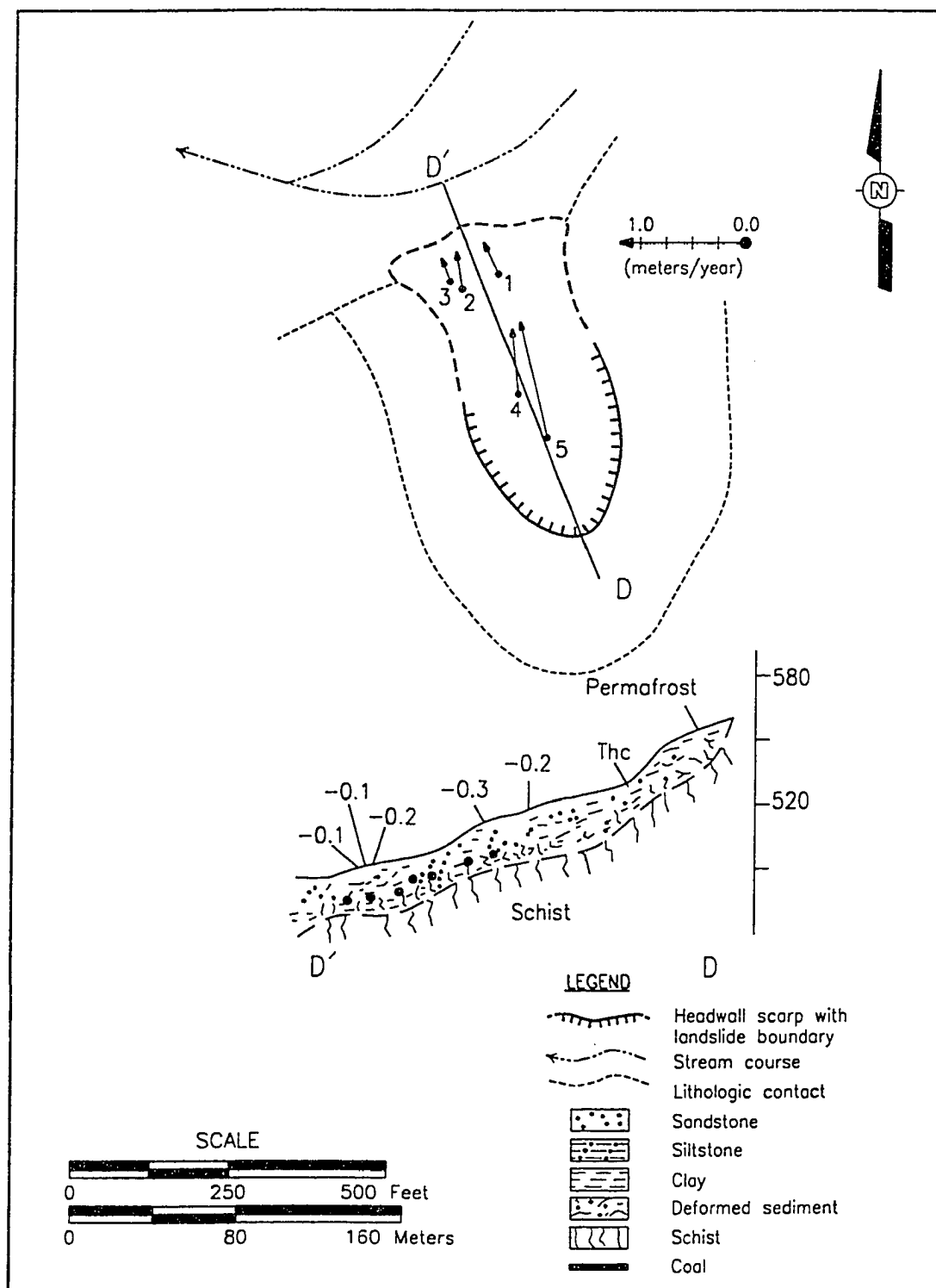


Figure 3.3-5. Geologic cross section and plan view of LV.

Landslide V was first visited in August of 1985. Five survey stakes were surveyed on the toe and mid section of the slide. In the following three years the stakes were surveyed four more times. For the five stakes, CHD's ranged from 0.7 to 1.9 m (or 0.2 to 0.6 m/yr), while CVD's ranged from -0.27 to -0.99 m (or -0.09 to +0.33m/yr) (Table 3.3-7). The maximum HDR and VDR measured on any one stake (LV-4) between successive surveys was 1.97 m/yr and -0.90 m/yr, respectively. These values are relatively low compared with some of the other more active slides, and they indicate a less active slide, with slow imperceptible movement.

The direction of movement of all stakes was relatively uniform, ranging from N6W and N26W (Table 3.3-7 and Figure 3.3-5). The minor variation in movement vectors is related to their position on the slide. The upper two stakes (LV-4 and LV-5) had the higher overall CHD and CVD and the higher CVD/CHD. The greater downward component and higher overall displacement in the upper region indicates extension up high with compression down low. In addition, LV-1 had positive VD during the first year (1985-86), being pushed up by movement from above. These are indicators of typical later stage activity that follows movement first at the toe, then by the mid slide area. This process has probably occurred episodically throughout the duration of slide activity. The average CVD/CHD for the all the stakes except LV-1, is around 0.5 (or about 27° from the horizontal). This movement vector is considerably greater than the slide's surface slope of 18.5°, and indicates that the slide mass is downwasting during translational or block sliding.

Table 3.3-7. Summary of Movement for LV.

Slide Section	Period of Record	Stake	CHD (m)	CHDR (m/yr)	Direction	CVD (m)	CVDR (m/yr)	CVD/HVD
LV	8/21/85-9/2/88	1	0.98	0.32	N26W	-0.27	-0.09	-0.28
		2	1.06	0.35	N9W	-0.50	-0.17	-0.48
		3	0.69	0.23	N22W	-0.34	-0.11	-0.49
		4	1.86	0.61	N6W	-0.99	-0.33	-0.53
		5	1.10	0.36	N14W	-0.55	-0.18	-0.50

Although LV is a considerable sediment producer as evidenced by the continued regrowth of the alluvial fan at its toe, it is relatively inactive; most of the movement occurred prior to 1985, and probably before 1949. The movement measured during the monitoring period likely represents the waning stages of movement for the slide in its present configuration. Unless Hoseanna Creek leaves its present course for a more southerly route, the toe area will continue to stabilize. The evidence at LV suggests that maximum sediment production coincides with or succeeds maximum landslide movement. That is, landslide movement exposes sediment to erosion and then the sediment is supplied to the creek. In addition, movement and sediment production over the landslide "life" are highly variable and episodic in nature.

3.3.1.6 Landslide VI

Landslide VI (LVI) is a relatively wide and short rotational slump block with a number of mudflow chutes that emanate from and are spaced across the mid section of the slide. The slide is approximately 70,000 m² and averages 180 m in length (Table 3.2-1), and is located at an elevation range of approximately 663 m (2175 ft) to 747 m (2450 ft) above m.s.l. in the northwest part of North Hoseanna Creek Watershed (10N) on a west-facing slope (Figure 3.1-1). A small northwest tributary of North Hoseanna Creek begins just upstream of the toe of the slide. The main slide block lies 55 m above the creek. Downward and headward creek incision has oversteepened the valley walls and caused headward gulley incision below the broad toe of the slump block. Mudflows that emanate from the mid slide area descend across the foot at steep angles to the channel below.

This slide was the least active of all the slides monitored. In the 1949 photo the slide boundary is not well defined. However, dramatic headward enlargement occurred between 1949 and 1968 (Tables 3.3-1 and 3.3-2); the slide area grew from 27,500 m² to 67,300 m² and from 120 to 180 m long. From 1968 to 1981, there were no significant change in area or length. This relative quiescence continued during the monitoring period.

The slide occurs wholly within the Lignite Creek Formation (Figure 3.3-6). Bedding dips gently 6-7°N and strikes N70°E. The pre-slide topographic slope is estimated at 27° to the west. Slump movement to the west is generally perpendicular to the

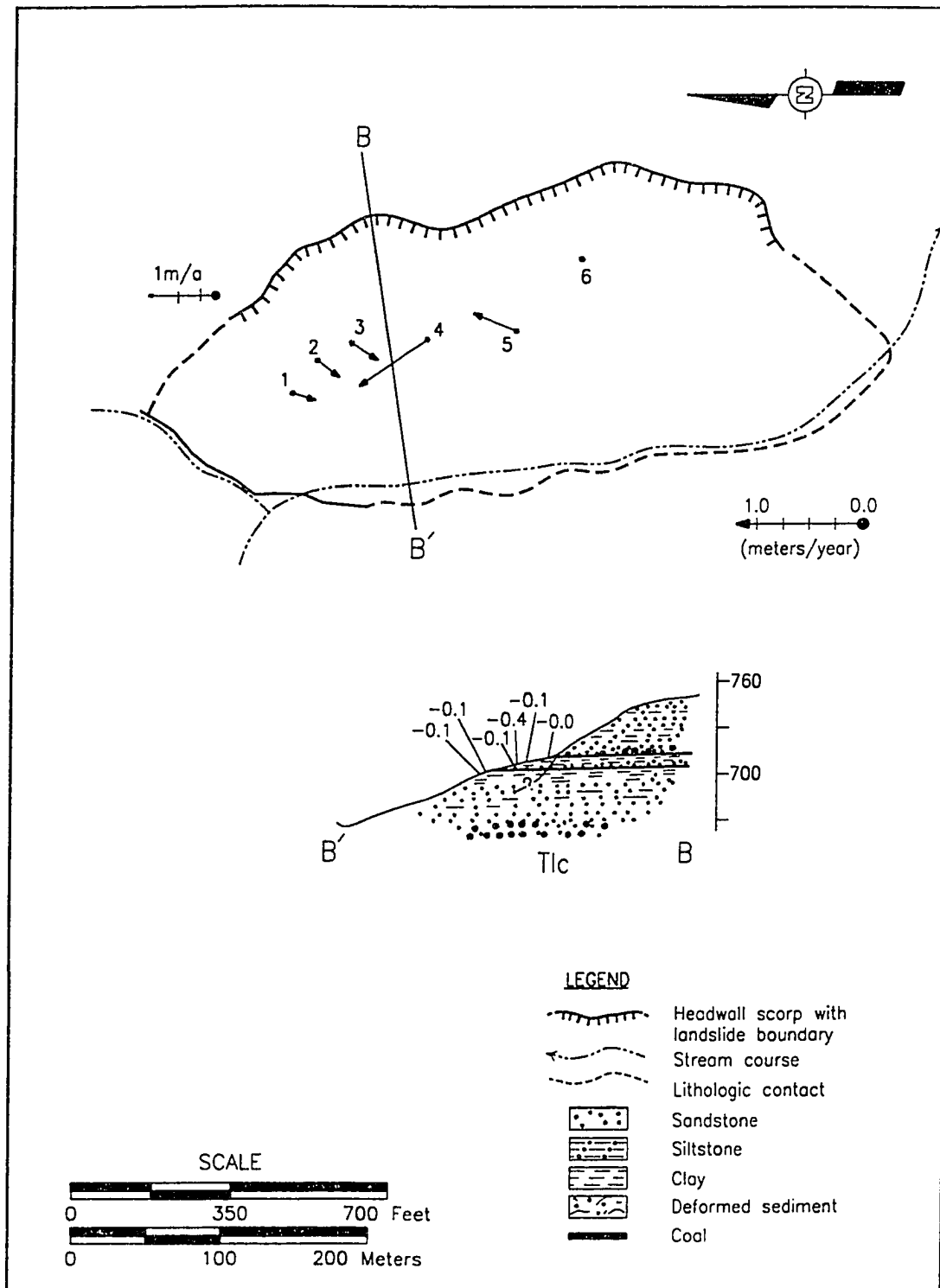


Figure 3.3-6. Geologic cross section and plan view of LVI.

strike of beds. The headward incision of the small tributary has undermined weak clays and triggered block slumping to the west. Most of the slide surface is vegetated with willows, alders and poplar, with occasional white spruce in more stable areas. The headscarp is not vegetated and has several amphitheater-like open areas with talus cones comprised of sand, silt and clay fill. Mudflows emanate from these areas during rainfall or snowmelt events.

The slide was first visited in August of 1985. Six survey stakes were surveyed across the mid section of the slide. In the following three years the stakes were surveyed three more times (once each year). For the six stakes, CHD's ranged from 0.11 to 2.17 m (or 0.04 to 0.77 m/yr), while CVD's ranged from -0.11 to -1.21 m (or -0.04 to -0.43 m/yr) (Table 3.3-8). The maximum HDR and VDR measured on any one stake (LVI-4) between successive surveys was 1.83 m/yr and -0.96 m/yr, respectively. This displacement was on a skin failure and is not representative of the slide mass as a whole. In general, the range in displacements is relatively low compared with some of the more active slides, and they indicate a less active slide with slow, imperceptible movement.

Table 3.3-8. Summary of Movement for LVI.

Slide Section	Period of Record	Stake	CHD (m)	CHDR (m/yr)	Direction	CVD (m)	CVDR (m/yr)	CVD/HVD
LVI Mid Section	8/28/85- 6/19/88	1	0.63	0.23	S16W	-0.38	-0.13	-0.60
		2	0.73	0.26	S36W	-0.31	-0.11	-0.42
		3	0.82	0.29	S32W	-0.20	-0.07	-0.24
		4	2.17	0.77	N34W	-1.21	-0.43	-0.56
		5	1.22	0.43	N22E?	-0.39	-0.14	-0.32
		6	0.11	0.04	S24W	-0.11	-0.04	-1.03

3.3.1.7 Landslide VII

Landslide VII (LVII) is a triangular-shaped disrupted block slide with lateral spread characteristics at the foot. The slide is approximately 52,500 m² and 360 m long (Table 3.2-1), with an elevation range of 613 m (2010 ft) to 704 m (2310 ft) above m.s.l. The slide foot is at the confluence of two small tributaries within the

northwest section of the North Hoseanna Creek Watershed (10N) (Figure 3.1-1). These tributaries join and flow along a fairly steep and heavily disturbed bank at the toe of the slide. The main slide block lies about 30 m above the creek channels. The slide appears much smaller and less defined in the 1949 photos than it does today. The slide grew from 23,500 m² in 1949 to 37,500 m² in 1968, and to 52,500 m² by 1974 (Tables 3.3-1 and 3.3-2). Although no size increases could be discerned between 1974 and 1981, the slide was fairly active during the monitoring period (1985-1988).

The slide mass encompasses the base of the Lignite Creek Formation and may incorporate (or sole out on) the upper part of the Suntrana Formation at the #6 coal seam (Figure 3.3-7). Bedding dips gently 6-10°N and strikes N70E, and the predominant movement direction is N78W in the slide mid section and S45W at the foot, so that the slide mass generally moves downslope obliquely across bedding surfaces. The pre-slide topographic slope is estimated at 16° to the west. Permafrost is not evident.

The slide was first visited in August of 1985. Six survey stakes were surveyed across the mid section and foot area of the slide. One stake from the mid section was lost after the first year; however, surveying this slide was very difficult and no new stakes were added. In the following three years the stakes were surveyed three more times (once each year). For the five stakes, CHD's ranged from 1.9 to 7.3 m (or 0.6 to 2.4 m/yr), while CVD's ranged from -8.9 to +0.2 m (or -2.9 to +0.08 m/yr) (Table 3.3-9). The maximum HDR measured on any one stake (LVII-3) between successive surveys was 6.1 m/yr, while the maximum VDR was -8.4 m/yr on LVII-2. These values are relatively high compared with some of the other slides, and indicate an active slide.

The predominant direction of movement for the foot area was to the SW (the directions of movement for the three stakes ranged from S27W to S64W), and the three stakes also experienced significant downward components as their CVD/CHD ratios ranged from -1.86 to -0.32. In contrast, the direction of the two stakes in the mid section was N78W, with lower CVD/CHD ratios (-0.26 and +0.07). The vectors of movement for the three in the foot area and the two in the mid section indicate changes in direction between the mid section and foot areas accompanied by divergent movement across bedding down a slope considerably steeper than the

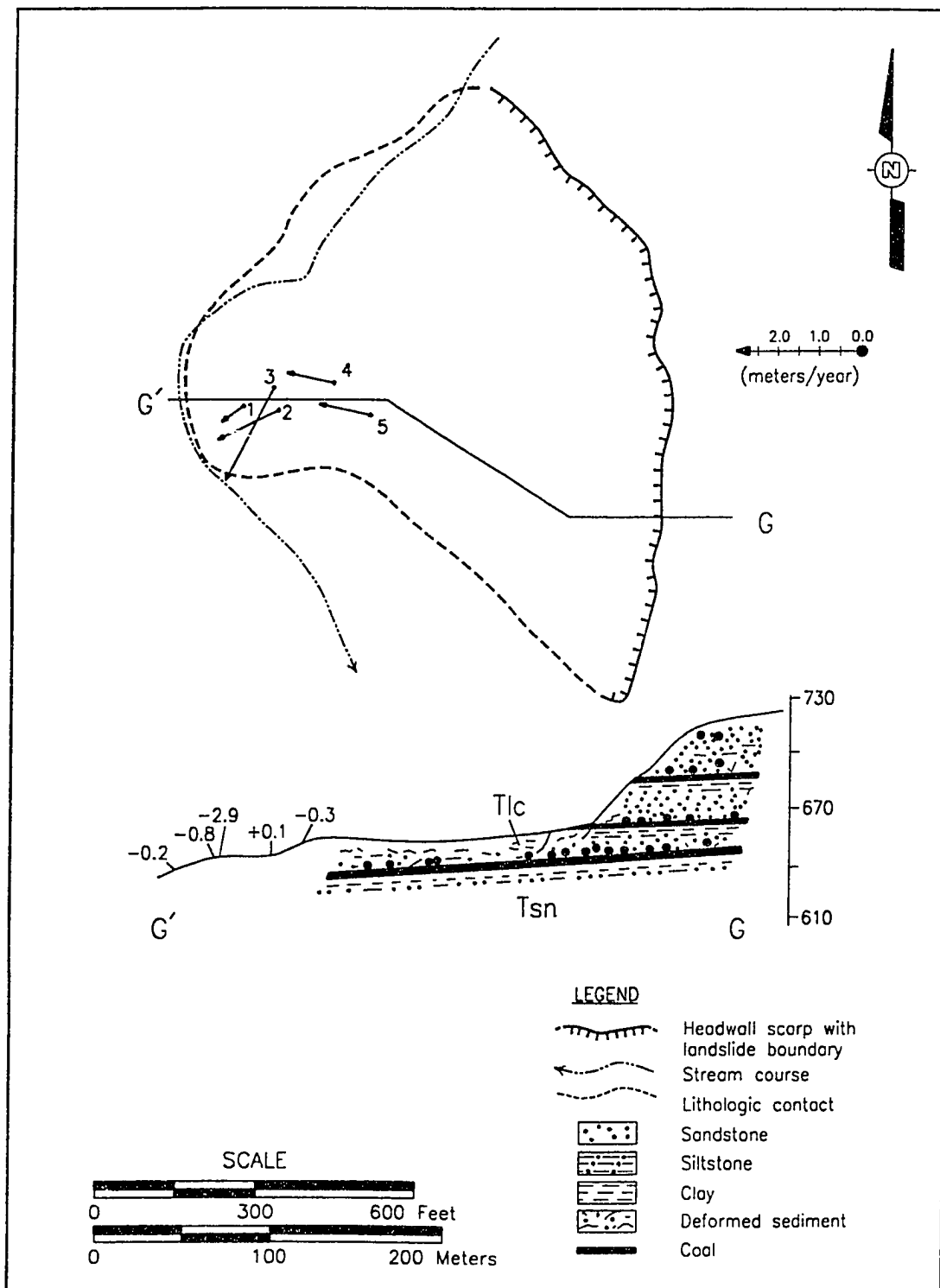


Figure 3.3-7. Geologic cross section and plan view of LVII.

pre-slide topographic slope. This pattern of motion is indicative of disrupted translational block slide movement in the mid section that develops downslope into a lateral spread.

Table 3.3-9. Summary of Movement for LVII.

Slide Section	Period of Record	Stake	CHD (m)	CHDR (m/yr)	Direction	CVD (m)	CVDR (m/yr)	CVD/HVD
LVII	8/28/85-9/2/88	1	1.88	0.62	S53W	-0.69	-0.23	-0.36
		2	4.77	1.58	S64W	-8.87	-2.94	-1.86
		3	7.32	2.43	S27W	-2.39	-0.79	-0.32
		4	3.38	1.12	N78W	+0.24	+0.08	+0.07
		5	3.72	1.23	N78W	-0.99	-0.33	-0.26

3.3.2 Summary of Change In Landslide Size (1949-1988)

All seven slides appear on the 1949 U.S. Army photos, suggesting that the landslides have stayed active for more than 40 years. Significant changes in the areas and lengths of these landslides has occurred during this time span (Tables 3.3-1 and 3.3-2, and Figures 3.3-8 and 3.3-9). Landslides I and IV, which were the most active during the monitoring period, were not well developed in 1949. Landslide IV, for example, enlarged headward over 280 m from 1949 to 1988 and almost 150 m since 1974. In contrast, some slides which appeared relatively active in earlier photos did not change much in later years. It is important to note that this spatial and temporal variety of slide activity occurred in slide-prone areas throughout Hoseanna Creek Watershed. For example, one of the largest slides in the basin in 1988 (over 500,000 m²: LVIII on Figure 3.1-1) could not be detected in the 1949 photograph. (Although LVIII was not part of the survey network, I was able to periodically visit the slide during the monitoring period, and between 1985 and 1988, LVIII experienced considerable changes in movement and in surface morphology.)

Landslide motion was not constant from 1949 through 1988. Initially, for each slide, incipient slow movement preceeded a period of relatively high activity, later

3-37

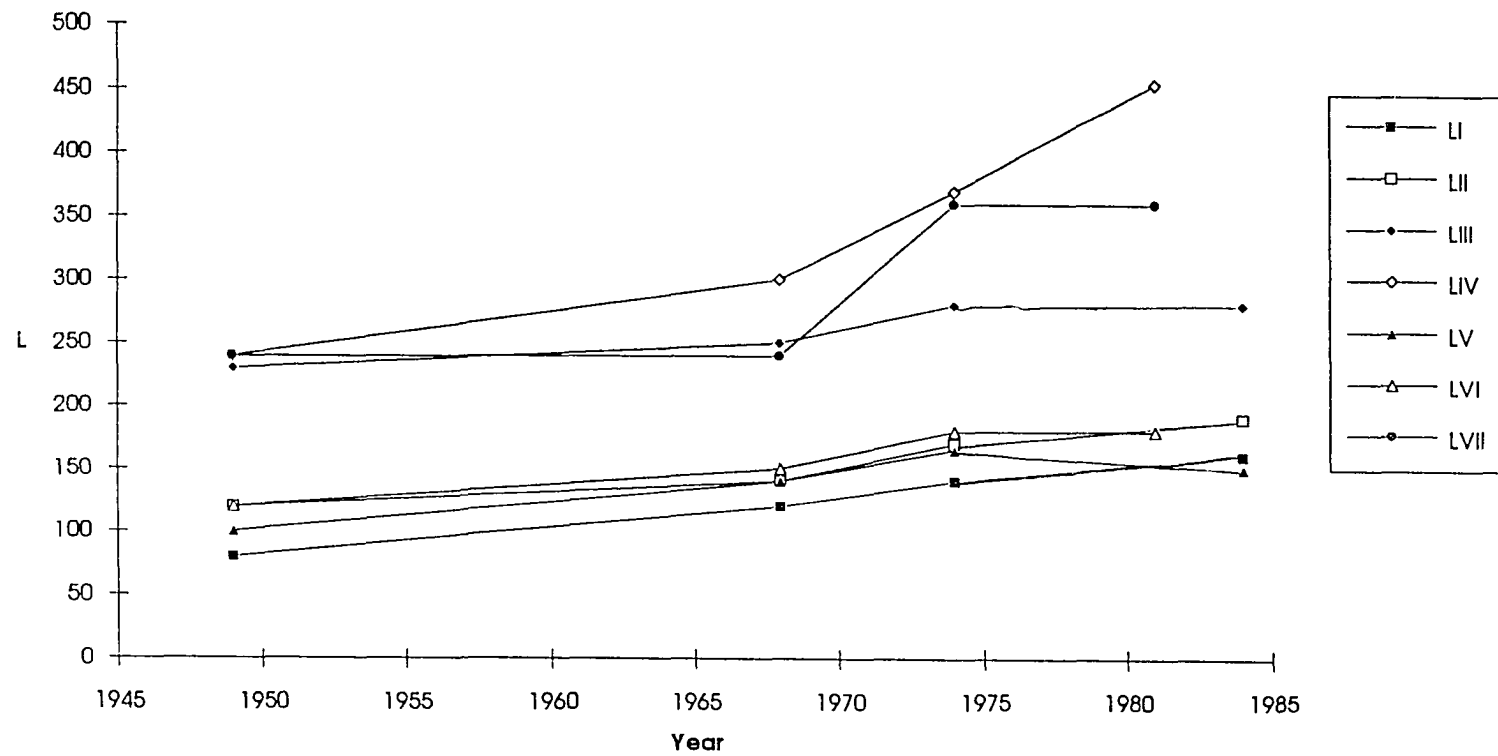


Figure 3.3-8. Changes in the length (L - m) of each monitored slide from 1949-1984.

3-38

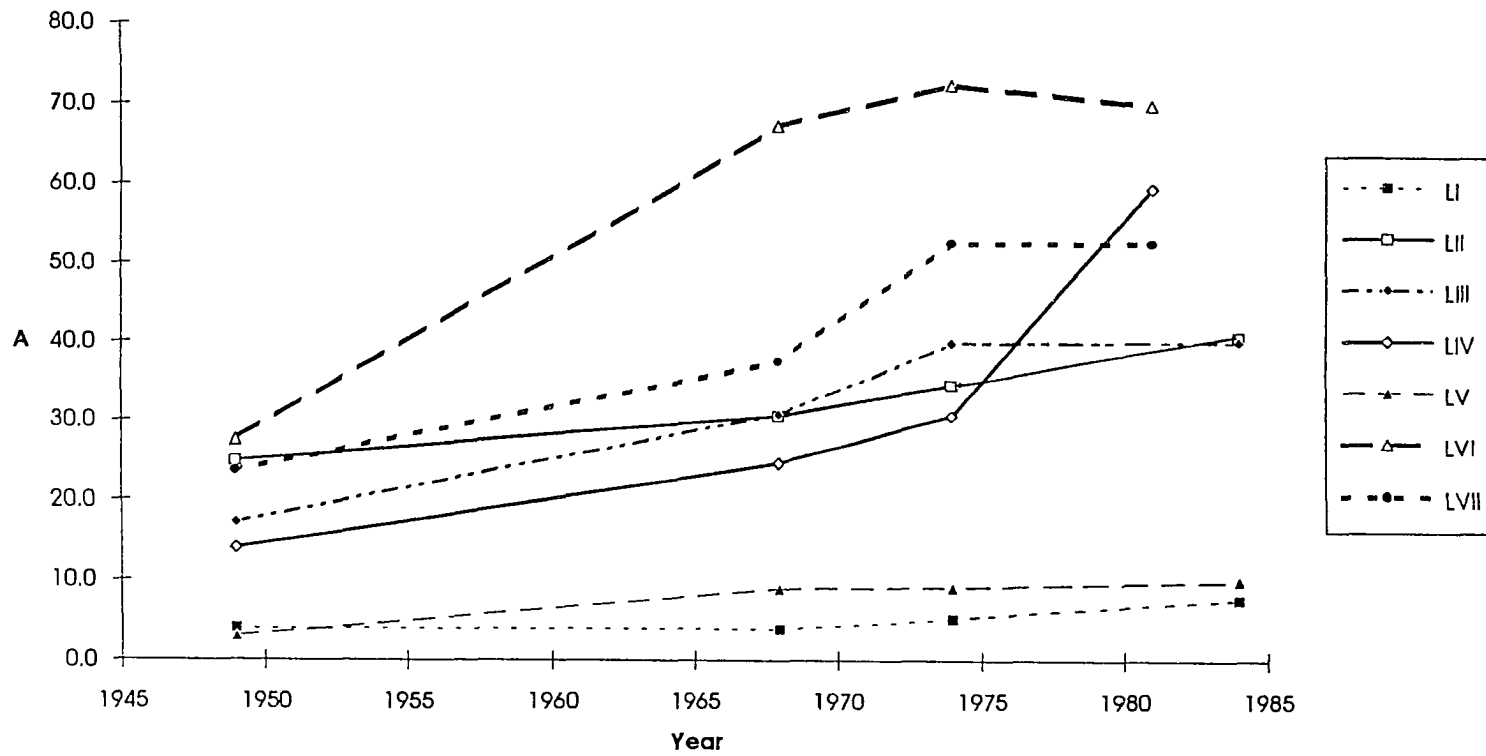


Figure 3.3-9. Changes in the area (A - km²) of each monitored slide from 1949-1984.

followed by progressively slower motion. In addition, slide motion appears to have been rejuvenated during periods of headward enlargement or stream-toe interactions.

Landslide motion was also not steady for the short period of record, 1985-1988 (discussed below in section 3.3.4). Non-steady activity appears to be the normal mode of movement and development as evidenced by the histories of slide motions discerned from air photos taken in 1949, 1968, 1974, 1981 and 1984, and from field surveys during 1985-1988. Figures 3.3-8 and 3.3-9 show the changes in area and length for the seven slides from 1949 to 1988. All slides have grown larger, but the rates of growth have not been constant. In addition, there does not appear to have been a time when all the slides were growing faster. However, from 1968-1974 most of the slides experienced considerable growth.

The most rapid growth has occurred in LIV, which doubled in size between 1974 and 1981. In addition, slides VI and VII have also experienced large growth periods. In contrast, periods when there were no increases in area have occurred in all but slides II and IV. Overall, the slides increased in area by a factor of about 1.7 to 4.2.

Growth in slide length correlates closely with growth in area, as the slides have increased in length from 1.2X to 2.1X. Length increases occur in two ways, by extending the slide front into the stream channel, and/or by headward enlargement. In most cases, headward enlargement accounts for most of the length increase, as well as the increase in area.

The best example of slide length and area increase is given by LIV, which also had the largest displacement rates. Figure 3.3-4 shows the plan view and longitudinal cross section of the slide, and changes it has experienced. Generally, since 1949, the upper section increased in area by retrogressive failure and sloughing of headscarp material into the upper basin. The unconsolidated sediments moved downslope by plug flow, which tended to pile up or spread laterally in the foot area. Consequently, the upper section has decreased in elevation while increasing in area and length, and the lower slide area increased in both elevation and area. In addition, the toe, which in 1949 abutted against the opposite valley wall, is turned downstream and now flows perpendicular to its original flow direction.

3.3.3 Summary of Movement 1985-1988

A summary of landslide movement for the seven slides is given in Tables 3.3-10. The slides are grouped by displacement rates and mechanism of movement into four groups: 1) LII, LIII and LV are disrupted translational block slides that move slowly and imperceptibly, 2) LI and LIV are earthflows that have moderate to rapid displacement rates and show significant surficial disturbance that is evidence for recent large displacements, 3) LVII is a fairly active block slide in the upper portion and may have characteristics of a lateral spread in the lower portion, and 4) LVI is a rotational slump block with very slow, imperceptible movement.

CHDR's for the translational slide group ranged from 0.15 m/yr on LII and LIII to 0.58 m/yr on LI and LIV, and for the rotational slump block 0.03 m/yr to 0.43 m/yr. CHDR's varied considerably for the earthflows and depend on location within the slide mass. In the foot areas, CHDR's ranged from 0.12 m/yr on LI to 5.2 m/yr on LIV, in the mid section from 0.43 m/yr on LI to 18.3 m/yr on LIV, and in the upper basin from 3.8 m/yr on LI to 26.4 m/yr on LIV. In general, CHDR's on LIV were much larger than on LI, which likely reflects the size differences; that is, all other things being equal larger earthflows have higher displacements than smaller earthflows (farther runout). The CHDR's for translational slide/spread were in between the translational slides and earthflows; CHDR's for LVII ranged from 0.6 m/yr to 2.3 m/yr.

Average CVDR's ranged from 0.24 m/yr to 0.49 m/yr for group 1, from 0.55 m/yr to 48.4 m/yr for group 2, from 1.2 to 1.6 for LVII and 0.21 m/yr for LVI. In a few cases vertical displacements were positive and indicated thickening on the lower reaches of some slides.

The average CVD/CHD for a slide section is related to the angle of basal shearing, and is a function of the threshold basal shear stress required to attain movement from the slide mass; CVD/CHD is likely parallel to the slope of the failure plane and is a good indicator of the stress regime. When CVD/CHD is positive or near horizontal, the shearing has left the basal zone due to the compressional stress field; this results in overall thickening of the slide mass.

Table 3.3-10. Summary of Movement for LI through LVII.

Slide/Group	Section	ACDHR (m/yr)	Direction of Movement	ACVDR (m/yr)	Average CVD/CHD
LI/2	Upper	2.0 ^a	N20W-N26W	-	1.0 to -0.2
	Mid	0.5	N9W-N5E		-0.2 to -0.51
	Foot	1.9	N26W-N21E		-0.28 to -0.13
LII/1	Foot	0.4	N34W-N8E	-0.06 to +0.09	-0.14 to +0.21
LIII/1	Foot	0.2	N9E-N28E	-0.09	-0.38
LIV/2	Upper	48.4 ^c	N49W-N36W	-8.2	-0.17
	Mid	18.7 ^b	N63W-N34W	-2.6	-0.14
	Foot	3.9 ^b	S40W-N57W	-0.4	-0.12
LV/1	Mid	0.5	N14W-N6W	-0.2	-0.50
	Foot	0.3	N26W-N9W	-0.1	-0.40
LVI/4	Mid	0.2	S36W-N34W	-0.09	-0.43
LVII/3	Mid	1.2	N78W	+0.09 to -0.3	+0.08 to -0.28
	Foot	1.6	S64W-S27W	-0.1	-0.84

Note: stakes moved by skin failures have been excluded

a: normalized for a full year

b: calculated using only stakes with three years of data

c: normalized for three years, based on correlations with other stakes with three full years of data, and excludes stake #1, which is outside of the lateral shear zone

In general, upper basin CVD/CHD is steeper than mid section and lower foot areas which is a product of extension up high in the slide and compression down low in the slide. The earthflows LI and LIV, which have the lowest CVD/CHD, deform by plastic plug flow and require lower shear stresses to achieve movement. In contrast, the block slides LV and LVI, which have the highest CVD/CHD, move by

overcoming friction along a basal slip surface and require higher basal stresses to achieve movement (Figure 3.3-10).

3.3.4 Displacement Histories

Understanding the timing of movement among all seven slides helps to discern the mechanism for movement and to determine whether the movement histories of the seven slides can be related to similar triggering (e.g., rainstorm) climatic events. It is important to note, however, that the data base for this analysis was compiled within the relatively short time period of August 1985 and October 1988. This period is just a small fraction of the entire history of each slide. The values reported here cannot be assumed to be constant nor necessarily representative of the entire slide history, and that during the evolution of a particular slide there are various movement patterns. The seven slides chosen for study not only represent a spectrum of slide types and modes of movement, but also represent slides at various stages in their evolution.

In general, substantial differences in the amount of slide displacement for each slide occurred in different seasons, and among from year to year (Figures 3.3-11 through 3.3-17). The patterns of the movement history reflect the slide type. For the slides moving predominantly by block sliding (LV), lateral spreading (LVII) and rotational block sliding (LVI), 82%, 51%, and 70%, respectively, of the average CHD occurred during the first year of the monitoring period, and decreased in each succeeding year (Figures 3.3-15, 3.3-16, 3.3-17 and 3.3-18). This pattern of movement suggests that the slide masses were stabilizing (a reduction of sliding potential) rather than building to slide again. In addition, survey data indicate that these slides move more or less uniformly as a unit, although some slides are sometimes comprised of several units decoupled from one another. For the two slides moving predominantly by disrupted translational sliding (LII and LIII), displacement rates were less variable over the entire monitoring period (between 11% and 40% of the average CHD during any one year), and the largest percentage of displacements did not necessarily occur during the first year of monitoring (Figures 3.3-12 and 3.3-13). The minor variations in HD and HDR over the three years probably reflect the process of the break up and decoupling of a single large block into several smaller blocks. In general, slides LII, LIII, LV, LVI, and LVII were

3-43

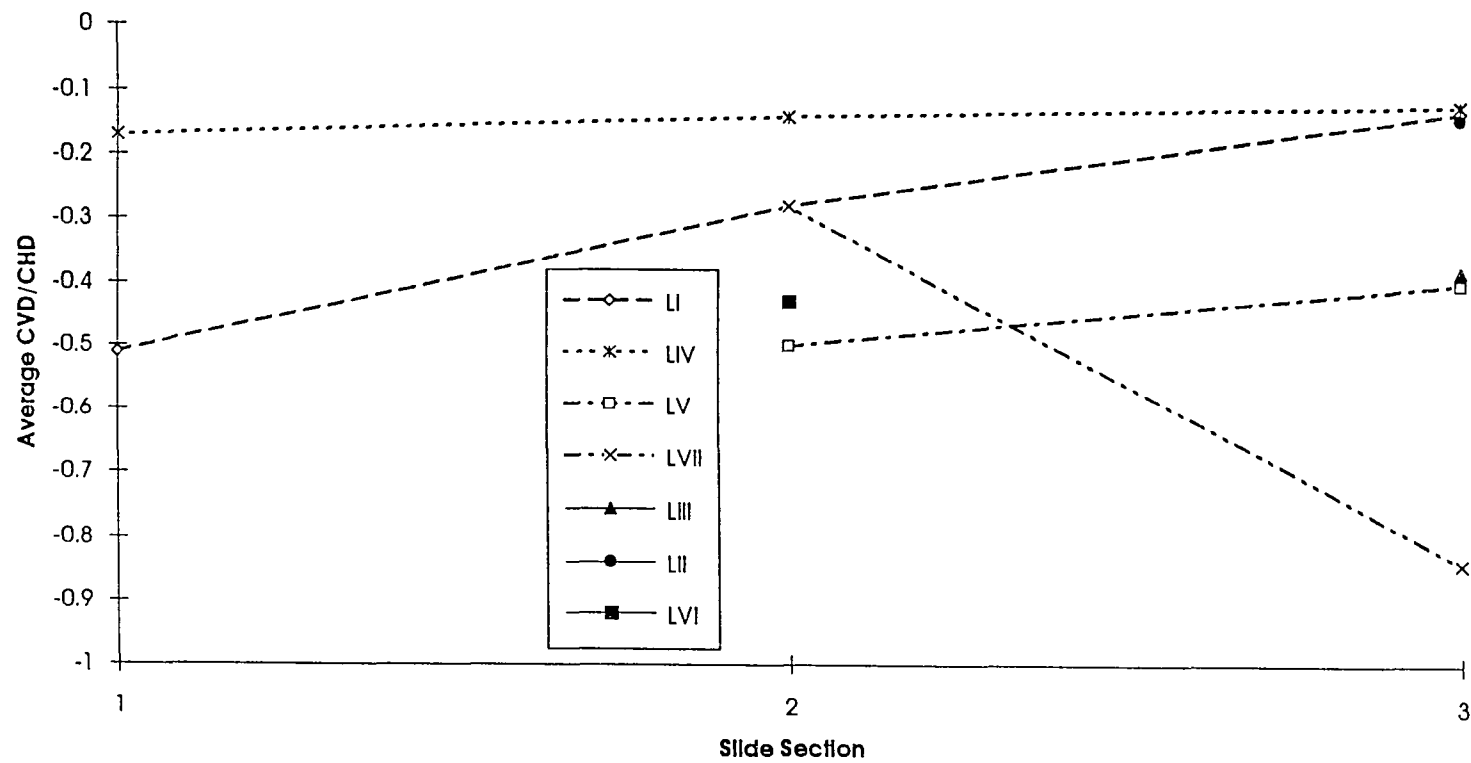


Figure 3.3-10. The average CVD/CHD for the upper (1), middle (2), and foot (3) sections of each monitored slide.

3-44

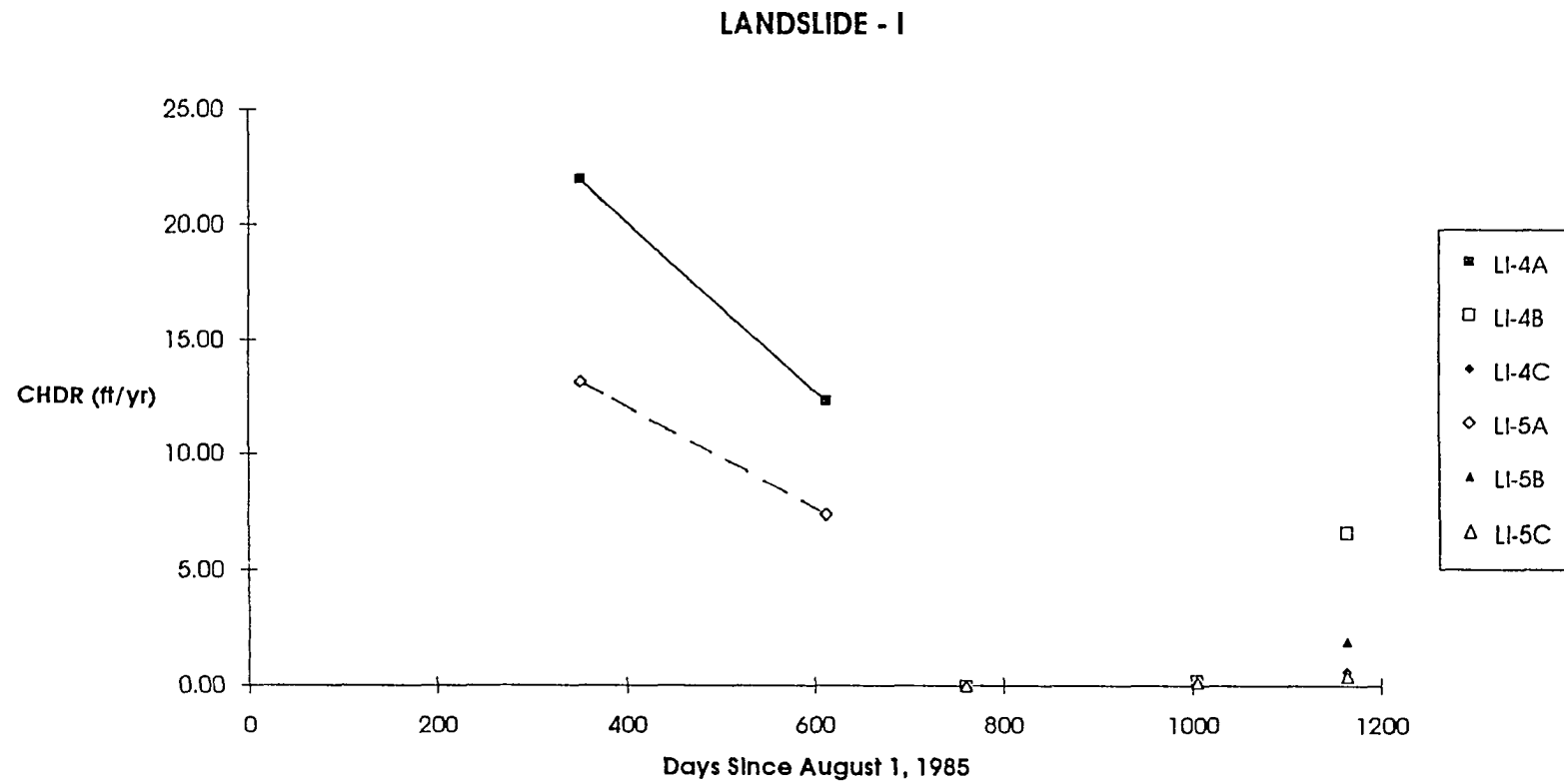


Figure 3.3-11a. Plot of cumulative horizontal displacement rate (CHDR) of LI stakes from the west foot area during the monitoring period. To make the time axis uniform, all the horizontal and vertical displacements are referenced to the number of days since August 1, 1985.

3-45

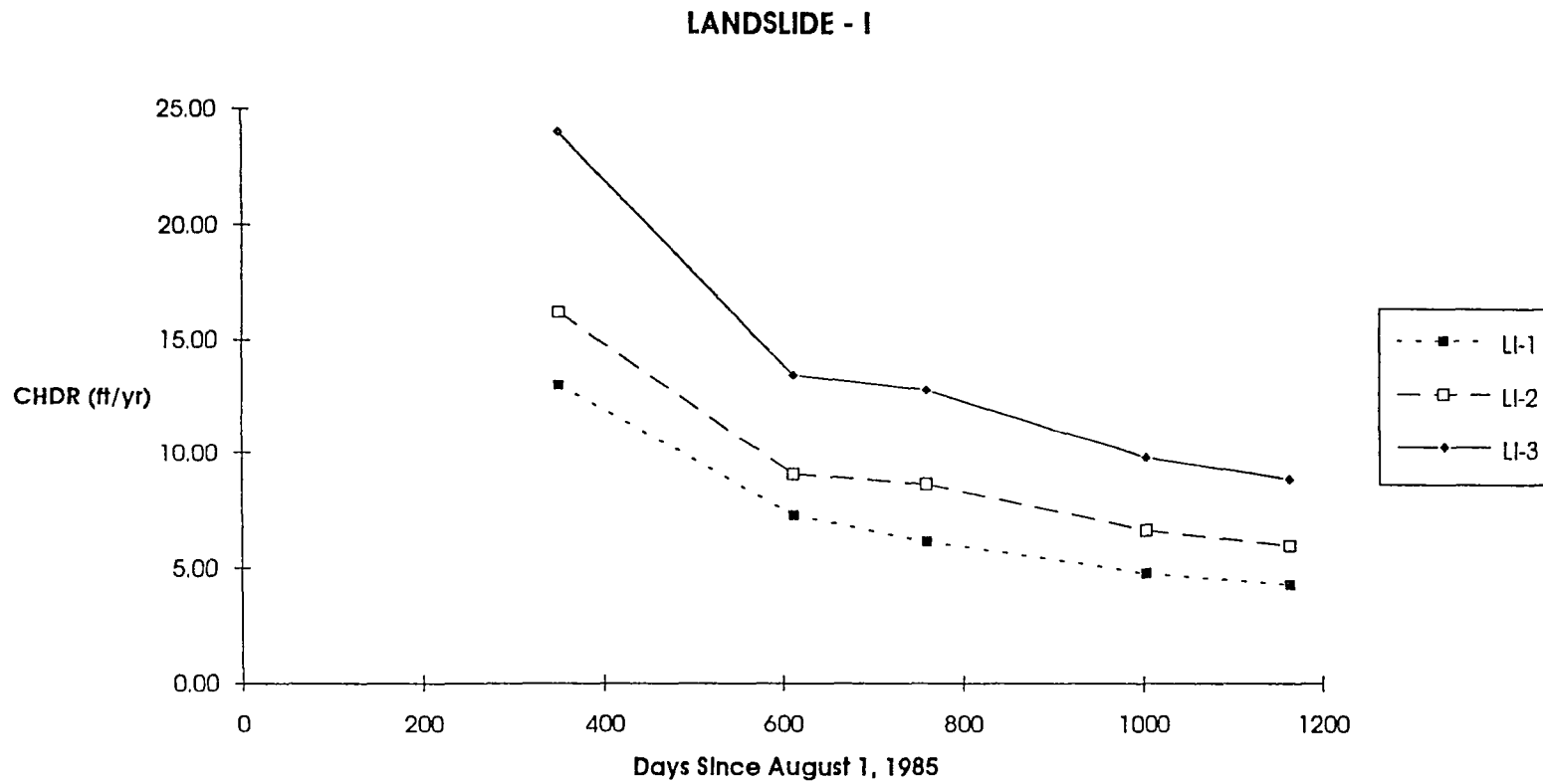


Figure 3.3-11b. Plot of cumulative horizontal displacement rate (CHDR) of LI stakes from the east foot area during the monitoring period. To make the time axis uniform, all the horizontal and vertical displacements are referenced to the number of days since August 1, 1985.

3-46

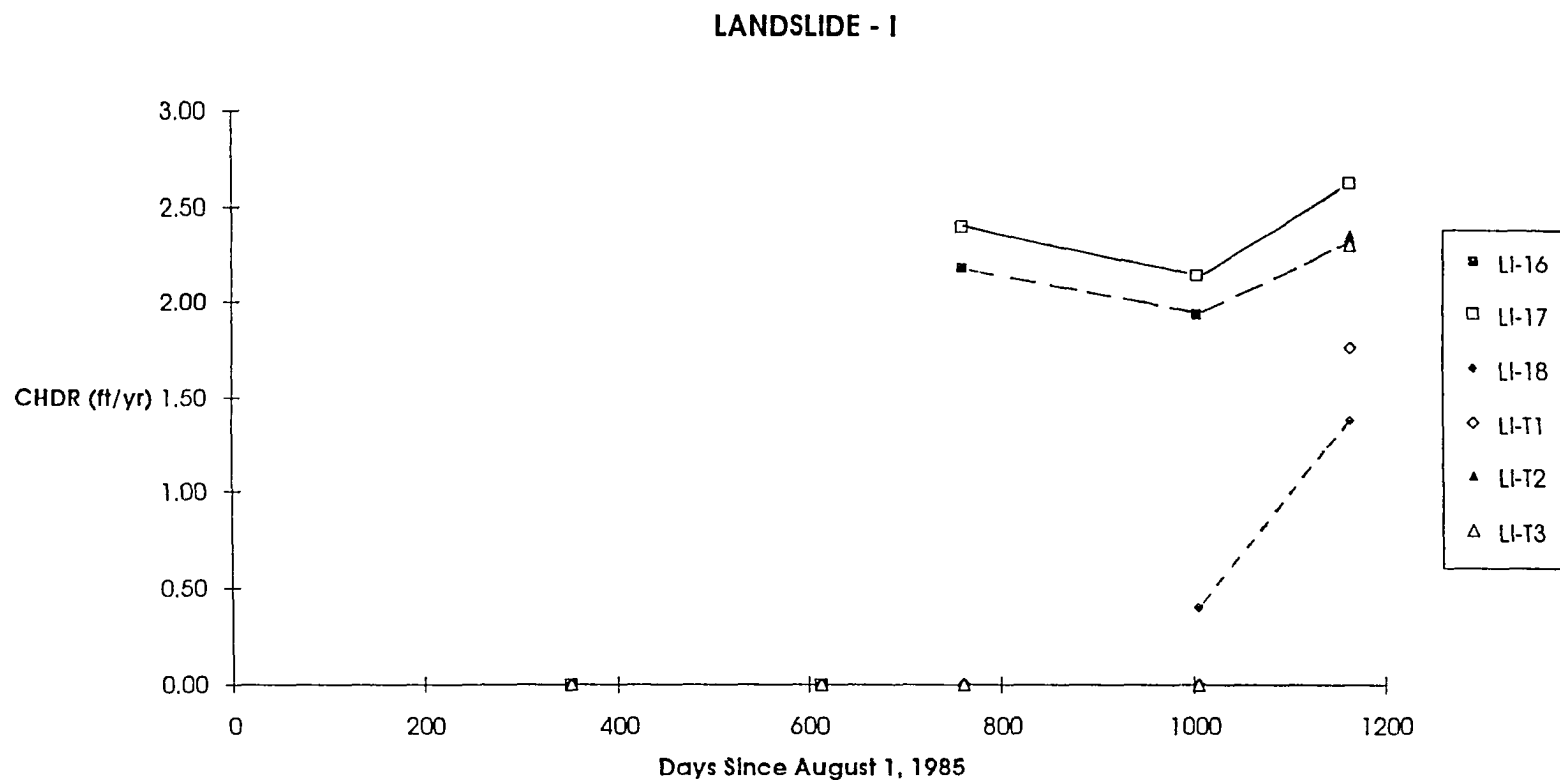


Figure 3.3-11c. Plot of cumulative horizontal displacement rate (CHDR) of LI stakes from the center mid section during the monitoring period. To make the time axis uniform, all the horizontal and vertical displacements are referenced to the number of days since August 1, 1985.

3-47

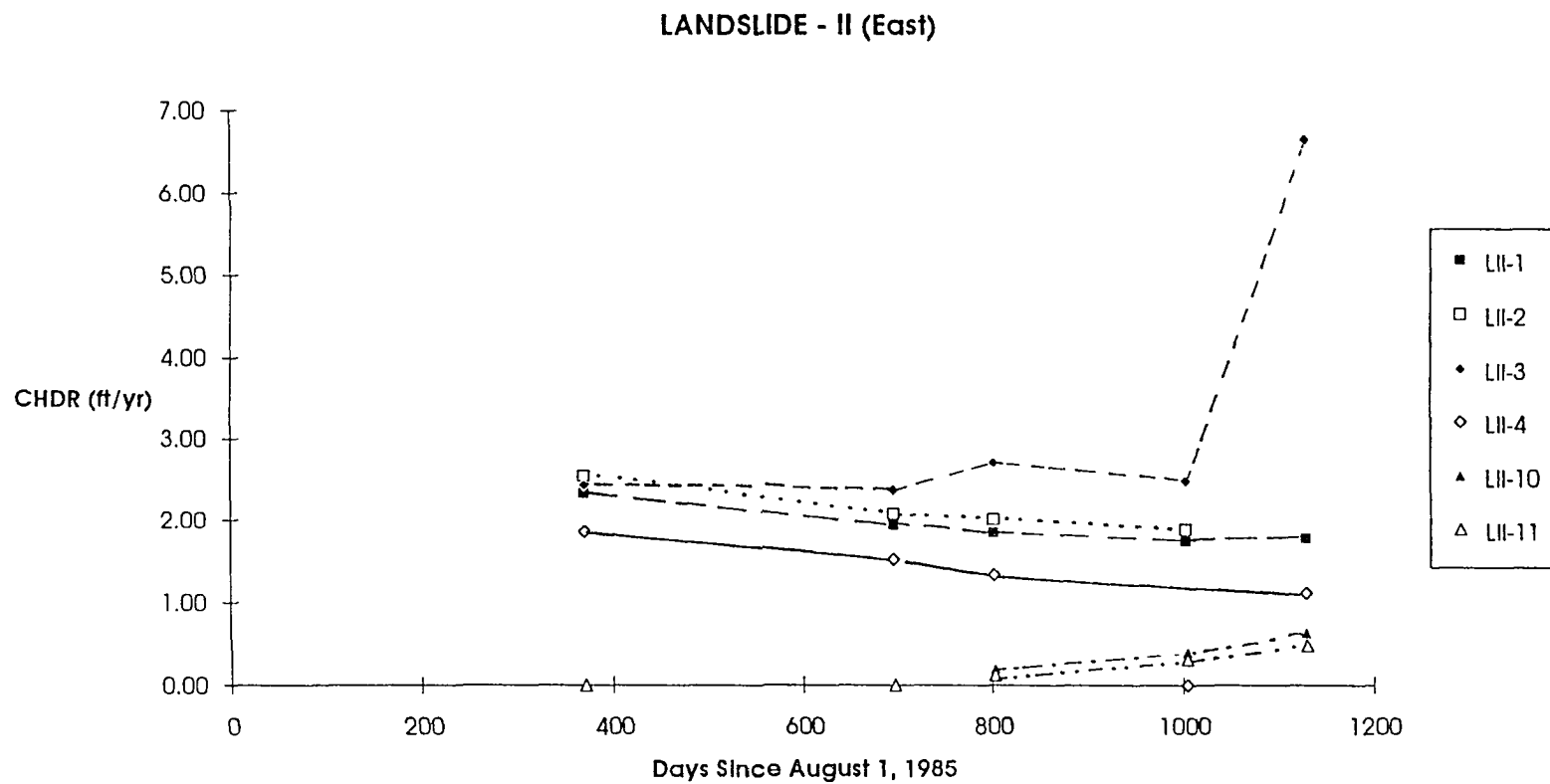


Figure 3.3-12a. The cumulative horizontal displacement rate (CHDR) of LII stakes from the east foot area during the monitoring period. To make the time axis uniform, all the horizontal and vertical displacements are referenced to the number of days since August 1, 1985.

3-48

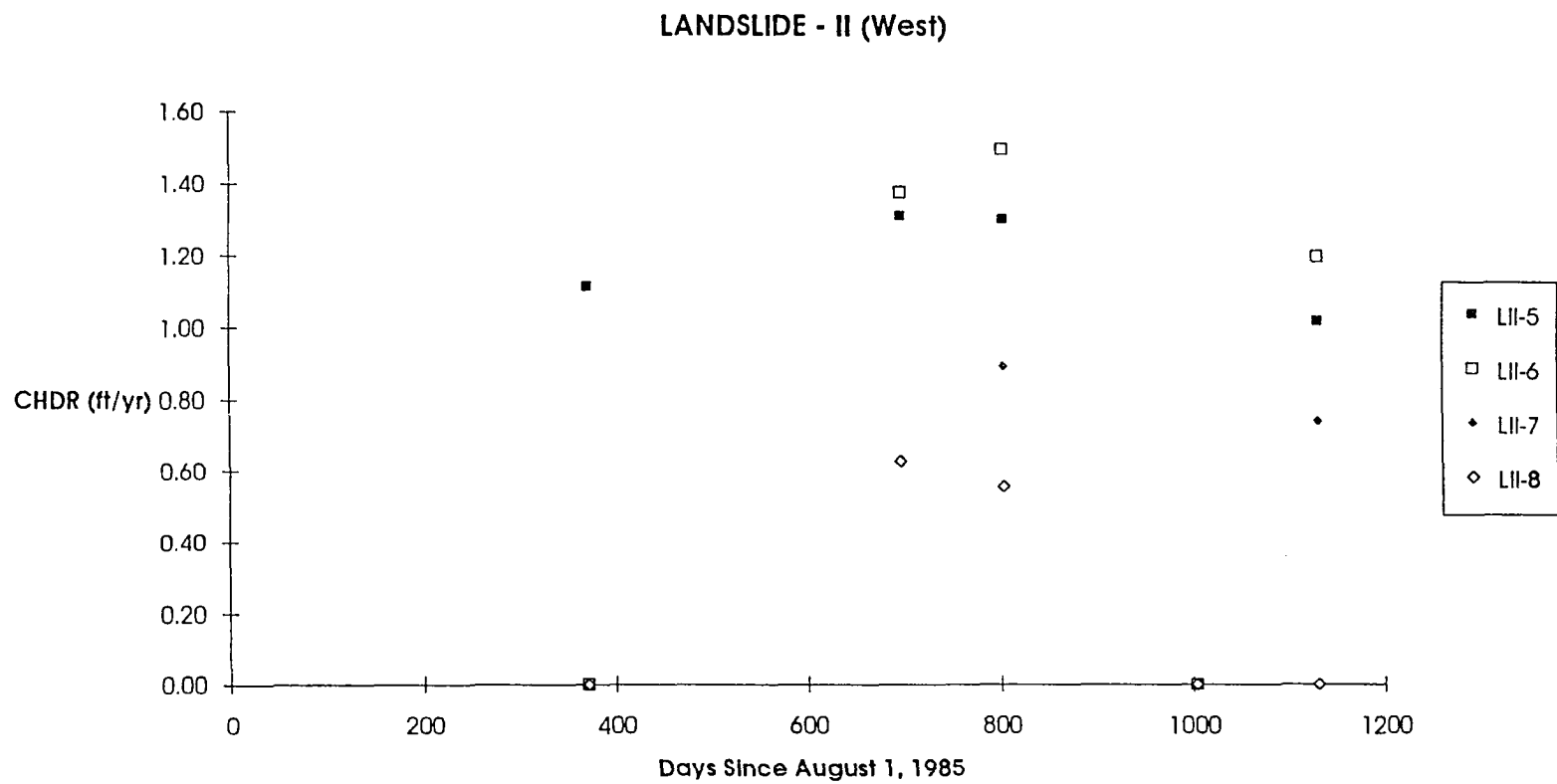


Figure 3.3-12b. The cumulative horizontal displacement rate (CHDR) of LII stakes from the west foot area during the monitoring period. To make the time axis uniform, all the horizontal and vertical displacements are referenced to the number of days since August 1, 1985.

3-49

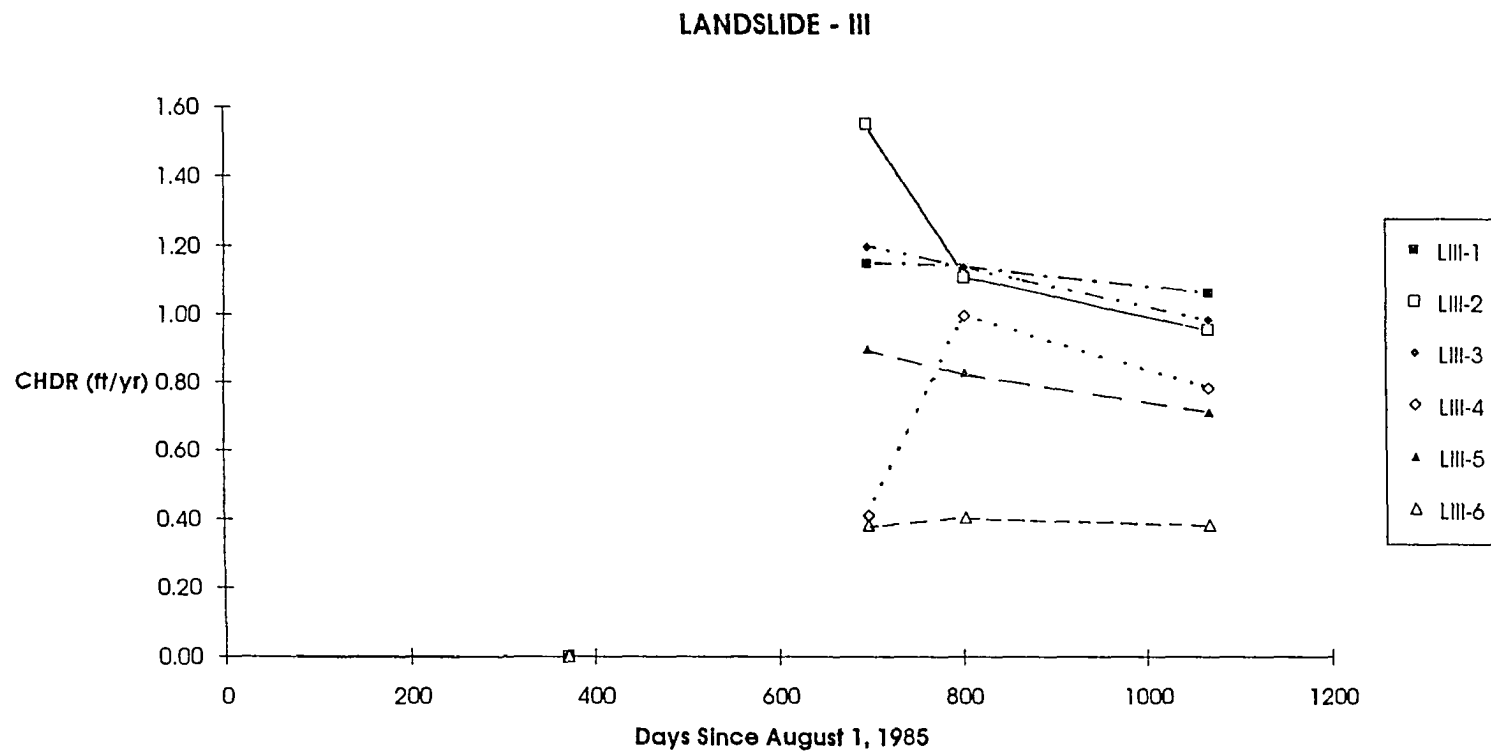


Figure 3.3-13. The cumulative horizontal displacement rate (CHDR) of all the LIII stakes during the monitoring period. To make the time axis uniform, all the horizontal and vertical displacements are referenced to the number of days since August 1, 1985.

3-50

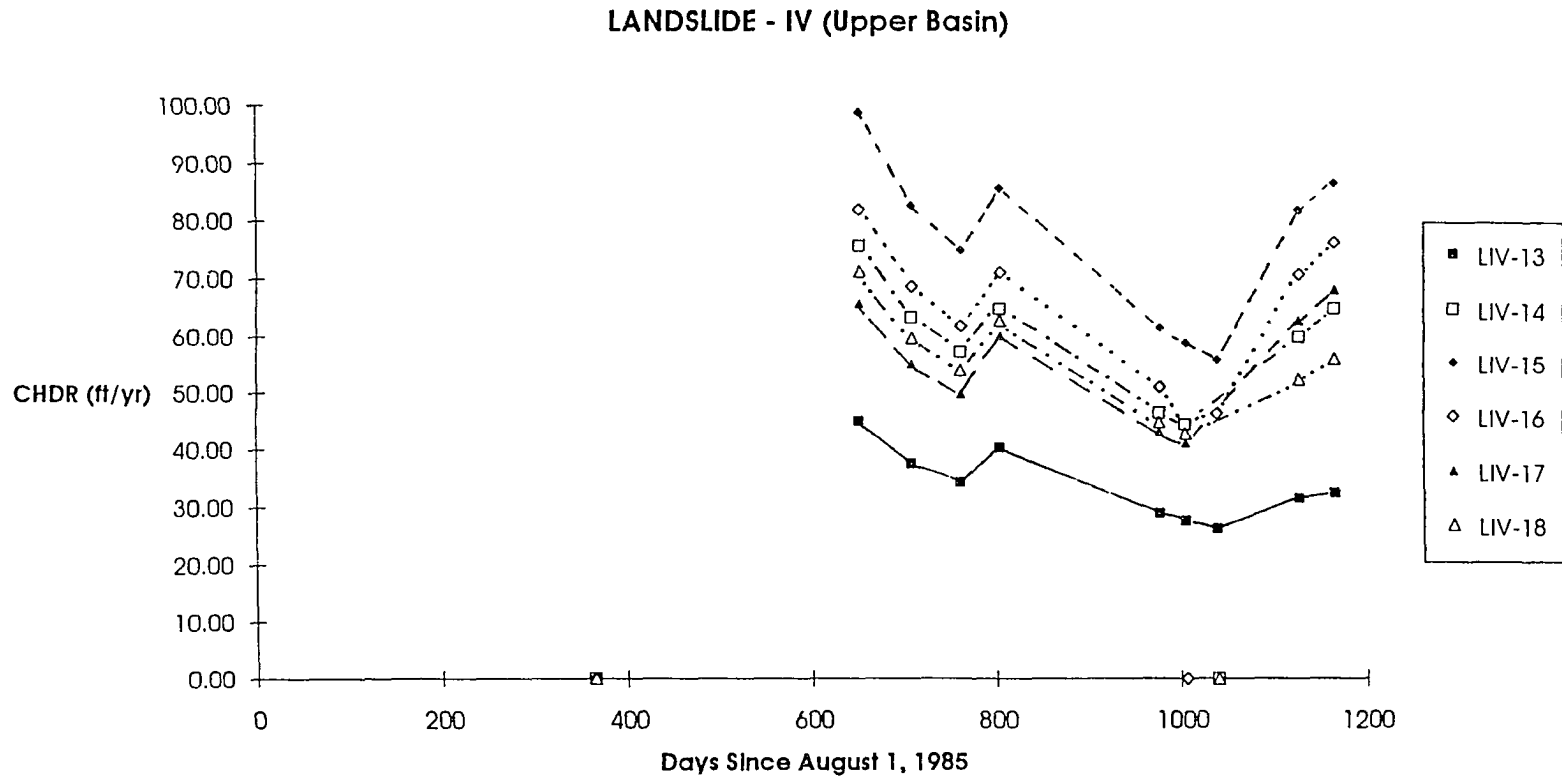


Figure 3.3-14a. The cumulative horizontal displacement rate (CHDR) of LIV stakes from the upper basin during the monitoring period. To make the time axis uniform, all the horizontal and vertical displacements are referenced to the number of days since August 1, 1985.

3-51

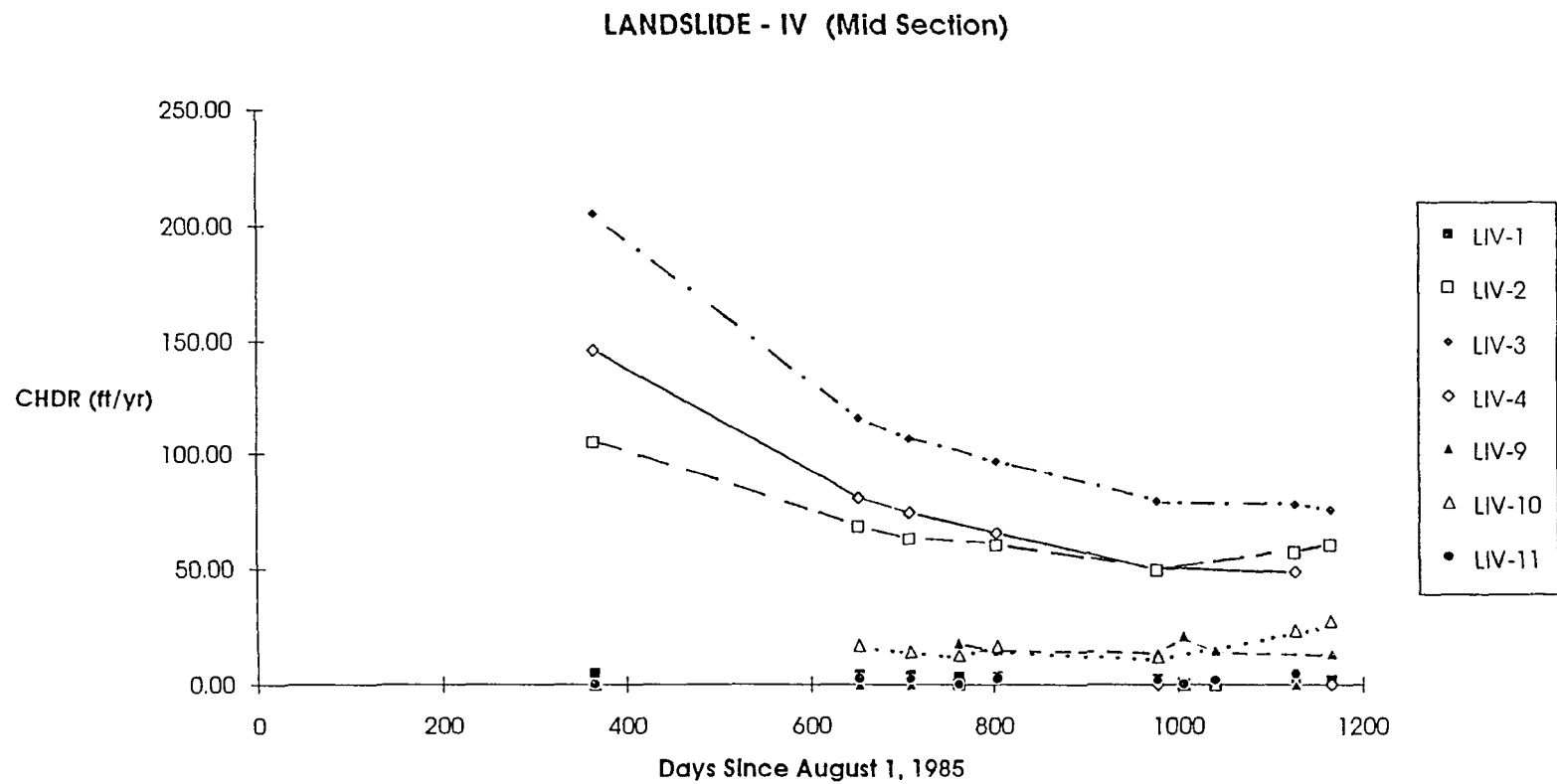


Figure 3.3-14b. The cumulative horizontal displacement rate (CHDR) of LIV stakes from the mid section during the monitoring period. To make the time axis uniform, all the horizontal and vertical displacements are referenced to the number of days since August 1, 1985.

3-52

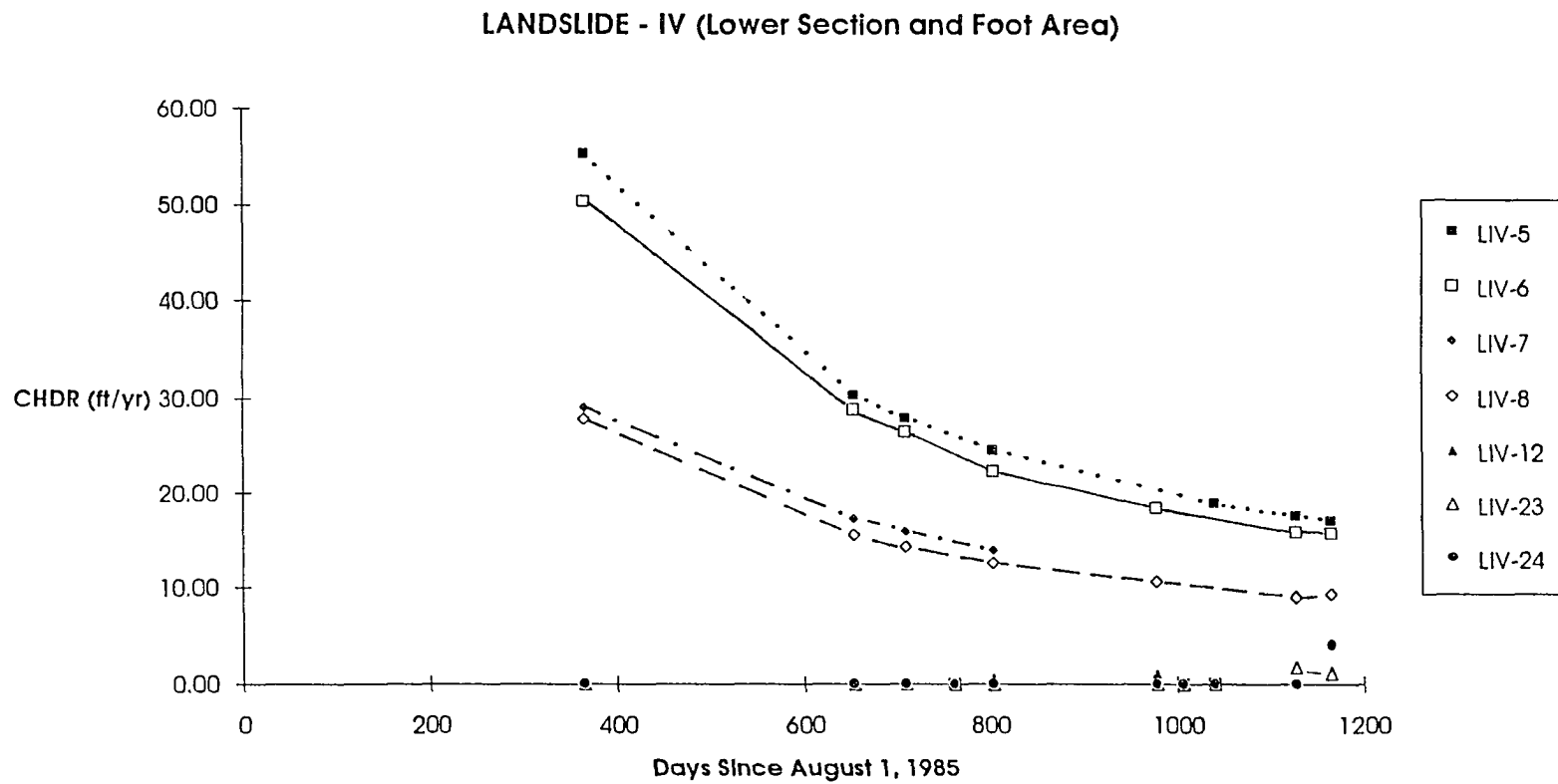


Figure 3.3-14c. The cumulative horizontal displacement rate (CHDR) of LIV stakes from the lower section and foot area during the monitoring period. To make the time axis uniform, all the horizontal and vertical displacements are referenced to the number of days since August 1, 1985.

3-53

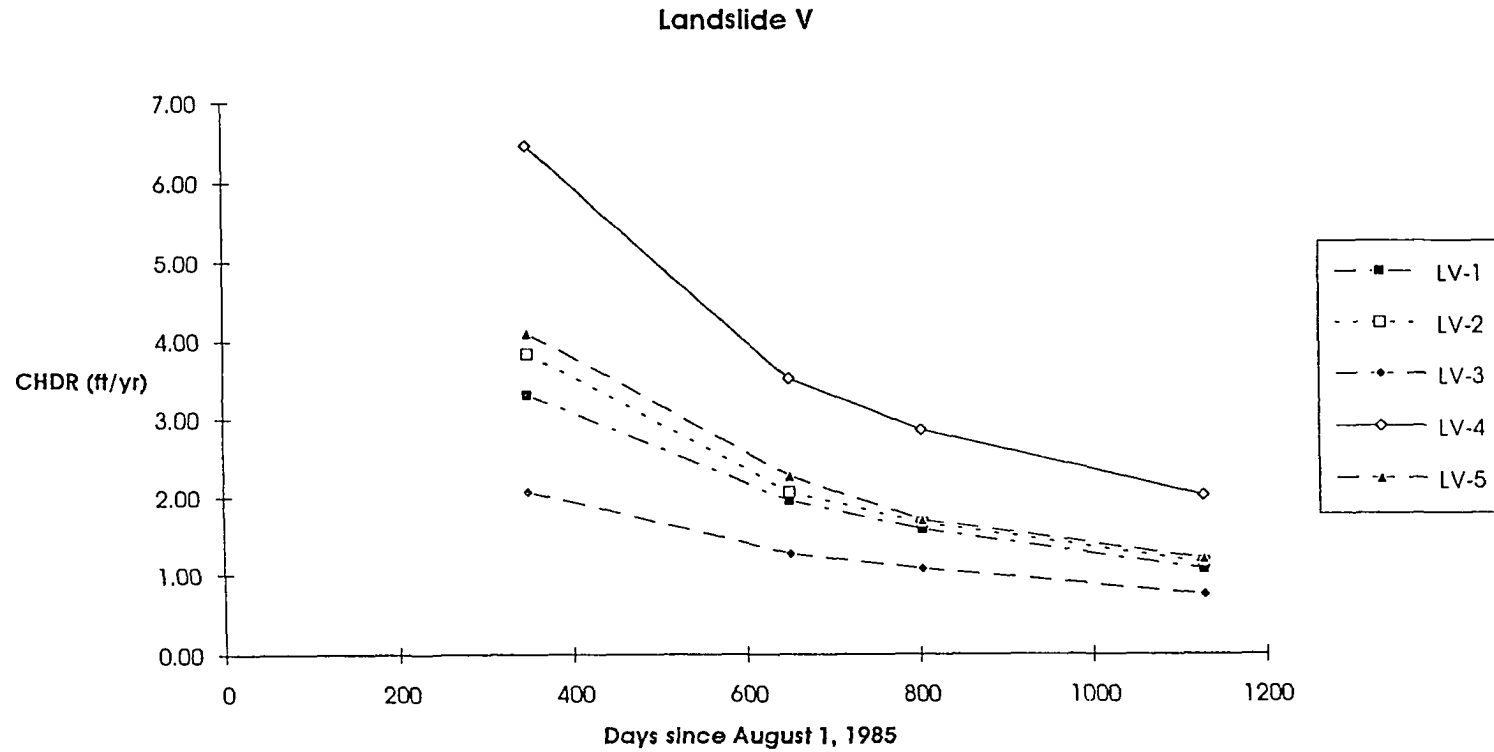


Figure 3.3-15. The cumulative horizontal displacement rate (CHDR) of all the LV stakes during the monitoring period. To make the time axis uniform, all the horizontal and vertical displacements are referenced to the number of days since August 1, 1985.

3-54

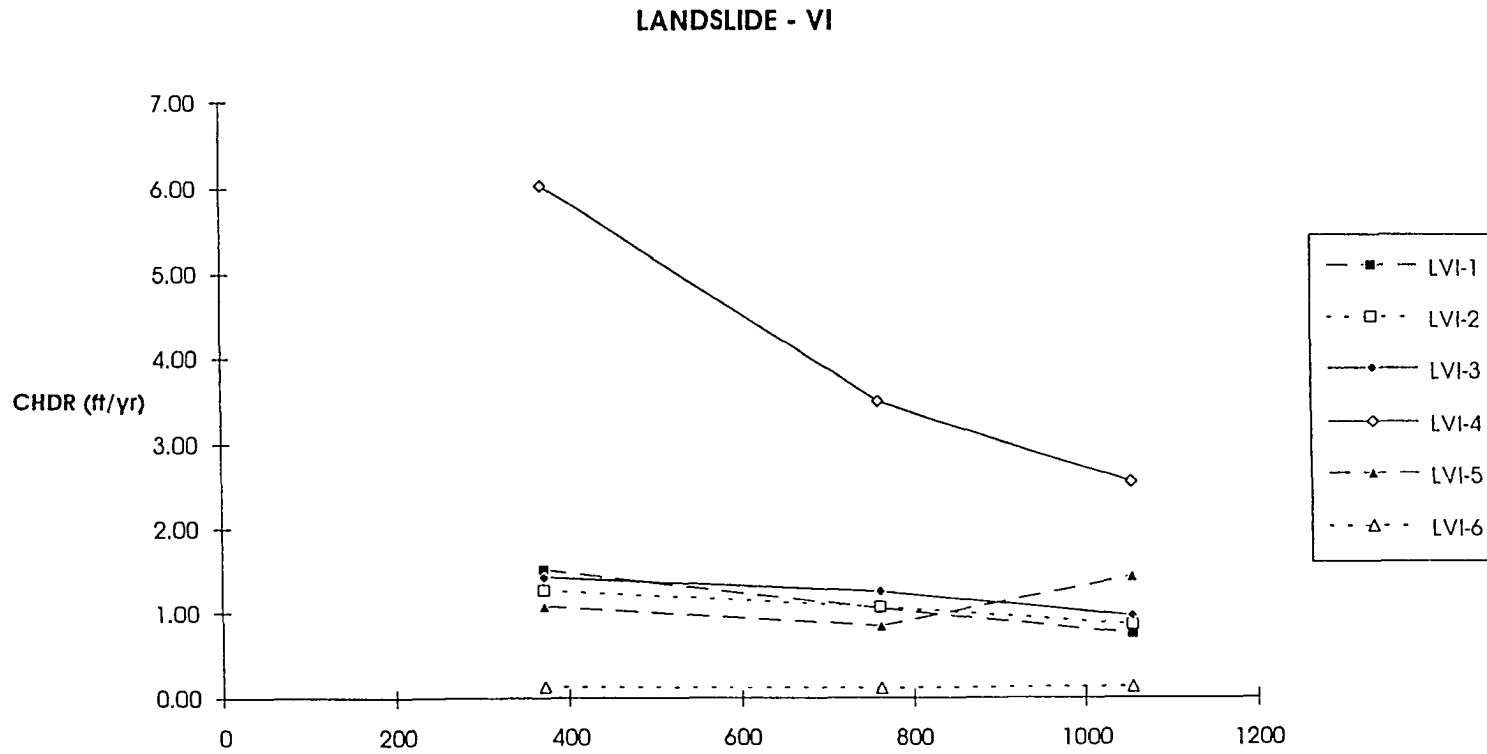


Figure 3.3-16. The cumulative horizontal displacement rate (CHDR) of all the LVI stakes during the monitoring period. To make the time axis uniform, all the horizontal and vertical displacements are referenced to the number of days since August 1, 1985.

3-55

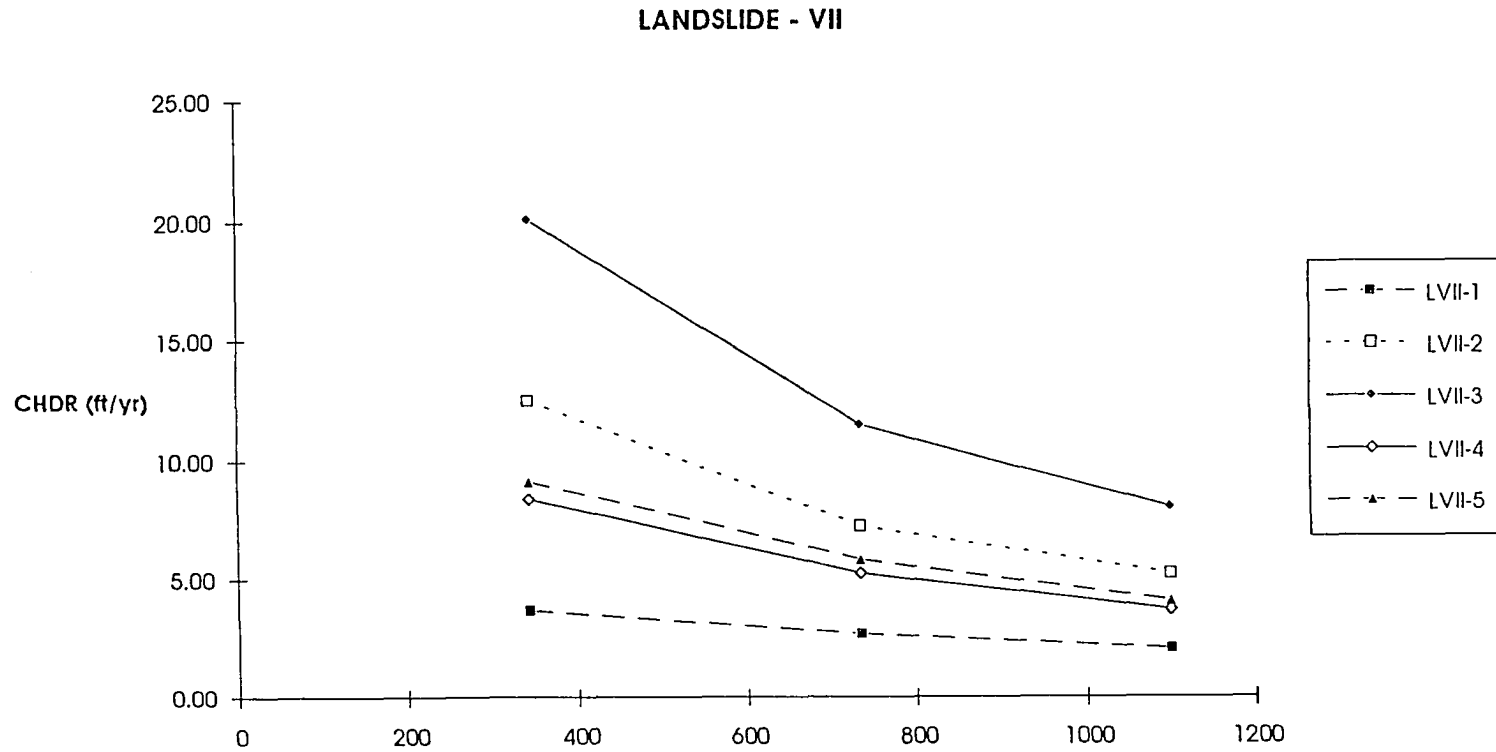


Figure 3.3-17. The cumulative horizontal displacement rate (CHDR) of all the LVII stakes during the monitoring period. To make the time axis uniform, all the horizontal and vertical displacements are referenced to the number of days since August 1, 1985.

3-56

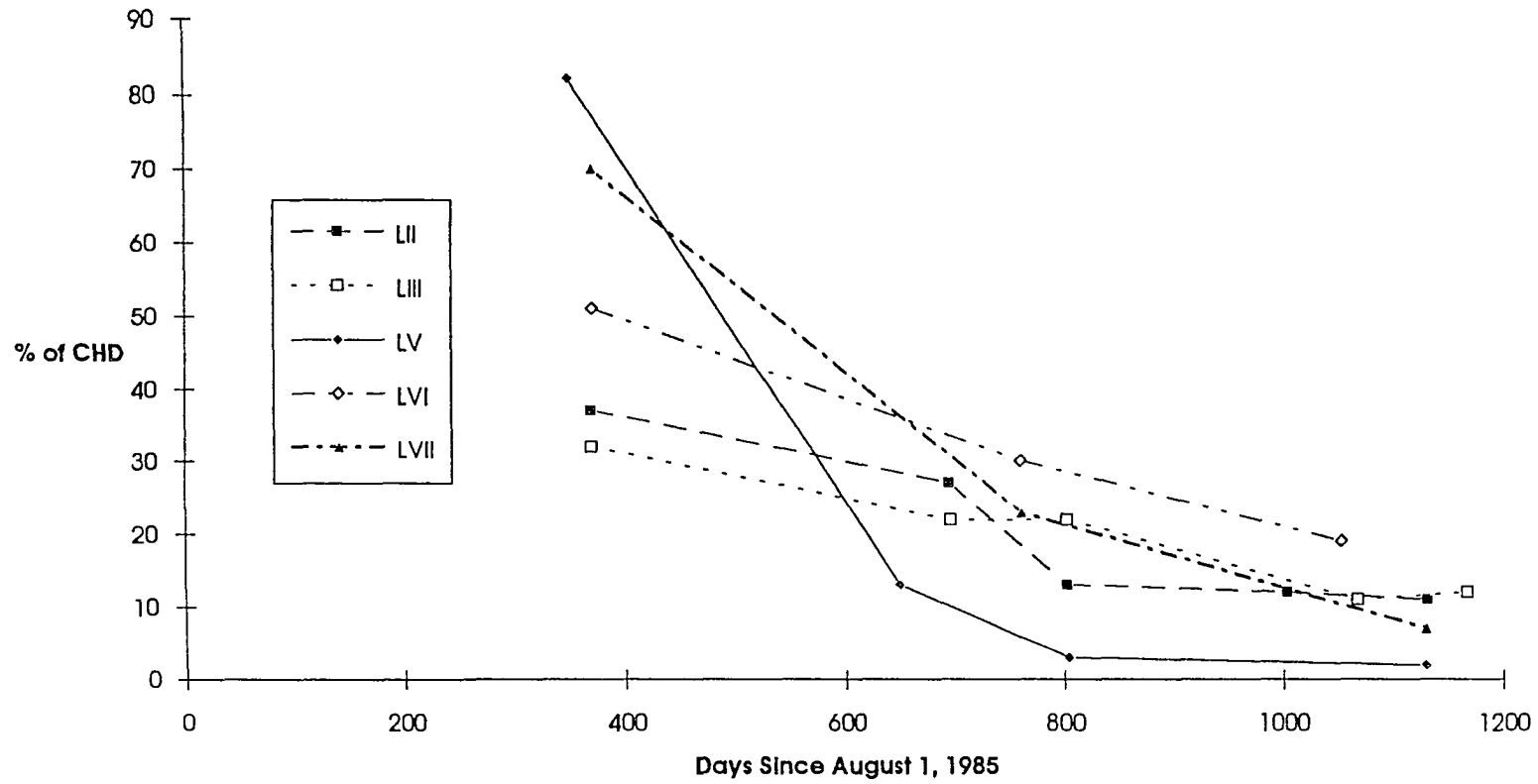


Figure 3.3-18. Percentage of Cumulative Horizontal Displacement (CHD) per year for slides LII, LIII, LV, LVI, and LVII.

not surveyed frequently enough to discern whether periods of non-movement occurred.

On the other hand, for the earthflows (LI and LIV), the temporal and spatial variability of their movement is more complex. Because the earthflow mass moves by shear deformation along grain boundaries, movement in the upper slide area is not coupled with the lower slide so that upper slide movement may not coincide with movement in the lower slide area. The timing and relationship of movements within the slide mass during adjustments in the stress field may span a year or more. In addition to the temporal variations in movement within a slide mass and the large year-to-year, and season to season variations in displacement, lengthy periods of no movement also occurred (Figure 3.3-11 and 3.3-14). At a minimum, the data document that no movement took place on LI from Day 352 (July 18, 1986) to Day 613 (April 5, 1987), while on LIV, at least two periods of no movement could be discerned, from Day 653 (May 15, 1987) to Day 804 (July 10, 1987), and from Day 978 (April 4, 1988) to Day 1040 (June 5, 1988).

3.3.5 Triggering Processes

It is apparent from Figures 3.3-11 through 3.3-18 that there is some temporal connection between the magnitude and timing of displacements among the seven slides. What geomorphic or climatic triggering events account for the apparent relatively high average displacements that occurred during the first year of monitoring in three separate slides (LV, LVI, and LVII)? In addition, why did some storms apparently have no effect on landslides, while other storms apparently triggered large displacements?

3.3.5.1 Climatic Factors

Precipitation and temperature records (see Section 2.2) were reviewed to identify possible relationships between climatic triggering events (e.g., rainstorms, breakup) and earthflow movement, a connection readily made for earthflows in other areas (Keefer and Johnson, 1983). All the rainfall events greater than 2 cm in any 24 or 48 hour period at Poker Flats (1985-1988), and Gold Run Pass (1987 and 1988) are listed in Table 3.3-11. In addition, Table 3.3-11 lists the approximate day (assuming day 1 = August 1, 1985) when freeze-up, winter, break-up and

Table 3.3-11. Summary of significant rainfall events and movement of LI and LIV.

DATE	SURVEY	POKER	POKER	GOLDRUN	FIRST	LIV-UPPER	LIV-MID	LIV-FOOT	LI-UP	LI-MID	LI-FOOT
	DAY	24 hour	48 hour	48 hour	DAY OF						
31259											
9/8/85	39	2.79									
9/16/85	47				FU						
10/17/85	78				W						
4/30/86	273				BU						
5/30/86	303				S						
6/2/86	306	3.78	3.78								
7/18/86	352								NM	NM	HIGH
7/20/86	354	6.65	6.91								
7/31/86	365					NM	HIGH	HIGH-MOD			
8/20/86	385	3.56	5.49								
9/9/86	405	2.79									
9/23/86	419				FU						
10/10/86	436		2.20								
11/5/86	462				W						
3/22/87	599				BU						
3/5/87	613								NM	NM	NONE
4/25/87	633				S						
5/15/87	653					HIGH	MOD-LOW	LOW-NONE			
5/25/87	667	3.71									
6/1/87	670	3.58									
7/8/87	707										
7/10/87	709		3.30	3.30		NONE	NONE	NONE			
7/21/87	720	2.39		4.11							
7/26/87	725	0.00		2.13							
7/29/87	728	3.51	4.17								
7/31/87	730			3.35							
8/19/87	749	2.03	2.26								
9/20/87	750	5.18		2.28							
8/31/87	761								NM	MOD	MOD-LOW
9/1/87	762					LOW	LOW-NONE	NONE			
9/16/87	777			2.74							
9/28/87	789				FU						
10/13/87	804					MOD	LOW	MOD-LOW			
10/26/87	817				W						
4/4/88	978					NONE	NONE	NONE			
4/10/88	984				BU						
5/1/88	1005								NM	LOW	LOW
5/2/88	1006										
5/18/88	1022				S						
5/30/88	1034	3.51		3.05							
6/5/88	1040					NONE	NONE	NONE			
6/11/88	1046			2.74							
6/18/88	1053	3.33									
6/22/88	1057			3.05							
7/8/88	1073			3.06							
7/10/88	1075		3.30								
7/21/88	1086		3.35	5.47							
9/1/88	1128					HIGH	MOD	LOW			
9/28/88	1155				FU						
10/8/88	1165								MOD	MOD	LOW
10/9/88	1166					MOD	MOD-LOW	LOW			
10/28/88	1185				W						

Table 3.3-11. Summary of significant rainfall events and movement of LI and LIV.

DATE	SURVEY	POKER	POKER	GOLDRUN	FIRST	LIV-UPPER	LIV-MID	LIV-FOOT	LI-UP	LI-MID	LI-FOOT
	DAY	24 hour	48 hour	48 hour	DAY OF						
3/22/9											
9/8/95	39	2.79									
9/10/95	47				FU						
10/17/95	73				W						
4/30/96	273				BU						
5/10/96	303				S						
5/2/96	306	1.13	3.79								
7/15/96	352								NM	NM	HIGH
7/20/96	354	5.55	5.91								
7/31/96	365					NM	HIGH	HIGH-MOD			
8/20/96	385	3.58	5.49								
9/9/96	405	2.79									
9/23/96	419				FU						
10/10/96	436		2.20								
11/5/96	462				W						
3/22/97	599				BU						
4/5/97	613								NM	NM	NONE
4/25/97	633				S						
5/15/97	653					HIGH	MOD-LOW	LOW-NONE			
5/29/97	667	3.71									
6/1/97	670	3.58									
7/3/97	707										
7/10/97	709		3.30	0.30		NONE	NONE	NONE			
7/21/97	720	2.39		4.11							
7/25/97	725	0.00		2.13							
7/29/97	729	3.51	4.17								
7/31/97	730			3.35							
8/19/97	749	2.03	2.35								
8/20/97	750	3.51		2.29							
8/31/97	761								NM	MOD	MOD-LOW
9/1/97	762					LOW	LOW-NONE	NONE			
9/16/97	777			2.74							
9/28/97	789				FU						
10/13/97	804					MOD	LOW	MOD-LOW			
10/25/97	817				W						
4/4/98	978					NONE	NONE	NONE			
4/10/98	984				BU						
5/1/98	1005								NM	LOW	LOW
5/2/98	1006					NONE	NONE	NONE			
5/18/98	1022				S						
5/30/98	1034	3.51		3.05							
6/5/98	1040					NONE	NONE	NONE			
6/11/98	1045			2.74							
6/19/98	1053	3.33									
6/22/98	1057			3.05							
7/9/98	1073			3.05							
7/10/98	1075		3.30								
7/21/98	1086		3.35	5.49							
9/1/98	1123					HIGH	MOD	LOW			
9/28/98	1155				FU						
10/8/98	1165								MOD	MOD	LOW
10/9/98	1166					MOD	MOD-LOW	LOW			
10/29/98	1185				W						

summer began and the day when slides I and IV were surveyed. The magnitudes of displacement measured since the previous survey are ranked as follows: high (> 50% of the maximum HD), moderate (> 10% of the maximum HD), low (displacement < 10% of the maximum HD), and none (no detectable movement). In addition, refer to Table 2.2-1 for monthly temperature and precipitation data for the monitoring period.

In all, from 5 to 10 significant rainfall events occurred each year; however, the timing and spatial distribution of the events differed between the Poker Flats and Gold Run Pass stations, so that although most storms were basin-wide, some large storms may have only been local (e.g., days 667, 670, 709, 725, 777, 1046, 1053, and 1057). In addition, since neither one of the precipitation stations are located near any of the slides, certain rainfall events listed in Table 3.3-11 may not have occurred in some slide areas, or some rainfall events that occurred in the slide area were not measured. However, it is a good assumption that all the very large storms were detected and were basin-wide.

In general there is no consistent correlation between any single rainfall event and earthflow motion. High to moderate displacements were measured on both LI and LIV after the June and July 1986 storms (days 354 and 385); however, no rainfall events preceded the high to moderate displacements in LIV on days 653 and 1166. In addition, on three occasions after significant rainfall events (survey days 709, 762 and 1040), no significant displacements (none or low) were detected. Furthermore, there were five survey days recorded for either LI or LIV during freeze-up or during or immediately after break-up not preceded by a significant rainfall event (days 613, 653, 804, 1006 and 1166), when high, moderate, low or no displacements were measured.

As described earlier, when LIV was first visited in early June 1985 (prior to surveying) and then again in late May 1986 (not surveyed), its upper section was crossed by large extensional cracks; a "bergschrand" had developed as the upper section material moved away from the scarp talus. These features indicated very recent and substantial movement. By mid-summer (the first survey and on day 365), in spite of several large rainstorms, these features had mostly disappeared (i.e., erosion but not movement). Indeed, the summer rainstorms generally eroded the fresh flow features developed during the spring. Also recall that in May 1987

(survey day 653), when the slide surface again showed evidence of very recent movement, the sediment was found to be frozen about 30-60 cm below the surface even though a large crevasse field covered the entire upper section. The survey data indicate that high to moderate displacements occurred in the upper section; however, no significant rainfall event had occurred. Clearly there is no general rule that can be applied to the timing of movement with rainfall events or break-up and freeze-up periods. Other triggering processes must be operating.

Some of the displacement variability may be attributed to a more complex interaction between the timing and duration of break-up or freeze-up with rainfall events, so that the resultant volume and rate of release or retardation of the availability of liquid water may vary considerably. For example, 2.20 cm of rain fell on day 436, already 17 days into freeze-up. Much of the movement of water from this rainfall was likely retarded by snow, aufeis, ice and frozen soils, so that the soils could not effectively drain before winter set in. In this case, high to moderate displacements were measured on slide IV the following spring (day 653). In contrast, the last significant rainfall of 1987 (day 777) was 12 days before freeze-up began, so that most of this water left the soil fabric before freeze-up and winter. In this case, no displacements were measured the following spring (day 1006) during break-up, nor by the next survey day (day 1040) following a significant rainfall event on day 1034. In this case, the 1988 high to moderate displacements occurred on slides I and IV at the end of summer following as many as five significant rainfall events.

Figures 3.3-19 and 3.3-20, and Tables 2.2-1 and 3.3-11 indicate that there was a warm winter and spring during 1986-87 and 1987-88. From February to May during these years, there were many days of above freezing temperatures as well as freeze-thaw days. Winter field observations indicated that in many places the snowpacks had melted before the next snow occurred. Conversely, during the winter of 1985-86 the snowpack remained largely intact until May, when most of it melted during breakup in a relatively short time.

In summary, major differences in the magnitude and timing of slide motion may be attributed to varying climatic conditions which include major annual and seasonal fluctuations in the timing of rainfall events, the timing of break-up or freeze-up, and general weather conditions.

3-61

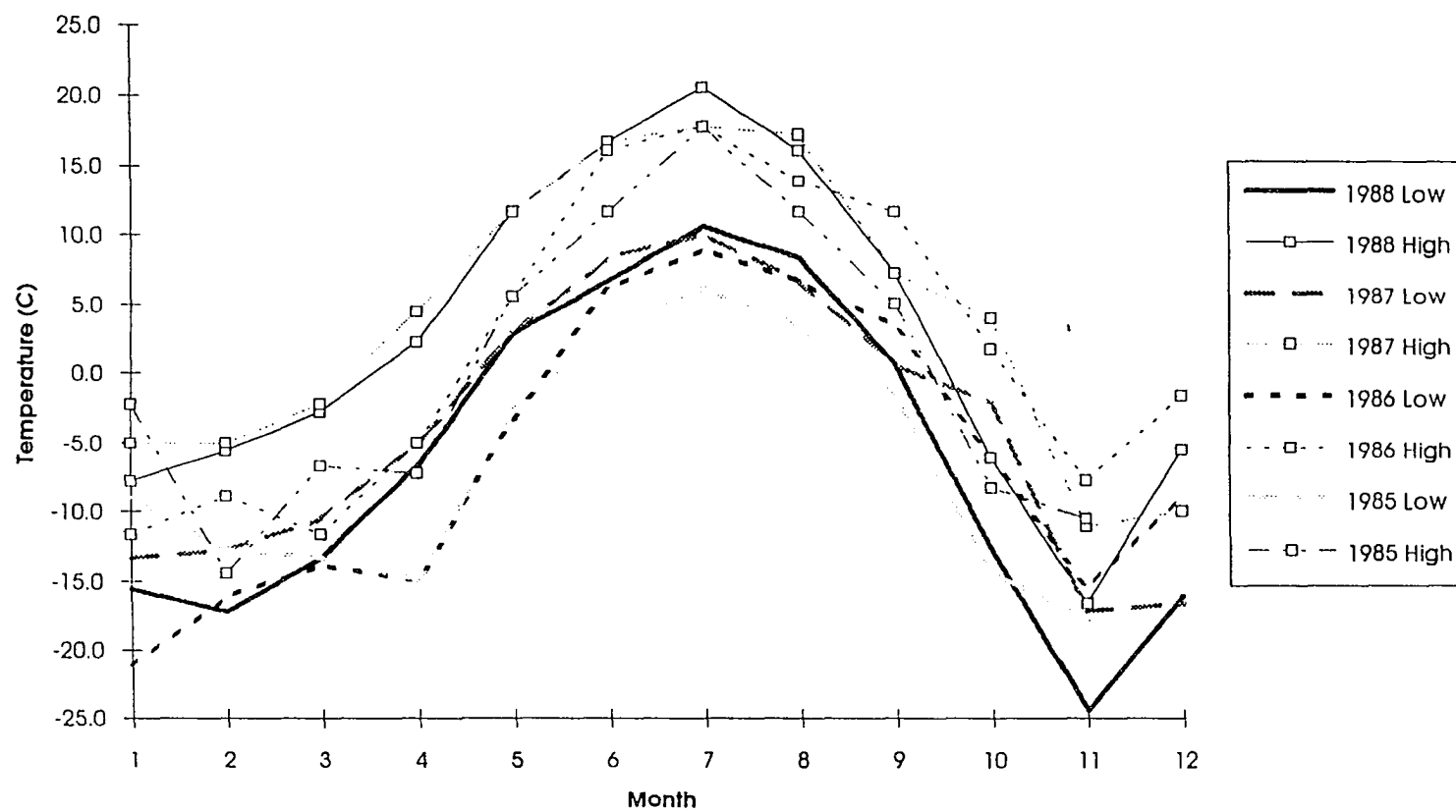


Figure 3.3-19. Plot of 1985, 1986, 1987, and 1988 mean monthly temperature highs and lows for Poker Flats.

3-62

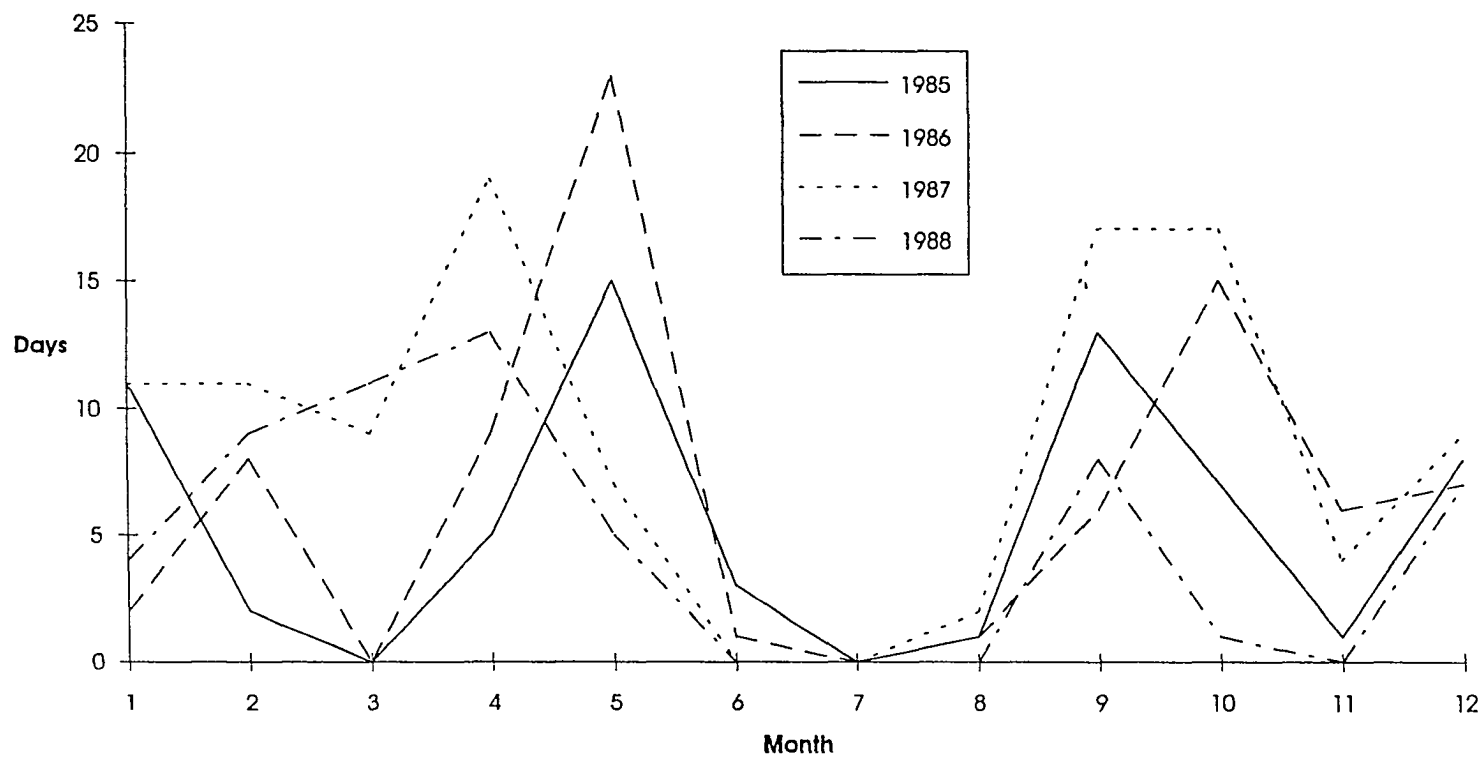


Figure 3.3-20. Plot of the number of freeze-thaw days during 1985, 1986, 1987, and 1988 for Poker Flats.

3.3.5.2 Geologic Factors

Several interactive geologic processes operate in Hoseanna Creek Watershed to either predispose certain hillslopes to failure, or serve as active agents in the initiation or continuance of hillslope movement. The prevalence of landsliding in specific areas is due to a structural predisposition to failure (gentle dipslopes with bedding dips less than the topographic slope), and the weakly consolidated sedimentary formations. The weakly consolidated Usibelli Group units contribute to lithostatic loading by grain-to-grain collapse or block toppling/falling into the upper slide basins.

There is a dynamic interaction between fluvial and hillslope processes. Slope movement is preceded by lateral corrasion of a slide toe, which is linked to channel changes induced by high runoff (migration and avulsion) in Hoseanna Creek. The timing of freeze-up of creek water and the break-up of aufeis contribute to the timing and magnitude of slope movement. The breakup of the vegetative mat catalyzes thawing of permafrost and likely results in the loss of binding strength, which further induces permafrost degradation (i.e., thermal erosion). The effect of isothermally warm permafrost is not obvious.

Some clays have freezing point depressions which would make them unfrozen while silts and sands are still frozen; this would enable the clays to behave plastically instead of rigidly in conditions just below freezing. Triplehorn (1976) gives clay compositions for all of the Usibelli Group, which include montmorillonite, and kaolinite-chlorite. These clays have freezing point depressions of up to -0.5 degrees C (Osterkamp, personal communication). Since the warm permafrost varies from 0.0 to -1.0 degrees C, it is likely that in some instances fine sand and silt are frozen, mechanically rigid, and less permeable (Chamberlain, 1985, Anderson and others, 1983) overlies impermeable, unfrozen, moist, deformable clays.

3.4 Discussion

3.4.1 Sliding Mechanics

In most cases horizontal displacements within individual slides were fairly variable (the staked locations were not uniformly sliding together) indicating that decoupling processes occur in all slides. However, the variability of direction and magnitude of motion for adjacent survey stakes was still small enough in LII, LIII, LV, LVI and LVII, and in portions of LI and LIV to suggest that a component of translational-slide motion occurs in all slides. Disrupted translational sliding (Varnes, 1978) may be especially significant in LII and LIII, where field and air (helicopter) observations indicate that large coherent blocks have fragmented into many disrupted independent blocks during downslope transit. In these slides, slow steady shearing over an undulatory surface occurs. As downslope displacement occurs, the slides begin to fragment into individual blocks. In the case of LVII, the fragmentation into many small blocks may have resulted in lateral spreading. Spreading is likely the cause for LVII to leave the dipslope and move obliquely to the dipslope on its way down to the tributary creek. Considerable oversteepening by headward incision of this tributary has catalyzed this process.

The vertical components were greatest in LV and LVI (as indicated by higher VHD/CHD ratios), and reflect the late stage erosion and general denudation of LV and the dominant downward component typical of rotational slump blocks in LVI. The CVD/CHD ratios were lowest in the earthflows and reflect low-angle basal shearing accompanied by plastic flow.

Earthflow processes (Keefer and Johnson 1983) predominate in LI and LIV, where rates of motion are greater and highly variable throughout the slide. Displacement in these slides is dominated by low-angle episodic surge-like movements; they undergo plug flow with considerable lateral and basal shear and internal granular displacements with minor to no block-like sliding. In all cases, slide mechanics are somewhat complex in that the predominance of a particular sliding mechanism reflects the lithologic, structural and permafrost characteristics of a given hillslope. For example, in the earthflows LI and LIV, movement in the upper section was much greater than in both the mid-slide and the lower slide areas, which are covered by furrows and ridges indicative of thickening and compression. In these

lower slide areas, lateral spreading occurred at the toe of LI and the foot of LIV, as indicated by the divergent horizontal displacement vectors (Figures 3.3-1 and 3.3-4).

3.4.2 Temporal Processes

3.4.2.1 Earthflows

The reasons for annual and seasonal differences in earthflow motion, and apparent insensitivity of the earthflows to major summer rainstorms are not obvious, although the data suggest that liquid water content (as compared to ice content) must reach a threshold value to initiate movement. Most models of earthflows envision a direct connection between precipitation and motion (Keefer and Johnson, 1983). However, seasonal earthflow motion in the subarctic may reflect additional processes.

Generally, continual earthflow/slide activity requires that the normal stress (lithostatic load) is maintained above or near a critical threshold, which here would mean a more or less episodic, but continual long-term supply of sediment from headscarp retreat. In this case, headscarp erosion appears to be accelerated during the winter and spring when freeze-thaw processes are most efficient. Thus lithostatic loading of the upper slide occurs through the winter and spring (Wahrhaftig, 1987), when most of the slide's surface skin (presumably the top 2-3 m) is frozen (Hutchinson and Bhandari, 1971). Second, stream erosion and debuttreasing of the toes of landslides are very active in spring. Streams carrying away snowmelt can periodically flow on aufeis 1-2 m above the summer creek channel, resulting in an especially efficient means of lateral corrasion. The maximum tangential stress occurs when the toe buttress (aufeis) is first melted and hydrostatic stress (i.e., piezometric surface) is highest. This usually occurs during the waning stages of spring break-up (Scott, 1978; and Kane, 1981). In effect, the thick aufeis serves as an effective buttress during the winter and early spring, but as it melts much of the landslide's toe support is removed.

As indicated by local climate data, high displacements in spring can be correlated with the coincidence of significant rainfall during freeze-up, or the occurrence of significant late spring rainfall during or after a late break-up. In addition, high

displacements in late summer followed many rainfall events. In every case, high pore pressures likely initiated movement. High pore pressures were attained by dumping a lot of water onto a freshly thawed and open soil fabric in a short period in June 1986, by releasing wintertime bound water in May 1987, and by the slow steady rise of the piezometric surface in September 1988.

Although soil conditions (e.g., temperature, ice content, and pore pressure) were not measured, the timing of motion and climate data suggest that the observed seasonal variation in motion may also reflect seasonal variations in the mechanical strength of the earthflows. Throughout winter the slide mass freezes downward. In the spring the slide mass begins to thaw unevenly with zones of open soil fabric down to the shearing zone. Prior to complete thaw consolidation, large amounts of water may be introduced from rain and/or snowmelt. The earthflows are easily mobilized when the water has infiltrated the open fabric and exceed threshold pore pressures. Later in the year, earthflow movement is less likely because motion and thaw consolidation have remolded the clayey material giving it greater mechanical strength. Because the slide mass is thawed, infiltration is more common throughout the slide, and the slide mass can accept more total water; thus the rate of pore pressure rise is less for the same volume of water introduced to the slide. In addition, if the slide mass has attained higher mechanical strength, then rapid displacement in the late summer may require higher pore pressures. Also, once the slide has moved, critical thresholds may be different and have to build again.

3.4.2 Block Slides

The survey data for Landslides II, III, V, VI and VII are not sufficiently frequent to determine whether periods of no movement occurred. Although it is logical to assume that wintertime motion is negligible, this still needs to be demonstrated. The movement history of these slides does not have any obvious connection to temporal processes, most likely because the monitoring period was too short to discern any connections. In addition, because displacement rates are slower in block slides, their movement history is less sensitive to single precipitation events. Movement in these slides probably correlates with longer term precipitation and temperature conditions.

Based on the observed physical characteristics, the block slides have wider, deeper

shear zones that need more water to reach critical thresholds. Based on the sediment type and physical characteristics observed at the surface (e.g., permafrost) and the higher overall CVD/CHD, they likely have higher basal shear strength and as such need higher pore pressures to fail. In addition, for those slides in permafrost terrain (LII, LIII, and LV), clay strength is greater when frozen or partially frozen. Permafrost degradation is a steady and slow process, and the loss of clay strength may take several years. Reactivation of these slides may be more dependent on geomorphic factors such as the loss of toe buttress by the seasonal break-up of aufeis, or the sudden avulsion of creeks to new channels during high runoff events that can laterally corrade a toe buttress.

3.5 Summary of Motion and Development

The initiation, development and long term evolution of mass movement failures within Hoseanna Creek Watershed have likely gone through several cycles during the Holocene. The existing climatic, tectonic and fluvial environments have aggravated lithologically and structurally predisposed hillslope areas to attain a considerable landslide density.

Several synergistic surficial processes have operated in the slides in Hoseanna Creek Watershed, including all the surveyed slides. These include:

- 1) Lateral corrasion (e.g., LI, LII, LIII, LV, and LVII) or headward incision by streams (e.g., LIV, LVI and LVII) oversteepened slopes. In some slides (e.g., LI, LII, LIII, LV and possibly LIV), the oversteepening initiated surficial skin failures and reduced the vegetative protection of the frozen dipslope sedimentary substrate. The oversteepening initiated incipient creep in all cases; extensional cracks developed upslope, headscarps formed and exposed more frozen sedimentary substrate (if present) to thermal degradation.
- 2) Weakly consolidated sandstone and silt fracture parallel to the headscarp walls (e.g., LI, LIV, LVI, and LVII). Winter and spring freeze-thaw processes opened cracks and caused large, frozen sediment blocks to fall to and lithostatically load the upper sections, where they thawed, if frozen, and disaggregated quickly into a chaotic jumble in earthflows (e.g., LI and LIV) or

remain intact for most of the slide history (e.g., LV and LVII).

3) During the winter, the slide masses freeze and have higher mechanical strength, liquid water is not available to increase pore pressures. In addition, stream channel aufeis grows and buttresses the toes of slides (e.g., LI, LII, and LIII).

4) During spring, earthflow material thaws nonuniformly and creates preferential pathways for water to reach shear zones and build pore pressures at higher rates than during summer time. Liquid water from break-up or early season rainfall events readily saturates the semi-frozen material. The majority of snowmelt precedes channel aufeis break-up, so that due to aufeis damming, water released into soils contributes to a higher piezometric surface and higher internal pore pressures. Thus the timing of loading relative to water availability provides a mechanism to inhibit or catalyze slope failures.

5) Local pore pressures rise in the chaotic sandy-silty-clayey material of earthflows and reduce shear strength. In some places, coal beds lying directly on clay beds act as aquifers and may introduce groundwater into soft clays at the base of the slide mass.

6) The removal of thick aufeis during spring and early summer debuttresses slide toes. The earthflows/slides are now especially prone to motion when a critical threshold is reached; the degree of movement is dependent on the amount of the new lithostatic load and the level of the piezometric surface. In the earthflows, there is rapid basal and lateral shearing, forming extensional crevasses perpendicular to movement in the upper basin and compressing older slide material into large hummocky furrows and ridges at the toe of the slide.

7) Generally, after substantial episodes of movement during any given year, high pore pressures attenuate. If the slide is not lithostatically loaded (i.e., loading commonly occurs during winter and break-up by block frost wedging) and pore pressures are lower than critical thresholds, failure and movement are not likely.

3.6 Summary and Conclusions of Landslide Movement and Evolution

Four major types of slides were investigated in Hoseanna Creek Watershed, including translational earth block slides, rotational block slides, earthflows and lateral earth spreads. In most cases, individual slides are characterized by more than one type of movement and are thus termed complex. In addition, each slide has a history that may include the evolution from one type of slide to another, typically from the more coherent types (block slides) to the more disrupted types (earthflows). Seven slides were surveyed at different stages of landslide development; for example, LIV was experiencing rapid growth during an early stage, while LV was experiencing movement typical of a late stage. The other five slides appear to have movement and physical characteristics typical of midstage. In all the slides, field and photo evidence suggest episodic activity when new slide material is added or when climatic triggers reach critical thresholds. The activity ranged from the slowest for LV and LVII, which had imperceptible movement indicative of rotational or block slides, to the fastest for LIV and LI, which reflects the rapid deformation typical of earthflows

Unique climatic and geomorphic processes operate in the subarctic. Although sliding occurs outside the subarctic, the permafrost terrain and Alaska climate produce processes not found in warmer climates that delay or precipitate failure. Freezing/thawing fronts affect soil strength and permeability; break-up/freeze-up processes affect the timing of the supply of water to the slide mass, and affect the development or breakdown of aufeis in the creeks. Typically the aufeis lasts longer than snow on the hillslopes in spring, but is the last thing to freeze in the winter (precedes snow build-up) (Kane, 1981).

Hillslope denudation rates are spatially and temporally dependent on episodic climatic and geomorphic triggers, and are a function of the stage in the cycle of a slide mass. Resurgent activity is less likely if no new material is added to the slide mass. The long-term evolution of slide masses within Hoseanna Creek is dependent on

- a) the lithologic resistance to denudation (e.g., differences between schist and sedimentary units, and the differences among sedimentary units);

- b) the prevailing east-west structure and resultant valley asymmetry;
- c) the subarctic climate (i.e., long cold winters and short warm summers, cyclonic summer precipitation patterns),
- d) the spatial distribution of discontinuous permafrost terrain, and
- e) tectonism (i.e., induced local base level changes).

Landsliding in the Hoseanna Creek Watershed is a significant part of natural erosion here, and delivers large amounts of sediment to the local streams. Because of continuing landslide activity, the poorly consolidated Tertiary rocks are constantly exposed to erosion. Where permafrost is present, the sliding exposes the frozen bedrock to thawing, collapse and disintegration, further increasing erosion.

Permafrost degradation leading to slope failure has occurred in LI, LII, LIII and LV, and possibly in LIV. In these slides, lateral migration of Hoseanna Creek into their toe regions resulted in incipient failure which initially exposed the permafrost, leading to its continued thermal degradation. Headward extension into permafrost terrain exposed frozen substrate, leading to collapse of the unlithified sediments or separation of frozen blocks within the upper slide section. These large coherent blocks of previously frozen ground have broken off from the headscarp along major fractures that parallel the vertical scarp. Thawing blocks have moved downslope and stayed fairly intact (e.g., LV), disintegrated into many blocks (e.g., LII and LIII), or became totally disaggregated and provided material for earthflows (e.g., LI and LIV)

Many other slides occur in Hoseanna Creek Watershed. Some are inactive and considerably older than 1949; and some are presently very active and were much more active less than 20 years ago. Episodic hillslope processes follow with some time-lag to changes in the grade of Hoseanna Creek. When the Hoseanna Creek fan is building into the Nenana River, the overall slope of the fan (and lower reach of Hoseanna Creek) decreases; this grade adjustment at the mouth moves upstream over time causing further adjustment in the hillslopes and tributaries. Thus, it is likely that the creeks active in the headwaters of Hoseanna Creek Watershed are now responding to a change in the Hoseanna Creek fan that occurred 1000-2000

years ago, based on the bracketing ages for the top and bottom of the Hoseanna Creek Fan (see Section 2.3). The higher portion of larger and inactive slides occur in the lower basin and may reflect this timing. If the Hoseanna Creek fan has a 2000-year cycle, there may be a similar cycle for the tectonic/fluvial triggering of landslides on the hillslopes.

The data gathered here can be related to other areas in the Nenana coal field which have similar densities of landslides, to other areas with similar lithologic and structural settings, and possibly even to similar climatic settings but somewhat different geology.

4.0 STREAMFLOW and SEDIMENT-DISCHARGE PROCESSES

4.1 Introduction

4.1.1 Field Studies

In 1985 a hydrology program designed to evaluate various sediment-discharge relationships for high gradient creeks within Hoseanna Creek Watershed was initiated. In the succeeding years up through 1988, I worked in conjunction with and/or coordinated the activities for the Usibelli Coal Mine, the State of Alaska Division of Geological Surveys (ADGGS - now Department of Water), and the United States Geological Survey (USGS). Together we worked to collect stream and sediment data, and established 23 hydrologic stations (Figure 4.1-1) either as short-term point record stations or as longer-term continuous record stations (USGS, 1986; USGS, 1987; USGS, 1988; USGS, 1989; USGS, 1990; USGS, 1991; USGS, 1992; USGS, 1993; Mack, 1987; Mack, 1988; Ray and Maurer, 1989; Ray, 1990; Ray and others, 1991; Ray and Vohden, 1992; Ray and Vohden, 1993). Streamflow and sediment data were collected at many other locations during the course of the investigation, but these are not considered hydrologic stations here. However, the data collected from these additional locations are included in Appendix C, along with all the other stream and sediment data.

The stations were located along the main channel of Hoseanna Creek or near the mouths of the north and south flowing tributaries. Most stations were positioned above the influences of mining and roads. The monitored creeks were chosen as draining representative basins by size (1.0 to 125 km²) underlain by the three principle lithologic basin types (described in Section 2.3) and that display widely varying hillslope and fluvial characteristics. The station locations were also chosen to represent the observed variations in sediment-discharge characteristics of all the creeks within the basin.

The purpose of this study was to collect and interpret discharge and sediment-transfer data which could be used to:

- 1) develop predictive relationships between discharge and sediment concentrations, and ascribe them to geologic and climatic factors;

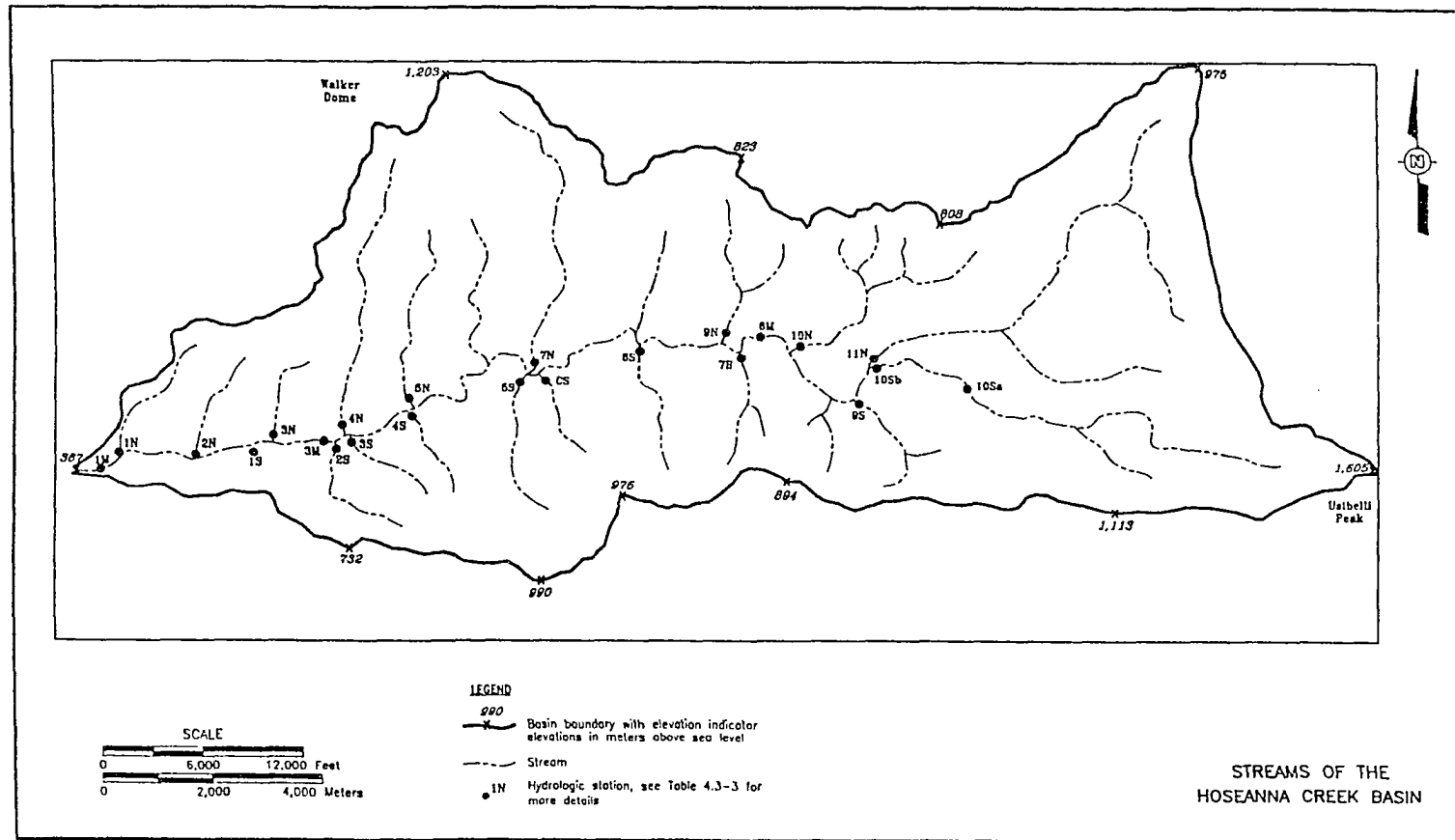


Figure 4.1-1. Locations of hydrologic stations. Continuous or point streamflow and sediment data were collected at 23 stations by the ADGGS, USGS, and UCM/UAF. The USGS monitored only 1M, while at various times, the ADGGS monitored 3M, 6M, 3N, 4N, 5N, 7N, 10N, 1S, 9S, and 10S. UCM/UAF monitored all the stations. Refer to Table 4.2-3 for creek names, years monitored and the type of data collected.

- 2) describe and quantify the spatial and temporal conditions which govern the observed variability; and
- 3) establish a baseline record of discharge and sediment concentration for creeks in Hoseanna Creek Watershed draining future coal-mining areas.

4.1.2 Background

Leopold and others, (1954), and Schumm's (1977) authoritative texts on river processes describe the fundamental relationships between discharge and sediment load, and demonstrate that the fluvial system interacts with many climatic, geologic and geomorphic parameters. The USGS improved and defined the methodology for obtaining empirical relationships between discharge and sediment load in their many reports on techniques of water investigation (see for example, Guy and Norman, 1970; Dalrymple and Benson, 1967; and Kennedy, 1984). This study has utilized concepts from a number of other sources, including but not limited to Van Sickle and Bechta's (1983) analysis of discharge-sediment concentration regressions, Gurnell and Clarke's (1986) compilations of subarctic and glaciofluvial processes, Guy's (1969) summary of fluvial sediment concepts, and Michel's (1971) report on subarctic rivers and lakes.

The relationships between discharge, sediment concentration, and sediment load are known to have high variances that can be attributed to many factors. However, in this paper, the focus is on quantifying discharge and sediment concentration, and relating the observed spatial and temporal variability to geologic and climatic influences found within the Hoseanna Creek Watershed. The observed natural spatial variability of sediment-transfer processes is attributed to the spatial distribution of lithologic and geomorphic features (e.g., permafrost distribution, drainage density, badland and landslide occurrences.) The observed temporal variability is related to sediment input and depletion and seasonal climate patterns. All of these were combined to test the predictability of discharge and sediment concentration when adjusted for systematic and quantifiable variables.

4.2 Methods

Because this was an intergroup effort, several different discharge measurement techniques and a number of different sediment sampling and laboratory methods were used (Tables 4.2-1, 4.2-2 and 4.2-3). The different techniques have different levels of accuracy; this affects sediment-discharge relationships. The use of alternative methods was also due, in part, to the field logistics required to cover the wide range in discharges and sediment concentrations present.

Table 4.2-1. Summary of techniques/tools used to measure streamflow velocities.

Technique/Tool	Conditions Used For	Performed By
Price AA Flowmeter (PAA)	25-400 cfs (0.71-11.3 m ³ /s), when depth x velocity < 12 ft ² /s (1.1 m ² /s), on mainstream and major tributaries	USGS, UAF/UCM
Price AA Flowmeter (PAA) on crane mounted on bridge	> 350 cfs (9.9 m ³ /s), when depth x velocity > 12 ft ² /s (1.1 m ² /s), at bridge 1	USGS
Marsh-McBirney 201 (MM201)	< 350 cfs (9.9 m ³ /s), when depth x velocity < 12 ft ² /s (1.1 m ² /s), and when depth > 0.3 ft (9 cm).	ADGGS
"Pygmy" Flowmeter (PYG)	low flows (< 25 cfs, or 0.71 m ³ /s) and on smaller creeks, and/or when depth > 0.3 ft (9 cm).	UAF/UCM
Floating Stick Method (FSM)	on the mainstream at very high flows and/or high velocities (when depth x velocity > 12 ft ² /s [1.1 m ² /s]), or on very small creeks with very low flows and/or when depth < 0.3 ft (9 cm).	UAF/UCM
Bucket Method (BKM)	on small creeks during low flows (< 1 cfs, or 0.28 m ³ /s) that discharge through a raised culvert	UAF/UCM

Two types of hydrologic data were collected: point data and continuous data. The effects of storm intensity and duration on sediment fluxes were evaluated from the continuous hydrologic records. In addition, continuous records provided for the calculations of sediment load over specified time intervals. Both continuous and point records were related to spatial information; for example, the parameters of sediment-discharge rating curves were interpreted in terms of hydrogeologic and geomorphologic factors such as lithology, drainage density, landslide density and permafrost distribution.

From 1986 through 1988, my assistant, Ted Clarke, and I collected discharge data, collected sediment samples, and monitored equipment at all the stations, including the ADGGS and the USGS stations. It was necessary to augment the USGS and ADGGS efforts to develop a more comprehensive data base. It was recognized early on that it would difficult for either the USGS or the ADGGS to be available to measure discharges or collect samples most of the time, so we coordinated our efforts as much as possible.

From 1985 to 1988, basin accessibility improved each year as the coal mine completed a haul road upstream to the Gold Run Pass mine site. Initially it took two long days at low flow conditions to reach every creek station. At high flows stream crossings were difficult and dangerous so only a few sites could be reached. In some cases, because of site inaccessibility and some high volume flows, other nearby sites upstream or downstream of the established station had to be used. By spring 1988, the road was completed. During the 1988 field season we were able to reach almost all the creek sites even during high flows, so that season was by far the most productive. I concluded my field studies at the end of summer in 1988. The USGS and ADGGS continued to collect streamflow and sediment concentration data through 1992 as part of Usibelli Coal Mine's efforts to establish a longer-term hydrologic database for the permitting requirements. This report utilizes discharge and sediment data primarily from the 1986-1989 data set; data and information from previous and later years are used only in a general manner.

Table 4.2-2. Summary of sediment sampling methods.

Sampling Technique	Sampling Tool	Sampling Type	Performed By
Grab of Suspended Load	Polyethylene Bottle	Point	ADGGS UAF/UCM
Equal-Transit Rate Sampling of Suspended Load	US-DH-48	Depth/Time-Integrated	ADGGS USGS
Automated Grab of Suspended Load	Isco	Point and/or Crest-Level Actuated	ADGGS UAF/UCM
Equal-Time Sampling of Bedload	60-lb/30lb Halley-Smith	Channel/Time-Integrated	USGS UAF/UCM
Bedload Trap	200 micron Flume Net	Time-integrated	ADGGS UAF/UCM

4.2.1 Hydrologic Stations

Hydrologic stations were chosen for 23 locations within the basin (Table 4.2-3 and Figure 4.1-1) to represent the streamflow and sediment transfer processes in specific lithologic-basin types. Nine of the sites were located on creeks on the north side of the valley; three of these (4N - Frances, 5N - Louise and 7N - Popovitch) are dominated by processes in the Nenana Gravel, three (9N - Slide, 10N - North Hoseanna and 11N - Upper Hoseanna) are dominated by processes in the coal-bearing formations, two (2N - Badlands and 3N - Two Bull) are dominated by processes occurring in gravels and/or coal-bearing formations, and one (1N - Terrace) is dominated by processes occurring in the coarse Quaternary terrace gravels. Eleven of the sites are located on creeks on the south side of the valley; five of these (4S - Schist, 5S - Iron, CS - Clear, 9S - Clinker and 10Sa - Sanderson above mining) are dominated by processes in the schistose terrain, one (1S - Runaway) is within only the Tertiary lithologies, while the remaining five sites (2S -

Table 4.2-3. Summary of hydrologic station records. The discharge measurement techniques and sediment sampling methods used by the ADGGS, USGS and UAF-UCM, from 1985-1992, are given for each Hoseanna Creek Watershed hydrologic station.

CREEK	Agency	Years Monitored	Discharge Methods		Sediment Sampling Methods		
			Measurement	Record Type	Technique	Tool	Type
Hoseanna Creek (Bridge 1)	USGS	1985-1992	Price AA Indirect	Continuous stage: bubble manometer with a Fisher-Porter recorder and a Stevens Chart recorder	grab ETR	polyethylene bottle US-DH-48	point depth-integrated
	UAF-UCM	1986-1988	Price AA Pygmy Floating Stick Indirect		grab bedload	polyethylene bottle 60 lb halley-smith	point channel-integrated
	ADGGS	1987-1990	MM201 Rating Curve		grab automated ETR	polyethylene bottle isco US-DH-48	point point depth-integrated
Hoseanna Creek (Bridge 3)	ADGGS	1986-1992	MM201 Indirect	Continuous stage: pressure transducer Omnidata DP320 Stage Recorder with a data storage module	grab automated	polyethylene bottle isco	point daily composite crest-level actuated depth-integrated
	UAF-UCM	1986-1988	Price AA Pygmy Indirect Rating Curve		ETR grab	US-DH-48 polyethylene bottle	point

Hoseanna Creek (Bridge 6)	ADGGS	1988-1990	MM201	Continuous stage: pressure transducer Omnidata DP320 Stage Recorder with a data storage module	grab	polyethylene bottle	point
	UAF-UCM	1988	Price AA Pygmy Rating Curve		automated	isco	daily composite crest-level actuated point
Terrace Creek (1N)	UAF-UCM	1986-1988	Floating Stick Pygmy Bucket	Non-stage: point	grab	polyethylene bottle	point
Badlands Creek (2N)	UAF-UCM	1986-1988	Floating Stick Pygmy	Non-stage: point	grab	polyethylene bottle	point
Two Bull Creek (3N)	ADGGS	1988-1990	MM201	Continuous stage: pressure transducer Omnidata DP320 Stage Recorder with a data storage module, Non-stage: point	grab	polyethylene bottle	point
	UAF-UCM	1986-1988	Floating Stick Pygmy Parshall Flume Rating Curve		automated	isco	crest-level actuated
					grab	polyethylene bottle	point

Frances Creek (4N)	ADGGS	1986-1989	9-in Parshall Flume	Continuous stage: pressure transducer Omnidata DP320 Stage Recorder with a data storage module, Non-stage: point	grab automated	polyethylene bottle isco	point daily composite crest-level actuated point
	UAF-UCM	1986-1988	Floating Stick Pygmy Bucket Rating Curve		grab bedload trap	polyethylene bottle 200 micron flume net	time-integrated
Louise Creek (5N)	ADGGS	1988-1989	9 in Parshall Flume	Continuous stage: pressure transducer Omnidata DP320 Stage Recorder with a data storage module, Non-stage: point	grab automated	polyethylene bottle isco	point daily composite crest-level actuated point
	UAF-UCM	1986-1988	Floating Stick Pygmy Rating Curve		grab	polyethylene bottle	
Popovitch Creek (7N)	ADGGS	1986-1988	9 in Parshall Flume	Continuous stage: pressure transducer Omnidata DP320 Stage Recorder with a data storage module, Non-stage: point	grab automated bedload trap	polyethylene bottle isco 200 micron flume net	point crest-level actuated time-integrated
	UAF-UCM	1986-1988	Floating Stick Pygmy Bucket Rating Curve		grab bedload trap	polyethylene bottle 200 micron flume net	point time-integrated
Slide Creek (9N)	UAF-UCM	1986-1988	Floating Stick Pygmy	Non-stage: point	grab bedload trap	polyethylene bottle 200 micron net	point time-integrated

North Lignite Creek (10N)	ADGGS	1986-1988	MM201	Continuous stage: pressure transducer Omnidata DP320 Stage Recorder with a data storage module, Non-stage: point	grab automated	polyethylene bottle isco	point daily composite crest-level actuated point
	UAF-UCM	1986-1988	Floating Stick Pygmy Indirect Rating Curve		grab	polyethylene bottle	
Upper Hoseanna Creek (11N)	ADGGS	1986-1987	MM201	Non-stage: point	grab	polyethylene bottle	point
	UAF-UCM	1986-1988	Floating Stick Pygmy Price AA	Non-stage: point	grab	polyethylene bottle	point
Sanderson Creek (above mining 10Sa)	ADGGS	1986-1988	MM201	Continuous stage: pressure transducer Omnidata DP320 Stage Recorder with a data storage module, Non-stage: point	grab automated	polyethylene bottle isco	point crest-level actuated
	UAF-UCM	1986-1988	Floating Stick Pygmy Price AA Rating Curve		grab	polyethylene bottle	point
Sanderson Creek (below mining 10Sb)	ADGGS	1987	MM201	Non-stage: point	grab	polyethylene bottle	point
	UAF-UCM	1986-1988	Floating Stick Pygmy Price AA	Non-stage: point	grab	polyethylene bottle	point

Clinker Creek (9S)	ADGGS	1991	MM201	Continuous stage: pressure transducer Omnidata DP320 Stage Recorder with a data storage module, Non-stage: point	grab automated	polyethylene bottle isco	point crest-level actuated
	UAF-UCM	1986-1988	Floating Stick Pygmy Bucket		grab	polyethylene bottle	point
Mosquito Creek (7S)	UAF-UCM	1986-1988	Floating Stick Pygmy	Non-stage: point	grab	polyethylene bottle	point
Sixth South Creek (6S)	UAF-UCM	1986-1988	Floating Stick Pygmy	Non-stage: point	grab	polyethylene bottle	point
Clear Creek (CS)	UAF-UCM	1986-1988	Floating Stick Pygmy	Non-stage: point	grab	polyethylene bottle	point
Iron Creek (5S)	UAF-UCM	1986-1988	Floating Stick Pygmy	Non-stage: point	grab automated	polyethylene bottle isco	point daily composite
Schist Creek (4S)	UAF-UCM	1986,1988	Floating Stick Pygmy	Non-stage: point	grab	polyethylene bottle	point
Pipe Creek (3S)	UAF-UCM	1986-1988	Floating Stick Pygmy	Non-stage: point	grab	polyethylene bottle	point
Slime Creek (2S)	ADGGS	1989	no data	no data	grab	polyethylene bottle	point
	UAF-UCM	1986-1988	Floating Stick Pygmy	Non-stage: point	grab	polyethylene bottle	point
Poker Creek	UAF-UCM	1986-1988	Floating Stick Pygmy	Non-stage: point	grab	polyethylene bottle	point

Runaway Creek (1S)	ADGGS	1989-1990	MM201	Continuous stage: pressure transducer Omnidata DP320 Stage Recorder with a data storage module,	grab	polyethylene bottle	point
	UAF-UCM	1986-1988	Floating Stick Bucket	Non-stage: point	grab	polyethylene bottle	point

Slime, 3S - Pipe, 6S - Sixth South, 7S - Mosquito and 10Sb - Sanderson below mining) have both schist and coal-bearing lithologies. Three of the sites (1M, 3M and 6M) were located at bridge sites on the main channel of Hoseanna Creek and also have mixed lithologic associations. A hydrologic station summary, including the responsible monitoring agency, the years monitored, and the type of discharge and sediment records that were collected is provided in Table 4.2-3.

Several other creeks (i.e., Dry Creek, Suntrana Creek, Nenana River, Squirrel Valley, Poker Creek, and many smaller creeks within Hoseanna Creek Watershed) were visited between 1986 and 1988. Discharge measurements and/or sediment samples were taken at these sites; in general, the data from these additional stations are used in only a cursory manner and are provided in Appendix C.

4.2.2 Discharge Measurements

4.2.2.1 Discharge Measurement Techniques

Discharge measurements were made following the guidelines set forth in Buchanan and Somers (1969). Discharge measurements were made by the three different agencies using a variety of equipment (Table 4.2-1). The ADGGS used a Marsh-McBirney Model 201 Flowmeter (MM201) most of the time and the USGS the standard Price AA Flowmeter (PAA) for all its velocity measurements. I used a PAA provided by the coal mine for many of the flows. At very low flows in small channels ($< 0.42 \text{ m}^3/\text{s}$ or 15 cfs) I used a "Pygmy" Flowmeter (PYG), or the floating stick method (FSM). At very high flows when wading was life-threatening only surface velocities could be measured by the FSM. In addition, the bucket method (BKM) was used for measuring discharge from small creeks which flowed through raised culverts.

The MM201, PAA, and PYG are accepted tools with standardized velocity calibrations. All the metered velocities were measured at the standard six-tenths depth for shallow flows in streams with high width-depth ratios. Discharges were calculated using the standard midpoint method (USDOL, 1981).

The FSM requires some calibration between the average surface velocity (U_s) and the average velocity (U_a) in a section; the relationship between U_s and U_a will vary

with stream gradient and channel geometry (Jarrett, 1988). In this case, for the high gradient streams in Hoseanna Creek Watershed, the relationship was determined to be $U_a = 0.70U_s$ by comparing discharge and velocity measurements made by the FSM and either the PYG, MM201 or the PAA. This value is less than the 0.86 value assumed for normal low-gradient streams (Burrows, personal communication, 1988). This is in accord with Jarrett's findings in which he showed that velocity profiles for high gradient streams (gradients generally greater than 0.1 m/m) are "s-shaped" and deviate slightly from a conventional profile; that is, surface velocities in high gradient streams can be expected to be higher than surface velocities in low gradient streams for similar average velocities.

The FSM was used in very small creeks at very shallow flows to determine average surface velocities. Discharges were calculated from surface velocity measurements and measurements of channel widths and depths. To do this, the channel was divided into three sections (in plan view). Each channel section was assumed to have a uniform velocity across its section. Repeated surface velocity measurements were made, from which average surface velocities were determined for each straight channel reach. The surface velocity was multiplied by 0.70 following the empirical relationship established between the metered velocity measurements and surface velocity measurements described above. The calculated average channel velocity was then multiplied by the average subarea in each channel subsection to determine section discharges.

The BKM involves filling a known bucket volume from a raised culvert outlet over a known time interval. If the conditions are favorable, this method is the most accurate method of measuring point discharge. A number of the creeks (i.e., Terrace, 1N; Frances, 4N; Slide, 9N; and Clinker, 9S) flow through raised culverts before discharging into the main channel of Hoseanna Creek. The culvert outlets typically rest in road fill from one to two meters above the main channel. This configuration allowed us to measure discharge directly at low flows (typically less than 0.50 cfs [0.014 m³/s]) by using the BKM.

4.2.2.2 Indirect Discharge Measurements

Since it was not always possible to measure the peak or near-peak discharge, indirect slope-conveyance discharge measurements of peak discharges were

performed following Benson and Dalrymple (1967) and Dalrymple and Benson (1967) for 10N, 10Sa, 1M, and 3M usually within a week of the high runoff event. For some of the higher discharges that were observed but where wading conditions were life threatening (greater than 500 cfs [$14.2 \text{ m}^3/\text{s}$]), surface velocities were measured using the FSM. After the flows subsided, channel cross sections were measured and the methods described by Dalrymple and Benson (1967) were used to calculate discharge. Normally there are large uncertainties involved in using the indirect method because of the uncertainty in estimating average channel velocity; however, in cases where the surface velocities were measured, indirect discharge calculations for these flows are more accurate. Nevertheless, when many of the creeks were observed at very high surface velocities, active scouring and channel filling was most likely occurring through the storm cycle; because the channel bed is not stable, the channel geometry measured after the storm may not represent the actual channel geometry that existed during the high velocity flows.

4.2.2.3 Channel Roughness

The accuracy of the estimate of discharge by an indirect measurement technique is largely dependent on the value assumed for channel roughness. At bridge 1, channel roughness was not constant, but changed significantly by a factor of 1/2X (as described below) with stream velocity and channel depth (Figure 4.2-1). Normally the magnitude of roughness decrease is much smaller and is attributed to the ratio of mean channel grain size to the mean channel depth (Limerinos, 1969), or is function of discharge only in streams of width:depth ratios greater than about 45 (Osterkamp and others, 1983). In the case observed here, the decrease in roughness can be attributed to a moving bed. A number of discharge measurements made at bridge 1 over the course of this study demonstrate this phenomenon. Velocity, depth and Manning's roughness (n) are plotted on Figure 4.2-1. Roughness decreases with increasing depth, and increasing velocity.

In general, the relationship portrayed in Figure 4.2-1 is a function of the sediment caliber (or grain size distribution) of the bed (Einstein, 1951). Fine-grained sand channels are more susceptible to changes in roughness due to a moving bed than coarse boulder-armored channels or clay-lined channels because the sand is much more easily entrained and therefore susceptible to moving at the bed (Schumm, 1960 and 1961). Generally, the phenomenon of decreasing roughness due to

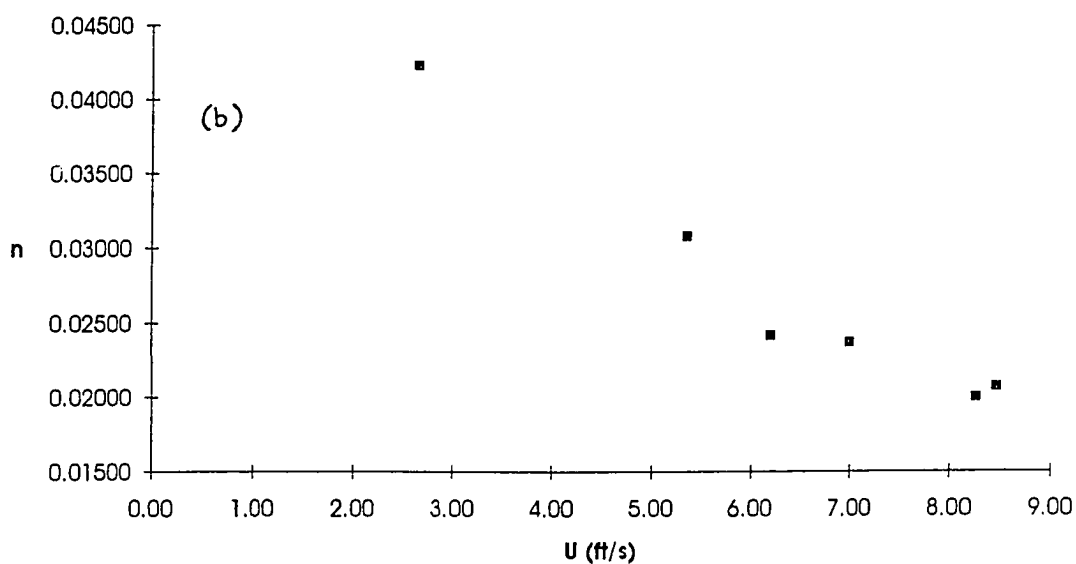
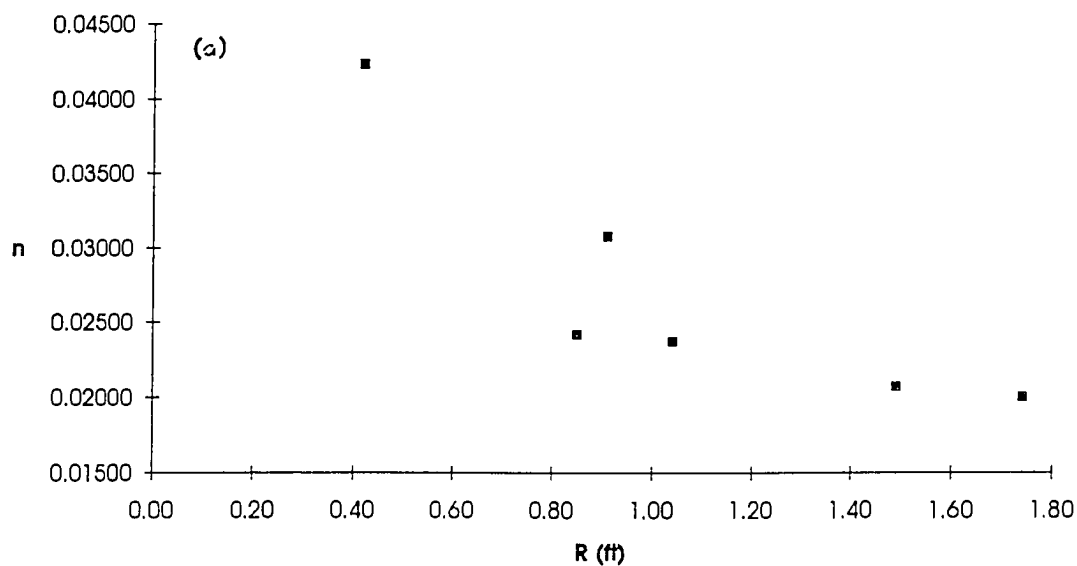


Figure 4.2-1. Channel roughness as a function of channel geometry. The roughness (Manning's n) is plotted versus hydraulic radius (R - ft) in Figure 4.2-2a and versus average channel velocity (U - ft/s) in Figure 4.2-2b for Hoseanna Creek at bridge 1 (1M). Roughness decreases with increasing hydraulic radius and with increasing average channel velocity.

moving beds is more common in the creeks draining the Tertiary lithologies which have a large fine sandy component and initially have moderately low roughness values ($n < 0.050$ when using English units).

4.2.3 Discharge Records

Discharge data were collected as continuous stage discharge records or nonstage point discharge records. Non-stage point discharge records were random discharge measurements made over a range of flows at specific creek locations. Obtaining the continuous stage data involved monitoring the head of the water column continuously through time with mechanical or electronic devices. The general procedure for gaging streams described by Carter and Davidian (1968) was followed for all stage data. Continuous discharge records were then calibrated from stage-discharge rating curves following Kennedy (1984).

Continuous stage record stations were not developed or monitored for all hydrologic stations because only point sediment-discharge relationships are necessary to demonstrate the spatial distribution of certain lithologic controls on sediment production. Thus, continuous discharge data were chosen for more specific research objectives related to temporal sediment transfer processes (i.e, the relationship of the storm hydrograph to sediment concentration), and secondly for logistic and financial reasons.

Establishing and monitoring a continuous gage station requires much more investment of equipment, time and energy than a non-stage point record station. Because not all channels are favorable for stage-discharge relationships and because of the large size of the study area, the sites for continuous records were chosen to be representative of fluvial conditions and geologic aspects present in Hoseanna Creek Watershed. The continuous records at these sites was then used to develop concepts for the sites with point records only. The ADGGS and the USGS concentrated their efforts on establishing continuous records at the locations listed in Table 4.2-3. From 1986-88, Ted Clarke and I helped the USGS and ADGGS maintain/monitor all the continuous stations, as well as establish and collect the point discharge data.

4.2.3.1 Nonstage Point Discharge Records

From 1986-1988, I collected point discharge data from over 40 locations in the area; data from 23 of these were collected more regularly than the others. Of the 23, two were continuous record stations only. Three point record stations were developed into continuous record stations by 1988, and from 1989-92 (after I finished my field work). The ADGGS developed three more of the point record stations into continuous record stations. Eleven of my point record stations were not visited by the ADGGS or the USGS. Stage-discharge ratings were not attempted at these sites. Discharge was measured each time a sediment sample was collected; this procedure was followed to ensure a good discharge value for each sediment concentration.

4.2.3.2 Continuous Stage Discharge Records

From 1986-1992, continuous discharge record stations were maintained over various time intervals for 11 hydrologic stations in Hoseanna Creek Watershed (Table 4.2-3 and Figure 4.1-1). Only 2 out of the 11 (1M and 3M) were maintained for the entire period. All the continuous discharge record stations were ADGGS stations except one, the station at bridge 1 (1M) located near the mouth of Hoseanna Creek, which was a USGS station.

Stage-Discharge Ratings

Stage-discharge rating curves were developed each year for all the continuous record stations. The continuous stage data were used to determine discharges. There were three different types of stage-discharge ratings: channel controlled bridge sites, noncontrolled open channel sites, and sites with Parshall flumes.

Of the eleven, three were bridge sites (1M, 3M and 6M) and flumes were used at five of the sites (3N, 4N, 5N, 7N and 1S) at various times, so are well suited for stage data. For the remaining three (10N, 10Sa and 9S) staff gage locations were chosen in straight stable channel reaches. The braided nature of some creeks made it necessary to look for the narrowest parts of the channel where the creek would always be confined. Rating curves were developed for each non-flume site by taking discharge measurements at different water levels throughout the season.

The rating curves were then used to estimate discharge for all the continuously recorded stage values.

For the non-flume sites, stage-discharge relationships vary from year to year, and from spring to fall (due to changing hydraulic geometries) so that a simple stage-discharge relationship does not exist. For some sites the bed level is not constant, as sediment flux is transferred down through the stream system. This is especially true for bridge sites, and for constrictions in general, which are scoured at high flows, and then fill during receding flows. In addition, spring break up flows carry large amounts of winter derived material (e.g., frost weathered debris) which clog the streams early in the year. This material is removed quickly during large storms and more slowly during lower flows throughout most of the season. At bridge 1, a 0.3 m difference of bed level was measured for similar discharges before and after a storm. However, this was not a significant factor for creeks draining schistose terrain (e.g., Sanderson Creek, 10Sa), which have coarser beds made of angular to subangular cobbles and boulders and so are relatively stable under all but extremely high flow conditions.

USGS Gage Station at Bridge 1

The USGS installed a bubble-gage sensor manometer device with continuous stage recorders at bridge 1 (1M) in June 1985. The manometer orifice was originally placed on the gravel bed 40 meters upstream from bridge 1 and connected through a 1 1/2-inch PVC pipe to the stage house on the south bank. Two major storms in 1986 washed out the orifice both times. The orifice was mounted directly on the northeast bridge wingwall in late May 1987 and then provided a good stage record for ice-free days only, which has generally occurred from early to mid June to late September. When ice was present, aufeis buildup produces higher stages for the same discharge without ice. In addition, no changes in stage are recorded when the standpipe freezes. Because of the different setups, the continuous stage data from 1985 and 1986 cannot be directly compared nor can they be directly compared with the 1987-92 data. Both a Stevens strip recorder and a Fisher-Porter punch recorder were used to keep the continuous record. The recorders and bubble manometer set-up was mounted in a mobile gage house provided by the coal mine in 1985.

ADGGS Gage Stations

The ADGGS maintained continuous stage recording devices in up to ten sites from 1986 through 1992 (i.e., Runaway, 1S; Two Bull, 3N; Frances, 4N; Louise, 5N; Popovitch, 7N; Clinker, 9S; North Hoseanna, 10N; Sanderson above mining, 10Sa; Bridge 3, 3M; and Bridge 6, 6M) (Figure 4.1-1). The year and type of discharge data for the ADGGS stations is summarized in Table 4.2-3. For a complete record of the ADGGS discharge data see Mack (1987 and 1988), Ray (1990), Ray and Maurer (1989), Ray and others (1991), Ray and Vohden (1992 and 1993). "At all ADGGS sites, continuous water surface levels were recorded with Omnidata DP320 Stream Stage Recorders. The DP320 is a small battery operated device with a submersible pressure transducer which measures and records water levels between 0 to ten feet to the nearest hundredth of a foot. Water level data are stored in a solid state memory called a data storage module. At all sites the water level recorders monitored water levels at 30 minute intervals," (Mack, 1988).

Parshall flumes (USDOI, 1981) were installed at Popovitch Creek (7N) (3.0 ft) in 1987 and 1988, Frances Creek (4N) (9 inch) in 1987, 1988, Louise Creek (5N) (9 inch) in 1989, and Two Bull (3N) and Runaway (1S) (9 inch) in 1990, and discharges were estimated from measured discharges and the ratings established by the USDOI (1981). During the 1986 season, we experimented with various weir and flume sizes and types, so the 1986 data is not directly comparable with the 1987 and 1988 data. The flume sizes were selected from estimated peak flows for each creek (which were greatly overestimated); hence, the sensitivity of the rating equations for the low normal flows is fair at best. The parshall flumes were equipped with stilling wells in which to place a transducer and record continuous stage data.

Generally, these recorders compiled continuous data. However, at times the recorder malfunctioned due to bad batteries or bad wiring. Hence, there are data gaps in the continuous records. In addition, at times the recorder gave inaccurate records (e.g.: very noisy due to random numbers); these time intervals were not used. This was particularly true for the 1988 continuous records compiled for Two Bull and Louise Creeks, which have unfavorable channel characteristics at low flows (depths less than 3 cm and high width:depth ratios).

4.2.4 Sediment Sampling

Various methods of measuring sediment concentrations have been developed (Guy and Norman, 1970), and the accuracy of the methods can vary depending on field and lab methods, instrumentation and operational error. For this study, the stream and sediment conditions differ widely across the watershed, so that it was necessary to use several techniques. Also, a wide range of techniques were used because each agency involved had different objectives for sediment-discharge data.

4.2.4.1 Suspended Load Sampling Techniques

Suspended sediment measurements were taken at all sites by three different techniques: grab, equal-transit rate (ETR) depth-integrated (Guy and Norman, 1970), and automated Isco sampling (Mack, 1988) (Table 4.2-2). These three techniques were selected for logistic, financial and research-directed reasons. The ETR depth-integrated sampling technique is the standard USGS sampling technique, and thus provides broad comparisons and sampling control. However, the ETR method involves considerable time both in the field and in the lab, and it was not feasible to rely solely on this technique. In this case the type and amount of data desired and the site-specific characteristics dictated that two other methods be used. Many of the creeks are very small (width less than 1 meter, depth less than 5 cm), so that only a point grab sample was feasible. In addition, one of the primary objectives of this study was to describe the temporal relationships of sediment concentrations before, during and after storms. An automated sampling system is better than grab samples for a continuous record through a storm cycle.

Point grab samples were collected at all sites whenever a discharge measurement was made. 300 ml polyethylene bottles were placed into the mid-channel, which was generally the well-mixed faster moving flow, facing upstream and turned at a slight angle to flow to allow the bottles to readily fill. For all these high-gradient creeks, mixing is thorough and quick so that the mid-channel flow is a good representation of the entire cross-section. In some cases, for the high flows that occurred in Hoseanna Creek, 1000 ml bottles were used.

Automated samples were taken by the Isco samplers at some of the ADGGS sites. Two different automated techniques were used. Composite samples were taken for

daily averages. Samples were collected through approximately 1/2-inch thick hollow polyethylene tubing at 3, 4 or 6 hour intervals and combined to fill 1000 ml bottles for each day. In other cases, crest stage sampling was activated by a trip level actuator and then samples were taken of the storm-generated flows at 45, 60, 90, 120 or 180 minute intervals depending on creek size and expected storm duration. In addition, the Isco was at times manually activated to collect a point sample that could be directly compared to a grab sample taken at the same time and from the same location. The types of the sampling techniques used on each creek are listed in Table 4.2-3.

4.2.4.2 Bedload Sampling Techniques

Bedload was measured at Hoseanna Creek bridge 1 (1M), Popovitch Creek (7N), and Frances Creek (4N) (Table 4.2-3). At bridge 1, the USGS measured bedload using a 30-lb (13.6 kg) three inch orifice Halley-Smith sampler, while I used at the same site the heavier 60-lb (27.3 kg) version provided by the coal mine. Bedload samples collected by the Halley-Smith samplers followed procedures described in USDOI (1981). Total bedload was calculated using the standard midpoint method with discharge and channel cross section data.

The number of bedload samples is small, so the data set can only be used in a preliminary manner. The data can be used to infer bedload processes but not to estimate the total bedload. The nature and use of this data are similar to the point suspended sediment concentration data. Variance within the results can be expected due to the different samplers used.

For Frances and Popovitch Creeks, a flume net bedload trap technique (Mack, 1988) was developed. A 250 micron mesh net with an aluminum frame was constructed large enough to collect all the coarse bed material from the outflow flume end. These samples were collected for specific time intervals at known discharges.

The flume-net technique gives accurate bedload measurements because all the moving bed material coarser than 250 microns is trapped in the net, and discharge values are known by the well calibrated flume stage-discharge data. However, the method assumes that all the material greater than 250 microns is bedload, which is

not true all the time. Bedload size fractions change with flow rate, stream power and sediment supply, and bed motion is not constant even for the same flow rate (Einstein, 1951; Schumm, 1960; Guy and Norman, 1970). In addition, portions of the size fraction finer than 250 microns were always trapped by the coarser fractions already in the net, but in general this was usually less than 5% of the total load. Operational error increases at very high flows, because the flume net fills very quickly and thus reduces the sampling period. This effect was lessened by taking many repeated composite samples during relatively constant discharges.

4.2.5 Laboratory Analyses

4.2.5.1 Suspended Load

Due to the large number of sediment samples (2926 in 7 years - excluding ETR-type samples, Table 4.2-4) and the multiple-agency effort, laboratories affiliated with the ADGGS, the USGS and the UCM were utilized. The bulk of the analyses (81%) were done at the ADGGS Water Resource Center joint facility at the University of Alaska after the field season. Almost all (99%) of the automated (which constitute 61% of all the samples) and 53% of the grab samples were processed there. Because the ETR samples represent less than 0.5% of all the samples and are not directly comparable, they are not used in this report.

Many (47%) of the grab samples were processed "on-site" during the field seasons at the Usibelli Coal Mine (UCM) laboratory. These field season results provided necessary data for on-going field strategy and to test various working hypotheses about field relationships, which could not have been done until the following year if one waited for the ADGGS lab results. To determine sediment concentration the ADGGS samples were filtered through a 46 micron filter, dried and measured for total weight (see Mack, 1988, page 13; and Guy, 1969). However, the analyses that I (or my assistant) performed at the UCM lab varied slightly from the ADGGS techniques. All the coal mine lab samples were oven-dried in crucibles and not filtered. Hence, suspended and dissolved components were combined. This method was performed to estimate total bedrock erosion, whether derived from chemically or physically weathered processes.

Table 4.2-4. Quantity of various sample types taken during each year of study. All samples analyzed at ADGGS were filtered and then evaporated before weighing; all samples analyzed at UCM were unfiltered and evaporated before weighing.

Year	Grab Samples Analyzed At		Automated Isco Samples Analyzed At		
	ADGGS	UCM	ADGGS (point)	ADGGS (composite)	UCM
1986	35	78	4	95	16
1987	124	131	156	0	0
1988	189	324	300	0	0
1989	140	0	404	184	0
1990	106	0	245	146	0
1991	0	0	8	146	0
1992	0	0	0	95	0
Total	594	533	1117	666	16

4.2.5.2 Comparison of Sampling Techniques

Grab sampling was done concurrently with Isco sampling. Comparative results are compiled in Table 4.2-5. A linear regression analysis between grab and Isco samples was used to compare results of the sampling methods. Although there is not a perfect 1:1 relationship, as shown in Figure 4.2-2, the r^2 value of 0.87 indicates there is a good correlation. The variance is due primarily to natural mixing variability with both channel width and depth, although minor operational variance also occurs. The sampling inlet for the Isco is at a fixed position with respect to the channel. During rising and falling stages, the sampling inlet is at various depths from the water surface. In contrast, grab samples were typically collected within the first 10 cm from the surface. Since sediment concentration increases with water depth (Guy and Norman, 1970), we can expect the Isco values to be lower than grab samples for low flows, but to be higher for high flows.

Table 4.2-5. Comparison of grab sampling and Isco automated sampling techniques.

Hydrologic Station	Date	Grab (g/l)	Isco (g/l)
Bridge 3 (3M)	09/04/86	3.73	4.27
	07/31/87	1.54	1.47
	07/09/88	8.01	7.46
	07/10/88	5.99	3.91
	07/10/88	6.80	7.13
	07/11/88	6.27	5.96
	07/21/88	3.13	3.08
	07/21/88	5.94	5.24
	04/27/89	0.99	1.04
	05/05/89	1.21	1.09
	06/06/89	12.40	11.60
	06/25/89	14.60	14.10
	06/25/89	29.20	28.60
	08/05/89	8.83	8.72
Brdige 6 (6M)	08/10/88	0.23	0.27
	06/25/89	19.30	18.70
	06/25/89	13.00	10.60
	08/05/89	5.70	5.30
Frances (4N)	07/21/88	2.38	2.12
Louise (5N)	06/06/89	89.30	80.30
	06/24/89	16.60	19.80
	06/24/89	18.10	13.80
	06/25/89	37.60	27.90
	06/25/89	78.00	33.00
	06/25/89	74.30	80.30
North Hoseanna (10N)	07/09/88	4.00	3.88
	08/12/88	1.62	1.60
Sanderson (10Sa)	06/30/88	0.045	0.040
Two Bull (3N)	06/24/89	35.20	38.60

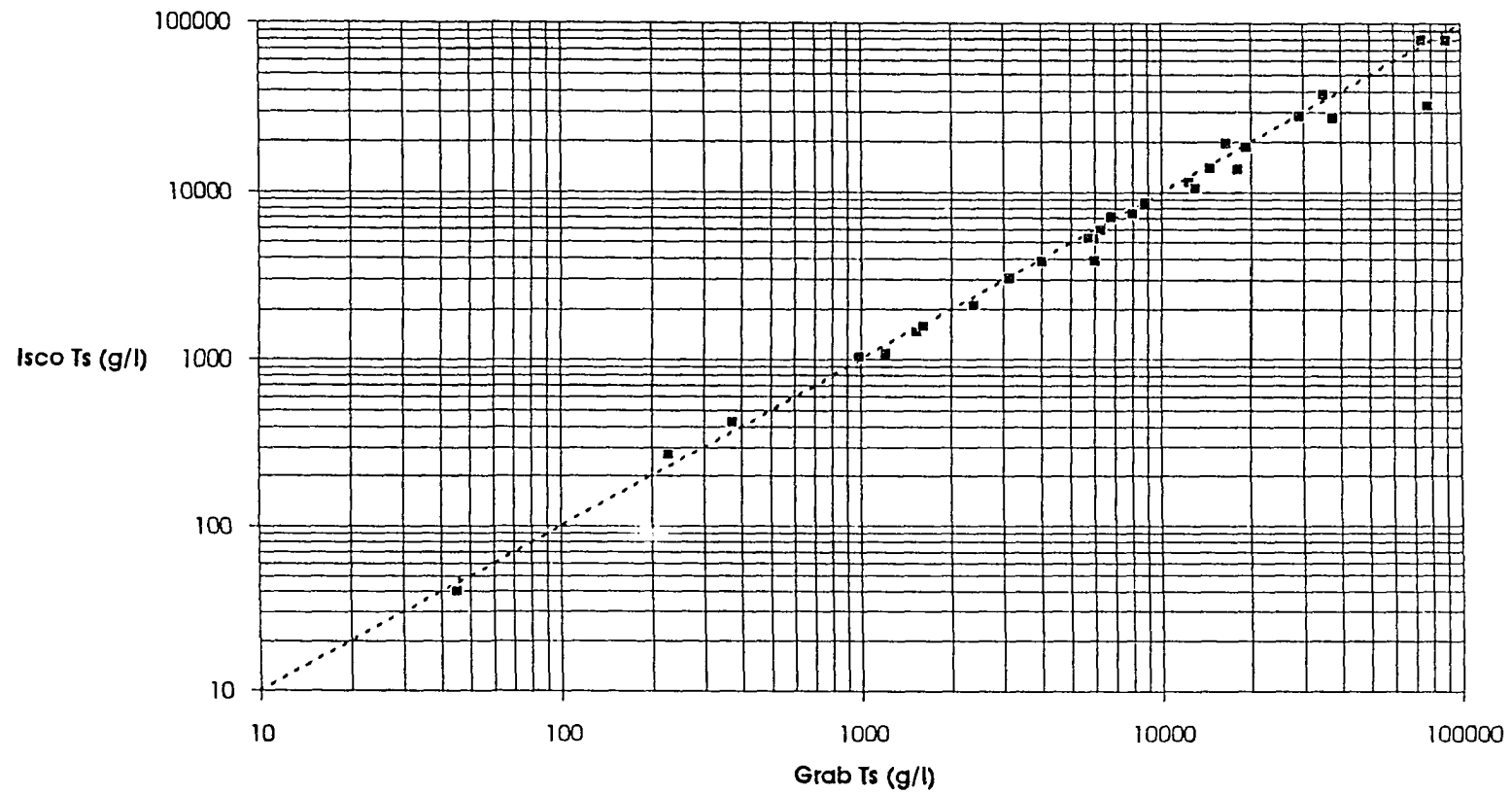


Figure 4.2-2. Comparison of grab sampling and Isco automated sampling techniques. Suspended sediment concentration values from automated Isco samples and grab samples compare fairly well over three orders of magnitude. Minor variance is due to both natural variability and operational error.

4.2.5.3 Comparison of Laboratory Techniques

As described above, the analyses performed at the UCM lab varied slightly from the ADGGS techniques, so that the suspended and dissolved components were combined. A number of duplicate samples were sent to the ADGGS lab and filtered. A comparison of the duplicates is shown in Table 4.2-6, and in Figure 4.2-3.

In general, the filtered samples have much lower values of T_s at lower T_s , and most of the values for the unfiltered samples are slightly higher than the filtered values. Because the filtered values are almost all systematically lower than the unfiltered values and the same sampler and sampling technique was employed for all the samples, this variance is due to laboratory methods, rather than natural processes.

For the low T_s values, the higher unfiltered values are due to the additional dissolved constituents in the unfiltered samples. Estimations of the dissolved portions made from Figure 4.2-3 by determining the difference between the unfiltered value and the 1:1 line range from 50 to 500 mg/L. The dissolved concentrations determined for the ETR depth-integrated ADGGS samples from 1M and 3M ranged from 245-364 mg/l (Mack 1988) and show that the estimations from the above method are reasonable.

However, the differences at very high T_s values (where dissolved portions are too small to detect) are likely due to a difference in lab technique. To decrease the volume of sample being analyzed, the ADGGS made splits of each sample using magnetic stirrers. However, because magnetic stirrers may not always be effective in dispersing the coarse fraction, some of the coarse fraction may have sorted out in mixing. In an effort to alleviate the potential errors due to splitting the samples, we analyzed the total grab sample (i.e., not just the split fraction) at the coal mine lab. A comparison between the ADGGS and UCM duplicates showed that at very high concentrations ADGGS may have underestimated total weight by as much as 10-15%.

Table 4.2-6. Results of lab analysis comparisons between ADGGS (filtered) and UCM (unfiltered) of duplicate suspended sediment samples taken during 1988.

Creek	Sample Date	Sample Time	ADGGS (g/L)	UCM (g/L)
Two Bull (3N)	7/8/88	16:55	21.287	21.640
	7/11/88	15:50	113.497	158.800
	8/16/88	11:05	0.534	0.465
	9/29/88	10:35	0.008	0.208
	7/21/88	08:50	14.566	16.131
Frances (4N)	7/8/88	17:20	5.913	6.977
	7/10/88	13:15	4.593	4.992
	7/11/88	16:20	19.100	19.853
	7/17/88	18:30	0.019	0.482
	7/25/88	15:05	0.173	1.433
	8/16/88	12:20	0.079	0.441
	8/29/88	12:10	0.023	0.498
	9/29/88	18:20	0.019	0.505
	5/26/88	11:20	1.467	1.530
	7/21/88	19:30	4.080	6.080
	7/22/88	23:50	20.564	21.130
Louise (5N)	7/8/88	19:40	19.112	20.140
	7/10/88	13:25	33.968	35.594
	7/22/88	11:00	105.916	140.700
	8/29/88	12:25	0.086	0.587
North Hoseanna (10N)	7/9/88	10:40	3.996	4.669
	7/10/88	19:15	1.297	1.834
	7/25/88	15:40	1.579	0.713
	8/21/88	17:05	0.212	0.327
	9/29/88	14:10	0.096	0.257
	8/14/88	19:20	0.843	0.456
Popovitch (7N)	7/8/88	19:55	0.173	0.241
	7/10/88	13:40	1.514	1.419
	7/10/88	18:00	1.116	1.236
	7/22/88	11:30	22.157	25.521
	8/14/88	19:35	0.048	0.165
	8/29/88	12:30	0.024	0.149
Sanderson (10Sa)	7/17/88	15:40	0.018	0.604
	7/25/88	16:15	0.091	0.512
	9/3/88	15:00	0.032	0.793
	9/29/88	12:05	0.031	0.740
Hoseanna at Bridge 3 (3M)	7/9/88	09:10	8.011	7.939
	7/10/88	13:10	5.985	6.660
	7/10/88	18:10	6.797	7.343
	7/11/88	16:15	6.265	6.231
	7/22/88	23:40	21.098	22.920
	7/23/88	07:55	6.540	6.999
	7/25/88	14:55	0.409	0.785
	8/14/88	18:20	0.224	0.563
	8/29/88	12:00	0.092	0.449
	9/29/88	17:50	0.541	0.918
Hoseanna at Bridge 6 (6M)	7/9/88	10:25	3.924	5.426
	7/22/88	12:55	8.444	9.919

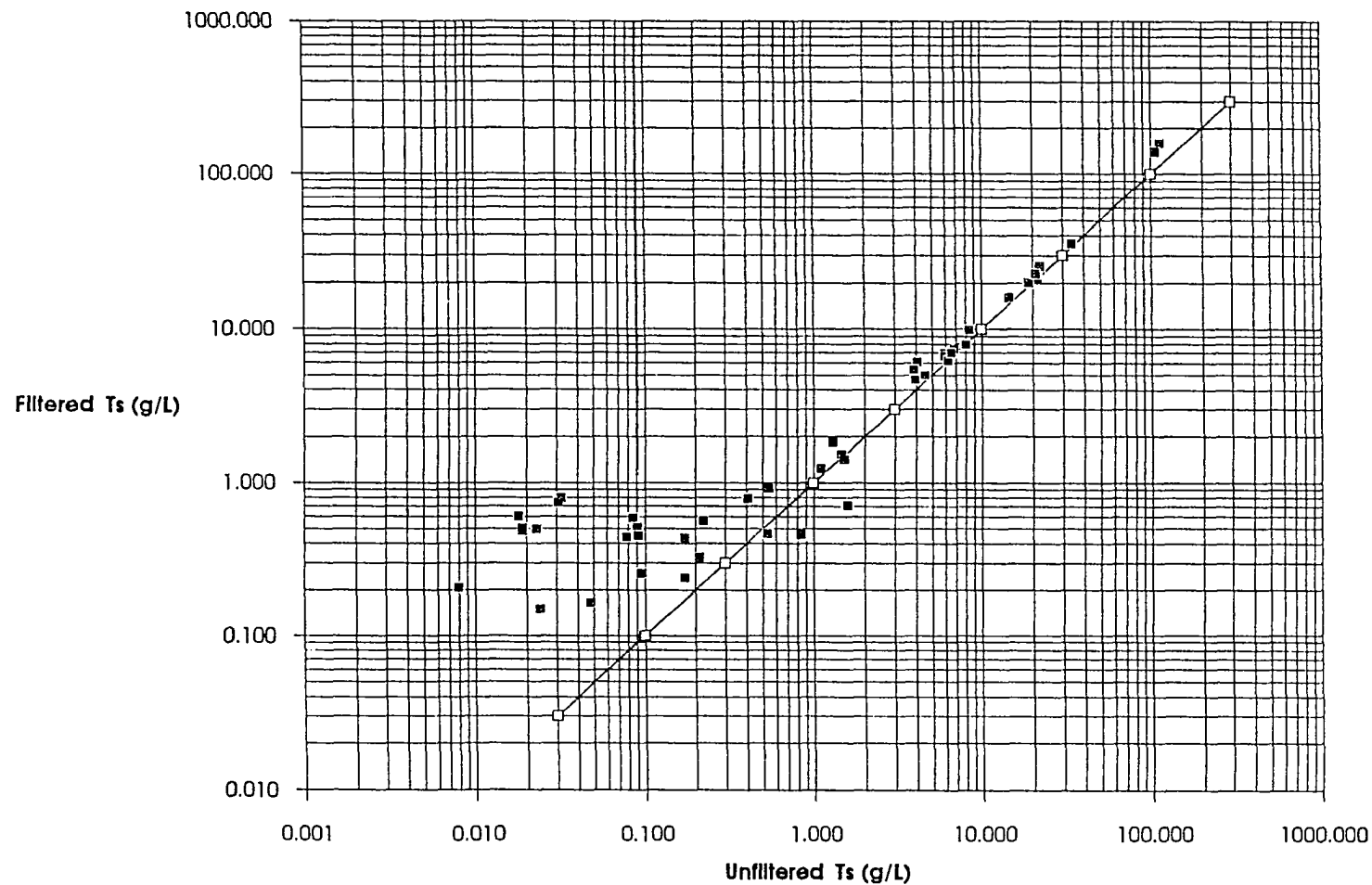


Figure 4.2-3. Comparison of filtered and unfiltered samples. The ADGGS samples were filtered to determine only the suspended constituents, whereas, the UCM samples were not filtered to determine the sum of suspended and dissolved constituents. Total dissolved solids can be estimated from the difference between the unfiltered and filtered results. Although the dissolved component is relatively high at lower Ts concentrations, at high Ts concentrations, the dissolved component is negligible and cannot be estimated.

4.2.5.4 Bedload

Bedload and channel samples were oven-dried on low heat in open flat-bottomed cake pans. The entire dried sample was weighed on a gravimeter to the nearest gram, and then sieved into 32 mm, 16 mm, 8 mm, 4 mm, 2 mm, 1.18 mm, 0.425 mm, 0.250 mm, 0.125 mm, and 0.063 mm sizes. The bedload mass was then divided by the time interval over which the sample was collected to determine the bedload component of sediment flux.

4.3 Results

Complete stream discharge and sediment data for the ADGGS stations are reported in Mack (1987), Mack (1988), Ray and Maurer (1989), Ray (1990), Ray and others (1991), Ray and Vohden (1992), and Ray and Vohden (1993), and the the USGS bridge 1 station in USGS (1986, 1987, 1988, 1989, 1990, 1991, 1992, and 1993). Because only portions or summaries of individual station data are discussed or utilized here, a summary of the more pertinent data to this report is compiled in the Appendix. All of the data not reported in the ADGGS or USGS reports are also presented in the Appendix.

4.3.1 Discharge Data

There are two kinds of discharge data, point discharge and continuous discharge data. Table 4.3-1 summarizes the point discharge data, and Table 4.3-2 summarizes the continuous discharge data. The tables include the number of observations (n - for point records only) of sample collection, the maximum measured discharge (Q_{max}), the minimum measured discharge (Q_{min}), the minimum specific discharge ($Q_{sp(min)}$), and the maximum specific discharge ($Q_{sp(max)}$) for each station. The specific discharge (Q_{sp}) is defined as the discharge per basin area or Q/A . For some stations, point records were collected in a particular year, and continuous records for another year. This is because the ADGGS either added or dropped a station in their monitoring network, before or after I had collected point data from that station.

Discharge (Q) was measured for each creek over ranges of 10-100X. Generally the larger creeks had smaller ranges in $\log[Q]$. An evaluation of the magnitude of discharge variations among creeks is made by comparing the $Q_{sp_{min}}$ and $Q_{sp_{max}}$. $Q_{sp_{min}}$ ranged from 0.006 cfs/mi² in 5N to greater than 0.50 cfs/mi² in 9N, 10N and 9S. $Q_{sp_{max}}$ (including only those with a measured range of $Q > 10X$) ranged from a minimum of 1.35 cfs/mi² in 7N to 48.7 cfs/mi² in 3S. The data in Tables 4.3-1 and 4.3-2 suggest that peak flow and base flow are dependent on the geohydrologic-basin type.

Table 4.3-1. Summary of point discharge records. At non-continuous stations only one discharge measurement and sediment sample were collected each time.

Creek	Basin Area		Lithology Type	Years Monitored	n	Q _{sp_min} (cfs/mi ²)	Q _{min} (cfs)	Q _{sp_max} (cfs/mi ²)	Q _{max} (cfs)
	mi ²	km ²							
1N Terrace	0.79	1.79	Qg	1986-88	17	0.29	0.23	5.72	4.52
2N Badlands	0.61	1.58	Tu/Qg	1986-88	14	0.17	0.106	13.13	8.01
3N Two Bull	0.90	2.33	Tu/Qg	1986,1988	14	0.08	0.071	5.33	4.80
5N Louise	1.56	4.04	Tn/Tu	1986-88	22	0.02	0.035	1.67	2.61
9N Slide	2.08	5.39	Tu	1986-88	19	0.52	1.09	13.57	28.23
UH Upper Hoseanna	8.64	22.37	Tu	1986-88	19	0.51	4.38	17.81	153.85
10Sb Sanderson below mining	5.26	13.63	p ₂ m	1986-88	15	0.19	0.988	27.45	144.40
9S Clinker	1.72	4.45	p ₂ m/Tu	1986-88	14	0.16	0.282	18.67	32.11
7S Mosquito	0.85	2.20	Tu/p ₂ m	1986-88	11	0.42	0.353	1.41	1.20
6S Sixth South	0.84	2.17	Tu/p ₂ m	1986-88	12	0.38	0.318	10.71	9.00
CS Clear	0.63	1.63	p ₂ m	1986-88	11	0.17	0.106	13.49	8.50
5S Iron	1.79	4.64	p ₂ m	1986-88	19	0.24	0.423	19.20	34.37
4S Schist	0.74	1.92	p ₂ m	1986,88	7	0.38	0.282	10.64	7.87
3S Pipe	0.69	1.79	p ₂ m/Tu	1986-88	15	0.15	0.106	48.68	33.59
2S Slime	0.80	2.07	p ₂ m/Tu/Tn	1986-88	13	0.22	0.176	26.64	21.31
1S Runaway	0.32	2.33	Tu	1989	22	0.32	0.10	24.69	7.9
Poker	6.02	15.59	Qg/Tn	1986-88	15	0.27	1.61	2.91	17.50

Table 4.3-2. Summary of Continuous Stage Discharge Records.

Creek	Basin Area		Lithology Type	Years Monitored	$Q_{sp_{min}}$ cfs/mi ²	Q_{min} cfs	$Q_{sp_{max}}$ cfs/mi ²	Q_{max} cfs
	mi ²	km ²						
3N Two Bull	0.90	2.33	Tu/Qg	1988-90	0.078	0.07	5.78	5.20
4N Frances	1.70	4.41	Tn/Tu	1986-88	0.021	0.035	2.49	4.23
5N Louise	1.56	4.04	Tn/Tu	1989-90	0.006	0.01	7.05	11.0
7N Popovitch	4.14	10.73	Tn	1986-88	0.068	0.28	1.35	5.58
10N North Hoseanna	3.13	8.11	Tu	1986-88	0.393	1.23	6.74	21.1
10Sa Sanderson above mining	5.07	13.13	p \bar{c} m	1986-88	0.286	1.45	44.38	225
9S Clinker	1.72	4.45	p \bar{c} m/Tu	1991	0.517	0.89	5.67	9.75
1S Runaway	0.32	2.33	Tu	1990	0.375	0.12	3.40	1.09
1M Bridge 1 Hoseanna	48.1	124.6	Tu/Tn/p \bar{c} m	1985-92	0.310	14.9	27.2 (49.5)	1310 (2380)
3M Bridge 3 Hoseanna	43.0	111.3	Tu/Tn/p \bar{c} m	1986-92	0.333	14.3	27.9	1200
6M Bridge 6 Hoseanna	20.9	54.0	Tu/p \bar{c} m	1988-90	0.397	8.3	23.73	496

4.3.1.1 Base Flows

Base flow is the sustained "fair-weather" runoff (Langbein and Iseri, 1960) composed primarily of effluent groundwater; it may also include runoff delayed by the slow passage through lakes, swamps or other supra-groundwater terrains. The term generally refers to the natural flow of a stream, unaffected by the works of man (Bates and Jackson, 1987).

In this study, base flow is defined as the minimum measurable runoff occurring during any season. For the Hoseanna Creek Watershed, base flows are generally highest in the early summer following break-up. Base flow supply will be charged

following a summer storm and continue to recede following the annual trend (groundwater recession curve). The magnitude of the base flow increase will depend on the extent (frequency, magnitude and duration) of summer storms. In addition to the climatic induced effect on base flow, base flow discharges also depend on geologic setting.

The records for non-stage and continuous-stage discharge data were reviewed to determine if the effect of climate and geology on base flow could be estimated. To eliminate the effects of spring break-up and fall freeze-up, the base flow minimum (Q_{min}) was defined as the minimum measured discharge that occurred during any ice-free time. Figure 4.3-1 is a plot of Q_{min} versus drainage basin area (A). There is no obvious distinction between northern and southern basins; however, the Nenana Gravel basins have very low $Q_{sp_{min}}$ compared to the other basins, and in general, it appear that base flows for Usibelli Group basins > than schistose basins which are > Nenana Gravel basins, and basins with mixed lithologies have intermediate $Q_{sp_{min}}$.

4.3.1.2 Peak Flows

Peak flow is defined as the maximum rate of streamflow discharge at a given point or from a given area, during a specified period (Bates and Jackson, 1987). For continuous-stage discharge stations, peak flows are usually not measured but are extrapolated from established stage-discharge ratings for a particular gage station. For non-stage point discharge stations, the stage of the peak flow is not known, and is usually estimated using indirect discharge measurement techniques (Benson and Dalrymple, 1967).

Mack (1987, 1988) estimated peak flows after Jones (1983), and Wilbur and Clarke (1987) estimated peak flows after Lamke (1978) for several creeks within Hoseanna Creek Watershed. However, it is apparent that both methods gave flows erroneously high for the northern basins underlain by coal-bearing and gravel lithologies, while they were relatively low for the southern basins underlain by permafrost and metamorphics. The methodologies used to predict peak flows did not work here, because they do not incorporate aspectual and geological factors, as will be discussed below.

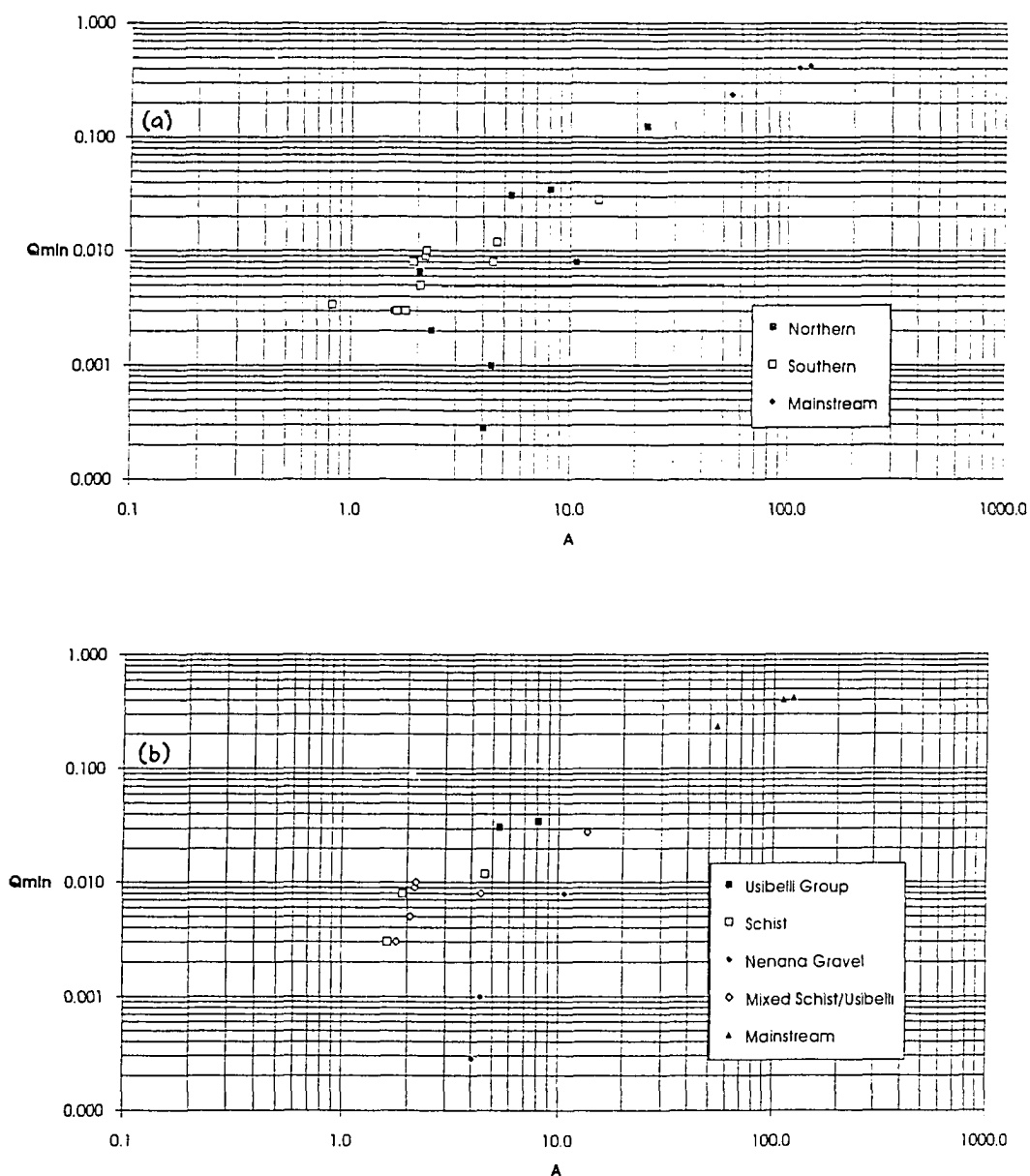


Figure 4.3-1. Plot of minimum discharge versus basin area. The minimum discharge (Q_{min} - m^3/s) or base flow is a function of basin area (A - km^2), aspect (Figure 4.3-1a) and lithology (Figure 4.3-1b). Northern basins underlain by Nenana Gravel have very low Q_{min} , whereas, northern basins underlain by coal-bearing rocks have relatively high Q_{min} . Southern schistose basins are less variable and have relatively moderate Q_{min} .

For most of the hydrologic stations observed in this study, the peak flow was generally not measured; however, in many cases during a single storm, the near peak flows were measured at both the continuous and point record stations. A near peak flow occurred when the measured water depths were within 10-20% of the peak flow depths as interpreted from observed highwater marks on the channel banks. Assuming that depth varies with $Q^{2.86}$ for creeks in Hoseanna Creek Watershed (Osterkamp, 1983), then measured depths 10-20% less than the peaks will correspond to discharges roughly 1.3 to 1.6 times the measured values. With this sampling variance accounted for, the sample set of maximum measured discharges (Q_{max}) for creeks with sufficient data and information was compiled in Tables 4.3-1 and 4.3-2. Figure 4.3-2 is a plot of (Q_{max}) versus drainage basin area (A).

The value of Q_{max} depends first on aspect, and southern basins have higher $Q_{sp_{max}}$ than the northern basins, and in general the demarcation between the two groups can be approximated by the sub-parallel line on Figure 4.3-2 where $Q_{sp_{(max)}}$ is approximately 10. The relationship between aspect and peak discharge reflects the influence of permafrost on the peakedness of storm hydrographs and the higher interception and transpiration rates of the south-facing slopes. In addition, the influence of aspect is amplified by geologic controls. For basins with only one primary lithology (i.e., 10Sa, 9S, 5S, CS, 4S, 10N, 9N, 7N, and 4N), $Q_{sp_{(max)}}$ for the schistose basins ranges from 10 to 45, $Q_{sp_{(max)}}$ for the Usibelli Group basins range from 6 to 14, and $Q_{sp_{(max)}}$ for the Nenana Gravel basins range from 1 to 3. In general, $Q_{sp_{(max)}}$ for the schistose basins is roughly twice that of the coal-bearing basins and ten times the gravel basins. In other words, a design storm event (i.e., 1.25, 10, or 50-year flood) for a north-facing schistose basin will produce roughly ten times the peak discharge of a south-facing gravel basin.

As a consequence of the aspectual and geological factors, current models that rely only on area (Kane and Janowicz, 1988) or do not include geological or aspectual components for predicting peak discharges (Jones, 1983; Lamke, 1978; AHC, 1987; Clarke, 1987) are not valid here. In addition, there are no consistently accurate models for small subarctic creeks (less than 10 km²). The data base for creeks this size in Alaska (Lamke, 1978; Jones, 1983) is not sufficient to extrapolate for the small creeks in this basin.

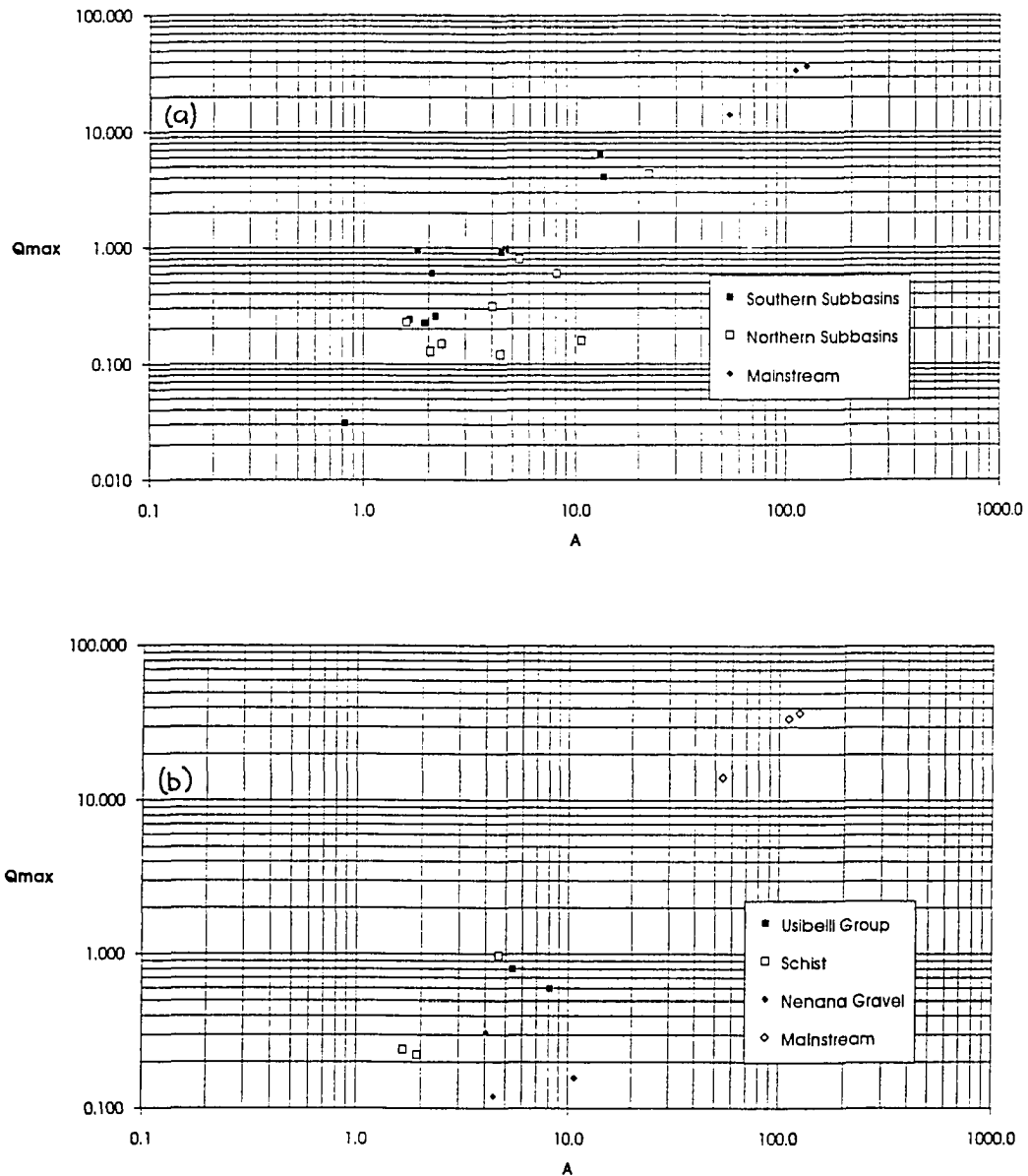


Figure 4.3-2. Plot of maximum discharge versus basin area. The observed peak or near peak flow (Q_{max} - m^3/s) is a function of basin area (A - km^2), aspect (Figure 4.3-2a) and lithology (Figure 4.3-2b). For any given area, southern basins with predominantly schist have relatively high Q_{max} , whereas, northern basins underlain by gravels and sands have relatively low Q_{max} .

Therefore predicted peak discharges for the 2, 5 and 50 year storms were estimated for each creek using a modified method from Kane and Janowicz (1988), where $Q_{peak} = k(Q_{kj})$, where (Q_{kj}) is empirically derived by Kane and Janowicz for Alaskan streams, and the coefficient (k) is derived from Figure 4.3-2 and tabulated in the Appendix, such that k is a function of aspect and lithology where $k_{(north-facing schist)} \sim 2k_{(south-facing coal)} \sim 10k_{(south-facing gravel)}$. Using this empirical relationship, predicted discharges were estimated for the 2, 5, or 50-year floods (Table 4.3-3).

4.3.1.3 Continuous Discharge Records

As described above, base and peak flows for Hoseanna Creek Watershed streams are controlled primarily by basin area, aspect and lithology. These factors also influence the shape of the annual and storm hydrographs. From the rating curves and the continuous stage data, continuous hydrographs were developed for 1M, 3M, 6M, 3N, 4N, 5N, 7N, 10N, 10Sa, 9S and 1S. Continuous discharge data for bridge 1 (1M) are summarized in the annual USGS data reports (USGS, 1986; USGS, 1987; USGS, 1988; USGS, 1989; USGS, 1990; USGS, 1991; USGS, 1992; USGS, 1993), and discharge data for the remainder of the continuous stations are summarized in the ADGGS data reports (Mack, 1987; Mack, 1988; Ray and Maurer, 1989; Ray, 1990; Ray and others, 1991; Ray and Vohden, 1992; and Ray and Vohden, 1993). Representative 1987 and 1988 hydrographs for three different creek sizes, 3M, 10Sa, and 4N, are reproduced in Figures 4.4-3 and 4.4-4 from ADGGS reports (Mack, 1988; and Ray and Maurer, 1989).

Two processes are apparent on all of the hydrographs. First, the creeks do not flow in the winter (or have negligible sub-aufeis flow), so that there are diurnally phased high and low flows during the spring break-up and fall freeze-up transition periods, and during the summer, relatively low base flows are punctuated by peaked high runoff events. Second, the aspectual and geological controls described above modify the amplitude and duration of these two trends. Figure 4.3-5 is a plot of the 2-year peak flow versus the base flow. The southern basins underlain by permafrost in predominantly schist terrain have much higher peak flows than the northern basins in non-permafrost in predominantly sedimentary terrain for a given base flow. This translates to more peaked hydrographs and shorter duration recession curves for the southern basins.

Table 4.3-3. Predicted discharges of Hoseanna Creek Watershed streams for the 2, 5 and 50 year recurrence intervals.

Creek	Q _{2.0} (cfs)	Q _{5.0} (cfs)	Q _{50.0} (cfs)
<u>Northern:</u>			
Terrace (1N)	4.1	9.5	31.1
Badlands (2N)	3.3	7.8	26.1
Two Bull (3N)	3.5	7.9	25.6
Frances (4N)	4.0	8.8	27.2
Louise (5N)	3.7	8.2	25.5
Popovitch (7N)	4.3	9.1	26.0
Slide (9N)	14.3	31.1	94.5
North Hoseanna (10N)	20.4	43.3	127.3
Upper Hoseanna (11N)	93.1	186.9	506.6
<u>Southern:</u>			
Runaway (1S)	2.8	6.8	24.1
Slime (2S)	12.5	28.7	94.1
Pipe (3S)	11.0	25.5	84.5
Schist (4S)	13.6	31.4	103.7
Iron (5S)	29.3	64.3	197.6
Clear (CS)	11.8	27.6	92.2
Sixth South (6S)	8.7	19.9	65.0
Mosquito (7S)	8.8	20.1	65.6
Clinker (9S)	24.2	53.3	164.5
Sanderson (10Sa)	109.6	226.7	641.4
Sanderson (10Sb)	117.1	241.8	682.1
<u>Hoseanna Creek:</u>			
Bridge 1 (1M)	725.3	1320.3	3119.5
Brdige 3 (3M)	658.2	1205.7	2874.4
Bridge 6 (6M)	264.1	504.1	1273.2

In addition, the southern basins are likely frozen (i.e., their channels filled with aufeis) for longer periods, so that maximum spring break-up flow occurs later than the maximum in the northern basins. In addition, the north-flowing creeks (i.e., draining southern basins) freeze before the south-flowing creeks and therefore have less total time to deplete groundwater storage.

4-40

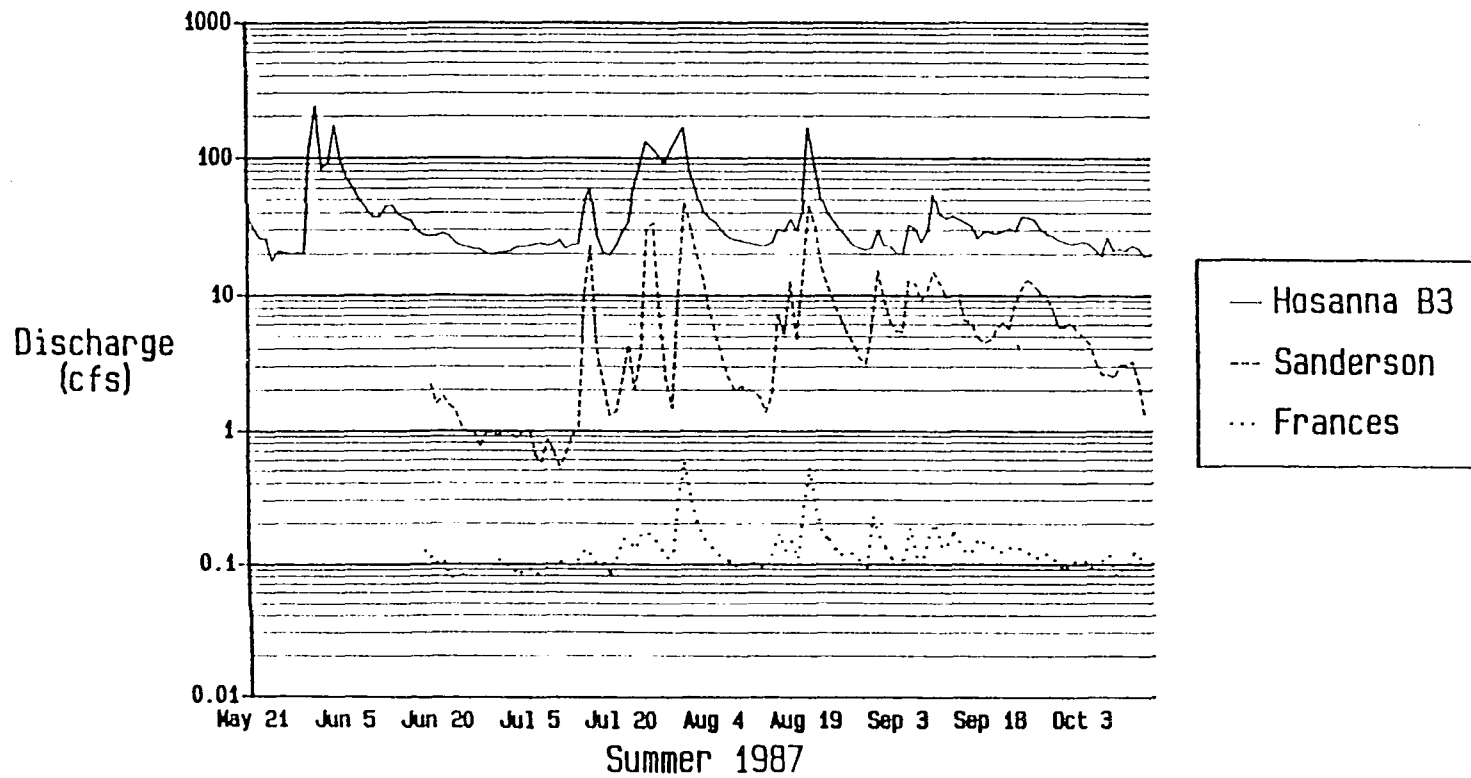


Figure 4.3-3. Composite 1987 summer hydrographs for Hoseanna Creek at bridge 3 (3M), Sanderson Creek above mining (10Sa), and Frances Creek (4N) (from Mack, 1988).

4-41

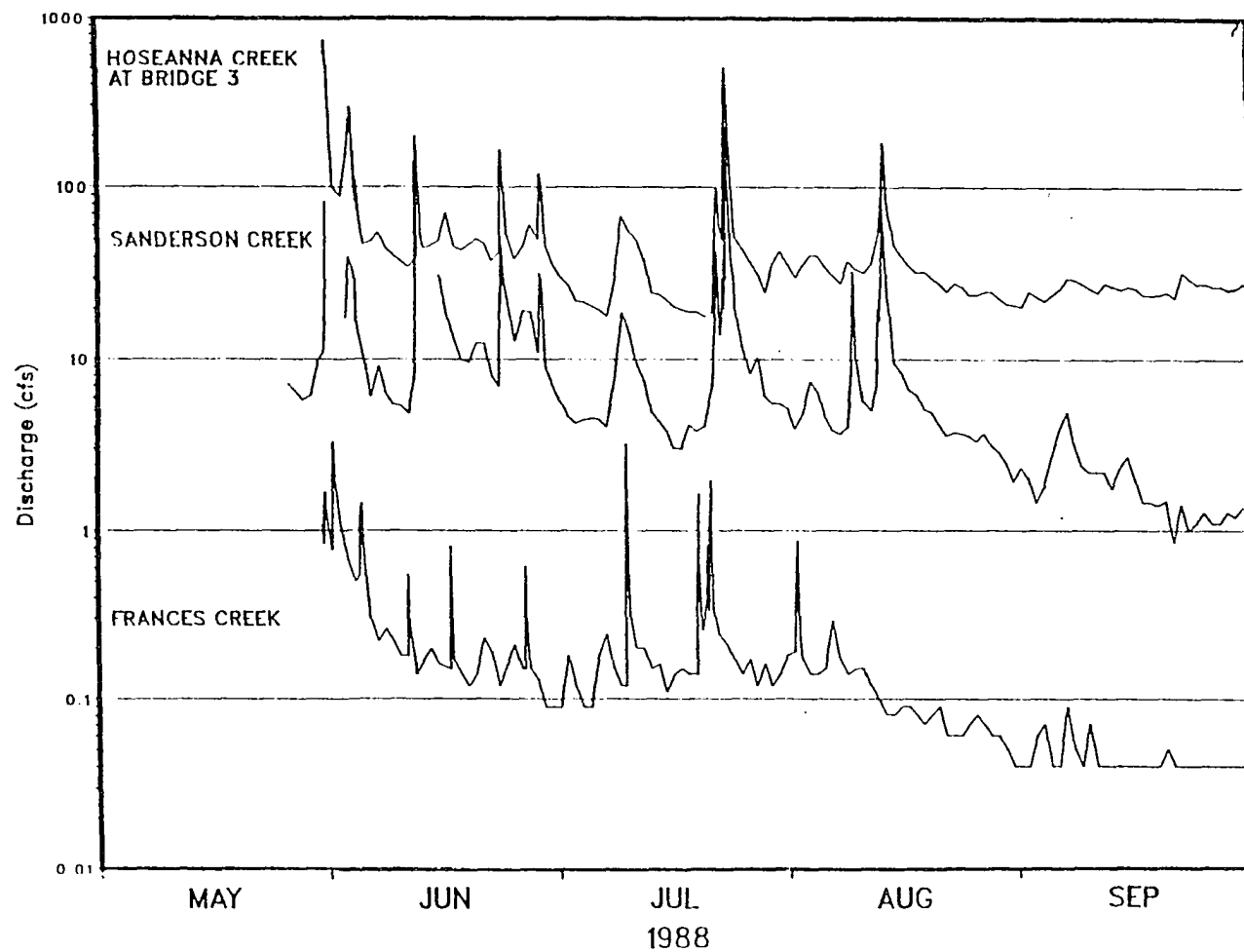


Figure 4.3-4. Composite 1988 summer hydrographs for Hoseanna Creek at bridge 3 (3M), Sanderson Creek above mining (10Sa), and Frances Creek (4N) (from Ray and Maurer, 1989).

4-42

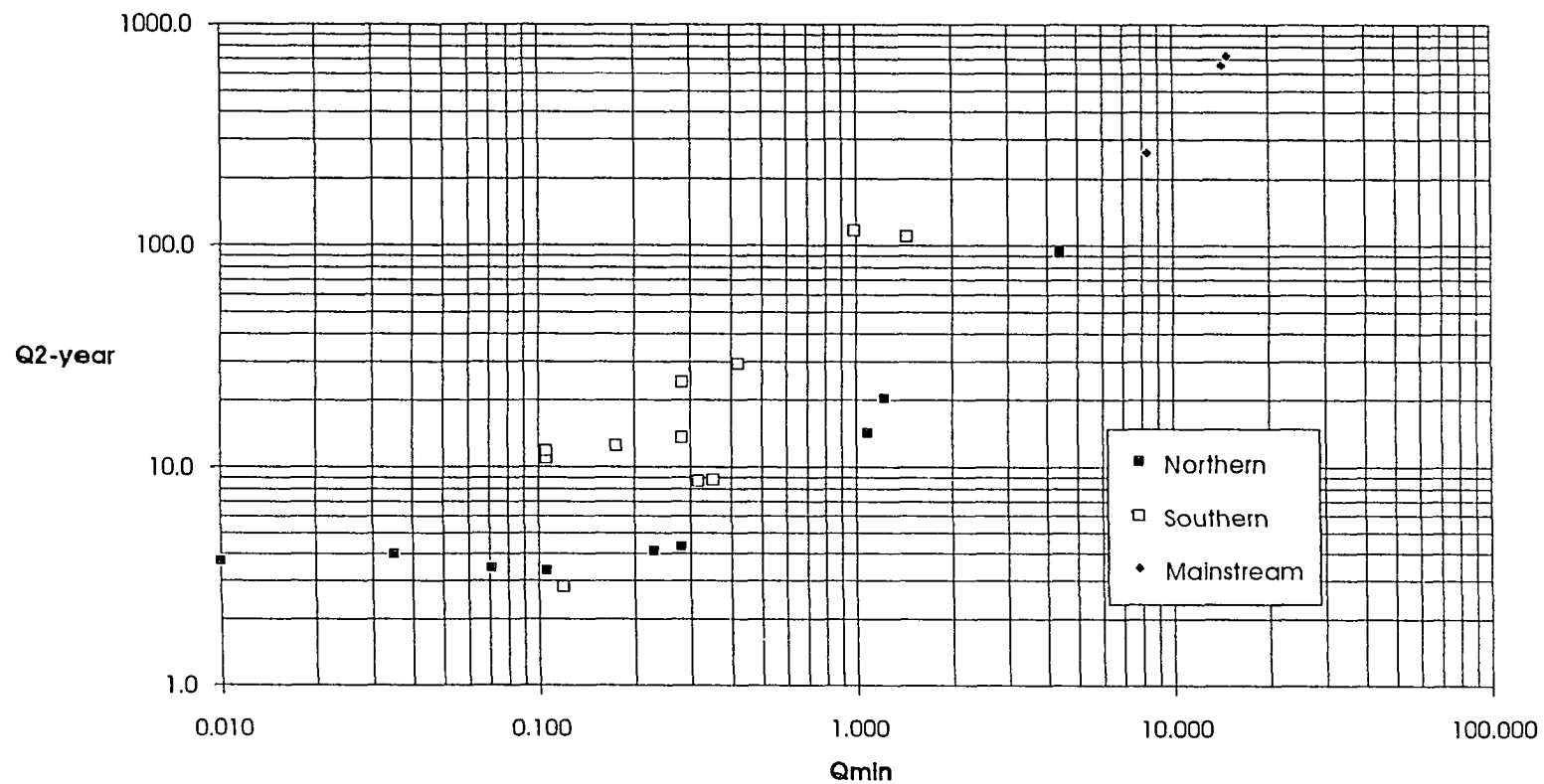


Figure 4.3-5. Plot of base flow versus estimated 2-year peak flow. Variations in aspect and lithology control the relationship between peak flows (i.e., the 2-year event) to base flows, such that southern basins underlain predominantly by schist have significantly higher peak to base flow ratios.

In many creeks, aufeis can build up to 1.5 to 2.0 meters thick. This covers 25 year-old terraces on the main channel, and completely inundates and overtops the entire channel in the small creeks. Springtime runoff on the aufeis surface is then capable of corradng stream banks that only summertime floods with 25-100 year return intervals could reach.

4.3.1.4 Controls on Discharge Variations

Hoseanna Creek Watershed is atypical in that the high latitude, geologic structure and three basic lithologies have produced markedly asymmetric drainage characteristics. The prevailing climate and discontinuous permafrost of the subarctic combined with this geologic asymmetry support distinct plant community characteristics with different transpiration and interception rates, and distinct geomorphic conditions with different degrees of cryogenic processes. The result is three distinct geohydrologic-basin types. This is demonstrated by the range of peak and base flows and the shape of the storm and annual hydrographs measured for the different basin types.

The north-flowing creeks are predominantly underlain by highly deformed basement metamorphics (quartz-sericite schist), are at a higher overall elevation and are in permafrost. Typically, the active layer is no more than 30-60 cm, and a *Sphagnum*-dominated community or stunted black spruce forest with a thick organic layer is the only cover. Hence, groundwater storage is limited, interception and evapotranspiration are low, but orographic influences provide more rainfall so peak discharges can be very high. In contrast, some of the south flowing creeks are underlain by the highly porous and permeable Nenana Gravels that have very low base and peak flows for their areas. As noted earlier, these basins (4N, 5N, and 7N) are unlike the other basins, and have thick sequences (over 300 m) of sandstones and gravels with no aquitards. Very little permafrost is evident, while the sands and gravels provide high infiltration potential. However, because vegetation is more lush, more evapotranspiration and higher amounts of interception occur. In addition, due to the ample supply of sediment, the channel bottoms are box-shaped and thick with sediment so that channel-interflow processes operate. These factors combine to yield very low base flows. Also, because infiltration capacity is high, peak discharges are smaller than those in the north-flowing creeks.

The layered sand-silt-clay-coal sequences of the Usibelli Group include thick fractured coal seams as relatively high volume storage aquifers. Usually, where there is extensive basin groundwater storage, baseflows are higher and maintained for longer periods. Conversely, in low storage basins baseflows are lower. The effect observed here in the Hoseanna Creek Watershed is a limited basin storage contained in highly porous Nenana Gravel sandy-gravel that depletes rapidly to a low base level. The higher base flows in the coal-basins dominated by coal-bearing lithologies reflect more groundwater storage released at a more steady rate. In addition, the higher elevation of the southern basins (and potential orographic influences on rainfall) may be responsible for the south creeks having higher overall larger peak and base flows.

4.3.2 Sediment Concentration Data

4.3.2.1 Suspended Load

A summary of suspended sediment concentration records for the nonstage point and continuous discharge record stations is provided in Tables 4.3-4 and 4.3-5. Grab samples were collected at all nonstage point record stations while both automated Isco samplers and grab sampling techniques were used at the continuous stage discharge record stations. Measured discharge (Q) during sediment sampling ranged from 0.03 to 1264 cfs (0.00042 to 17.90 m³/s) and suspended sediment concentration (Ts) ranged from 0.0013 in relatively clear creeks to 1635 g/l during mudflows in other creeks. Generally, creeks underlain by the poorly consolidated sedimentary rocks draining from the northern basins were turbid for any flow above base flow, and typically did not "clear up" until well into the summer season (late July to early August).

Generally, all creeks attained fairly low Ts sometime during the year, as the minimum Ts for each creek ranged from 0.0013 g/l to 0.039 g/l for filtered samples, and from 0.096 g/l to 0.96 g/l for unfiltered samples. However, the maximum Ts for each creek had a much larger range of values. The maximum Ts for each (a) schistose-type creek ranged from 1.07 g/l in Schist Creek (4S) to 59.3 g/l in Sanderson Creek (10Sa), (b) coal-bearing-type creek from 16.1 g/l in Upper Hoseanna Creek (11N) to 949 g/l in Badlands Creek (2N), and (c) sandy-gravel-type creek from 25.5 g/l in Popovitch Creek (7N) to 1635 g/l in Suntrana Creek.

Table 4.3-4. Summary of suspended sediment concentration records for nonstage point discharge record stations.

Creek	Lithology Type	Years Monitored	Sample Type	n	Ts _{min}	Ts _{max}
1N Terrace	Qg	1986	Ug	2	0.157	0.261
		1987	Ug	5	0.166	0.551
		1988	Ug	9	0.174	17.82
2N Badlands	Tu/Qg	1986	Ug	2	0.544	1.136
		1987	Ug	4	1.337	44.06
		1988	Ug	8	0.160	949.0
3N Two Bull	Tu/Qg	1986	Ug	2	3.732	3.870
		1988	Ug	12	0.208	327.0
			Fg	13	0.0075	113.0
4N Frances	Tn/Tu	1989	Fg	2	4.070	6.010
5N Louise	Tn/Tu	1986	Ug	3	0.446	18.175
		1987	Ug	7	0.560	20.55
		1988	Ug	12	0.462	140.7
			Fg	14	0.0594	106.0
9N Slide	Tu	1986	Ug	3	0.784	1.038
		1987	Ug	6	0.444	9.349
		1988	Ug	8	0.364	28.88
11N Upper Hoseanna	Tu	1986	Ug	3	0.180	0.373
			Fg	1	1.740	---
		1987	Ug	4	0.428	2.685
			Fg	3	0.793	1.030
		1988	Ug	12	0.143	16.07
10Sb Sanderson below mining	p = m	1986	Ug	3	0.731	0.802
		1987	Ug	3	0.850	2.651
			Fg	2	0.162	1.050
		1988	Ug	9	0.769	13.507
9S Clinker	p = m/Tu	1986	Ug	2	0.190	0.193
		1987	Ug	2	0.347	0.780
		1988	Ug	10	0.208	13.54

7S Mosquito	Tu/p \bar{m}	1986	Ug	2	0.601	0.710
		1987	Ug	4	0.707	1.290
		1988	Ug	5	0.689	6.887
6S Sixth South	Tu/p \bar{m}	1986	Ug	1	0.963	---
		1987	Ug	4	1.413	2.810
		1988	Ug	7	1.212	5.349
CS Clear	p \bar{m}	1986	Ug	2	0.107	0.763
		1987	Ug	3	0.134	0.470
		1988	Ug	6	0.126	2.076
5S Iron	p \bar{m}	1986	Ug	5	0.242	0.437
			Ua	6	0.265	0.328
		1987	Ug	6	0.390	2.080
		1986	Ug	8	0.252	4.079
4S Schist	p \bar{m}	1986	Ug	2	0.471	1.071
		1988	Ug	5	0.192	0.676
3S Pipe	p \bar{m} /Tu	1986	Ug	2	0.432	13.526
		1987	Ug	4	0.481	7.103
		1988	Ug	9	0.350	19.971
2S Slime	p \bar{m} /Tu/Tn	1986	Ug	2	0.743	2.636
		1987	Ug	3	0.427	3.350
		1988	Ug	8	0.300	14.347
		1989	Fg	2	1.780	26.100
1S Runaway	Tu	1986	Ug	2	0.179	0.368
		1987	Ug	1	---	15.760
		1989	Fg	23	0.0073	23.200
Poker	Tn	1986	Ug	1	0.096	---
		1987	Ug	3	0.110	0.120
		1988	Ug	12	0.106	2.222

Table 4.3-5. Summary of suspended sediment concentration records for continuous discharge record stations. Sample types: Ug - unfiltered grab, Fg - filtered grab, Fa - filtered automated, Fac - filtered automated composite.

Creek	Lithology Type	Years Monitored	Sample Type	n	Ts _{min}	Ts _{max}
3N Two Bull	Tu/Qg	1989	Fg	14	0.0097	35.20
			Fa	28	5.66	99.40
		1990	Fg	22	0.0225	9.26
			Fa	43	3.36	94.40
4N Frances	Tn/Tu	1986	Ug	3	0.330	7.671
			Fg	10	0.0212	4.130
			Fac	37	0.0183	3.160
		1987	Ug	4	1.697	11.757
			Fg	30	0.0046	8.330
			Fa	2	7.20	12.50
		1988	Ug	23	0.416	43.0
			Fg	26	0.0052	56.90
			Fa	35	0.219	125.0
5N Louise	Tn/Tu	1989	Fg	32	0.0013	89.30
			Fa	76	5.330	99.70
			Fac	5	1.910	9.780
7N Popovitch	Tn	1986	Ug	4	0.454	23.541
			Fg	10	0.0665	17.00
			Fa	4	0.340	24.80
		1987	Ug	4	0.134	0.823
			Fg	24	0.0023	1.33
		1988	Ug	22	0.159	25.52
			Fg	21	0.0171	22.20
10N North Hoseanna	Tu	1986	Ug	4	1.376	5.702
			Fg	2	0.986	2.960
			Fac	29	0.306	26.80
		1987	Fg	14	0.136	7.200
			Fa	7	4.91	17.80
		1988	Ug	10	0.257	6.542
			Fg	21	0.020	7.830
			Fa	52	0.660	16.60

10Sb Sanderson above mining	p Ξ m	1986	Ua	10	0.477	3.99
			Ug	2	0.480	-.-
			Fg	2	0.0168	0.060
		1987	Ug	1	1.001	-.-
			Fg	11	0.0094	2.720
			Fa	52	0.456	59.30
		1988	Ug	5	0.512	0.793
			Fg	15	0.0063	26.50
			Fa	94	0.0402	27.80
9S Clinker	p Ξ m/Tu	1990	Fg	47	0.0139	1.880
			Fa	69	0.116	27.20
1M Bridge 1 Hoseanna	Tu/Tn/p Ξ m	1986	Ug	16	0.540	47.83
		1987	Ug	55	0.450	16.56
			Fe	3	0.198	1.850
		1988	Ug	79	0.382	35.74
			Fg	21	0.040	11.70
			Fe	3	0.0786	2.360
		1989	Fg	6	0.314	1.496
			Fe	1	0.234	-.-
		1990	Fa	72	0.719	11.00
			Fg	2	0.0172	0.427

3M Bridge 3 Hoseanna	Tu/Tn/pΣm	1986	Ug	10	0.540	47.83
			Fg	10	0.214	2.990
			Fac	29	0.372	14.80
		1987	Ug	8	0.849	13.279
			Fg	37	0.0283	19.00
			Fa	95	0.0743	40.70
		1988	Fe	3	0.275	1.970
			Ug	22	0.512	28.17
			Fg	35	0.0241	21.10
		1989	Fa	92	0.756	63.10
			Fe	3	0.842	1.440
			Fg	35	0.0824	29.20
		1990	Fa	181	0.141	30.10
			Fac	159	0.0675	47.80
			Fe	1	0.113	---
		1991	Fg	2	0.0172	0.427
			Fa	93	0.895	19.80
			Fac	97	0.0517	12.70
		1992	Fe	2	0.0669	0.578
			Fa	8	4.390	129.00
			Fac	146	0.0496	15.90
6M Bridge 6 Hoseanna	Tu/pΣm	1988	Ug	5	0.651	31.45
			Fg	23	0.113	19.70
			Fa	27	0.114	12.40
		1989	Fg	25	0.191	19.30
			Fa	119	0.158	43.30
			Fac	20	0.362	2.64
		1990	Fac	49	0.0394	6.490
			1S Runaway	Tu		
		1990		Fg	33	0.000
			Fa	40	0.560	44.90

Sediment concentrations in creeks draining terrain underlain by mixed lithologies were dominated by the lithology within the lower half of the basin.

During spring break-up flows and during high intensity summer storms some transitional muddy streamflows and even bouldery mudflows were observed emanating from creeks draining either the coal-bearing or sandy-gravel basins. A

summary of these exceptional sediment concentrations is compiled in Table 4.3-6. Creeks underlain by schist were "clear" or only slightly turbid except during major storm events. However, during the fall season the schistose creeks took on a very turbid iron-rich orange-brown color most likely indicative of cold temperature induced precipitation of chemically weathered iron.

4.3.2.2 Bedload

Concurrent measurements of bedload, suspended load, stream gradient, discharge, and grain size distributions taken from Hoseanna, Frances and Popovitch Creeks are summarized in Table 4.3-7. In addition to the bedload samples, samples were collected from the channel bed during low flow conditions. Grain size distribution charts for the bedload and channel samples are shown on Figures 4.3-6 through 4.3-8. The three creeks show a wide range in sediment load and channel caliber characteristics (Wilbur and Clarke, 1988).

Sediment samples were collected from Hoseanna Creek (1M) using the Halley-Smith sampler (with a 3-inch [7.6 cm] sample orifice) and were taken at discharges from 66 to 178 cfs (0.93 to 2.52 m³/s), where the average channel gradient ranged from 0.004 to 0.017. Total sediment concentrations ranged from 1.7 to 16.8 g/l in which the bedload comprised from 0.9 to 33.5%. The bedload percentage, %BL, was lowest at the highest discharges (Figure 4.3-9), and the bedload concentration decreased with increased discharge (Figure 4.3-10). The proportionate increase in T_s with Q indicates a fine-grained sediment caliber dominated by sediment supply from the fine-grained coal-bearing rocks. The grain size distribution chart (Figure 4.3-6) indicates that coarse material is present in the channel. Although the D_{50} and D_{90} grain size increased with increased discharge, the proportion of coarse bedload at low flows decreases at high flows because there is a larger increase in fine sediment at high flows.

Sediment samples collected from Popovitch Creek (7N) using the flume-net bedload trap were taken at discharges from 0.28 to 1.54 cfs (0.0040 to 0.022 m³/s), where the average channel gradient ranged from 0.035 to 0.070. Total sediment concentrations ranged from 0.024 to 19.7 g/l, in which %BL, ranged from 34 to 94%. No simple relationship between discharge and %BL existed (Figure 4.3-9).

Table 4.3-6. Exceptional sediment concentrations (greater than 50 g/L) sampled during storms from 1986-1992. The last three sites are located outside Hoseanna Creek Watershed. Sample Type: Ug - unfiltered grab, Fg - filtered grab, Fa - filtered automated.

Site	Date	Time	Sample Type	Ts (g/l)
Badlands Ck (2N)	06/03/88	05:50	Ug	105.9
	06/18/88	14:50	Ug	823.0
	07/08/88	16:30	Ug	962.1
	07/08/88	16:32	Ug	935.2
	07/08/88	16:34	Ug	731.8
	07/08/88	16:36	Ug	624.4
Two Bull Ck (3N)	06/18/88	15:10	Ug	327.0
	07/08/88	16:55	Ug	66.0
	07/11/88	15:45	Ug	158.8
	07/11/88	15:50	Fg	113.5
	06/25/89	00:00	Fa	72.0
	06/25/89	00:30	Fa	99.4
	06/25/89	01:00	Fa	59.0
	06/25/89	01:30	Fa	55.8
	06/25/89	02:30	Fa	95.4
	06/25/89	03:00	Fa	71.1
	07/03/89	16:30	Fa	70.1
	08/26/90	17:00	Fa	94.4
	08/26/90	17:30	Fa	59.9
Frances Ck (4N)	06/01/88	19:00	Fg	56.9
	07/21/88	06:15	Ug	124.8
	07/21/88	07:45	Fa	62.0
	07/21/88	17:30	Fa	298.0

Louise Ck (5N)	05/31/88	01:10	Ug	72.5
	07/22/88	11:00	Ug	105.9
	07/22/88	11:05	Ug	140.7
	06/06/89	10:15-15:30	Fa	56.4-91.6
	06/25/89	05:15	Fa	90.7
	06/25/89	10:30	Fg	78.0
	06/25/89	12:00	Fa	80.3
	06/25/89	12:15	Fg	74.3
	08/04/89	22:15	Fa	99.7
	08/04/89	23:00	Fa	56.5
	08/05/89	02:00	Fa	68.7
Hoseanna Ck (3M)	05/31/88	02:00	Fa	63.1
	07/01/91	21:30	Fa	101.0
	07/01/91	22:30	Fa	129.0
	07/01/91	23:30	Fa	82.3
	07/02/91	00:30	Fa	70.3
	07/02/91	01:30	Fa	67.1
Suntrana Ck	07/09/88	00:10	Ug	148.8
	07/22/88	22:50	Ug	804.5
	07/22/88	23:08	Ug	1635.1
	07/22/88	23:10	Ug	1240.9
Squirrel Valley	06/18/88	14:45	Ug	866.7
	07/11/88	15:20	Ug	613.0
Dry Ck	07/08/88	23:00	Ug	67.9
	07/08/89	23:10	Ug	58.7

However, bedload concentration increased with increased discharge (Figure 4.3-10), and bedload percentage was generally a very significant portion of the total load, reflecting the coarse sediment associated with Nenana Gravel (Figure 4.3-7). In addition, the D50 and D90 grain sizes increased with discharge.

Sediment samples collected from Frances Creek (4N) using the flume-net bedload trap were taken at discharges from 0.10 to 0.73 cfs (0.0014 to 0.010 m³/s), where the average channel gradient ranged from 0.052 to 0.105. Total sediment concentrations ranged from 0.66 to 21.1 g/l in which %BL ranged from 8.5 to 71.2%. In this case, both %BL and bedload concentration increased with

Table 4.3-7. Summary of bedload samples collected at Hoseanna Creek Bridge 1 (1M), Frances Creek (4N), and Popovitch Creek (7N), where Q = streamflow discharge during sampling, T_{bl} = total bedload rate, T_s = total suspended sediment concentration, T_b = total bedload concentration, $\%T_b$ = percent bedload of the total sediment load.

<u>Creek:</u> Sample Date	Sampling Duration (secs)	Sample Weight (g)	Q (cfs)	T_{bl} (g/s)	T_s (g/L)	T_b (g/L)	$\% T_b$
<u>Frances:</u>							
6/25/88	120	109.8	0.14	0.92	0.6720	.231	25.57
7/2/88	240	38.1	0.10	0.16	0.6000	.056	8.55
7/8/88	60	1098.4	0.21	18.31	6.9770	3.079	30.62
7/22/88	21.3	6623.9	0.73	310.98	6.0800	15.046	71.22
<u>Popovitch:</u>							
7/8/87	300	49.4	0.28	0.16	0.0032	0.021	86.65
7/20/87	120	489.0	0.55	4.08	0.3290	0.262	44.30
7/20/87	120	570.0	0.55	4.75	0.3290	0.305	48.11
7/21/87	600	272.0	0.33	0.45	0.0080	0.049	85.85
7/30/87	60	2040.0	0.61	34.00	1.3000	1.969	60.23
7/31/87	240	1890.0	0.44	7.88	0.3130	0.632	66.88
8/3/87	300	123.0	0.33	0.41	0.0232	0.044	65.41
8/4/87	600	70.8	0.33	0.12	0.0250	0.013	33.56
8/19/87	60	7240.0	0.71	120.67	1.1900	6.002	83.45
9/15/87	120	3930.0	0.61	32.75	0.1190	1.896	94.09
5/13/88	30	717.7	1.40	23.92	4.3500	0.604	12.18
5/26/88	30	1262.3	1.84	42.08	0.6900	0.808	53.93
5/30/88	30	15900.8	3.40	530.03	7.5890	12.156	61.56
6/26/88	60	187.6	0.33	3.13	0.1630	0.335	67.25
7/10/88	120	3943.9	0.52	32.87	1.4190	2.232	61.14
8/21/88	120	486.1	0.55	4.05	0.1500	0.260	63.43
<u>Hoseanna Creek Bridge 1:</u>							
7/22/88	20	15457.0	156.00	772.85	14.5200	0.175	1.19
7/24/88	20	21310.0	65.90	065.50	1.1300	0.571	33.57
8/12/88	20	14623.0	178.10	731.15	16.6500	0.145	0.86

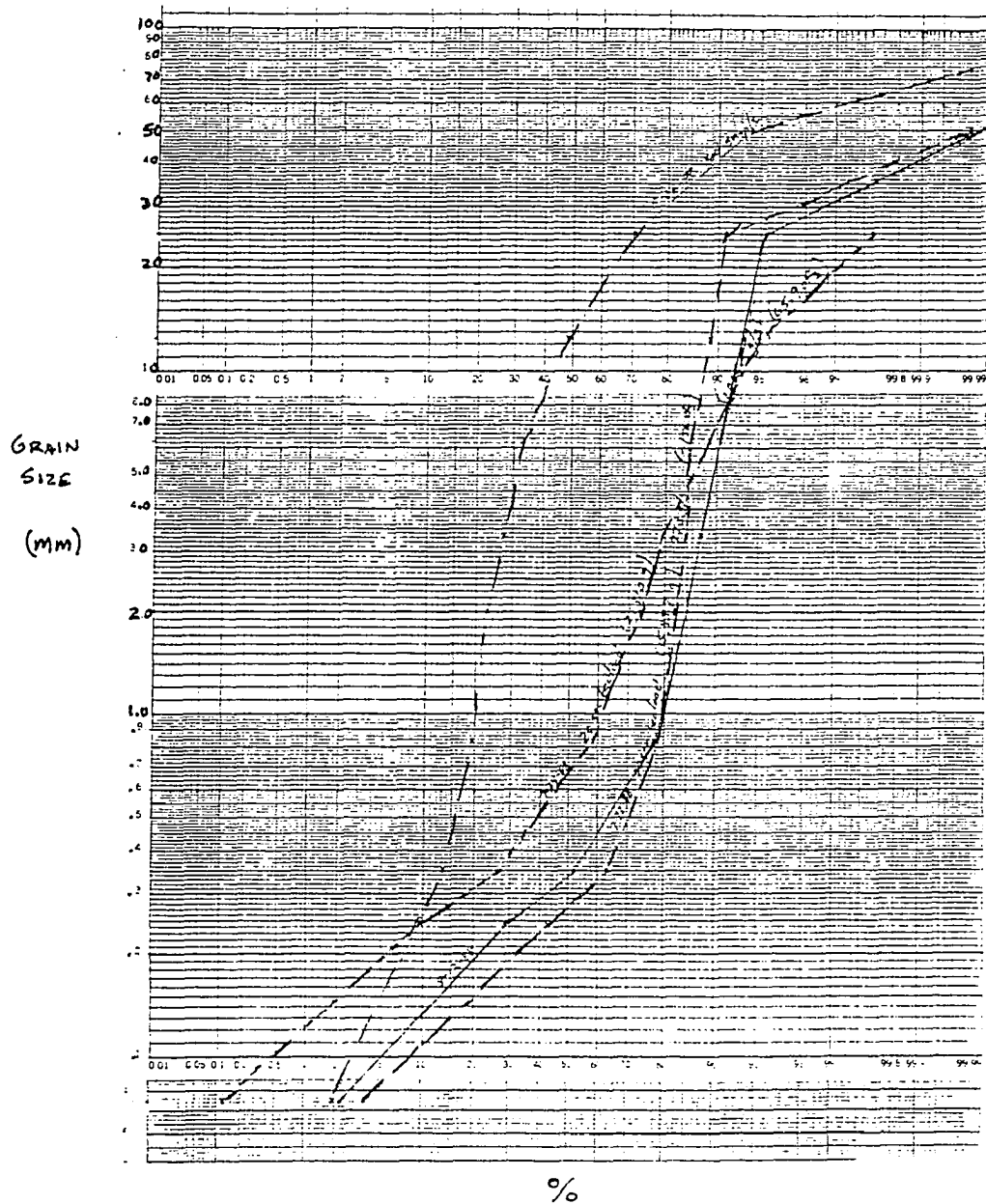


Figure 4.3-6. Grain size distribution curves for bedload and channel bottom samples from Hoseanna Creek at bridge 1 (1M). Channel bottom samples were collected following Wolman (1954), while bedload samples were collected using a flume-net or a Halley-Smith sampler. Channel bottom sample curve represents the maximum grain size distribution that bedload sample curves approach with increasing stream energy.

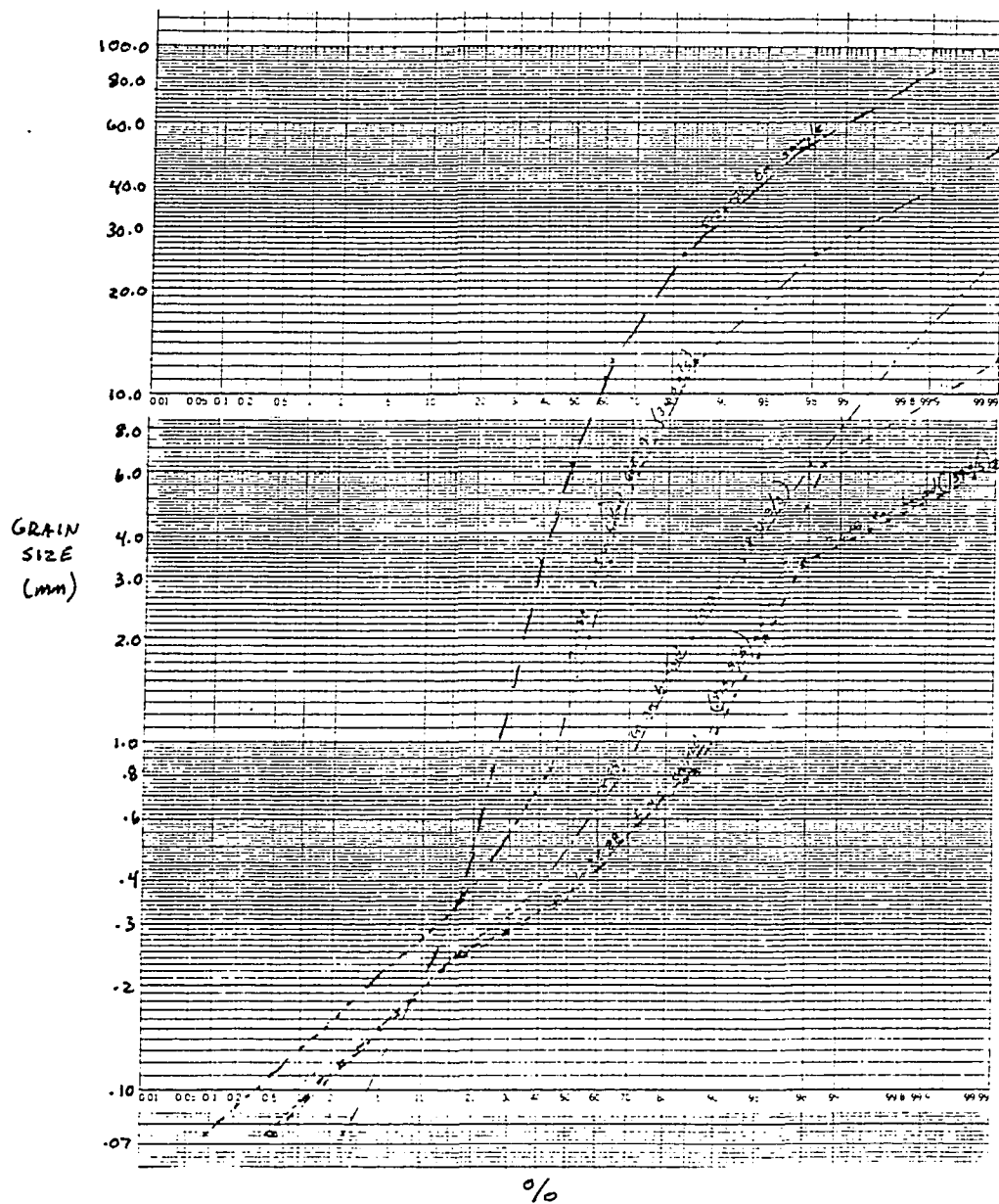


Figure 4.3-7. Grain size distribution curves for bedload and channel bottom samples from Frances Creek (4N). Channel bottom samples were collected following Wolman (1954), while bedload samples were collected using a flume-net or a Halley-Smith sampler. Channel bottom sample curve represents the maximum grain size distribution that bedload sample curves approach with increasing stream energy.

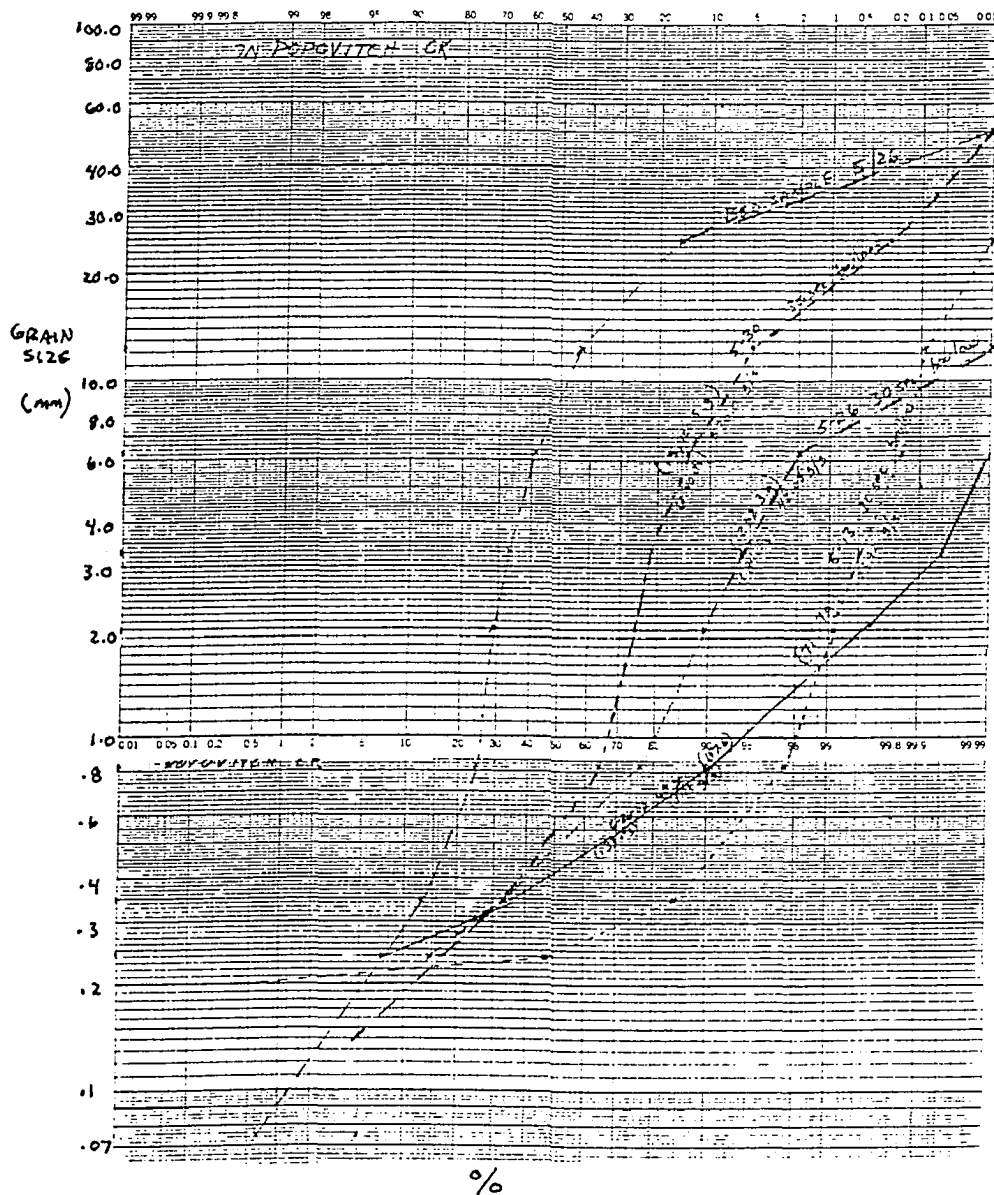


Figure 4.3-8. Grain size distribution curves for bedload and channel bottom samples from Popovitch Creek (7N). Channel bottom samples were collected following Wolman (1954), while bedload samples were collected using a flume-net or a Halley-Smith sampler. Channel bottom sample curve represents the maximum grain size distribution that bedload sample curves approach with increasing stream energy.

discharge (Figures 4.3-9 and 4.3-10). The proportionate decrease of Ts is indicative of the tendency of coarse material from Nenana Gravel to dominate at high flows, and that the supply of fines has reduced by the time higher flows are attained. Again the D50 and D90 grain sizes increased with discharge (Figure 4.3-8).

Although %BL and Tb were not uniformly related to discharge, in all three cases, both the D50 and the D90 grain size components increased with increased discharge, and tended towards the D50 and D90 concentration of the channel bed sample. The bed sample is representative of the maximum attainable sediment caliber from the available supply in a particular basin, and is a reflection of the dominant lithologies beding eroded upstream from the sample location. The tendency of grain size distribution curves sampled from increasing discharges to approach the type curve sampled from the channel is attributed to the existence of maximum entrainment thresholds associated with each creek.

4.3.2.3 Dissolved Load

The dissolved concentrations determined for the ETR depth-integrated ADGGS samples from 1M and 3M ranged from 201-350 mg/l (Ray, 1990). Although the measurement of dissolved load was not an objective of this study, an estimate of the dissolved load can also be made from a comparison of the duplicate samples taken and analyzed by the filtering and non-filtering techniques described in Section 4.2.5.3. This essentially is a comparison of the analyses of duplicate samples made between the UCM Lab (non-filtered) and the ADGGS Lab (filtered) results. That is

$$T_d = T_{ucm(lab)} - T_{dggs(lab)},$$

where Td is the dissolved concentration. Operational errors between labs can be expected as well as natural variation between duplicate samples. The relationship is shown in Figure 4.2-3; generally, the estimated dissolved concentration is a significant component only at very low flows, and typically is in the 50-500 mg/l range. Dissolved solids are difficult to estimate for high flows with high sediment concentrations because errors are large; that is, an estimation cannot be made by subtracting two very large numbers to get a small one. A review of the results

4-58

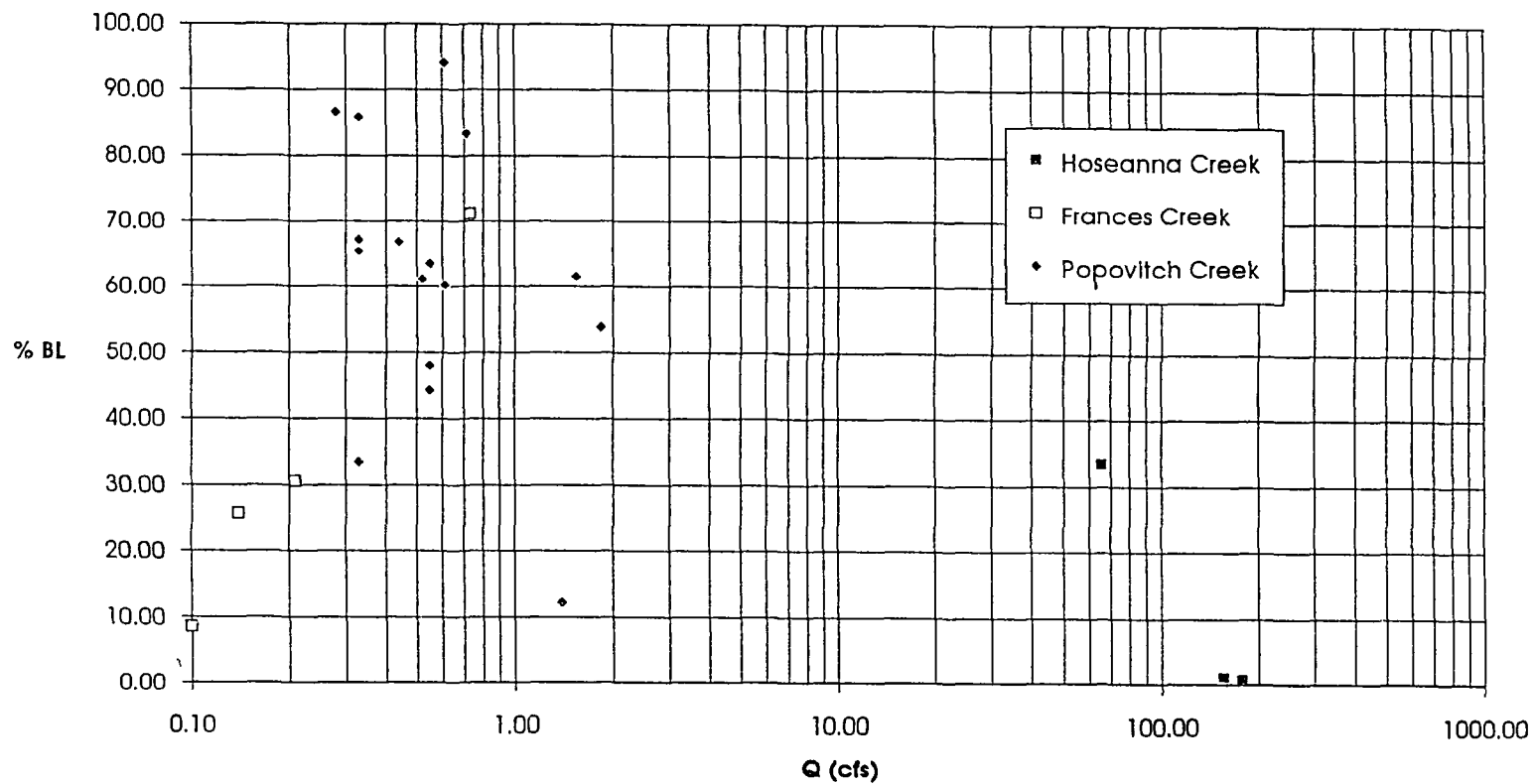


Figure 4.3-9. Plot of bedload percentage versus discharge. The relationship between bedload percentage (%BL) and discharge (Q) varies, such that for Hoseanna Creek at bridge 1, %BL decreases with increasing Q, and for Frances Creek, %BL increases with increasing Q, while for Popovitch Creek, there is no apparent relationship between %BL and Q.

4-59

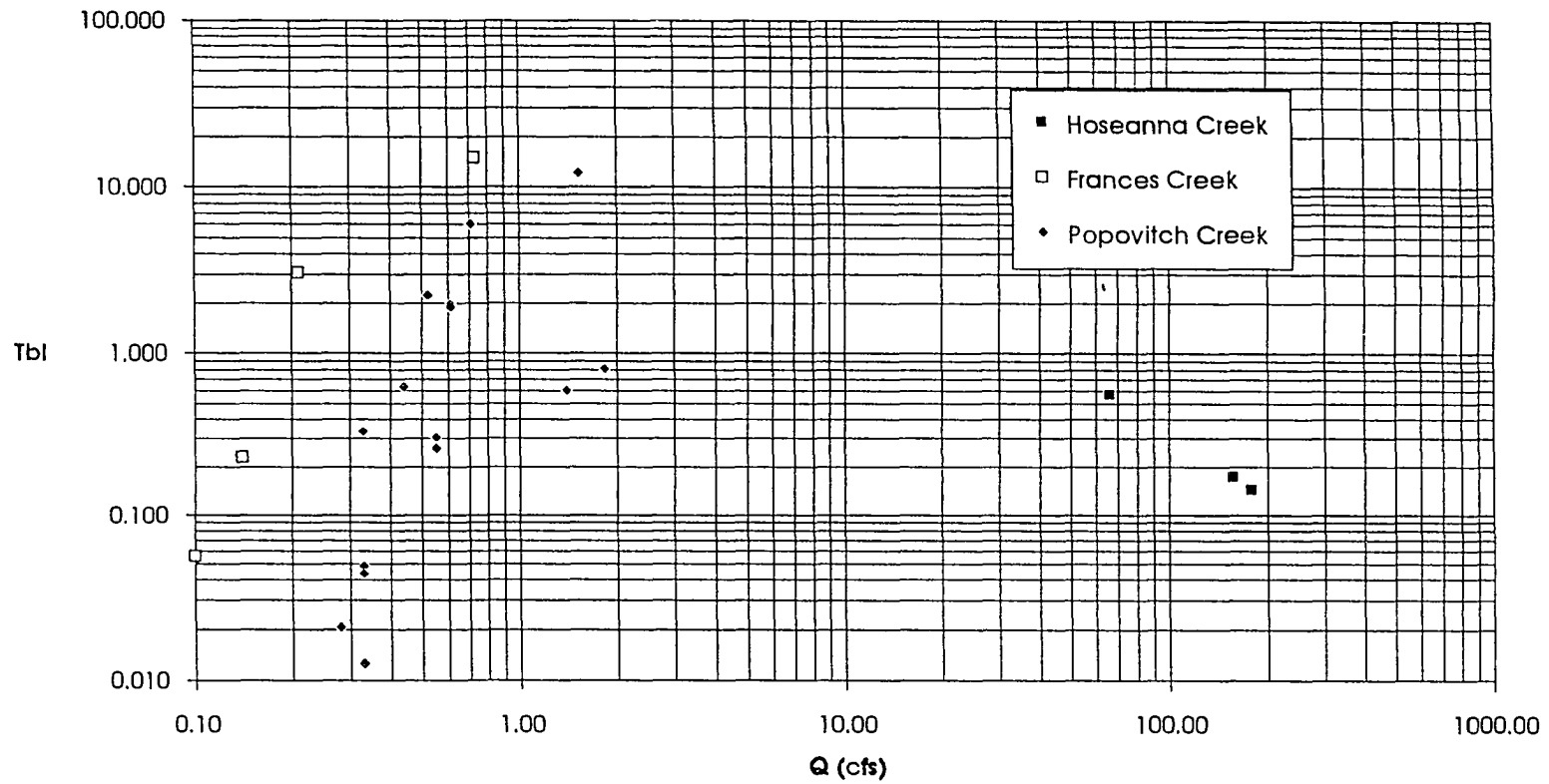


Figure 4.3-10. Plot of bedload concentration versus discharge. The relationship between bedload concentration (T_{bl}) and discharge (Q) varies, such that for Hoseanna Creek at bridge 1, T_{bl} decreases with increasing Q , and for Frances and Popovitch Creeks, T_{bl} increases with increasing Q .

(Table 4.2-6) suggests that the schistose creek (e.g., 10S) had higher dissolved components than the creeks in the sedimentary basins (e.g., 4N, 7N, and 10N).

4.4 Sediment-Discharge Relationships

4.4.1 Linear Regression Analyses of Sediment-Rating Curves

4.4.1.1 Theoretical Relationship

Sediment-discharge rating equations are fundamental quantitative expressions that relate sediment concentration to discharge (Guy, 1967). Theoretically, as discharge increases, the stream power to lift and entrain sediment and the stream capacity to carry sediment both increase; the net result is an increase in high sediment concentration. In general, the desired relationship can be expressed by the equation

$$T_x = aQ^b$$

where T_x is the sediment concentration, and $x = bm$ (bed material) or s (suspended material), Q is discharge, and a and b are the coefficient and exponent. This equation is another form of the linear expression

$$\log T_x = \log a + b \log Q ,$$

where b is the slope and a the y-intercept of the linear power function. In this relationship, both a and b increase with increasing sediment concentration. However, the relationship is not simple and the regression equation typically yields considerable variance (Walling, 1977). The values of a and b vary spatially and in this case, from creek to creek depending on many factors. In general, a and b are controlled the most by lithology (i.e., erosion potential) and drainage basin area. The relationship is even more complex, because both a and b are not constant for a particular basin or hydrologic station, but are sensitive to temporal changes in storm intensity, storm duration, sediment supply, channel characteristics, upgradient hillslope processes and other weather conditions.

In general, to establish sediment rating curves one must predict what the expected

natural variations of a and b are at any time and location. Sediment discharge rating equations were determined and used to help understand the variability of temporal and spatial sediment transfer occurring in Hoseanna Creek Watershed. The objective of the analyses was to explain the observed variance of the regression parameters and then attribute the variances to basin characteristics such as lithology, landform, vegetation or morphology. Large ranges in r^2 values for the regression equations reflect both natural and operational variances. We are asking why and when is the variance high (low r^2), and different from the simple theoretical log-log linear relationship between increasing Q and increasing T_s .

4.4.1.2 Operational Variances

Operational factors can increase the variance (reduce r^2) of the sediment rating regression equations, and need to be evaluated before comparing the regression parameters between unlike data sets (i.e., automated versus grab samples). Linear regressions were performed on four different types of data sets represented by the different sampling or laboratory techniques. Four different types of sediment concentration data exist:

- U_g unfiltered grab samples of suspended sediment analyzed at UCM,
- F_g filtered grab samples of suspended sediment analyzed at ADGGS, and
- F_a filtered automated samples of suspended sediment analyzed at ADGGS.
- F_{a+g} filtered grab and automated samples analyzed together

First, grab samples (F_g and U_g) were sampled over greater ranges of discharges than the automated samples (F_a), which were sampled only at higher crest-level actuated flows. As a consequence, the slopes of the regression lines b for the grab samples (F_g) are greater than the automated samples (F_a) for the same creek. In addition, unfiltered samples (U_g) include dissolved constituents (see Section 4.2.5) so that the minimum sediment concentration for unfiltered will theoretically always be greater than the filtered minimums for the same sample. Hence, b for the filtered samples will be greater than the unfiltered samples for the same creek. For example, compare the slope b for all the F_g 's and U_g 's for each creek on Table 4.4-1.

Table 4.4-1. Summary of sediment-discharge regression parameters, where $\log T_s = \log a + b \log Q$.

Creek	Years	Sample Type	n	b	log a	r ²
<u>Northern Streams:</u>						
Terrace (1N)	1986-88	Ug	16	0.93	-0.25	.79
Badlands (2N)	1986-88	Ug	14	2.18	1.24	.81
Two Bull (3N)	1986-88	Ug	14	1.59	1.40	.83
	1988-90	Fa+g	115	1.75	4.18	.66
Frances (4N)	1986-88	Ug	32	1.02	0.94	.64
	1986-88	Fa+g	98	1.86	4.12	.48
	1988	Fg	22	2.22	1.21	.79
	1988	Fa	35	0.53	0.95	.05
Louise (5N)	1986-88	Ug	22	1.20	1.31	.71
	1988-89	Fa+g	116	1.21	3.94	.72
Popovitch (7N)	1986-88	Ug	32	1.81	0.08	.69
	1986-88	Fg	52	4.50	3.13	.57
Slide (9N)	1986-88	Ug	19	1.36	-0.30	.80
North Hoseanna (10N)	1986-88	Ug	14	1.70	-0.80	.49
	1986-88	Fa+g	93	1.40	2.59	.46
	1988	Fa	52	0.89	0.15	.21
	1988	Fg	18	2.79	-1.53	.67
Upper Hoseanna (11N)	1986-88	Ug	19	1.16	-1.27	.58

<u>Southern Streams:</u>						
Runaway (1S)	1989-90	Fa + g	94	2.47	3.57	.60
Slime (2S)	1986-88	Ug	13	0.62	0.03	.41
Pipe (3S)	1986-88	Ug	15	0.67	0.04	.65
Schist (4S)	1988-90	Ug	7	0.37	-0.31	.59
Iron (5S)	1986-88	Ug + a	19	0.45	-0.42	.29
Clear (CS)	1986-88	Ug	11	0.54	-0.46	.51
Sixth South (6S)	1986-88	Ug	12	0.38	0.38	.32
Mosquito (7S)	1988-89	Ug	11	1.05	0.24	.28
Clinker (9S)	1986-88	Ug	14	0.86	-0.37	.62
Sanderson (10Sa)	1991	Fa + g	112	2.16	1.16	.65
	1986-88	Ug	15	0.74	-0.38	.80
	1986-88	Fa + g	173	1.82	0.52	.72
	1988	Fg	14	2.13	-2.79	.69
	1988	Fa	94	1.87	-2.47	.80
Sanderson (10Sb)	1986-88	Ug	15	0.74	-0.38	.80
Poker	1986-88	Ug	16	1.12	-1.46	.78
<u>Hoseanna Creek:</u>						
Bridge 1 (1M)	1986-88	Ug	150	1.10	-1.57	.76
Bridge 3 (3M)	1986-88	Ug				
	1988	Fa	92	1.26	-1.92	.76
	1988	Fg	31	2.07	-3.49	.66
	1986-92 ^a	Fa + g	710	1.30	0.91	.71
Bridge 6 (6M)	1988	Fa	16	1.96	-3.25	.93
	1988	Fg	23	2.09	-3.17	.77
	1988-90 ^a	Fa + g	261	1.61	0.44	.77

a: 1991 and 1992 bridge 3 and 1990 bridge 6 samples were collected as composite samples and are not included here

The r^2 values from the sediment rating regressions ranged from .05 to .93 indicating that some creeks have large variance and no apparent sediment-discharge relationship, while others are highly correlated. Generally, smaller creeks had lower r^2 values (Figure 4.4-1). Although the number of samples can reduce r^2 (Figure 4.4-2), there is a maximum attainable r^2 specific to each creek that is due to the inherent natural variability of sediment supply and sediment transfer processes.

If all (or most) of the operational variance (e.g., sample number, sampling technique) can be accounted for, then the measure of the natural variance of Ts

4-64

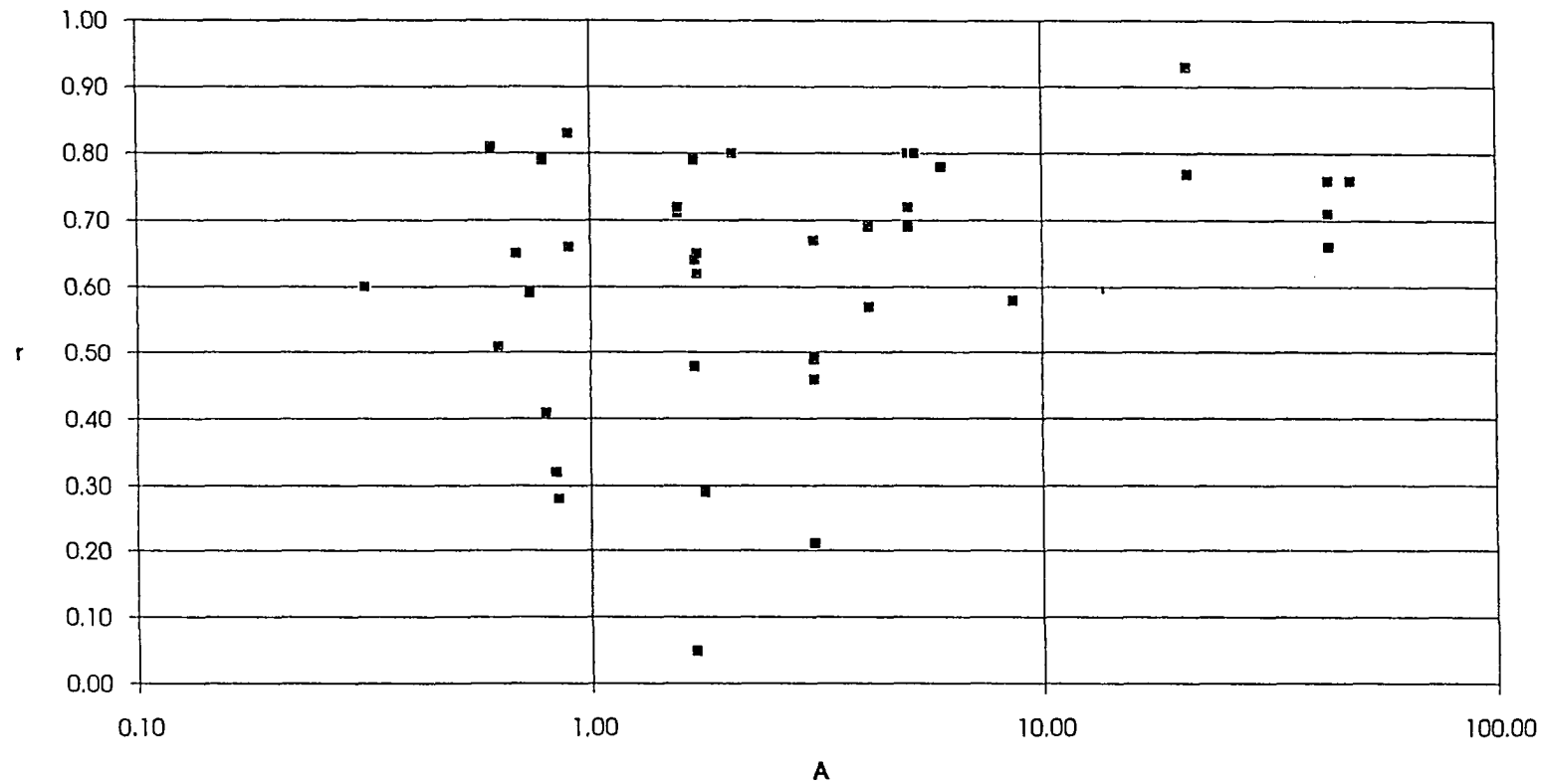


Figure 4.4-1. Plot of sediment-discharge regression goodness of fit (r^2) versus basin area (A - km²). Maximum r^2 values apparently are no higher than about 0.85 (with one exception), and are indicative of intrinsic natural variability. In addition, the range in r^2 values apparently decrease with increasing area, which suggests that there is less natural variability in sediment-discharge relationships for larger channel systems. However, see Figure 4.4-2.

4-65

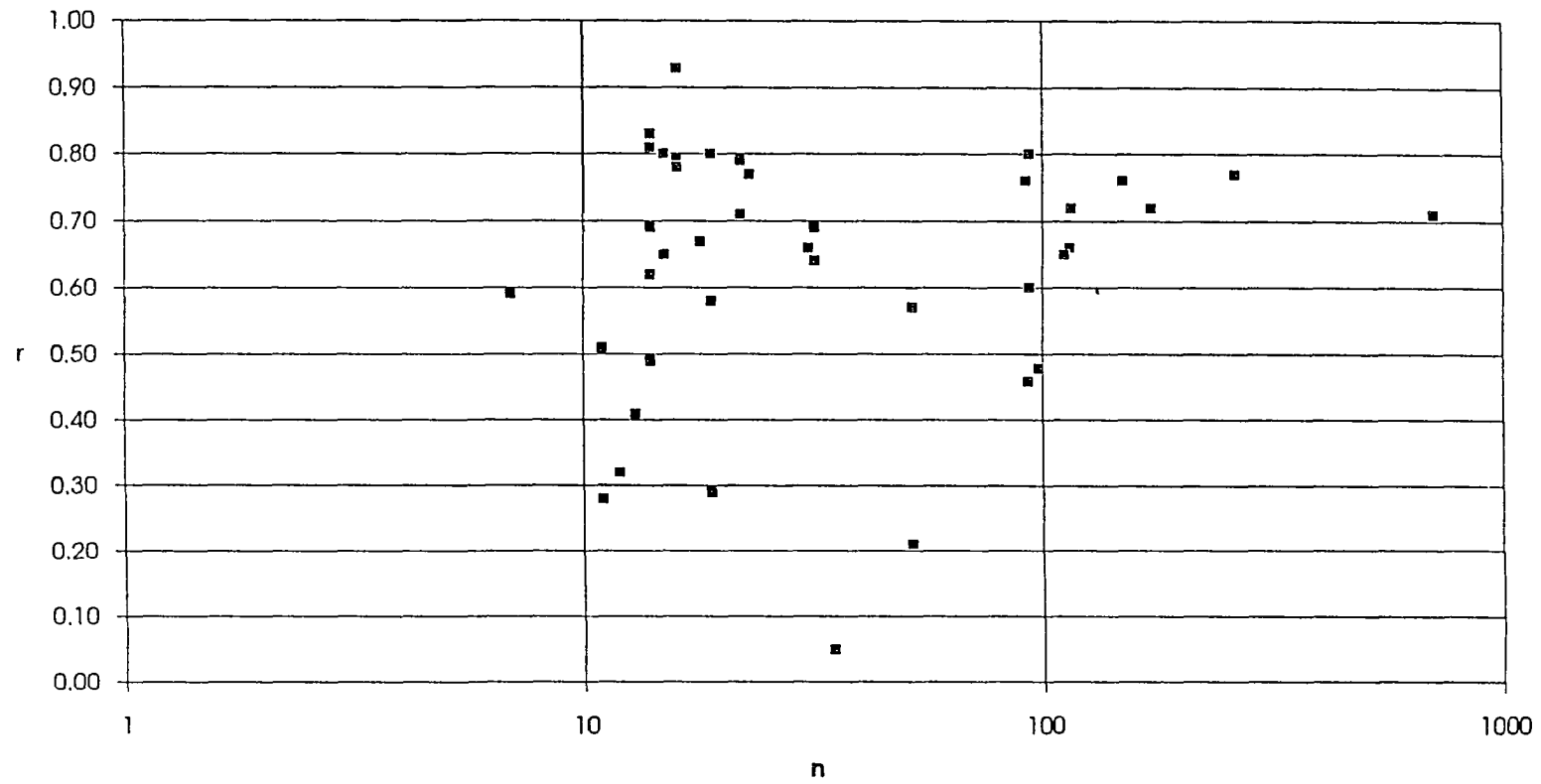


Figure 4.4-2. Plot of sediment-discharge regression goodness of fit (r^2) versus the number of samples (n). Intrinsic natural variability limits the goodness of fit correlation. In addition, better correlations were obtained with larger sampling numbers (increasing n).

per Q for each creek is r^2 . Generally, the northern basins had higher r^2 values (0.70 ± 0.11) than the southern basins (0.50 ± 0.17). Nine examples of sediment-rating regression plots are shown on Figure 4.4-3.

4.4.1.3 Natural Variances

Natural variance (at a specific sample collection station) expressed by the regression relationship exists spatially among basins, and temporally within a basin. The slope b and y-intercepts a are reflections of this variance, in that a and b vary systematically due to both spatial and temporal conditions.

Spatial Factors

Generally, for a given geohydrologic-basin type the slope b decreases with basin area. For the same basin area, the slope of northern basins > southern basins and the slope of Nenana Gravel > Usibelli Group > p- basins with basins with mixed lithologies having intermediate slopes. In addition, there is an apparent threshold of maximum slope b for any given area (Figure 4.4-4). This relationship suggests that the slope is a function of the rate of sediment supply (or the erosion potential) of a particular geohydrologic-basin type, and in essence the slope is an indicator of how fast the creek can become turbid.

The y-intercept a is also dependent on basin area and has similar thresholds for geohydrologic-types, but the distinction between types is not as clear and the range of values is higher (Figure 4.4-5). The y-intercept is a function of the amount of readily available sediment supply and is an indicator of how clean the creek is before increasing discharge. Larger creeks have lower a values (for a given discharge) and are relatively cleaner at lower flows due to two factors. First, sustained recession base flows dilute other Ts sources and armor the channel and prevent the entrainment of fine-grained particles (i.e., the channel armor is coarser and wider). Second, sediment load is diluted by discharge from non sediment-producing landscapes; this becomes more prevalent with increasing basin area. The values of both a and b are influenced by other spatial factors such as the proximity to sediment supply, percent upstream area in slide or in badlands, and the local channel gradient.

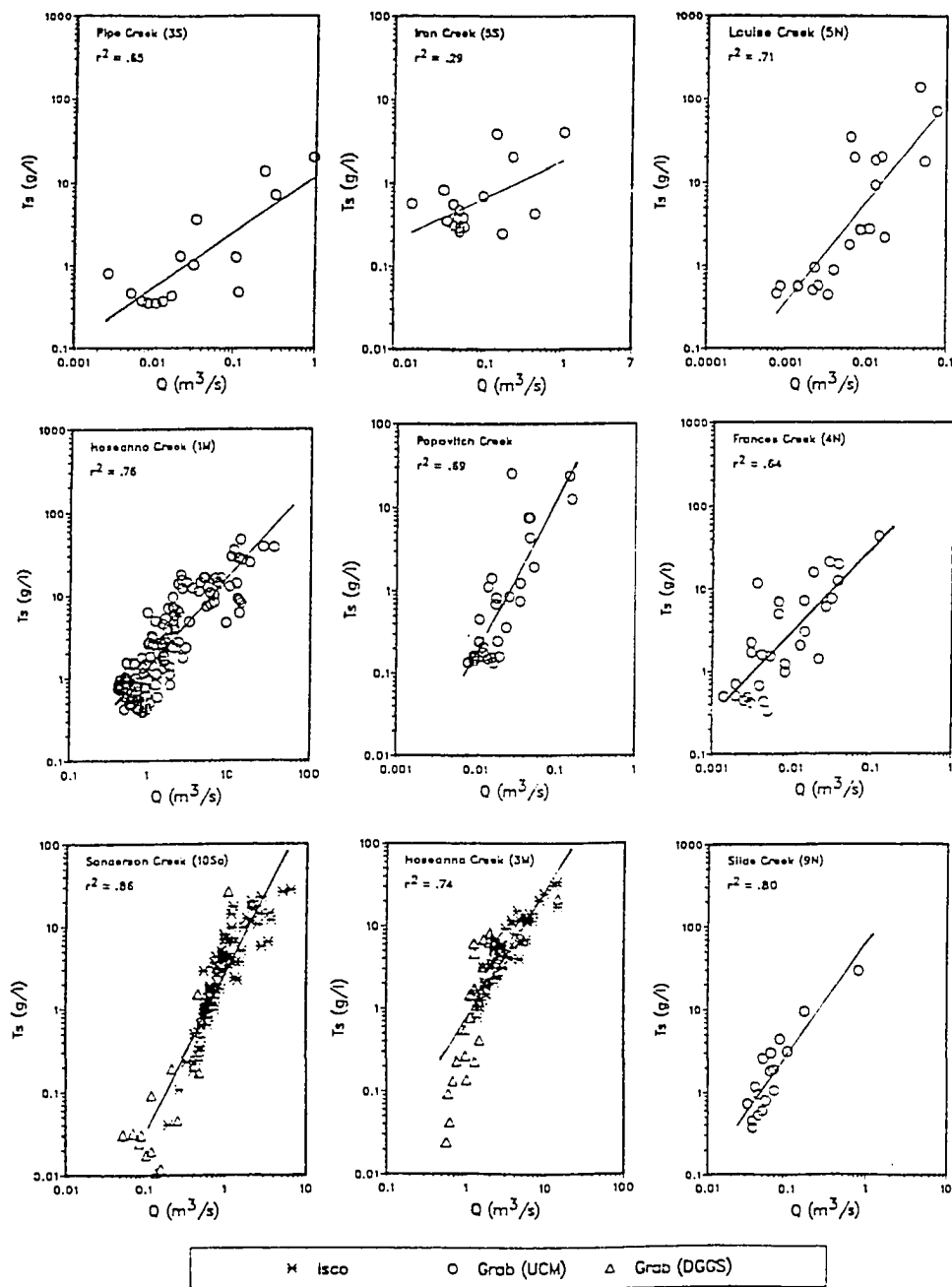


Figure 4.4-3. Nine examples of sediment-rating regression lines. All lines are plotted through 3 orders of magnitude for x-axes and through 4 orders of magnitude for y-axes (from Ray and Maurer, 1989). Variations in sediment-rating regression lines are attributed to variations in basin area, lithology, and aspect which can be measured by differences among the slopes and y-intercepts (see Table 4.4-1).

4-68

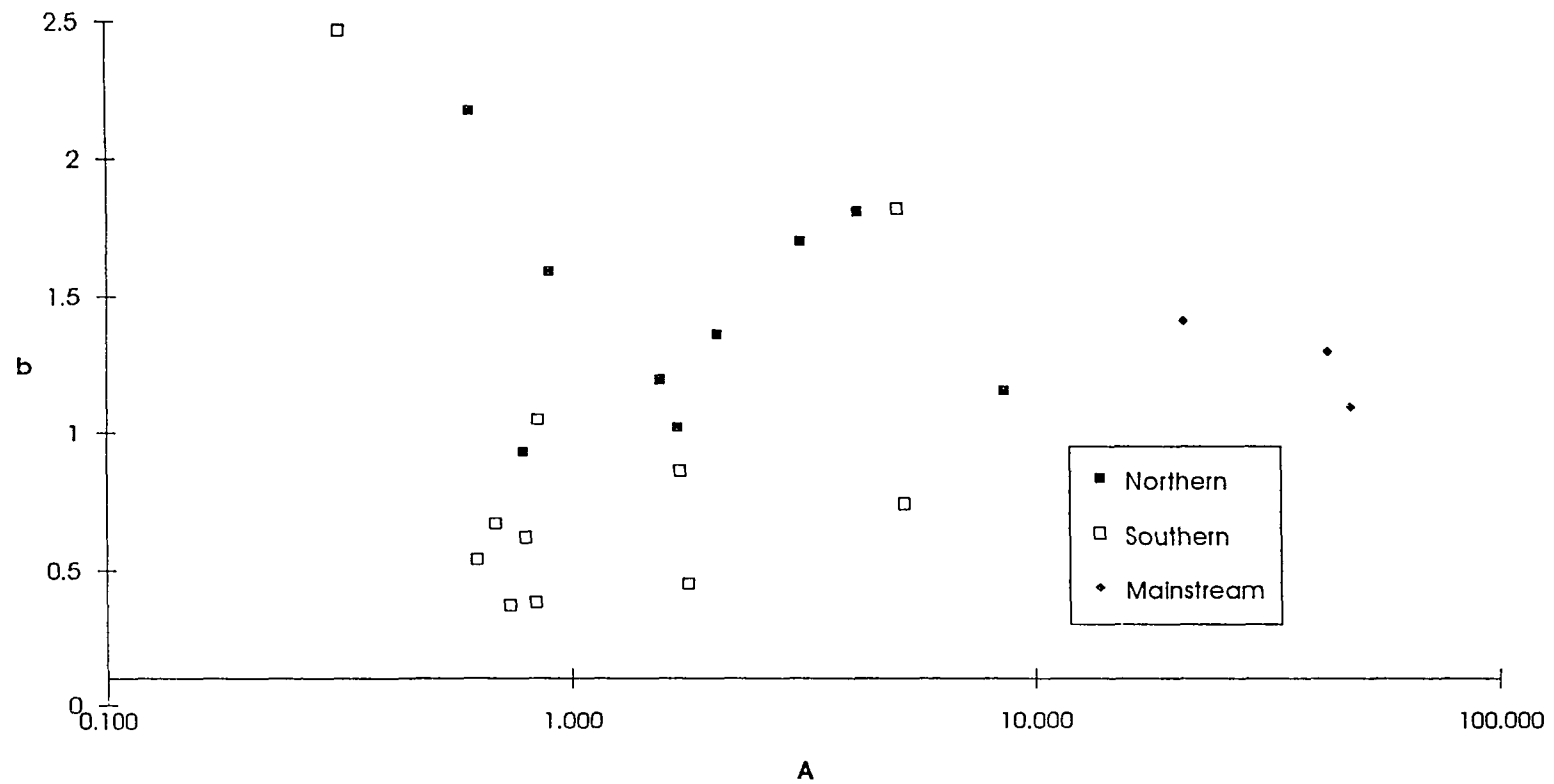


Figure 4.4-4. Plot of the sediment-discharge slope regression parameter (b) versus basin area (A - km^2). In general, northern basins underlain by the Usibelli Group and the Nenana Gravel have higher b values (i.e., become more sediment rich faster) for any given area.

4-69

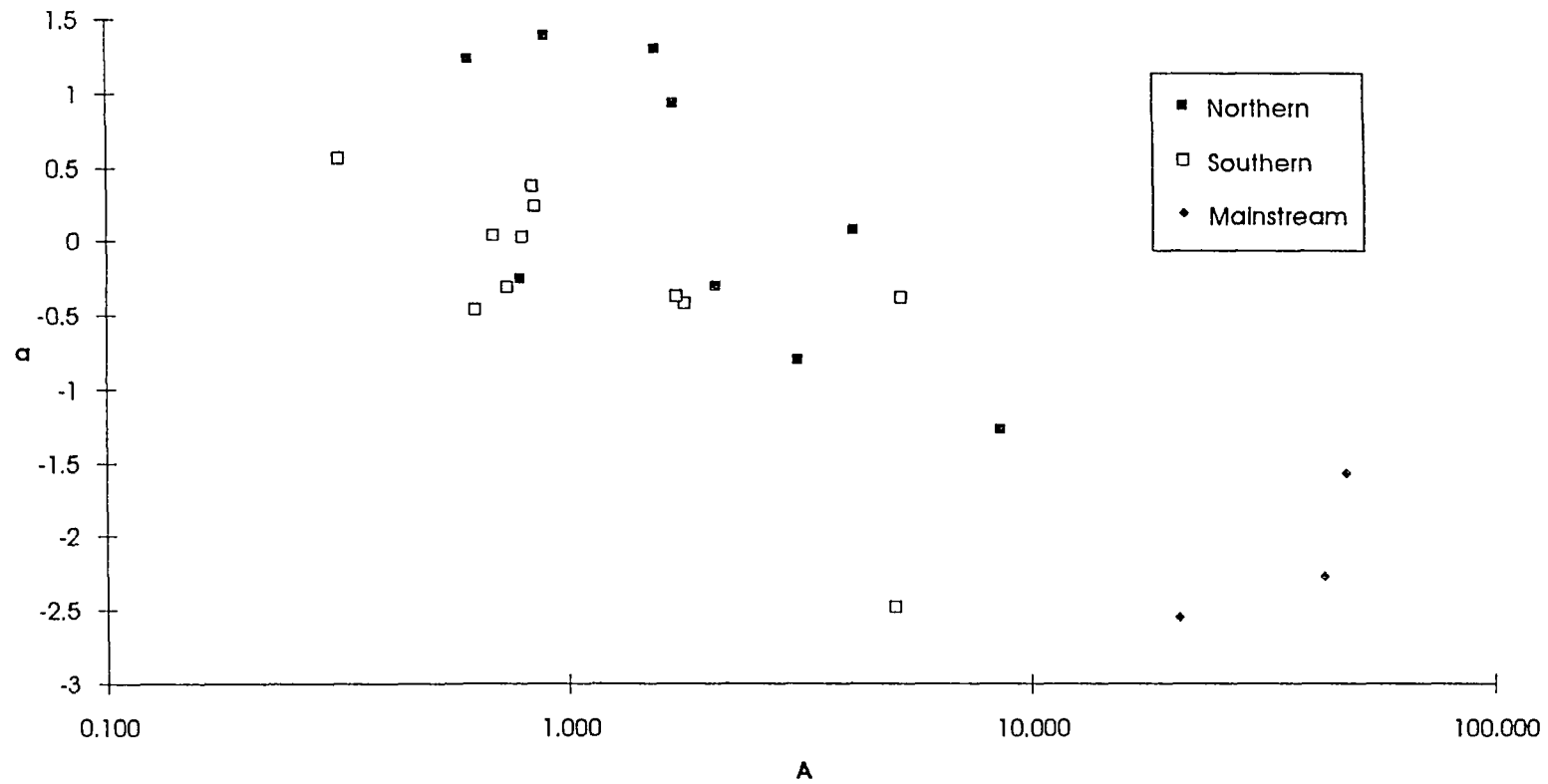


Figure 4.4-5. Plot of the sediment-discharge y-intercept regression parameter (a) versus basin area (A - km^2). In general, northern basins underlain by the Usibelli Group and the Nenana Gravel have higher a values (i.e., more readily available sediment supply) for any given area.

Temporal Factors

Besides the variations of *a* and *b* among basins, there is significant natural variation at a given location, reflecting the natural temporal change in sediment concentration from one year to the next, during the course of a season, or during a storm. This process can be shown by taking a closer look at regressions performed for different years and for different times of the year.

Figure 4.4-6 depicts four creeks (Iron Creek, 5S; Clear Creek, CS; Upper Hoseanna, UH; Louise, 5N) in which year to year and season to season shifts in the y-intercept occur. Note the higher y-intercepts measured during 1987. Also, for most of the creeks for most of the years, from spring to fall a downward shift in the y-intercept with no change in slope occurred, and is indicative of sediment supply depletion. In addition to the systematic shift from year to year and through the year, another shift occurs during each storm such that rising stage is more sediment rich (slope of T_s versus Q is steeper) than falling stage; this process is termed hysteresis. Thus, quantification of the three major temporal components can explain much of the natural variance in a regression. Theoretical changes to sediment-discharge regression lines are shown on Figure 4.4-7. Changes are due to both spatial (i.e., area and lithology) and temporal (i.e., storm hysteresis, seasonal sediment supply depletion or enrichment) variability. The magnitude of the variance (the amount of unexplained or lower r^2) is specific to each basin's sediment supply, sediment caliber and its entrainability, and basin area. The residual r^2 , or that remaining unexplained variance after accounting for the major temporal (i.e., seasonal change and hysteresis) and additional storm related (i.e., storm intensity, duration) trends, is likely due to local spatial conditions (i.e., a mass wasting event that is proximal to the sample collection point and briefly supplies an inordinate amount of sediment).

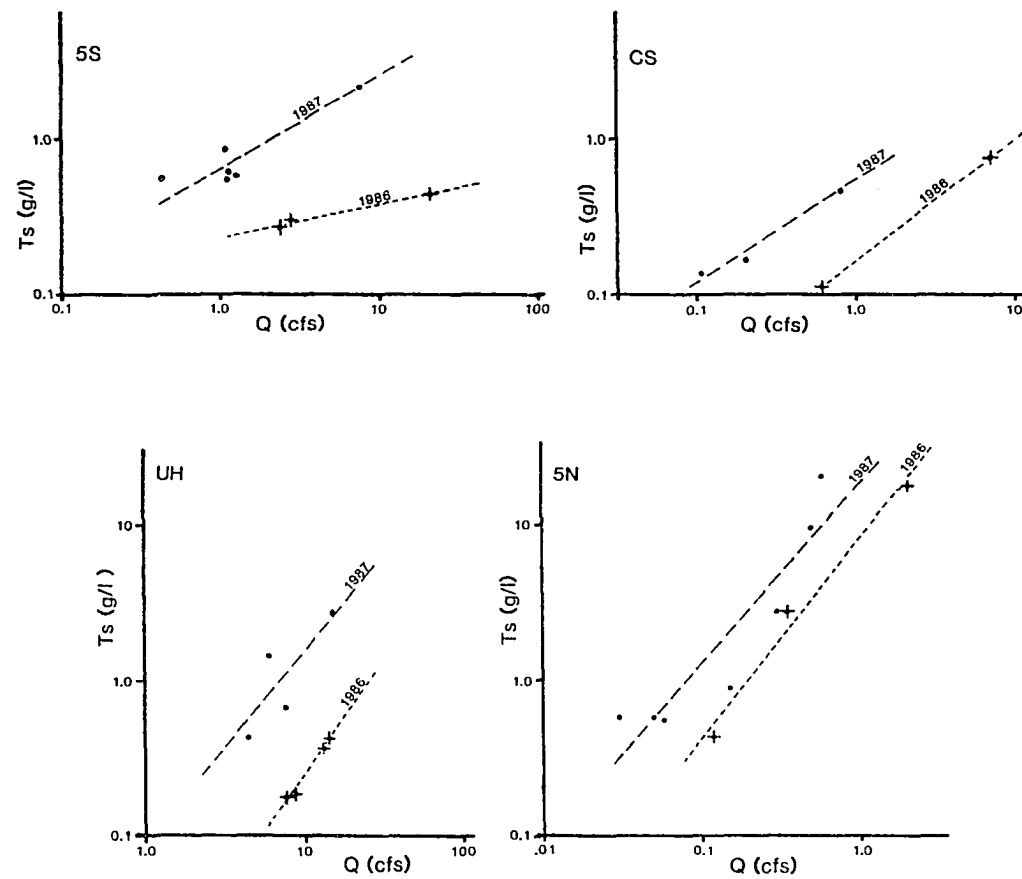


Figure 4.4-6. Four examples of annual related shifts in the slope (b) and y-intercept (a) of sediment-discharge regression equations.

4-72

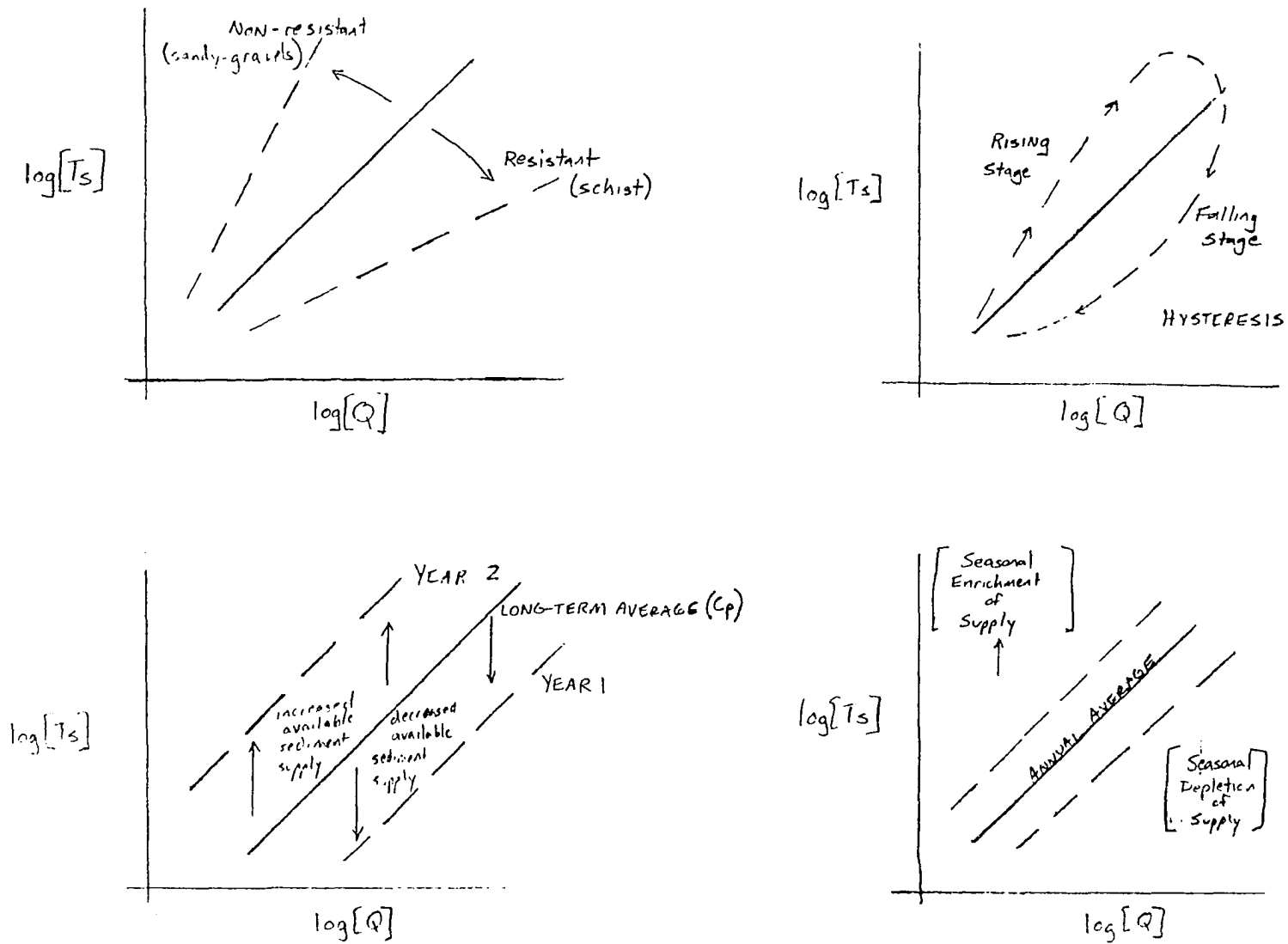


Figure 4.4-7. Theoretical changes to sediment-discharge regression lines due to spatial and temporal variability.

4.5 Sediment Supply and Transfer Processes

4.5.1 Sediment Rating Regression Residuals

The residuals from the sediment rating regressions are defined as:

$$R = \log Ts_{[\text{observed}]} - \log Ts_{[\text{predicted}]}$$

where R is the residual, $\log Ts_{[\text{observed}]}$ is equal to the sampled sediment concentration during the storm, and

$$\log Ts_{[\text{predicted}]} = \log a + b \log Q$$

where $\log Ts_{[\text{predicted}]}$ is the predicted sediment concentration from the regression equation.

The observed response of sediment-transfer processes in a stream system during a storms to changes in sediment supply can be represented by the plots of Q and R versus time. The response of five different stations (3M, 4N, 10Sa, 6M and 5N) were examined for several 1988 and 1989 storm events (Figures 4.5-1 through 4.5-3). Several obvious processes are apparent from the figures for all storms on all basins. First, later season storms have either lower (4N, 10Sa, 3M and 5N) or higher (6M) R values than early season storms, indicating that readily available sediment supply can decrease or increase through the summer. Second, R is not random, but is time dependent and its value changes systematically (i.e., not randomly) during the storm runoff cycle. In addition, peak R values do not generally coincide with peak discharges, and typically precede the peak discharge.

Nevertheless, there are some exceptions, most notably with Frances Creek (4N) on July 21, where high R values associated with the second sediment pulse do not relate well with the hydrograph. Variant R 's not associated with changes in Q may reflect local mass wasting events, inefficient mixing zones or unique ephemeral channel sediment characteristics. This factor probably has a larger impact on smaller creeks, where mixing is not as thorough, and mass wasting effects can have a larger impact on smaller stream sizes. In addition, small increases in Q can result in major changes in R values (e.g., 10Sa), and points to the inherent

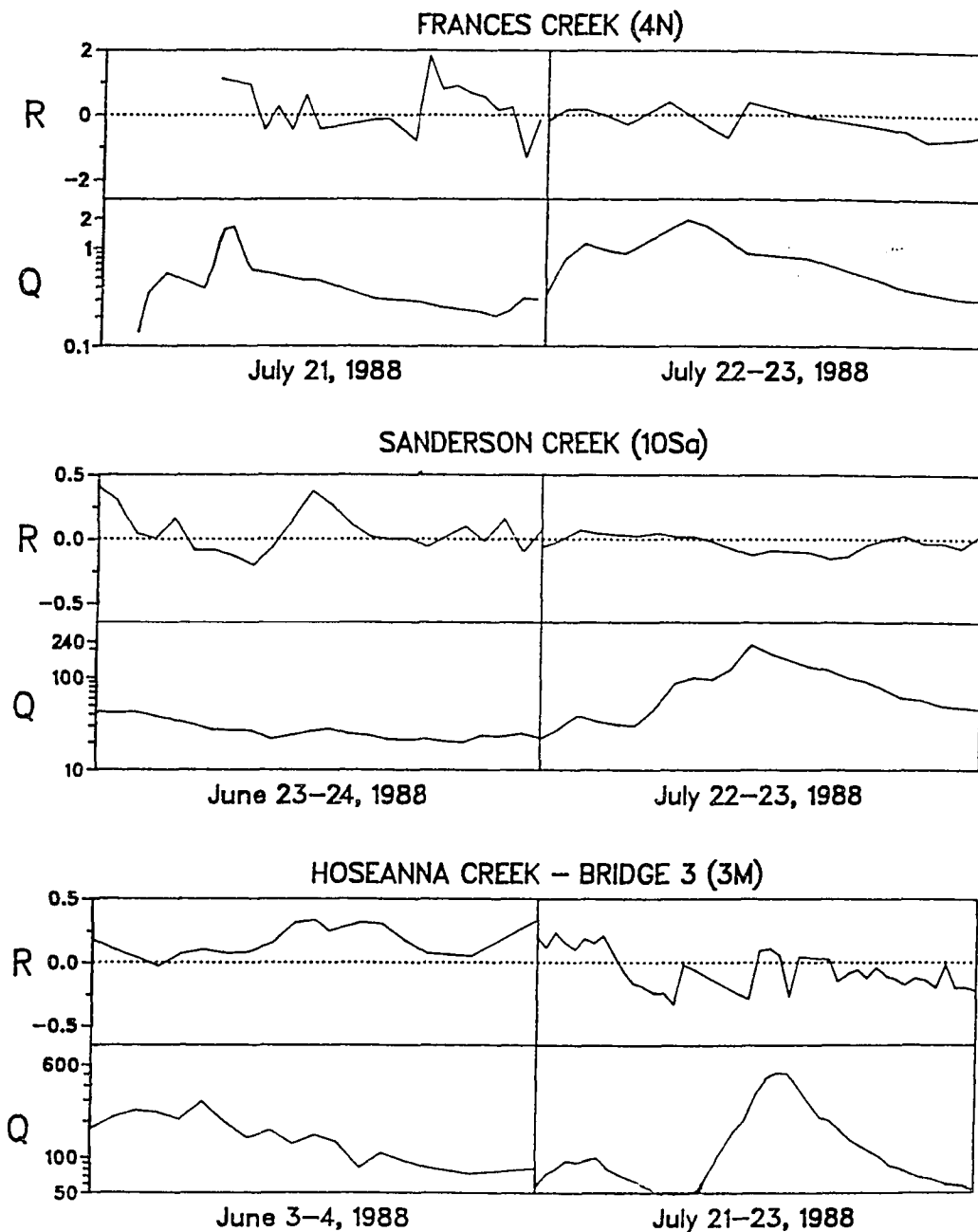


Figure 4.5-1. Plot of the regression residual (R - g/l) and discharge (Q - cfs) during 1988 storms for Frances Creek, Sanderson Creek and Hoseanna Creek at Bridge 3.

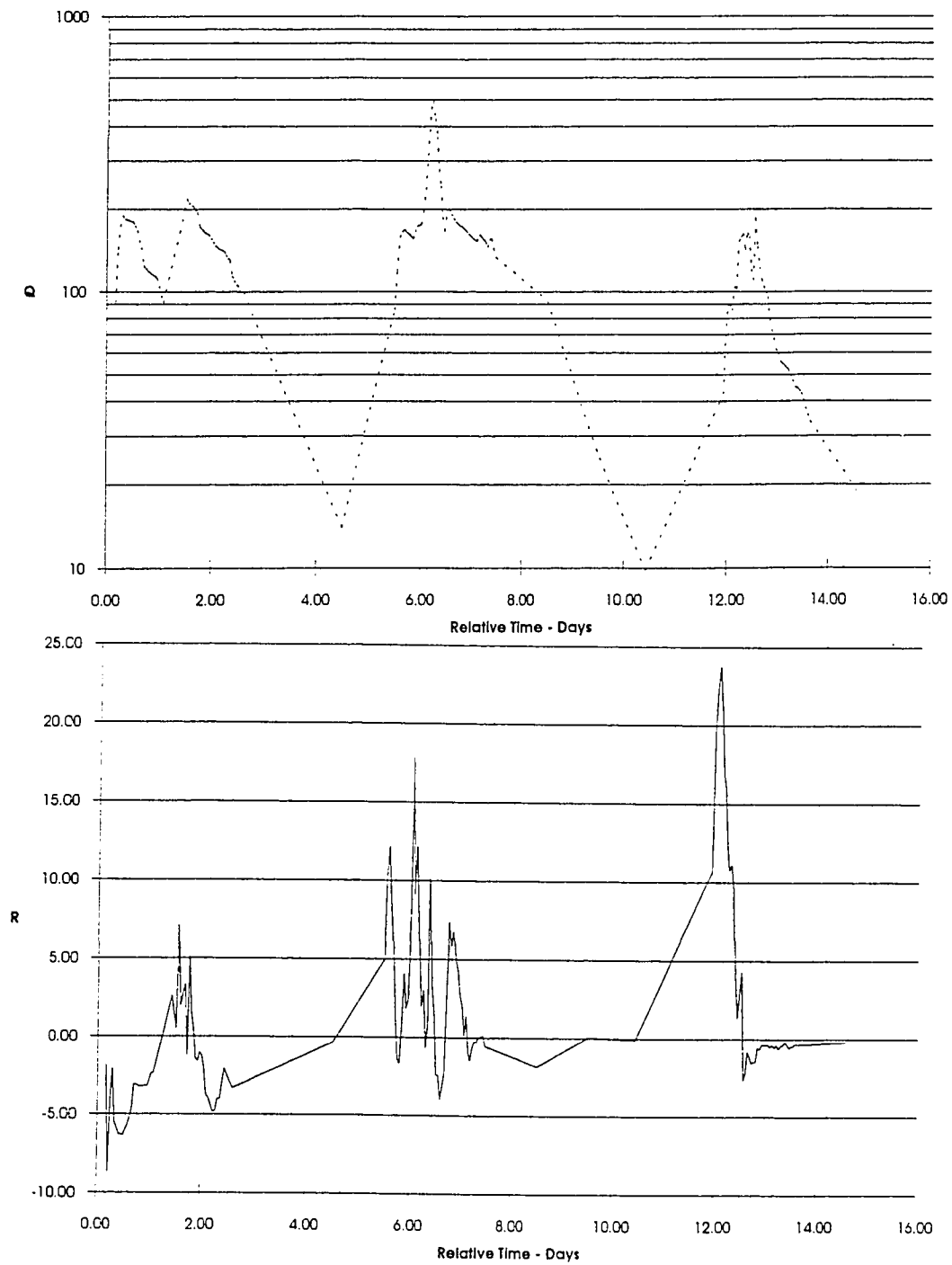


Figure 4.5-2a. Plot of the regression residual (R - g/l) and discharge (Q - cfs) during three 1989 storms for Hoseanna Creek at Bridge 6.

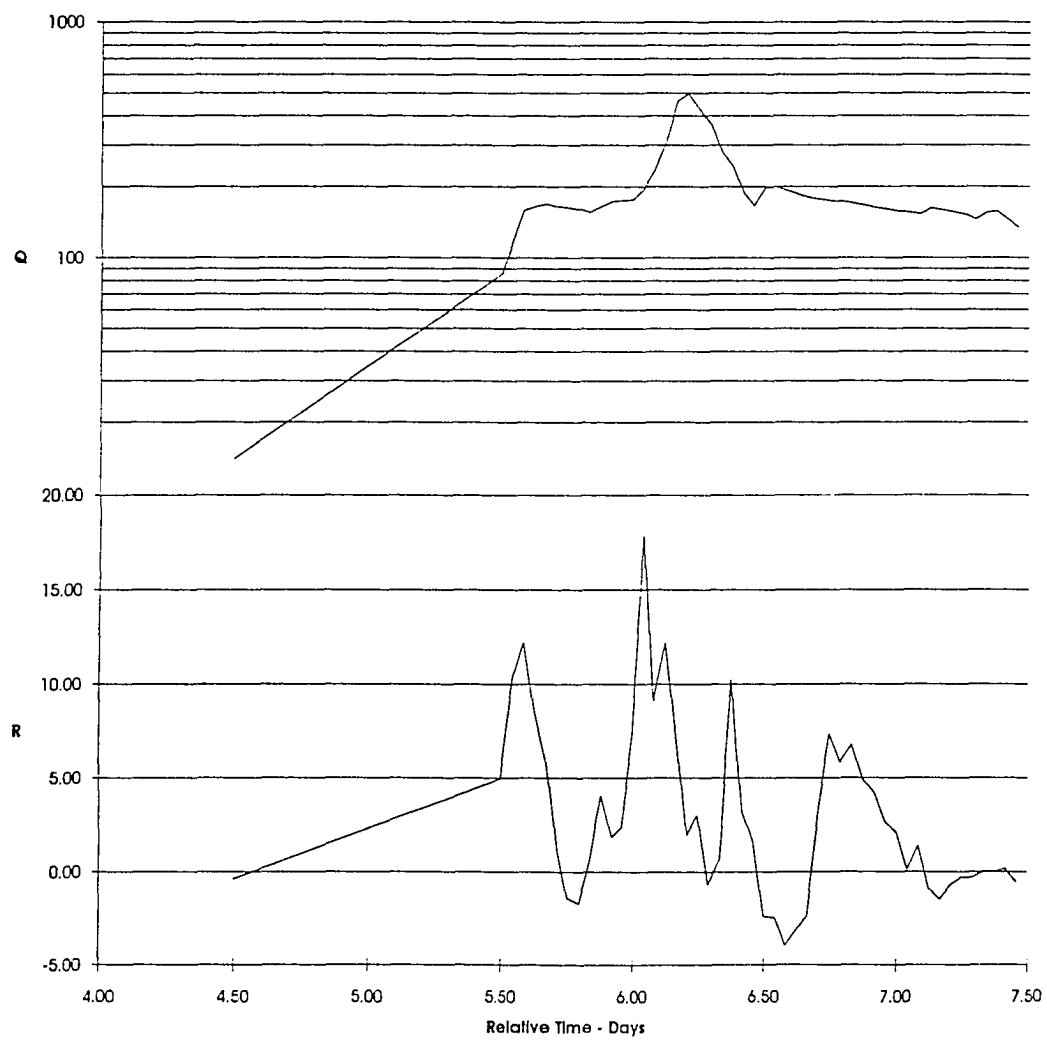


Figure 4.5-2b. Plot of the regression residual (R - g/l) and discharge (Q - cfs) during the June 24-26, 1989 storm for Hoseanna Creek at Bridge 6.

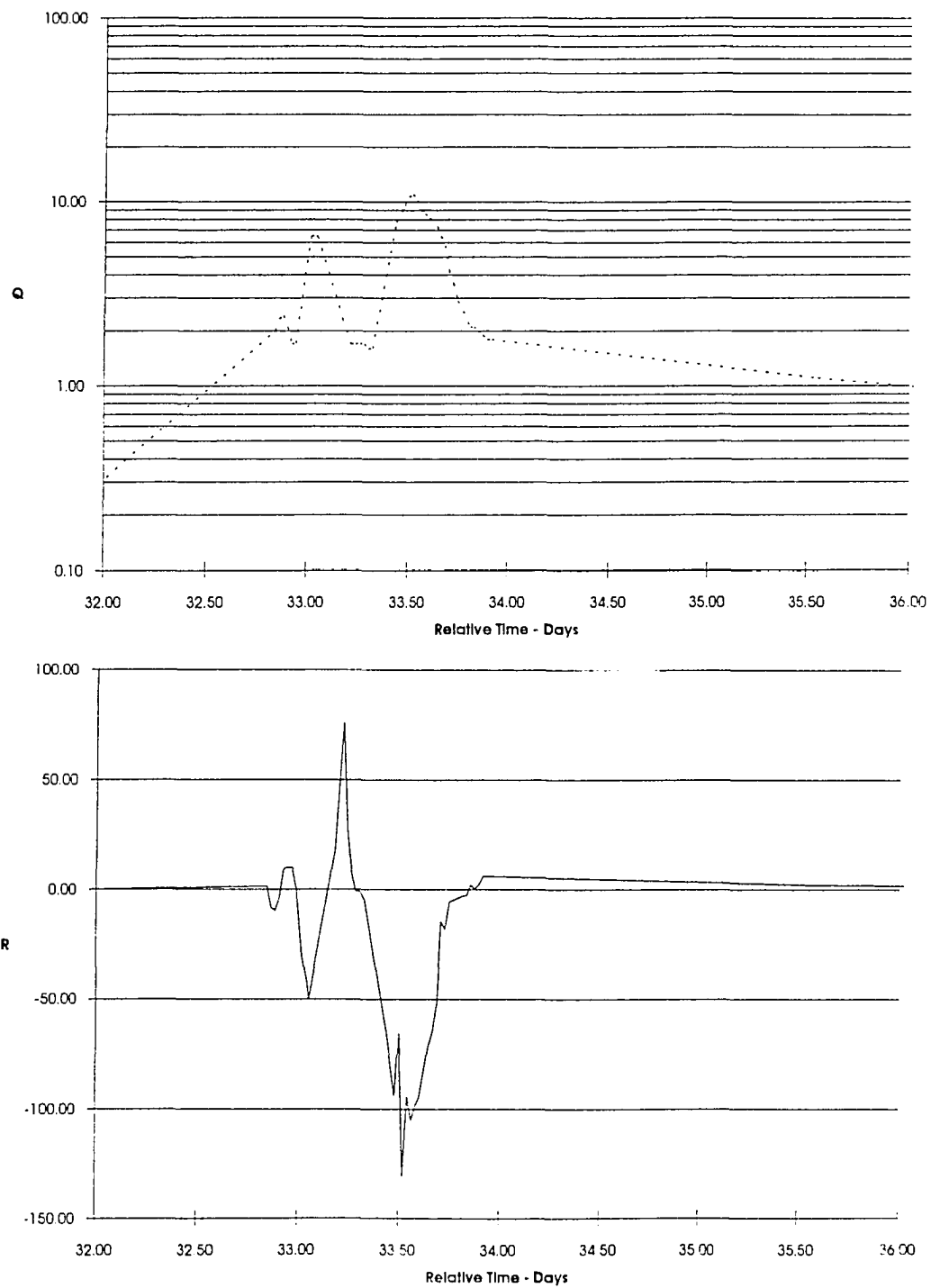


Figure 4.5-3. Plot of the regression residual (R - g/l) and discharge (Q - cfs) during the June 24-25, 1989 storm for Louise Creek.

sensitivity of sediment concentrations to storm surges.

4.5.2 Mean Sediment Concentration Potential and the Maintenance Rate

The mean sediment concentration potential C_p for each basin is expressed by the unique T_s versus Q sediment rating regression equation determined for each creek. Over time, R will vary with respect to C_p . R is a function of the potential of the readily available sediment supply to meet stream demand (carrying capacity) in order to maintain C_p , stream constance and a steady state channel geometry. If there were no temporal variance (e.g., no hysteresis) and $R = 0$, then supply would equal demand and the steady state channel geometry would be maintained. However, the fluvial system is dynamic and R and the rate of change in R (i.e., the sediment concentration maintenance rate or R^*) can be either positive or negative at any given time. The value of R is dependent on the site-specific spatial and temporal variability unique to each basin.

When $R < 0$, demand is greater than supply; if R^* is positive when $R < 0$ ($R/t > 0$), then the stream is restoring to meet demand by cutting and corradging. If R^* is negative when $R < 0$ ($R/t < 0$), then the stream is depleting its supply by dilution and deposition. When $R > 0$, supply is greater than demand; if R^* is positive when $R < 0$, then the stream is loading and augmenting its supply from sediment influx sources (e.g., mass wasting, bank corrasion) with erosion; if R^* is negative when $R > 0$, then the stream is dropping its load and the channel is aggrading. The wavelength of the plot of R versus time is a function of the storm, season and year.

The magnitude of hysteresis is a function of the proximity of the sediment source. With a proximal source there is less mixing time, and more intense supply-related surges; with a distal source there is more mixing time and more attenuated supply-related surges. The smaller the creek or basin, the larger the residuals (or more variance) that can be attributed to supply surges and supply ebbs; the larger the creek or basin, the smaller residuals (or less variance) can be attributed to more thorough mixing and less supply-related surges. The magnitude of R is related to the relative magnitude of a sediment pulse to a stream system or the scale of a mass wasting event to a creek size.

4.5.3 Changes in Supply and Runoff Rates

In the simplest case, when increasing R correlates with rising Q , stored sediment on bars and banks is readily acquired by the storm surge. Similarly, when decreasing R 's correlate with falling Q , stream power is attenuated so that sediment supply has been diminished and results in reduced sediment load. However, additional and more complex responses typically occur during a storm cycle. Hypothetical responses of sediment-transfer processes in a stream system to changes in sediment supply are represented in Figure 4.5-4 which shows plots of Q , T_s and R versus time. The figure demonstrates that annual, seasonal and storm-related changes in sediment supply show a pronounced effect on sediment concentrations. This process is likely more important for creeks with high proportions of readily available finer grain sizes which are easily entrained and can produce high suspended sediment concentrations. These temporal effects may be heightened in subarctic creeks because of the long winter dormancy of sediment transfer processes and must be accounted for in developing realistic and accurate sediment-discharge relationships.

4.5.4 Geologic and Climatic Controls on Supply and Demand and Stream Maintenance

The mean sediment concentration potential [C_p] varies from creek to creek depending upon climate, lithology and basin area. These three controls interact to yield variations in vegetation, aspect, and the presence or absence of permafrost.

South-facing non-permafrosted Nenana Gravel basins have high C_p (a and b are both high). Badlands provide the primary source of sediment; sediment influx is provided by sediment block falls of poorly consolidated material and by grain-grain collapse from the badlands to form loose talus at the base of the badlands. When the talus becomes saturated (either during spring break-up or during a major summer storm) transitional flows to mud flows commonly occur and provide a rapid means of sediment transfer to the main tributary streams. The channel caliber is predominantly texturally mature (sub- to well-rounded grains) and coarse, bedload transport increases with increasing discharge, and the percentage of bedload transport to total load increases. Because base flows and peak flows are relatively low, Q_s is reduced. However, high magnitude storms generate transitional flows

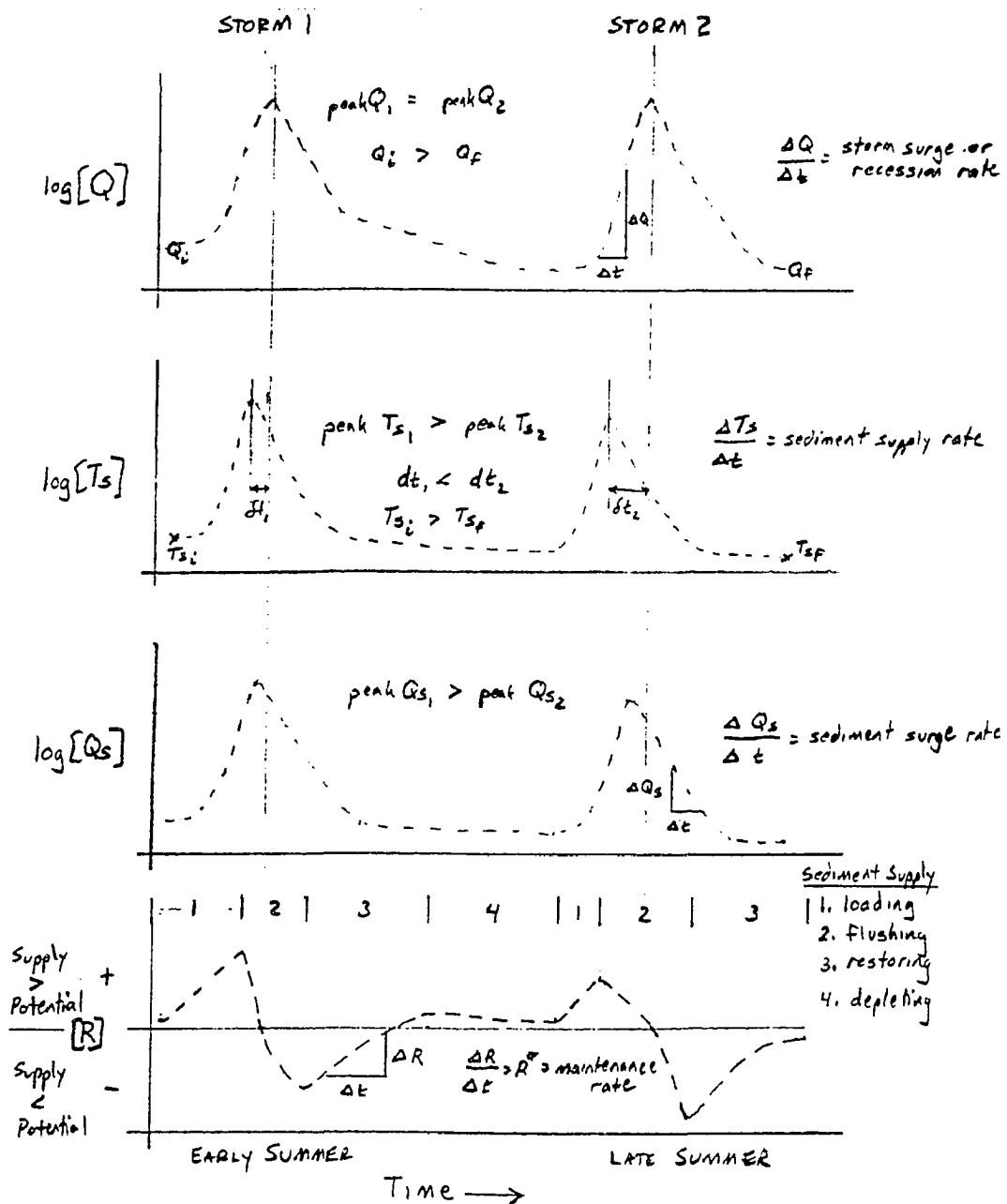


Figure 4.5-4. Hypothetical relationships of discharge (Q), sediment concentration (Ts), sediment load (Qs), and the sediment concentration residual (R) over time. Variations in R during a storm event reflect the adjustments of the channel maintenance rate to changes in sediment supply.

and mudflows. During these times, T_s and R are highly variable and reflect the hydrodynamic processes of sediment transfer in super-concentrated flows.

Both north-facing or south-facing coal-bearing basins have relatively moderate C_p , although the north-facing Usibelli Group basins have higher peak Q , probably due to the effect of permafrost. Sediment influx is provided by earthflows, landslides, or badlands which are corraded or washed into creeks during spring break-up or during major summer storms. The channel caliber is predominantly fine to medium and there is a moderate but steady sediment influx. Bedload transport is important at low volume flows. As Q increases, the $\%T_s$ increases and reflects the fine-grained caliber. As a result, R is more sensitive to storm surges and sediment supply, and has characteristic hysteresis due to the ample supply of fines on braid bars and channel banks.

Permafrosted north-facing metamorphic basins have relatively low C_p . Sediment influx is provided by localized frost heaves, frost scars, mud boils, rockfall block failures and by chemically weathered dissolved constituents precipitated by freeze-up conditions. Peak flows are relatively higher and of shorter duration than flows in south-facing sedimentary basins, but they yield low to moderate sediment supply rates. The sediment caliber is mixed but is dominated by texturally immature (angular blocks) cobbles and boulders which provide armor to the channel bottoms.

In all cases the readily available supply is increased during winter and spring because there is little or no sediment transfer. Physical weathering occurs during winter and spring due to direct sunlight on badland outcrops or by freeze-thaw processes. Grain-grain collapse and block collapse are common and fall on growing auefs and snow banks and clog the channel with readily transported material in the form of talus cones and blocky talus debris at the base of slopes.

During spring break-up sediment influx from the hillslopes to the fluvial system is high and the sediment transfer rate in the streams is high. During the summer supply is generally being depleted; however, large mass wasting events triggered by summer storms may temporarily restore supply to meet or exceed the sediment concentration potential in each creek. During fall freeze-up discharges attenuate, mass wasting processes are inhibited and sediment transfer in the fluvial system becomes negligible.

4.6 Sediment Load

Sediment load Q_s is defined as the product of discharge Q and sediment concentration T_x , such that

$$Q_s = kQT_x.$$

where k is a unit constant. Sediment rating equations can be used with stream hydrographs to calculate sediment load over time where

$$Q_{s_t} = \int Q \, dt \text{ (from } t = 0 \text{ to } n\text{);}$$

in practice this becomes

$$Q_{s_t} = \sum kQT_x t \text{ (from } t = 0 \text{ to } n\text{),}$$

where t is the time interval for the weighted Q and T_x .

4.6.1 Peak Sediment Loads

4.6.1.1 Observed

The large volume of sediment contributed by landslides and badlands results in unusually turbid waters with high suspended sediment concentrations (up to 2000 mg/l) being carried during normal base flow conditions. Hoseanna Creek and many of its Tertiary basins are turbid almost every day during the summer. Coarser sediment, and some silt and clay, are temporarily stored in alluvial fans, talus cones, braid bars and stream banks. Large cyclonic storms greatly increase stream discharge, depth and velocity and make it possible for the streams to entrain large amounts of this readily available stored sediment. Maximum sediment loads occur during either brief high magnitude summer storms, or during spring break-up.

From 1985-1991 the proportionate load from twelve large storms (> 500 cfs, or $14.2 \text{ m}^3/\text{s}$) was estimated (also see Ray and others, 1992). Table 4.6-1 demonstrates the importance of the magnitude and number of high runoff induced storm events in determining the annual sediment load. Up to 95% of the seasonal

Table 4.6-1. Seasonal proportions of sediment load. Proportion of sediment load occurring during short periods showing number of events greater than 500 cfs, the seasonal load, the percentage of the seasonal load transported during 1,2,3,5, and 10 days. The 1985 and 1986 data are for bridge 1, 1987 data for bridge 1 and bridge 3 (Ray and others, 1992), and the 1988 through 1992 data for bridge 3 (Ray and others, 1992). Spring break-up discharge and sediment concentration data are generally lacking; because the daily discharge and sediment concentration have large diurnal fluctuations during spring break-up, all sediment load estimations for spring break-up are suspect.

Year	Period of Discharge Record	Number of Days of Discharge Record	Number of Events > 500 cfs	Seasonal Sediment Load (metric tons)	Percentage of seasonal sediment load occurring in number of days				
					1	2	3	5	10
1985 (1M)	5/30/85 9/30/85	124	2	93,000 ^(b)	8	14	19	25	38
1986 (1M)	7/19/86 8/14/86	26	1 ^(a)	134,000 ^(d)	40	65	77	84	95
	(8/26/86)	(38)	(2)	~234,000	43	79	85	90	95
1987 (1M)	6/21/87 8/28/87	69	0	17,500 ^(d)	12	19	26	38	56
1987 (3M)	5/21/87 10/12/87	135	0	40,000 ^(c)					77
1988 (3M)	5/31/88 10/4/88	127	2	59,200 ^(c)	44	55	65	78	87
1989 (3M)	5/1/89 10/4/89	157	4	103,000 ^(c)	42	56	63	78	91
1990 (3M)	5/30/90 9/30/90	124	3	64,000 ^(c)	29	40	50	62	73
1991 (3M)	5/16/91 9/30/91	138	1	47,300 ^(c)	20	33	45	58	70

(a) does not include the August 21-22, 1986 storm (with a peak discharge of over 2000 cfs and additional estimated 100,000 tons) which washed out the gage stations on both bridge 1 and bridge 3.

(b) sediment load estimates made using mean daily discharges in sediment rating equation established from 1986-1988 (underestimates effect of peak discharge but overestimates peak sediment concentration due to hysteresis).

(c) sediment load calculated using mean daily Q and mean daily Ts (underestimates total load)

(d) sediment load calculated using time-weighted measured or rated discharges with time-weighted measured sediment concentrations (generally good estimate of total load).

load (the seasonal load is somewhat less than the annual load because the spring break-up load was not fully accounted for) is transported in only 10 days, and up to 90% of the seasonal load in only 5 days. Although spring break-up flows are not well represented in the database and likely transport a significant proportion of the annual sediment load, the nature of sediment transfer in Hoseanna Creek Watershed is such that most of the sediment transported during the year occurs during relatively short periods of time.

In general, comparisons of the sediment transfer capacity for large storms can be approximated by the peak sediment load (assuming that the shapes of different storm hydrographs are relatively similar for the same hydrologic station at bridge 1). For example, a storm on July 20, 1986 increased the discharge at bridge 1 of Hoseanna Creek from about 50 cfs ($1.42 \text{ m}^3/\text{s}$) to about 1310 cfs ($37.1 \text{ m}^3/\text{s}$). Prior to the storm, Hoseanna Creek was delivering approximately 1,400 g/s. The estimated average suspended concentration during maximum discharge was about 39,000 mg/l. This corresponds to a sediment load of 1,470,000 g/s or about 1.62 short tons of sediment per second (or roughly 1000 times the rate prior to the storm). Similarly, a second storm on August 22, 1986 yielded about 1,680,000 g/s or about 1.85 short tons per second. Thus, the sediment production rates during the two storms increased by more than three orders of magnitude above the pre-storm conditions. These two storms accounted for roughly 40% and 55%, respectively, of the total estimated load for the 1986 period of record, and delivered more sediment load than each total seasonal load for 1987, 1988, 1990 and 1991!

4.6.1.2 Predicted

The effect storms of various magnitudes have on sediment production for each basin was estimated. The predicted discharges for the 2, 5, and 50 year flood discharges (Table 4.3-3) were used with the regression parameters from the sediment-discharge rating equations (Table 4.4-1) to determine peak suspended sediment concentrations (Ts_2 , Ts_5 and Ts_{50}) and peak sediment loads (Qs_2 , Qs_5 and Qs_{50}) for each flood in each basin (Table 4.6-2). Regression parameters for only the Ug type samples were used in this analysis for several reasons. First, it is the only sample type that exists for all the basins. Second, some of the automated sample sets (Fa) had higher unexplained variances or gave unrealistic (and high) Ts_{pre} values. In addition, we expected the automated sample sets to yield much different

Table 4.6-2. Predicted peak sediment concentrations (Ts), peak sediment loads (Qs) and peak erosion rates (ER) for the predicted 2-year (Q₂), 5-year (Q₅), and 50-year (Q₅₀) flow events.

Subbasin	area (mi ²)	slope a	Intercept log b	Q (cfs) 2	Tspre (g/l) 2	Qs (kg/s) 2	ER (mm/day) 2	Q (cfs) 5	Tspre (g/l) 5	Qs (kg/s) 5	ER (mm/day) 5	Q (cfs) 50	Tspre (g/l) 50	Qs (kg/s) 50	ER (mm/day) 50
1N	0.790	0.93	-0.25	4.1	2.1	0.2	0.0045	9.5	4.5	1.2	0.0224	31.1	18.7	12.1	0.2222
2N	0.610	2.18	1.24	3.3	240.9	22.8	0.5424	7.8	1529.5	338.0	8.0403	26.1		1184.9	28.1841
3N	0.900	1.59	1.4	3.5	180.4	17.7	0.2848	7.9	670.6	150.0	2.4177	25.6		1162.3	18.7381
4N	1.700	1.02	0.94	4.0	35.8	4.1	0.0346	8.8	80.1	20.0	0.1706	27.2	252.9	194.9	1.6633
					53.5	6.1	0.0518		105.2	26.3	0.2241		287.9	221.8	1.8935
5N	1.560	1.2	1.31	3.7	98.5	10.4	0.0264	8.2	255.5	59.5	0.5533	25.5	996.6	721.1	6.7071
7N	4.140	1.81	0.08	4.3	17.0	2.1	0.0073	9.1	64.9	16.6	0.0583	26.0	438.6	323.5	1.1340
					62.0	7.6	0.0266		314.3	80.6	0.2826			1503.9	5.2707
9N	2.080	1.36	-0.3	14.3	18.7	7.6	0.0527	31.1	53.7	47.4	0.3305	94.5	243.5	652.2	4.5497
10N	3.130	1.7	-0.8	20.4	26.6	15.4	0.0712	43.3	96.0	117.8	0.5463	127.3	600.5	2167.0	10.0453
11N	8.640	1.16	-1.27	93.1	10.3	27.3	0.0458	186.9	23.2	122.8	0.2062	506.6	73.7	1058.1	1.7769
2S	0.800	0.62	0.03	12.5	5.1	1.8	0.0329	28.7	8.6	7.0	0.1266	94.1	17.9	47.8	0.8671
3S	0.690	0.67	0.04	11.0	5.5	1.7	0.0357	25.5	9.6	6.9	0.1455	84.5	21.4	51.3	1.0781
4S	0.740	0.37	-0.31	13.6	1.3	0.5	0.0097	31.4	1.8	1.6	0.0306	103.7	2.7	8.0	0.1572
5S	1.790	0.45	-0.42	29.3	1.7	1.4	0.0117	64.3	2.5	4.5	0.0365	197.6	4.1	23.0	0.1863
CS	0.630	0.54	-0.46	11.8	1.3	0.4	0.0102	27.6	2.1	1.6	0.0374	92.2	4.0	10.4	0.2401
6S	0.840	0.38	0.38	8.7	5.5	1.3	0.0232	19.9	7.5	4.2	0.0728	65.0	11.7	21.6	0.3729
7S	0.850	1.05	0.24	8.8	17.0	4.2	0.0721	20.1	40.6	23.1	0.3943	65.6	140.4	260.9	4.4542
9S	1.720	0.86	-0.37	24.2	6.6	4.5	0.0383	53.3	13.0	19.7	0.1663	164.5	34.4	160.2	1.3510
10Sb	5.260	0.74	-0.38	117.1	14.2	47.0	0.1295	241.8	24.2	165.8	0.4575	682.1	52.1	1007.5	2.7792
1M	48.100	1.1	-1.57	725.3	37.7	775.4	0.2339	1320.3	72.9	2727.5	0.8228	3119.5	187.7	16594.5	5.0058
3M	43.000	1.3	-2.28	658.2	24.2	451.4	0.1523	1205.7	53.2	1816.4	0.6129	2874.4	164.5	13398.4	4.5211
6M	20.900	1.41	-2.55	264.1	7.3	54.8	0.0380	504.1	18.2	260.3	0.0002	1273.2	67.3	2427.5	1.6853
Poker	6.020	1.12	-1.46	6.0	0.3	0.0	0.0001	12.3	0.6	0.2	0.0005	34.2	1.8	1.8	0.0042

$T_{s_{pre}}$ values because they were sampled only during higher flows, and thus have biased sample sets.

A maximum threshold for sediment concentration exists where T_s cannot exceed about 1600 to 2000 g/l (i.e., the largest T_s collected from a mudflow during the study was 1600 g/l). Without the threshold, some of the regressions with high slope values would yield predicted sediment concentrations that are not physically possible. This points to the danger of using linear regressions without caution. In some cases, it also reflects the lack of fit for a simple linear regression (e.g., see 10Sa and 3M regression plots in Appendix C), and that a slight curve might give better representation of natural thresholds.

$T_{s_{pre}}$ values ranged from 0.3 g/l to 241 g/l for the Q_2 event, 0.6 g/l to 1530 g/l for the Q_5 event, and 1.8 g/l to threshold concentrations for the Q_{50} event. Mudflows commonly have T_s values greater than 800 g/l. Mudflow exceedance thresholds were reached by 2N, 3N and 7N for the Q_{50} event, thus mudflows concentrations were predicted for 2N, 3N, 5N, and 7N for the Q_{50} event, and for 2N for the Q_5 event. In addition, transitional flows have T_s concentrations that range from 200 to 800 g/l; three more creeks (4N, 9N and 10N) had predicted T_s in this range. All seven of the creeks with very high predicted T_s concentrations emanate from the Tertiary basins with much of their landscape exposed in badlands. Mudflows were observed emanating from 2N and transitional flows were observed emanating from 3N, 4N, 5N and 7N during this study.

The T_{s_5} predicted values are well within the range of actual T_s values measured in each creek during the study, while the $T_{s_{50}}$ values are high for some basins, they seem plausible because T_s concentrations of this magnitude were measured. However, sustaining the predicted $T_{s_{50}}$ concentration would require an ample supply of readily available sediment, which could only be accommodated by large mass wasting events. The Q_{50} event would likely result in a tremendous flushing of the basin and a downstream transfer of much of the coarser stored sediment.

4.6.2 Erosion Rates

4.6.2.1 Peak Erosion Rates

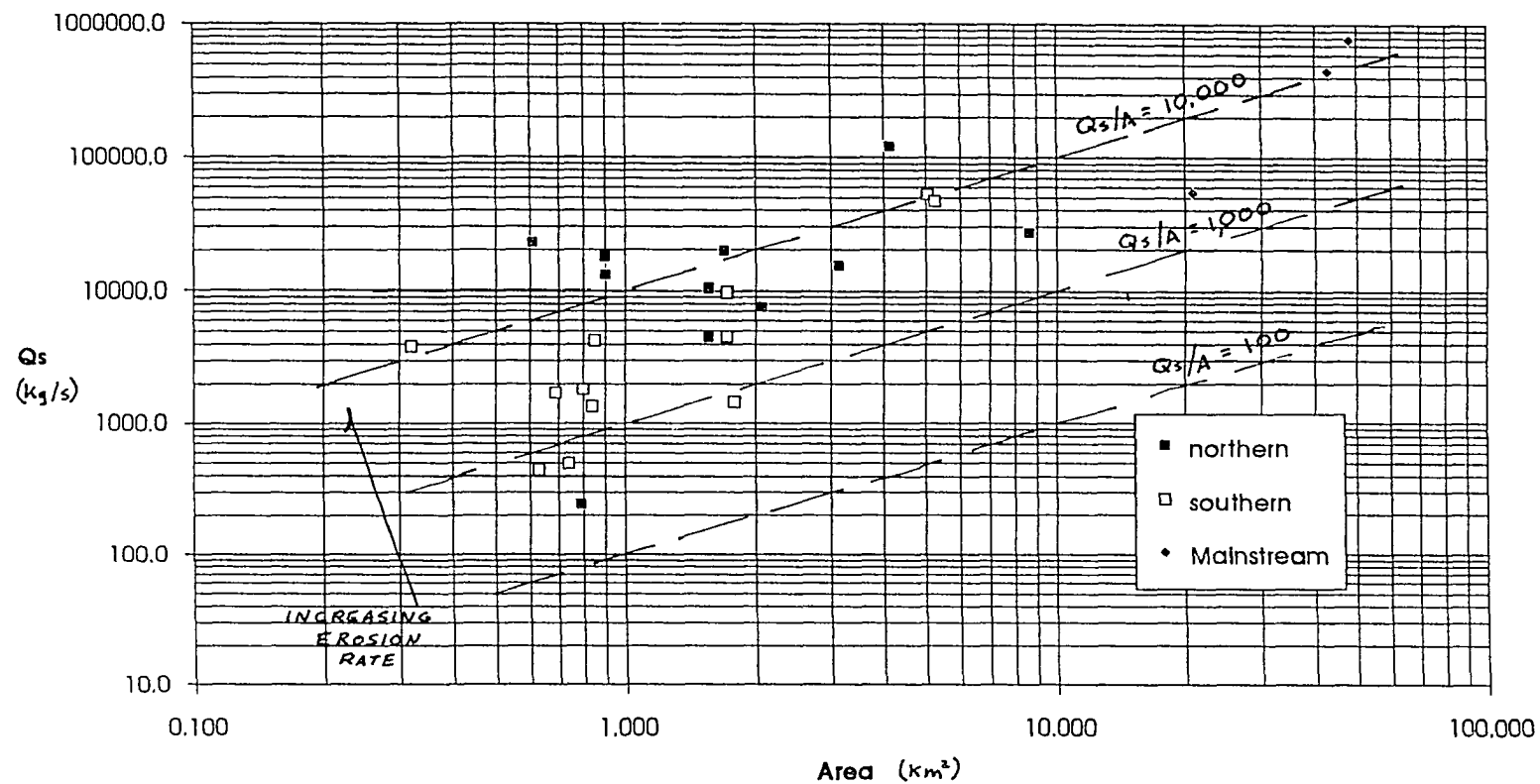
Peak sediment concentrations or loads alone do not accurately indicate what effect a given storm has on the various basins. To establish an index of which basins are eroding slowly and which are eroding quickly, the peak sediment discharge rate ($Q_{s_{peak}}$) was divided by the basin area (A) and the average density of the eroded material (2.3 g/cm^3 for unconsolidated sedimentary rock and 3.0 g/cm^3 for schist) in each respective basin to determine a daily "erosion rate" (mm/day) for each basin. Since the peak erosion rate cannot be sustained during a storm, and is in essence the instantaneous erosion rate, it is greater than the erosion rate over the entire storm. However, since the $Q_{s_{peak}}$ is proportional to the ratio of $Q_{s_{storm}}/Q_{s_{peak}}$, it is thought to be a reasonable index of erosion rate differences between basins.

Calculated erosion rates are summarized in Table 4.6-2 and represented graphically on Figures 4.6-1 through 4.6-3. In general, the badland-dominated sand and gravel basins (2N, 3N, 5N, and 7N) are eroding 10 to 25 times faster than the other Tertiary basins, which in turn are eroding at least ten times faster than the schistose basins. The average basin-wide erosion rate is approximately 0.23 mm/day for the Q_2 event, 0.82 mm/day for the Q_5 event and 5.0 mm/day for the Q_{50} event. Based on the sediment loads predicted for the 2, 5 and 50 year storms, which likely yield from 50 to 99% of the annual sediment load (Ray and others, 1992), the annual erosion rates can be estimated from the daily erosion rates such that the annual erosion rates are as much as two times the values listed in Table 4.6-2.

4.6.2.2 Estimated Long-term Erosion Rates

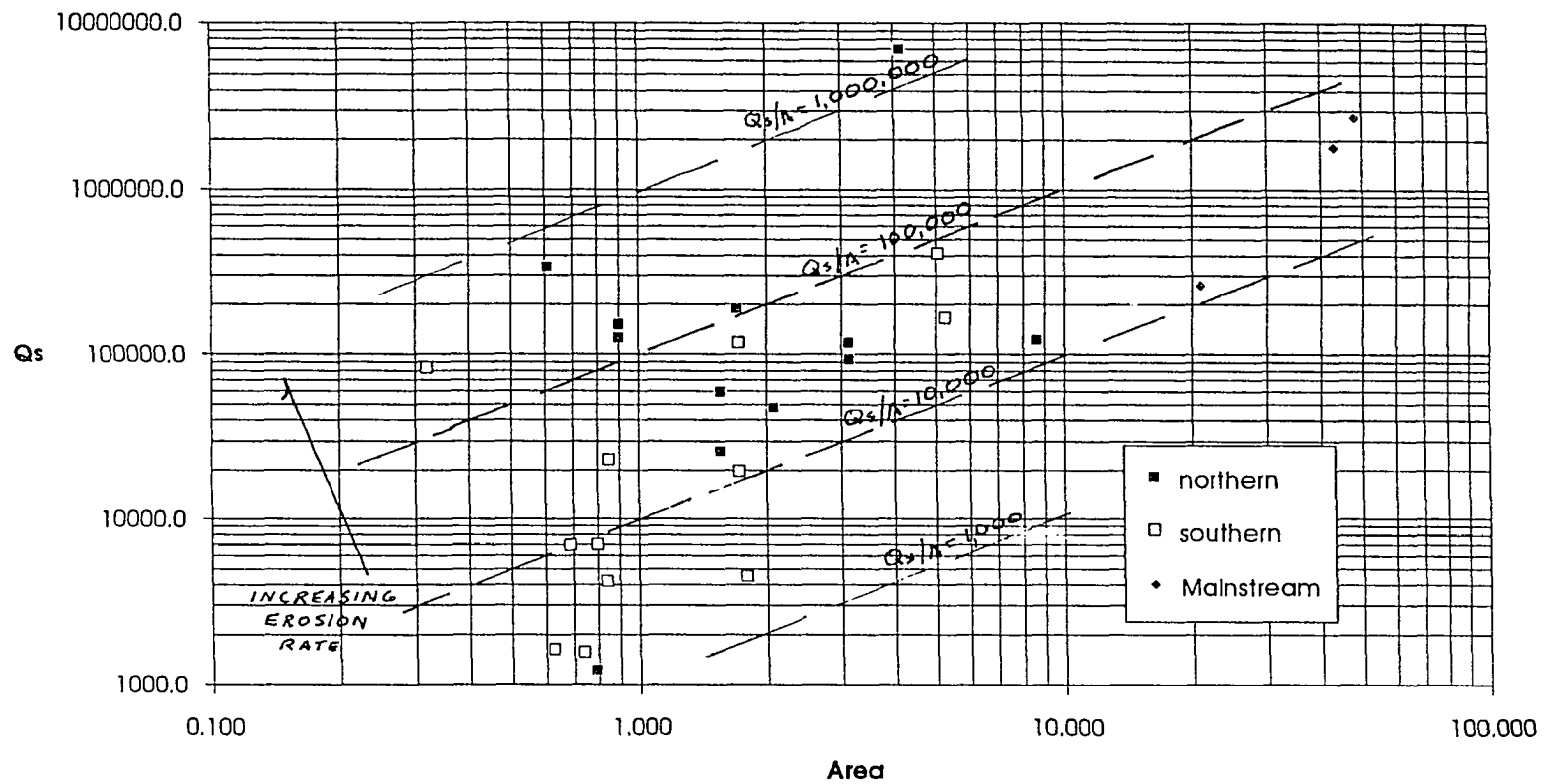
During the Late Quaternary, land surface lowering in Hoseanna Creek Watershed was not uniform throughout the basin. The Nenana Valley bottom aggraded during glaciation and outwash progradation, and degraded during tectonic uplift that has been accompanied by deglaciation and outwash incision (Section 2.3). Since the end of the Late Wisconsin, the rate of lowering has likely increased due to the changes in local base level (Figure 2.3-5); the local base level lowering has allowed the geologic variation to exhibit its control on erosion and landscape development.

4-88



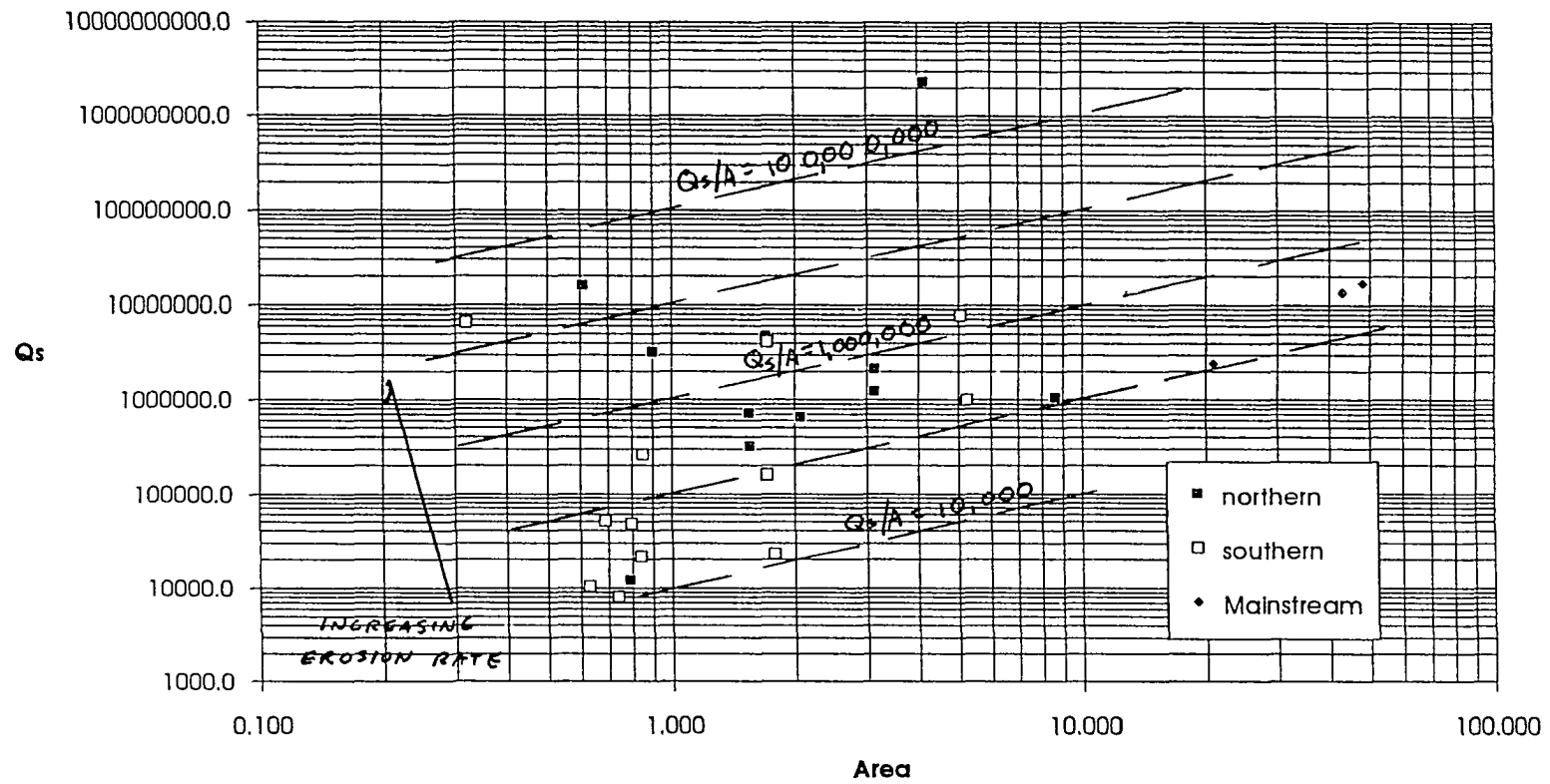
Figures 4.6-1. Plot of peak sediment load versus basin area for a 2-year storm event. The daily erosion rate (estimated from the quotient of Q_s/A) is controlled by aspect and lithology. Erosion rates vary over two orders of magnitude for the 2-year event, such that northern basins underlain by Nenana Gravel are eroding up to 100 times the rate of southern basins underlain by schist.

4-89



Figures 4.6-2. Plot of peak sediment load versus basin area for a 5-year storm event. The daily erosion rate (estimated from the quotient of Q_s/A) is controlled by aspect and lithology. Erosion rates vary by more than two orders of magnitude for the 5-year event, such that northern basins underlain by Nenana Gravel are eroding over 260 times the rate of southern basins underlain by schist.

4-90



Figures 4.6-3. Plot of peak sediment load versus basin area for a 50-year storm event. The daily erosion rate (estimated from the quotient of Q_s/A) is controlled by aspect and lithology. Erosion rates vary by over two orders of magnitude for the 50-year event, such that northern basins underlain by Nenana Gravel are eroding over 170 times the rate of southern basin underlain by schist.

If just the Qs_{50} predicted erosion rates are extrapolated over the Holocene and averaged over the terrain then the schist would have eroded roughly 1.5 to 2.4 meters, the coal-bearing rocks 18 to 100 meters, and the Nenana Gravel up to 280 meters. Thus, erosion has been insignificant in the areas underlain by the schist, while areas underlain by the Tertiary lithologies have undergone rapid degradation.

The estimated erosion rates of 1.5 to 280 meters over the last 10,000 years are within the necessary range of values to account for the rate of base level decrease (i.e., 6.2 to 18.0 m/ka) that has occurred at the mouth of Hoseanna Creek during the Late Quaternary (Figure 2.3-5). Hence, it is safe to assume that the processes contributing to very high sediment yields today have occurred in Hoseanna Creek for much of the Late Quaternary, although the spatial distribution and site-specific rates have probably changed.

4.7 Summary and Conclusions of Streamflow and Sediment Discharge Processes

The objectives of the streamflow and sediment-discharge study were to:

- 1) describe and quantify the natural variations of discharge and sediment concentrations as functions of climate and geology,
- 2) determine what governs sediment-discharge relationships so that the observed variance in the Q-Ts regressions could be explained, and
- 3) determine what portions of the observed variance is due to operational factors (e.g., sampling and laboratory techniques), and what part is controlled by natural processes (e.g., spatial and temporal variability).

The primary methodology was to collect streamflow and sediment concentration data from the variety of geohydrologic-type basins within Hoseanna Creek Watershed and relate the data to the climatic and geologic characteristics described in Section 2.0. The analyses utilized standard regression techniques to describe and quantify the variability of measured discharge and sediment concentration.

A major conclusion is that natural spatial and temporal controls on discharge and sediment concentration are related to basin's aspect, lithology and climate regime. North-facing higher relief permafrost basins underlain by resistant schistose rocks have relatively high peak flows of short duration that decline during the summer to

low base flows. In contrast, south-facing non-permafrost lower relief basins underlain by coal-bearing rocks have reduced peak flows due to higher interception and infiltration while base flows are relatively higher and sustained due to high volume aquifer storage in thick fractured coal seams. South-facing non-permafrosted basins underlain by the Nenana Gravel have very low peak and base flows due to higher overall evapotranspiration, infiltration, interflow and likely a very short groundwater storage residence time.

Variations among basins of suspended and bedload sediment concentrations are controlled by lithology and basin area such that the north-facing schistose basins have relatively low sediment concentrations, basins underlain by coal-bearing formations have relatively high suspended sediment concentrations and moderate bedload concentrations. Basins underlain by Nenana Gravel have moderate suspended sediment concentrations and very high bedload concentrations. However, the variability of sediment concentrations is a function of discharge.

Discharge and sediment concentration are spatially and temporally associated; their relationship is expressed by the sediment-rating regression equation. Each basin has a unique sediment concentration-discharge relationship referred to here as the mean sediment concentration potential C_p . The regression parameters (a and b) of the sediment-discharge power function indicate that geologic and basin size largely define the mean sediment concentration potential, while systematic changes in the sediment concentration regression residual R (here referred to as the maintenance rate R^*) describes the unique temporal variability of sediment concentration through time with respect to C_p .

The relationships of Q , T_s , C_p , R , and R^* are developed from continuous discharge and sediment concentration data and provide quantitative and qualitative expressions of supply and demand. These expressions can be used to explain the nature of sediment transfer processes (i.e., filling, cutting, corradng), with respect to differences in climate and geology. In addition, from the residual curve, one can measure or interpret the effect of proximity and supply, the magnitude of the supply event, and the effect of spring break-up or summer storms on stream channel maintenance.

Peak flow erosion rates were estimated and are used as an index of long-term

erosion rates, and suggest that Nenana Gravel basins are eroding 260 times faster than the schistose basins and ten times the coal-bearing basins. Estimated basinwide erosion rates for various size storm events are comparable to the rate of base level incision at the mouth of Hoseanna Creek and are thus reasonable indicators of the long-term erosion rate.

The analyses indicate that natural spatial and temporal variations as well as operational methods limit the accuracy of models based on linear regressions, and should govern their application. In addition, the wide ranges in measured discharges (0.001 to 2350 cfs, or 0.000028 to 66.5 m³/s) and sampled sediment concentrations (0.005 to 1600 g/l) necessitates the use of log-log scales, so that the regression equations are necessarily power functions.

The success of predicting sediment concentrations is complicated by several factors. The sensitivity of base, peak, and recession discharges to a) the seasonal timing, intensity, frequency and duration of storm events, b) variations in break-up, summer and freeze-up conditions, c) the geohydrologic basin type, d) the presence and thickness of permafrost and the role of the active layer, e) additional geomorphic characteristics (e.g., drainage density), and f) vegetation-controlled aspectual variations. In addition, the timing and size of mass wasting events, the proximity of the sediment supply to the sampling site, and the timing of data collection during events all affect the accuracy of the regression equations.

In order to provide reliable models for predicting sediment concentrations one must first establish a rigorous field program in which both storm and base flow sediment data are closely monitored. This is especially important during spring breakup when a very large portion of the annual sediment load is transported. Second, one must account for strong geologic influences on the sediment supply and the surface and subsurface hydrology. The geologic control is inherently linked to other environmental factors such as aspect, permafrost and plant communities. Third, almost all natural and spatial variables are dependent on watershed area. For example, larger basins will have attenuated storm hydrographs and more chances for mixing and dilution of sediment sources so that larger creeks have lower sediment concentrations than smaller creeks even though all other factors are equal.

The natural variance of sediment concentration is time dependent, which implies a relationship with the shape of the storm hydrographs, and non-steady surges in sediment supply. Therefore, the application of only linear regression models without considering the temporal influences will have limited accuracy and applicability, and in some cases are not statistically warranted. In any case, linear regressions have a limited accuracy where the natural variation of sediment concentration is very large.

5.0 SUMMARY and CONCLUSIONS

Hoseanna Creek Watershed of central Alaska is a rapidly eroding drainage basin that provides an excellent opportunity to describe and quantify various hillslope and fluvial processes. An extensive four-year field investigation of these processes integrating the resources of the United States Geological Survey, the Alaska Division of Geological and Geophysical Surveys and Usibelli Coal Mine, Inc. yielded new or revised geologic, geomorphic and hydrologic data which were used to describe and quantify the geologic and climatic controls governing the surface processes in Hoseanna Creek Watershed.

5.1 Climatic and Geologic Controls

Subarctic climate patterns have produced discontinuous permafrost and provide an environment for cryogenic processes to operate. Spring break-up and major cyclonic summer storms produce large changes in the hydrologic regime that catalyze mass wasting and sediment-transfer.

The mildly folded Tertiary strata and ubiquitous presence of clay horizons are conducive to landsliding. Poorly consolidated Tertiary lithologies are exposed on cliffed badlands and rapidly break down to yield large quantities of sediment. Repeated late Quaternary glaciations in the Nenana Valley concurrent with continued faulting and deformation associated with the rising Alaska Range, (most recently the resurgent displacement of the Poker Flats fault - approximately 40 m between 25,000 and 10,000 yrs BP) have dropped local base level (the confluence of the Nenana River and Hoseanna Creek) at least 100 m, enhancing stream power and causing Hoseanna Creek Watershed to enlarge headward through weak Tertiary lithologies.

All the surface morphology in Hoseanna Creek Watershed is late Pleistocene or younger. Differences in drainage densities of headwater 3rd order streams are indicators of non-uniform erosion rates operating throughout the last approximately 200,000 years. Weaker Tertiary sedimentary lithologies have relatively higher drainage densities with many short 1st order streams and thus are much more dissected and able to provide more sediment to trunk streams for any given storm.

Late Holocene alluvial fans grew at the mouths of basins emanating from weak sedimentary lithologies and also at the mouth of Hoseanna Creek in response to the increased sediment production and sediment-transfer adjustments to the changes in creek grade. The most recent adjustment appears to have taken approximately 2000 years to reach the headwaters of tributary streams.

5.2 Landslide Processes and Evolution

More than 5% of Hoseanna Creek Watershed is covered by landslide deposits, of which 98% occur in coal-bearing lithologies. The slides (0.002 to 0.6 km²), form in weakly consolidated clayey sedimentary formations in response to lateral corrasion of toes by avulsing streams or to undermining of foot areas by headward incising streams. The slides move predominantly as remobilized earthflows, disrupted translational block slides, rotational slide blocks or lateral spreads or some combination of the four types. In addition, each slide has a history that may include the development from one type of slide to another, typically from a more coherent type (e.g., block slide) to a more disrupted type (e.g., earthflow) or more fragmented type (e.g., lateral spread). Many other mass wasting forms such as soil slips, frost boils, frost scars and solifluction occur but are less significant erosion agents and sediment producers.

Landslides in Hoseanna Creek Watershed exhibit all stages of evolution. Some are experiencing rapid growth during an early stage, others are experiencing movement periods typical of a late stage, while other slides exhibit movement and physical characteristics typical of midstage. In all the slides, there is field and photo evidence that suggests episodic activity when new slide material is added or when climatic triggers reach critical thresholds. Seven slides were surveyed at different periods of landslide evolution or stage. Average horizontal rates of motion between August 1985 and September 1988 ranged from 0.2 m/yr in rotational slide blocks to 48 m/yr in the upper sections of earthflows.

Landslide motion is not constant throughout the year, nor during the period of landslide activity. In areas of permafrost, thermal erosion (or permafrost degradation) catalyzes slide activity. Major differences in the timing of rainfall events, the timing of break-up or freeze-up, and general weather conditions in any one year cause major differences in the magnitude and timing of slide motion.

Lithostatic loading of slides due to crown retreat (retrogressive enlargement) occurs primarily during the late winter and spring and in some slides reflects thermal degradation of permafrost. Major slide motion occurs during spring and early summer when large volumes of water become available from snowmelt; however, warm winters appear to reduce the magnitude of spring motion. Large summer rainstorms sometimes have major effect on motion, while at other times have little or no effect on motion.

There are unique climatic and geomorphic processes operating in the subarctic. Although sliding mechanisms are not unique to the subarctic, the permafrost terrain and cold climate provide unique processes that cause delays or catalysts for failure that would not occur in a warmer climate. Freezing/thawing fronts affect soil strength and permeability; break-up/freeze-up processes affect the timing of the supply of water to the slide mass, and affect the development or breakdown of aufeis in the creeks. Typically the creek aufeis lasts longer than snow in spring but the creeks are the last thing to freeze in the winter.

Hillslope denudation rates are spatially and temporally dependent on variable and episodic climatic and geomorphic triggering processes, and are also a function of the stage in the cycle of a slide mass. Resurgent activity is less likely if no new material is added to the slide mass. The long-term evolution of slide masses within Hoseanna Creek Watershed are dependent on: (a) the lithologic resistance to denudation (e.g., schist versus sedimentary units); (b) the prevailing east-west structure and valley asymmetry; (c) the subarctic climate (i.e., long cold winters and short warm summers, and cyclonic summer precipitation patterns); (d) discontinuous permafrost terrain (and the related thermal erosion of permafrost); and (e) tectonism (i.e., local base level changes).

5.3 Streamflow and Sediment Transfer Processes

High latitude aspectual differences and lithologic variations combine to yield valley asymmetry with three geohydrologic-basin types which govern the range of peak (Q_{\max}) and base (Q_{\min}) flows. North-facing permafrosted schistose basins have relatively low Q_{\min} with high Q_{\max} , south-facing nonpermafrosted coal-bearing basins had relatively low Q_{\max} but high Q_{\min} , and the south-facing nonpermafrosted Nenana Gravel basins had very low Q_{\max} and low Q_{\min} .

Linear regression analyses were performed on sediment-discharge (Ts-Q) data to help describe the influence of both operational and natural variables on sediment concentrations. The analyses indicate that natural spatial and temporal variations as well as operational methods limit the accuracy of models based on linear regressions, and should govern their application. Regression variance (r^2) was found to have both minimum and maximum limits; a maximum r^2 exists such that all Ts-Q relationships have a minimum amount of natural variability, and minimum r^2 tended to increase with basin area and with number of samples. In addition, the wide ranges in measured Q (0.001 to 2350 cfs, or 0.000028 to 66.5 m³/s) and sampled Ts (0.005 to 1600 g/l) necessitates the use of log-log scales, so that the sediment-rating regression equations are necessarily power functions.

The discharge and sediment concentration function is spatially and temporally related, and can be expressed by the sediment rating regression equation $\log T_s = \log a + b \log Q$. Each subbasin has a unique sediment concentration-discharge relationship referred to here as the mean sediment concentration potential C_p . Systematic differences in the regression parameters (a - y-intercept and b - slope) of the discharge-sediment power function reveal that specific spatial (e.g., geologic variability and basin area) conditions define the mean sediment concentration potential, while systematic changes in the sediment concentration regression residual R (here referred to as the maintenance rate R^*) describe the temporal variability of sediment concentration through time with respect to C_p .

The relationships of Q , T_s , C_p , R , and R^* are developed from continuous discharge and sediment concentration data and provide quantitative and qualitative expressions of supply and demand. These expressions can be used to explain the nature of sediment transfer processes (i.e., filling, cutting) with respect to differences in climatic and geologic input. In addition, from the residual curve, one can measure or interpret the effect of proximity and supply, the magnitude of the supply event, and the effect of spring break-up or summer storms on stream channel maintenance. The regression techniques indicate that the observed variance can be attributed to geologic variability, systematic temporal changes in sediment supply, hysteretic processes during a storm cycle, and the shapes of site-specific storm hydrographs.

50-95% of the annual sediment load is produced during large infrequent summer storms or during spring break-up. Peak flow sediment load estimates were used to establish an index of long-term erosion rates and suggest that Nenana Gravel basins are eroding 260 times faster than the schistose basins and ten times faster than the coal-bearing basins. Estimated basinwide erosion rates for various size storms are comparable to the rate of base level incision at the mouth of Hoseanna Creek and are thus reasonable indicators of the long-term erosion rate.

REFERENCES

AHC (1987). Sediment and drainage control for the Gold Run Pass Mine, prepared by Arctic Hydrologic Consultants for Usibelli Coal Mine, Healy, Alaska, February 1987, 27 pp.

Anderson, D. M., Williams, P. J., Guymon, G. L., and Kane, D. L. (1984). Principles of soil freezing and frost heaving, in Berg, R. L. and Wright, E. A., eds., Frost Action and its Control, New York, American Society of Civil Engineers, p. 1-21.

Bagnold, R. A. (1966). An approach to the sediment transport problem from general physics, U. S. Geological Survey Prof. Paper 422-I, 79 pp.

Barnes, F. F., Wahrhaftig, C., Hickcox, C. A., Freedman, J., and Hopkins, D. M. (1951). Coal Investigations in South Central Alaska, 1944-46, U.S. Geological Survey Bull. 963E, p. 141-165.

Bates, R. L. and Jackson, J. A. (1987). "Glossary of Geology, 3rd ed," Alexandria, Virginia, American Geological Institute, 788 pp.

Beget, J. E. and Keskinen, M. (1991). The Stampede tephra: a middle Pleistocene marker bed in glacial and eolian deposits of central Alaska, Can. J. Earth Sci., vol. 28, p 991-1002.

Benson, M. A. and Dalrymple, T. (1967). General field and office procedures for indirect discharge measurements, Techniques of Water Resources Investigations of the U.S. Geological Survey, Book 3, Ch. A1, 30 pp.

Brunsden, D. (1984). Mudslides, in Brunsden, D. and Prior, D. B., eds., Slope Instability, John Wiley & Sons, Ltd., p. 363-418.

Buchanan, T. J. and Somers, J. P. (1969). Discharge measurements at gaging stations, Techniques of Water Resources Investigations of the U.S.G.S., Book 3, Ch. A8, 64 pp.

Buffler, R. T. and Triplehorn, D. M. (1976). Depositional environments of the Tertiary coal-bearing group, central Alaska, in Miller, T. P., ed., Recent and ancient sedimentary environments in Alaska, Proceedings of Symposium, April 2-4, Anchorage, Alaska Geological Society, p. H1-H10.

Burrows, R. (1988). Oral communication, U.S.G.S. Water Resources Division, Fairbanks, Alaska.

Campbell, R. H. (1975). Soil slips, debris flows, and rainstorms in the Santa Monica Mountains and vicinity, southern California, U. S. Geological Survey Prof. Paper 851, 51 pp.

Campbell, R. H., Varnes, D. J., Fleming, R. W., Hampton, M. H., Prior, D. B., Sangrey, D. A., Nichols, D. R., and Brabb, E. E. (1985). Landslide classification for identification of mud flows and other landslides, Ch A, *in* Feasibility of a nationwide program for the identification and delineation of hazards from mud flows and other landslides, U. S. Geological Survey Open File Report 85-276A, 24 pp.

Capps, S. R. (1912). The Bonnifield region, Alaska, U. S. Geological Survey Bull. 501.

Capps, S. R. (1940). Geology of the Alaska Railroad region, U. S. Geological Survey Bull. 907, 201 pp.

Carter, R. W., and Davidian, J. (1968). General procedure for gaging streams, Techniques of Water Resources Investigations of the U.S. Geological Survey, Book 3, Ch. A6, 13 pp.

Chamberlin, E. J. (1985). Shear strength anisotropy in frozen saline and freshwater soils, *in* International Symposium on Ground Freezing, 4th, Sapporo, Japan, August 5-7, 1985, Proceedings, vol. 2, Rotterdam, A. A. Balkema, p. 189-194.

Clarke, T. (1987). Estimates of the 100-year and 50-year discharge events at the #6 bridge site on Hoseanna Creek, Alaska, prepared for Renshaw Consulting Engineers, Anchorage, Alaska, September 1987, 10 pp.

Coates, D. R. (1977). Landslide perspectives, in Reviews in Engineering Geology, Vol III, Geol. Soc. Am., p. 3-28.

Cruden, D. M. (1990). Suggested nomenclature for landslides, Bull. of the International Assn. of Eng. Geol, 4:13-16.

Csejtey, B., Jr., Mullen, M. W., Cox, D. P., Gilbert, W. G., Yeend, W. E., Smith, T. E., Wahrhaftig, C., Craddock, C., Brewer, W. M., Sherwood, K. W., Hickman, R. G., Stricker, G. D., St. Aubin, D. R. and Goertz, D. J. III (1986). Geology and geochronology of the Healy Quadrangle, Alaska, U. S. Geological Survey Open File Report 86-396.

Dalrymple, T. and Benson, M. A. (1967). Measurement of peak discharge by the slope-area method, Techniques of Water Resources Investigations of the U.S. Geological Survey, Book 3, Ch. A2, 12 pp.

Einstein, H. A. (1951). The bed-load function for sediment transportation in open channel flows, U. S. Dept. Agric. Tech. Bull. 1926, 71 pp.

Fisher, R. V. (1971). Features of coarse-grained, high concentration fluids and their deposits, J. Sed. Petrol., vol. 41, p. 916-927.

Golder (1985). Stability analysis of north facing spoil slopes at Poker Flats; prepared for Usibelli Coal Mine by Golder Associates, Inc., Anchorage, AK, Report 853-5016, 22 pp.

Gurnell, A. M. and Clarke, M. J. (1986). Glacio-fluvial Sediment Transfer: an Alpine Perspective, John Wiley & Sons, Inc., Chichester 524 pp.

Guy, H. P. (1967). Fluvial sediment concepts, Techniques of Water Resources Investigations of the U.S. Geological Survey, Book 3, Ch. C1, 55 pp.

Guy, H. P. (1969). Laboratory theory and methods for sediment analyses, Techniques of Water Resources Investigations of the U.S. Geological Survey, Book 5, Ch. C1, 58 pp.

Guy, H. P. and Norman, V. W. (1970). Field measurements for measurement of fluvial sediment, Techniques of Water Resources Investigations of the U.S. Geological Survey, Book 3, Ch. C2, 59 pp.

Hampton, M. A. (1975). Competence of fine-grained debris flows, J. Sed. Petrol., vol 45, no. 4, p. 834-844.

Hutchinson, J. N. and Bhandari, R. K. (1971). Undrained loading, a fundamental mechanism of mudflows and other mass movements, Geotechnique, vol 21, no. 4, p. 353-358.

Jarrett, R. D. (1988). Hydraulics of high-gradient streams, J. Hydraulic Eng, vol. 110, no. 11, p. 1519-1539.

Johnson, A. M. and Rodine, J. R. (1984). Debris flows, *in* Brunnsden, D. and Prior, D. B., eds., Slope Instability, John Wiley & Sons, Ltd., p. 257-361.

Jones, S. H. (1983). Floods from small drainage basins in Alaska, U.S. Geological Survey Open File Report 83-258, Anchorage, AK, 60 pp.

Kane, D. L. (1981). Physical mechanics of aufeis growth, Can. J. Civil Eng. vol. 8, no. 2, p. 186-195.

Kane, D. L. and Janowicz, J. R. (1988). Flood frequency estimation for Alaska, Alaska Division of Geological and Geophysical Surveys, Report of Investigations 88-17, 22 pp.

Keefer, D. K. and Johnson, A. M. (1983). Earthflows: morphology, mobilization, and movement, U.S. Geological Survey Prof. Paper 1264, 56 pp.

Kennedy, E. J. (1984). Discharge ratings at gaging stations, Techniques of Water Resources Investigations of the U.S. Geological Survey, Book 3, Ch A10, 59 pp.

Lamke, R. D. (1978). Flood characteristics of Alaska streams; U.S. Geological Survey, Water Resources Investigations, WRI 78-129, 61 pp.

Langbein, W. B. and Iseri, K. T. (1960). General introduction and hydrologic definitions, U. S. Geological Survey, Water -Supply Paper, 1541-A, 29 pp.

Leopold, L. B. and Maddock, T., Jr., (1953). The hydraulic geometry of stream channels and some physiographic implications, U. S. Geological Survey Prof. Paper 242, 57 pp.

Leopold, L. B., Wolman, M. G. and Miller, J. P. (1964). Fluvial Processes in Geomorphology, Freeman, San Francisco, 522 pp.

Limerinos, J. T. (1969). Determination of the Manning coefficient from measured bed roughness in natural channels, U. S. Geological Survey Water Supply Paper 1898-B, 47 pp.

Mack, S. F. (1987). Streamflow and sediment supply study of Hosanna Creek near Healy, Alaska: 1986 progress report, Alaska Division of Geological and Geophysical Surveys, Public-data File Report 87-4, 13 pp.

Mack, S. F. (1988). Streamflow and sediment study of Hosanna Creek near Healy, Alaska: 1987 progress report, Alaska Division of Geological and Geophysical Surveys, Public-data File Report 88-9, 57 pp.

Martin, G. C. (1919). The Nenana coal field, Alaska, U. S. Geological Survey Bull. 664, 54 pp.

Merritt, R. D. (1986). Alaska's coal resources, Alaska Division of Geological and Geophysical Surveys with the Alaska Coal Association, map (1:2,500,000) with text.

Michel, B. (1971). Winter regime of rivers and lakes, Cold Regions Research and Engineering Laboratory, Cold Regions Science and Engineering Monograph III-B1a, Hanover, New Hampshire, 130 pp.

Middleton, G. V. and Hampton, M. A. (1973). Sediment gravity flows: mechanics of flow and deposition, *in* Middleton, G. V. and Bouma, A. H., co-chairmen, Turbidites and deep-water sedimentation, short course lecture notes, Pacific Section S.E.P.M., Los Angeles, p. 1-38.

Nemcok, A. (1972). Gravitational slope deformations in the high mountains of the Slovak Carpathians, Sbornik Geologických ved, Rada HIG, no. 10, p. 31-37.

Nemcok, A., Pasek, J. and Rybar, J. (1972). Classification of landslides and other mass movements, Rock Mechanics, vol. 4, no. 2, p. 71-78.

Nye, J. F. (1951). The flow of glaciers and ice-sheets as a problem in plasticity, *Proc. R. Soc. London, Ser. A*, vol. 207, pp 554-572.

Osterkamp, W. R., Lane, L. J., and Foster, G. R. (1983). An analytical treatment of channel-morphology relations, U. S. Geological Survey Prof. Paper 1288, 21 pp.

Ray, S. (1990). Streamflow, sediment load and water-quality study of Hoseanna Creek near Healy, Alaska: 1989 progress report and 1986-1989 data summary, Alaska Division of Geological and Geophysical Surveys Public-data File Report 90-15, 99 pp.

Ray, S. R. and Maurer, M. (1989). Streamflow, sediment load and water-quality study of Hoseanna Creek near Healy, Alaska: 1988 progress report, Alaska Division of Geological and Geophysical Surveys Public-data File Report 89-10, 62 pp.

Ray, S. R., Vohden, J., and Roe, J. T. (1991). Streamflow, sediment load and water-quality study of Hoseanna Creek near Healy, Alaska: 1990 progress report, Alaska Division of Geological and Geophysical Surveys Public-data File Report 91-20, 65 pp.

Ray, S. R. and Vohden, J. (1992). Streamflow, sediment load and water-quality study of Hoseanna Creek near Healy, Alaska: 1991 progress report, Alaska Department of Natural Resources, Div. of Water, Alaska Hydrological Survey Public-data File Report 92-19, 51 pp.

Ray, S. R. and Vohden, J. (1993). Streamflow, sediment load and water-quality study of Hoseanna Creek near Healy, Alaska: 1992 progress report; Alaska Department of Natural Resources, Div. of Water, Alaska Hydrological Survey Public-data File Report 93-78, 43 pp.

Ritter, D. F. (1982). Complex river terrace development in the Nenana Valley near Healy, Alaska, *Geol. Soc. Am. Bull.*, vol. 93, p. 346-356.

Ritter, D. F. and Ten Brink, N. W. (1986). Alluvial fan development and the glacial-glaciofluvial cycle, Nenana Valley, Alaska, *J. Geol.* vol. 94, p. 613-625.

Schumm, S. A. (1960). The effect of sediment type on the shape and stratification of some modern fluvial deposits, *Am. J. Sci.*, v. 258, pp 177-184.

Schumm, S. A. (1961). Effect of sediment characteristics of erosion and deposition in ephemeral-stream channels, U. S. Geological Survey Prof. Paper 352-C, pp. 31-70.

Schumm, S. A. (1977). *The Fluvial System*, John Wiley & Sons, Inc., 338 pp.

Scott, K. M. (1978). Effects of permafrost on stream channel behavior in arctic Alaska, U. S. Geological Survey Prof. Paper 1068, 19 pp.

Sharpe, C. F. S. (1938). Landslides and related phenomenon, Columbia Univ Press, New York, 136 pp.

Ten Brink, N. W. (1982). North Alaska Range Project draft final report on the 1978-1982 geoarcheological studies, unpublished report submitted to the National Park Service and National Geographic Society, 960 pp.

Ten Brink, N. W. (1983). Glaciation of the northern Alaska Range, *in* Glaciation in Alaska, eds. Thorson, R. M. and Hamilton, T. D., Alaska Quaternary Center, University of Alaska Museum Occasional Paper no. 2, p 82-91.

Terzaghi, K. (1950). Mechanism of landslides, *in* Paige, S., Chairman, Applications of geology in engineering practice, Geol. Soc. Am. Berkey Volume, p. 83-123.

Thorson, R. M. (1975). Late Quaternary history of the Dry Creek area, central Alaska, M.Sc. thesis, University of Alaska, Fairbanks.

Thorson, R. M. (1978). Recurrent late Quaternary faulting near Healy, Alaska, Alaska Division of Geological and Geophysical Surveys, Short Notes on Alaskan Geology, Geologic Report 61, 14 pp.

Thorson, R. M. (1983). Pre-late Pleistocene glacial sequence for the Nenana Valley: a revision, *in* Glaciation in Alaska, eds. Thorson, R. M. and Hamilton, T. D., Alaska Quaternary Center, University of Alaska Museum Occasional Paper No. 2, p 92-95.

Thorson, R. M. (1986). Late Cenozoic glaciation of the northern Nenana Valley, *in* Glaciation in Alaska, the geologic record, eds., Thorson, R. M. and Hamilton, T. D., Alaska Geological Society, Anchorage, pp. 99-122.

Triplehorn, D. M. (1976). Clay mineralogy and petrology of the coal-bearing group near Healy, Alaska, Alaska Division of Geological and Geophysical Surveys Geologic Report No. 52, 14 p.

USDOI (1981). Water measurement manual, United States Department of Interior, Denver, CO, U.S. Bureau of Reclamation, U.S. Government Printing Office, 327 pp.

USGS (1986). Water Resources Data, Alaska, Water Year 1985, U. S. Geological Survey Water-Data Report AK-85-1.

USGS (1987). Water Resources Data, Alaska, Water Year 1986, U. S. Geological Survey Water-Data Report AK-86-1.

USGS (1988). Water Resources Data, Alaska, Water Year 1987, U. S. Geological Survey Water-Data Report AK-87-1.

USGS (1989). Water Resources Data, Alaska, Water Year 1988, U. S. Geological Survey Water-Data Report AK-88-1.

USGS (1990). Water Resources Data, Alaska, Water Year 1989, U. S. Geological Survey Water-Data Report AK-89-1.

USGS (1991). Water Resources Data, Alaska, Water Year 1990, U. S. Geological Survey Water-Data Report AK-90-1.

USGS (1992). Water Resources Data, Alaska, Water Year 1991, U. S. Geological Survey Water-Data Report AK-91-1.

USGS (1993). Water Resources Data, Alaska, Water Year 1992, U. S. Geological Survey Water-Data Report AK-92-1.

USBWR. United States Weather Bureau records for McKinley Park, Alaska 1925-1988.

Usibelli Coal Mine weather records. Daily temperature and precipitation 1979-1988 for Poker Flats, Gold Run Pass, and Two Bull Ridge, Usibelli Coal Mine, Healy, AK.

Van Sickle, J. and Beschta, R. L. (1983). Supply-based models of suspended sediment transport in streams, *Water Resources Research*, vol. 19, no. 13, p. 768-778.

Varnes, D. J. (1978). Slope movement types and processes, *in* Schuster, R. L., and Krizek, R. S., eds., *Landslides: Analysis and Control*, Ch. 2, United States National Academy of Sciences, Transportation Research Board Special Report (176), p. 11-33.

Wahrhaftig, C. (1958). Quaternary geology of the Nenana River Valley and adjacent parts of the Alaska Range, U.S. Geological Survey Prof. Paper 293, Part A, 68 pp.

Wahrhaftig, (1959). Draft of section on the lithology and conditions of deposition of the formations of the coal-bearing group in the Nenana coal field, Alaska, unpublished manuscript.

Wahrhaftig, C. (1968). Schists of the central Alaska Range; U.S. Geological Survey Bull. 1254E, p. E1-E22.

Wahrhaftig, C. (1970a). Geologic map of the Healy D-2 quadrangle, U.S. Geological Survey Map Series GQ-806.

Wahrhaftig, C. (1970b). Geologic map of the Healy D-3 quadrangle, U.S. Geological Survey Map Series GQ-807.

Wahrhaftig, C. (1970c). Geologic map of the Healy D-4 quadrangle, U.S. Geological Survey Map Series GQ-806.

Wahrhaftig, C. (1970d). Geologic map of the Healy D-5 quadrangle, U.S. Geological Survey Map Series GQ-807.

Wahrhaftig, C. (1970e). Geologic map of the Fairbanks A-2 quadrangle, U.S. Geological Survey Map Series GQ-806.

Wahrhaftig, C. (1970f). Geologic map of the Fairbanks A-3 quadrangle, U.S. Geological Survey Map Series GQ-807.

Wahrhaftig, C. (1970g). Geologic map of the Fairbanks A-4 quadrangle, U.S. Geological Survey Map Series GQ-806.

Wahrhaftig, C. (1970h). Geologic map of the Fairbanks A-5 quadrangle, U.S. Geological Survey Map Series GQ-807.

Wahrhaftig, C. (1970i). A late Cenozoic orogeny in the Alaska Range, Geol. Soc. Am. abs. with programs, part 7:713-714.

Wahrhaftig, C. (1970j). Late Cenozoic orogeny in the Alaska Range, paper presented at the symposium on the geology and geophysics of the Bering Sea region, June 26-28, 14 pp plus figures, unpublished.

Wahrhaftig, C. (1973). Coal reserves of the Healy and Lignite Creek Basins, Nenana coal field, Alaska, U.S. Geological Survey Open File Report 568, with plates and figures.

Wahrhaftig, C. (1987). The Cenozoic section at Suntrana, Alaska, Contribution for the Geological Society of America, Decade of North American Geology, Centennial Guide, Cordilleran Section, vol. 1, p 445-450.

Wahrhaftig, C., Hickcox, C. A., and Freedman, J. (1951). Coal deposits on Healy and Lignite Creeks, Nenana coal field, Alaska, *in* Barnes, F. F. and others, Coal Investigations in South Central Alaska, 1944-46; U.S. Geological Survey Bull. 963E, p. 141-165.

Wahrhaftig, C., and Birman, J. H. (1954). Stripping coal deposits on lower Lignite Creek, Nenana coal field, Alaska; U.S. Geological Survey Circular 310, 11 p, 5 pl.

Wahrhaftig, C., Wolfe, J., Leopold, E. B., and Lanphere, M. A., (1969). The coal-bearing group in the Nenana coal field, Alaska; U.S. Geological Survey Bull. 1274D, p. D1-D30.

Walling, D. E. (1977). Assessing the accuracy of suspended sediment rating curves for a small basin, Water Resources Research, vol. 13, no. 3, p. 531-538.

Washburn, A. L. (1980). Geocryology, 406 pp., John Wiley & Sons, New York.

Wilbur, S. (1989). Predicting sediment concentrations for small subarctic creeks in the Hoseanna Creek Basin, *in* Bandopadhyay, S. and Skudrzyk, F. J., eds, Proceedings, International Conference on Mining in the Arctic, University of Alaska, July 1989, Balkema Publishers, Rotterdam, Netherlands, p 145-156.

Wilbur, S. and Beget, J. (1988). Landslide motion in discontinuous permafrost, *in* Senneset, K., ed., Permafrost, Fifth International Conference, Proceedings, 1:897-902.

Wilbur, S. and Clarke, T. (1987). Relations among lithology, sediment production and drainage density for Hoseanna Creek basin near Healy, Alaska, *in* Huntsinger, R. G., ed., Water Quality in the Great Land, Alaska's Challenge, Proceedings, American Water Resources Association, Water Research Center, IWR 109:203-213.

Wilbur, S. and Clarke, T. (1988). Unusually high bedload concentrations in three subarctic Alaskan creeks, abs., EOS, Transactions, American Geophysical Union, 69:1218, no. 44.

Wilbur, S. and Renshaw, D. (1987). Geologic and climatic controls governing high erosion rates in the Hoseanna Creek Coal basin of central Alaska, *in* Rao, P. D. ed., Focus on Alaska's Coal '86, Mineral Industry Research Laboratory Report, 72:106-115, University of Alaska, Fairbanks.

Wolfe, J. A. and Tanai, T. A. (1980). The Miocene Seldovia Point flora from the Kenai Group, Alaska, U. S. Geological Survey Prof. Paper 1105, 52 pp.

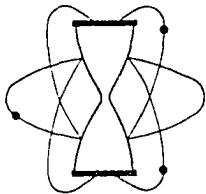
Wolman, M. G. (1954). A method of sampling coarse river-bed material, Transactions, AGU, vol. 35, no. 6, p. 951-956.

Zaruba, Q. (1952). Periglacial phenomena in the Turnov region, Sbornik Ustredniho Ustavu Geologickeo, vol. 19, p. 157-168.

Zaruba, Q. (1969). Landslides and their control, Elsevier, New York, and Academia, Prague, 205 pp.

APPENDIX A

GEOCHRONOLOGIC DATA



KRUEGER ENTERPRISES, INC.

GEOCHRON LABORATORIES DIVISION

24 BLACKSTONE STREET • CAMBRIDGE, MASSACHUSETTS 02139 • (617) 876-3691

RADIOCARBON AGE DETERMINATION

REPORT OF ANALYTICAL WORK

Our Sample No. GX- 12495

Date Received: 06-09-86

Your Reference: Letter of 05-31-86.

Date Reported: 09-30-86

Submitted by: Stephen Wilbur
401A Geophysical Institute
University of Alaska
Fairbanks, AK 99708

Sample Name: Sample 86C0t:1. Wood from palaeo-overbank silts near Healy, AK.

AGE = 1000 +/- 190 C-14 Years B.P. (C-13 corrected).

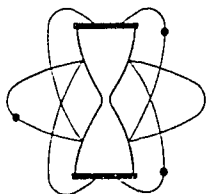
Description: Sample of wood.

Pretreatment: The wood was cleaned of dirt or other foreign material and was split into small pieces. It was then treated with hot dilute HCl to remove any carbonates and with hot dilute NaOH to remove humic acids and other organic contaminants. After washing and drying it was combusted to recover carbon dioxide for the analysis.

Comment:

$\delta^{13}\text{C}_{\text{PDB}} = -27.4 \text{ ‰}$

Notes: This date is based upon the Libby half life (5570 years) for ^{14}C . The error stated is $\pm 1\sigma$ as judged by the analytical data alone. Our modern standard is 95% of the activity of N.B.S. Oxalic Acid. The age is referenced to the year A.D. 1950.



KRUEGER ENTERPRISES, INC.

GEOCHRON LABORATORIES DIVISION

24 BLACKSTONE STREET • CAMBRIDGE, MASSACHUSETTS 02139 • (617) 876-3691

RADIOCARBON AGE DETERMINATION

REPORT OF ANALYTICAL WORK

Our Sample No. GX- 12496

Date Received: 06-09-86

Your Reference: Letter of 05-31-86.

Date Reported: 09-30-86

Submitted by: Stephen Wilbur
401A Geophysical Institute
University of Alaska
Fairbanks, AK 99708

Sample Name: Sample 86C0t:2. Wood from palaeo-overbank silts near Healy, AK.

AGE = 1045 +/- 70 C-14 Years B.P. (C-13 corrected).

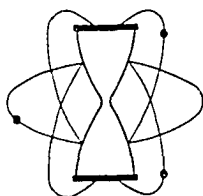
Description: Sample of wood.

Pretreatment: The wood was cleaned of dirt or other foreign material and was split into small pieces. It was then treated with hot dilute HCl to remove any carbonates and with hot dilute NaOH to remove humic acids and other organic contaminants. After washing and drying it was combusted to recover carbon dioxide for the analysis.

Comment:

$\delta^{13}\text{C}_{\text{PDB}} = -25.7 \text{ ‰}$

Notes: This date is based upon the Libby half life (5570 years) for ^{14}C . The error stated is $\pm 1\sigma$ as judged by the analytical data alone. Our modern standard is 95% of the activity of N.B.S. Oxalic Acid. The age is referenced to the year A.D. 1950.



KRUEGER ENTERPRISES, INC.

GEOCHRON LABORATORIES DIVISION

24 BLACKSTONE STREET • CAMBRIDGE, MASSACHUSETTS 02139 • (617) 876-3691

RADIOCARBON AGE DETERMINATION

REPORT OF ANALYTICAL WORK

Our Sample No. GX- 13066

Date Received: 01-22-87

Your Reference: Letter of 01-22-87.

Date Reported: 02-25-87

Submitted by: Stephen Wilbur
401A Geophysical Institute
University of Alaska
Fairbanks, AK 99708

Sample Name: 86 CVt:1.

AGE = 2465 +/- 80 C-14 Years B.P. (C-13 corrected).

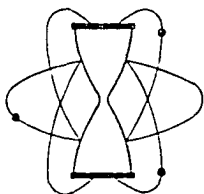
Description: Sample of wood.

Pretreatment: The wood was cleaned of dirt or other foreign material and was split into small pieces. It was then treated with hot dilute HCl to remove any carbonates and with hot dilute NaOH to remove humic acids and other organic contaminants. After washing and drying it was combusted to recover carbon dioxide for the analysis.

Comment:

$\delta^{13}\text{C}_{\text{PDB}} = -25.5 \text{ ‰}$

Notes: This date is based upon the Libby half life (5570 years) for ^{14}C . The error stated is $\pm 1\sigma$ as judged by the analytical data alone. Our modern standard is 95% of the activity of N.B.S. Oxalic Acid. The age is referenced to the year A.D. 1950.



KRUEGER ENTERPRISES, INC.

GEOCHRON LABORATORIES DIVISION

24 BLACKSTONE STREET • CAMBRIDGE, MASSACHUSETTS 02139 • (617) 876-3691

RADIOCARBON AGE DETERMINATION

REPORT OF ANALYTICAL WORK

Our Sample No. GX- 13067

Date Received: 01-28-87

Your Reference: Letter of 01-22-87.

Date Reported: 02-26-87

Submitted by: Stephen Wilbur
401A Geophysical Institute
University of Alaska
Fairbanks, AK 99708

Sample Name: 86 CVt:2.

AGE = 395 +/- 75 C-14 Years B.P. (C-13 corrected).

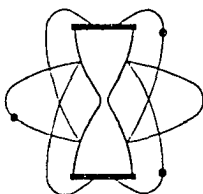
Description: Sample of wood.

Pretreatment: The wood was cleaned of dirt or other foreign material and was split into small pieces. It was then treated with hot dilute HCl to remove any carbonates and with hot dilute NaOH to remove humic acids and other organic contaminants. After washing and drying it was combusted to recover carbon dioxide for the analysis.

Comment:

$\delta^{13}\text{C}_{\text{PDB}} = -29.2 \text{ ‰}$

Notes: This date is based upon the Libby half life (5570 years) for ^{14}C . The error stated is $\pm 1\sigma$ as judged by the analytical data alone. Our modern standard is 95% of the activity of N.B.S. Oxalic Acid. The age is referenced to the year A.D. 1950.

**KRUEGER ENTERPRISES, INC.**

GEOCHRON LABORATORIES DIVISION

24 BLACKSTONE STREET • CAMBRIDGE, MASSACHUSETTS 02139 • (617) 876-3691

RADIOCARBON AGE DETERMINATION**REPORT OF ANALYTICAL WORK**

Our Sample No. GX- 13393

Date Received: 07-13-87

Your Reference: Sample submission form.

Date Reported: 08-12-87

Submitted by: Stephen Wilbur
401A Geophysical Institute
University of Alaska
Fairbanks, AK 99708

Sample Name: 87 CLF:1.

AGE = 1425 +/- 135 C-14 Years B.P. (C-13 corrected).

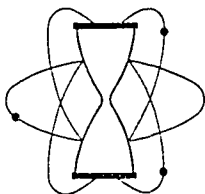
Description: Sample of wood.

Pretreatment: The wood was cleaned of dirt or other foreign material and was split into small pieces. It was then treated with hot dilute HCl to remove any carbonates and with hot dilute NaOH to remove humic acids and other organic contaminants. After washing and drying it was combusted to recover carbon dioxide for the analysis.

Comment:

 $\delta^{13}\text{C}_{\text{PDB}} = -25.6 \text{ ‰}$

Notes: This date is based upon the Libby half life (5570 years) for ^{14}C . The error stated is $\pm 1\sigma$ as judged by the analytical data alone. Our modern standard is 95% of the activity of N.B.S. Oxalic Acid.
The age is referenced to the year A.D. 1950.



KRUEGER ENTERPRISES, INC.

GEOCHRON LABORATORIES DIVISION

24 BLACKSTONE STREET • CAMBRIDGE, MASSACHUSETTS 02139 • (617) 876-3691

RADIOCARBON AGE DETERMINATION

REPORT OF ANALYTICAL WORK

Our Sample No. GX- 13394

Date Received: 07-13-87

Your Reference: Sample submission form.

Date Reported: 08-12-87

Submitted by: Stephen Wilbur
401A Geophysical Institute
University of Alaska
Fairbanks, AK 99708

Sample Name: 87 CLF:2.

AGE = 2170 +/- 140 C-14 Years B.P. (C-13 corrected).

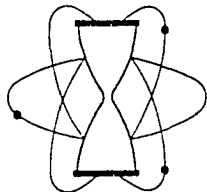
Description: Sample of wood.

Pretreatment: The wood was cleaned of dirt or other foreign material and was split into small pieces. It was then treated with hot dilute HCl to remove any carbonates and with hot dilute NaOH to remove humic acids and other organic contaminants. After washing and drying it was combusted to recover carbon dioxide for the analysis.

Comment:

$\delta^{13}\text{C}_{\text{PDB}} = -25.2 \text{ ‰}$

Notes: This date is based upon the Libby half life (5570 years) for ^{14}C . The error stated is $\pm 1\sigma$ as judged by the analytical data alone. Our modern standard is 95% of the activity of N.B.S. Oxalic Acid. The age is referenced to the year A.D. 1950.

**KRUEGER ENTERPRISES, INC.**

GEOCHRON LABORATORIES DIVISION

24 BLACKSTONE STREET • CAMBRIDGE, MASSACHUSETTS 02139 • (617) 876-3691

RADIOCARBON AGE DETERMINATION**REPORT OF ANALYTICAL WORK**

Our Sample No. GX- 13396

Date Received: 07-13-87

Your Reference: Sample submission form.

Date Reported: 08-12-87

Submitted by: Stephen Wilbur
401A Geophysical Institute
University of Alaska
Fairbanks, AK 99708

Sample Name: 87 CB2.

AGE = 620 +/- 95 C-14 Years B.P. (C-13 corrected).

Description: Sample of wood.

Pretreatment: The wood was cleaned of dirt or other foreign material and was split into small pieces. It was then treated with hot dilute HCl to remove any carbonates and with hot dilute NaOH to remove humic acids and other organic contaminants. After washing and drying it was combusted to recover carbon dioxide for the analysis.

Comment:

 $\delta^{13}\text{C}_{\text{PDB}} = -25.1 \text{ ‰}$

Notes: This date is based upon the Libby half life (5570 years) for ^{14}C . The error stated is $\pm 1\sigma$ as judged by the analytical data alone. Our modern standard is 95% of the activity of N.B.S. Oxalic Acid. The age is referenced to the year A.D. 1950.



ALPHA ANALYTIC INC.

(305) 667-5167

UNIVERSITY BRANCH

P.O. BOX 248113

CORAL GABLES, FLA. 33124

REPORT OF THERMOLUMINESCENCE DATING ANALYSES

FOR: Dr. Stephen Wilbur DATE RECEIVED: June 18, 1986
Usibelli Coal Mine, Inc. DATE REPORTED: August 12, 1986
Healy, Alaska

OUR LAB NUMBER	SUBMITTED SAMPLE I.D.	SAMPLE MATERIAL	TL age years B.P.
----------------	-----------------------	-----------------	-------------------

Alpha-3041	86TML:1	Lacustrine silts	> 63,800 +/- 10,500 *
			< 242,500 +/- 43,500 *

U = 6.5 ppm; Th = 18.7 ppm; K₂O = 2.71 %

* Sample exhibiting trap saturation. Greater-than age calculated from Regen technique, less-than age calculated from Residual technique. Data from R-beta technique unsuitable.

The above sediment was submitted for thermoluminescence dating on the individual basis. The 4 to 11 micron polymineralic fraction was separated for multiple glow analyses by the fine-grain technique using internal crosscheck dating methods: R-Beta, Residual, Regen. Mineral sensitivity & ED was determined by calibrated alpha & beta irradiations from Am-241 & Sr-90 sources. U, Th & K contents were measured by thick-source alpha counting & atomic absorption. Water content was estimated as 75% of lab measured saturation. Cosmic dose was taken as 0.014 rads/year.



ALPHA ANALYTIC INC.

(305) 667-5167

UNIVERSITY BRANCH

P.O. BOX 248113

CORAL GABLES, FLA. 33124

REPORT OF THERMOLUMINESCENCE DATING ANALYSES

FOR: Dr. Stephen Wilbur DATE RECEIVED: August 6, 1986
Geology Dept., UAF DATE REPORTED: September 28, 1986
Fairbanks, Alaska

OUR LAB NUMBER	SUBMITTED SAMPLE I.D.	SAMPLE MATERIAL	TL Age (years BP)
----------------	-----------------------	-----------------	-------------------

Alpha-3071	86-TFR:10	Sediment	205,000 +/- 28,000*
------------	-----------	----------	---------------------

*Sample TL characteristics represent multiple age components. The date represents an average age.

The above sample was submitted for thermoluminescence dating analysis on the individual sediment basis. The 4 to 11 micron particle size fraction was separated for multiple glow analysis by the fine-grain technique using the 3 dating methods: Regen, Residual, & R-Beta. Mineral sensitivity & ED were determined by Sr-90 beta irradiations. U, Th, & K contents were measured by thick source alpha counting and atomic absorption. Representative water content was taken as 75% of the laboratory measured saturation value. Cosmic dose was taken as 0.014 rads/yr.

A-10

APPENDIX B

LANDSLIDE DATA

LANDSLIDE I

Date	Jul.Day (day)	Time (days)	LI-1			LI-2		
			Easting (ft)	Northing (ft)	Elevation (ft)	Easting (ft)	Northing (ft)	Elevation (ft)
8/19/85	231	19	354.80	742.33	1657.38	356.09	705.20	1662.72
7/18/86	199	352	349.60	753.00	1656.46	352.10	719.40	1660.74
4/5/87	95	613	349.60	753.00	1656.46	352.10	719.40	1660.74
8/31/87	243	761	349.46	753.70	1654.92	351.09	722.02	1659.55
5/1/88	122	1005	349.24	754.02	1655.61	350.79	722.38	1659.51
10/8/88	282	1165	348.97	754.50	1655.66	350.45	723.12	1659.40
			Horiz. Dis.		Vert. Dis.	Horiz. Dis.		Vert. Dis.
			11.87		-0.92	14.75		-1.98
			0.00		0.00	0.00		0.00
			0.71	0.060	-1.54	2.81	0.190	-1.19
			0.39		0.69	0.47		-0.04
			0.55		0.05	0.81		-0.11
			Cum HD		Cum VD	Cum HD		Cum VD
0.79	11.87	0.88	-0.92			14.75	0.79	-1.98
0.00	11.87	0.00	-0.92			14.75	0.00	-1.98
0.11	12.56	0.05	-2.46			17.55	0.15	-3.17
0.02	12.94	0.03	-1.77			17.98	0.02	-3.21
0.08	13.49	0.04	-1.72			18.79	0.04	-3.32
			HD Rate		VD Rate	HD Rate		VD Rate
			13.01		-1.01	16.17		-2.17
			0.00		0.00	0.00		0.00
			1.76		-3.80	6.92		-2.93
			0.53		1.03	0.70		-0.06
			1.26		0.11	1.86		-0.25
			CHD Rate		CVD Rate	CHD Rate		CVD Rate
333	13.01	-1.01	16.17			-2.17		
594	7.29	-0.57	9.06			-1.22		
742	6.18	-1.21	8.63			-1.56		
986	4.79	-0.66	6.66			-1.19		
1146	4.30	-0.55	5.98			-1.06		
			-2.09			-3.18		
			N25.6W			N17.4W		

LANDSLIDE I (cont.)

LI-3			LI-4A			LI-4B		
Easting (ft)	Northing (ft)	Elevation (ft)	Easting (ft)	Northing (ft)	Elevation (ft)	Easting (ft)	Northing (ft)	Elevation (ft)
422.52	704.42	1668.78	413.33	751.99	1659.40			
428.33	725.53	1665.71	418.08	771.49	1657.42			
428.33	725.53	1665.71	418.08	771.49	1657.42			
429.66	729.39	1664.53	lost	lost	lost	416.54	770.91	1656.42
429.87	729.87	1664.07				416.69	771.43	1657.27
430.24	731.14	1664.20				424.06	790.27	1642.54
Horiz. Dis.		Vert. Dis.	Horiz. Dis.		Vert. Dis.	Horiz. Dis.		Vert. Dis.
21.89		-3.07	20.07		-1.98			
0.00		0.00	0.00		0.00			
4.08	0.186	-1.18	3.81	0.19		new		new
0.52		-0.46	0.57			0.63		0.85
1.32		0.13	1.50			20.16		-14.73
Cum HD		Cum VD	Cum HD		Cum VD	Cum HD		Cum VD
21.89	0.79	-3.07	20.07	0.77	-1.98			
21.89	0.00	-3.07	20.07	0.00	-1.98			
25.97	0.15	-4.25	23.88	0.15		new		new
26.49	0.02	-4.71	24.45	0.02		0.63		0.85
27.81	0.05	-4.58	25.95	0.06		20.77		-13.88
HD Rate		VD Rate	HD Rate		VD Rate	HD Rate		VD Rate
24.00		-3.37	22.00		-2.17			
0.00		0.00	0.00		0.00			
10.07		-2.91				new		new
0.78		-0.69				0.94		1.27
3.02		0.30				45.99		-33.60
CHD Rate		CVD Rate	CHD Rate		CVD Rate	CHD Rate		CVD Rate
24.00		-3.37	22.00		-2.17			
13.45		-1.89	12.33		-1.22			
12.78		-2.09				new		new
9.81		-1.74				0.23		0.31
8.86		-1.46				6.61		-4.42
3.46			4.11			2.57		
N16.1E			N13.7E			N21.3E		

LANDSLIDE I (cont.)

LI-4C			LI-5A			LI-5B		
Easting (ft)	Northing (ft)	Elevation (ft)	Easting (ft)	Northing (ft)	Elevation (ft)	Easting (ft)	Northing (ft)	Elevation (ft)
			386.90	776.96	1654.98			
			387.77	788.92	1653.19			
			387.77	788.92	1653.19			
414.79	761.19	1659.42	lost	lost	lost	386.87	789.91	1650.85
415.01	761.65	1659.27				387.01	790.30	1651.17
415.29	763.12	1658.99				388.12	795.98	1646.21
Horiz. Dis.		Vert. Dis.	Horiz. Dis.		Vert. Dis.	Horiz. Dis.		Vert. Dis.
			11.99		-1.79			
			0.00		0.00			
new		new	0.72	0.06		new		new
0.51		-0.15	0.43			0.41		0.32
1.50		-0.28	3.36			5.79		-4.96
Cum HD		Cum VD	Cum HD		Cum VD	Cum HD		Cum VD
			11.99	0.73	-1.79			
			11.99	0.00	-1.79			
new		new	12.71	0.04		new		new
0.51		-0.15	13.14	0.03		0.41		0.32
1.99		-0.43	16.51	0.20		6.20		-4.64
HD Rate		VD Rate	HD Rate		VD Rate	HD Rate		VD Rate
			13.14		-1.96			
			0.00		0.00			
new		new				new		new
0.76		-0.22				0.62		0.48
3.41		-0.64				13.20		-11.32
CHD Rate		CVD Rate	CHD Rate		CVD Rate	CHD Rate		CVD Rate
			13.14		-1.96			
			7.37		-1.10			
new		new				new		new
0.19		-0.06				0.15		0.12
0.63		-0.14				1.97		-1.48
3.86			13.75			4.86		
N14.5E			N4.2E			N11.6E		

LANDSLIDE I (cont.)

LI-5C			LI-6			LI-7		
Easting (ft)	Northing (ft)	Elevation (ft)	Easting (ft)	Northing (ft)	Elevation (ft)	Easting (ft)	Northing (ft)	Elevation (ft)
			354.20	793.09	1651.31	533.79	430.23	1751.43
			354.20	793.09	1651.31	533.79	430.23	1751.43
389.62	780.54	1656.18	354.13	794.99	1650.41	532.60	430.86	1750.05
389.71	780.98	1656.07	353.95	795.11	1650.51	530.61	431.44	1747.51
389.73	781.92	1655.99	354.26	796.24	1650.12	NM	NM	NM
Horiz. Dis.		Vert. Dis.	Horiz. Dis.		Vert. Dis.	Horiz. Dis.		Vert. Dis.
			new		new	new		new
			0.00		0.00	0.00		0.00
new		new	1.90		-0.90	1.35		-1.38
0.45		-0.11	0.22		0.10	2.07		-2.54
0.94		-0.08	1.17		-0.39			
Cum HD		Cum VD	Cum HD		Cum VD	Cum HD		Cum VD
			new		new	new		new
			0.00	0.00	0.00	0.00		0.00
new		new	1.90	0.60	-0.90	1.35		-1.38
0.45		-0.11	2.04	0.04	-0.80	3.40		-3.92
1.38		-0.19	3.15	0.35	-1.19			
HD Rate		VD Rate	HD Rate		VD Rate	HD Rate		VD Rate
			new		new	new		new
			0.00		0.00	0.00		0.00
new		new	4.69		-2.22	3.32		-3.40
0.67		-0.16	0.32		0.15	3.10		-3.80
2.14		-0.18	2.67		-0.89			
CHD Rate		CVD Rate	CHD Rate		CVD Rate	CHD Rate		CVD Rate
			new		new	new		new
			0.00		0.00	0.00		0.00
new		new	0.94		-0.44	0.66		-0.68
0.17		-0.04	0.75		-0.30	1.26		-1.45
0.44		-0.06	1.00		-0.38			
12.55			52.50			-0.38		
N4.6E			N1.1E			N69.2W		

LANDSLIDE I (cont.)

LI-8			LI-16			LI-17		
Easting (ft)	Northing (ft)	Elevation (ft)	Easting (ft)	Northing (ft)	Elevation (ft)	Easting (ft)	Northing (ft)	Elevation (ft)
512.29	346.75	1773.24	443.11	652.43	1679.51	444.90	622.32	1686.11
512.29	346.75	1773.24	443.11	652.43	1679.51	444.90	622.32	1686.11
512.19	347.42	1772.70	443.49	656.86	1667.84	444.53	627.19	1685.16
512.00	347.98	1772.61	443.69	657.62	1677.47	444.57	628.11	1684.87
NM	NM	NM	443.75	659.69	1677.15	444.32	630.56	1684.76
Horiz. Dis.		Vert. Dis.	Horiz. Dis.		Vert. Dis.	Horiz. Dis.		Vert. Dis.
new		new	new		new	new		new
0.00		0.00	0.00		0.00	0.00		0.00
0.68		-0.54	4.45		-11.67	4.88		-0.95
0.59		-0.09	0.79		9.63	0.92		-0.29
			2.07		-0.32	2.46		-0.11
Cum HD		Cum VD	Cum HD		Cum VD	Cum HD		Cum VD
new		new	new		new	new		new
0.00		0.00	0.00	0.00	0.00	0.00	0.00	0.00
0.68		-0.54	4.45	0.61	-11.67	4.88	0.59	-0.95
1.26		-0.63	5.22	0.11	-2.04	5.80	0.11	-1.24
			7.29	0.28	-2.36	8.26	0.30	-1.35
HD Rate		VD Rate	HD Rate		VD Rate	HD Rate		VD Rate
new		new	new		new	new		new
0.00		0.00	0.00		0.00	0.00		0.00
1.67		-1.33	10.97		-28.78	12.05		-2.34
0.88		-0.13	1.18		14.41	1.38		-0.43
			4.72		-0.73	5.62		-0.25
CHD Rate		CVD Rate	CHD Rate		CVD Rate	CHD Rate		CVD Rate
new		new	new		new	new		new
0.00		0.00	0.00		0.00	0.00		0.00
0.33		-0.27	2.19		-5.74	2.40		-0.47
0.47		-0.23	1.93		-0.76	2.15		-0.46
			2.32		-0.75	2.63		-0.43
-4.24 N13.3W			11.34 N5.0E			-14.21 N4.0W		

LANDSLIDE I (cont.)

LI-18			Tree-1			Tree-2		
Easting (ft)	Northing (ft)	Elevation (ft)	Easting (ft)	Northing (ft)	Elevation (ft)	Easting (ft)	Northing (ft)	Elevation (ft)
448.18	578.14	1693.14						
448.22	579.22	1692.91	459.05	503.35	1707.77	461.45	428.49	1724.77
447.50	582.43	1692.40	456.59	508.30	1706.13	458.65	435.38	1723.59
Horiz. Dis.		Vert. Dis.	Horiz. Dis.		Vert. Dis.	Horiz. Dis.		Vert. Dis.
new		new						
1.08		-0.23	new		new	new		new
3.29		-0.51	5.53		-1.64	7.44		-1.18
Cum HD		Cum VD	Cum HD		Cum VD	Cum HD		Cum VD
new		new						
1.08		-0.23	new		new	new		new
4.34		-0.74	5.53		-1.64	7.44		-1.18
HD Rate		VD Rate	HD Rate		VD Rate	HD Rate		VD Rate
new		new						
1.62		-0.34	new		new	new		new
7.50		-1.16	12.61		-3.74	16.97		-2.69
CHD Rate		CVD Rate	CHD Rate		CVD Rate	CHD Rate		CVD Rate
new		new						
0.40		-0.09	new		new	new		new
1.38		-0.24	1.76		-0.52	2.37		-0.38
-6.31			-2.01			-2.46		
N9.0W			N26.4W			N22.1W		

LANDSLIDE I (cont.)

Tree-3		
Easting (ft)	Northing (ft)	Elevation (ft)
491.09	406.15	1731.57
488.57	412.95	1730.02
Horiz. Dis.		Vert. Dis.
new		new
7.25		-1.55
Cum HD		Cum VD
new		new
7.25		-1.55
HD Rate		VD Rate
new		new
16.54		-3.54
CHD Rate		CVD Rate
new		new
2.31		-0.49
-2.70		
N20.3W		

LANDSLIDE II

Date	Jul. Day (day)	Time (days)	LII-1			LII-2		
			Easting (ft)	Northing (ft)	Elevation (ft)	Easting (ft)	Northing (ft)	Elevation (ft)
8/19/85	231	19	175.25	498.61	1702.85	193.35	447.54	1717.31
8/6/86	218	371	174.98	500.84	1704.17	193.09	449.97	1717.97
6/28/87	179	697	174.91	502.18	1703.96	192.95	451.36	1717.52
10/12/87	285	803	174.94	502.55	1704.09	193.08	451.83	1717.45
5/1/88	121	1004	174.89	503.26	1703.49	193.05	452.58	1716.49
9/4/88	247	1130	174.82	503.95	1704.28	192.90	453.23	1717.33
			Horiz. Dis.		Vert. Dis.	Horiz. Dis.		Vert. Dis.
			2.25		1.32	2.44		0.66
			1.34		-0.21	1.40		-0.45
			0.37		0.13	0.49		-0.07
			0.71		-0.60	0.75		-0.96
			0.69		0.79	0.67		0.84
			Cum HD		Cum VD	Cum HD		Cum VD
			2.25		1.32	2.44		0.66
			3.59		1.11	3.84		0.21
			3.95		1.24	4.30		0.14
			4.66		0.64	5.05		-0.32
			5.36		1.43	5.71		0.02
			HD Rate		VD Rate	HD Rate		VD Rate
			2.33		1.37	2.53		0.68
			1.50		-0.24	1.56		-0.50
			1.28		0.45	1.68		-0.24
			1.29		-1.09	1.36		-1.74
			2.01		2.29	1.93		2.43
			CHD Rate		CVD Rate	CHD Rate		CVD Rate
352			2.33		1.37	2.53		0.68
678			1.93		0.60	2.07		0.11
784			1.84		0.58	2.00		0.07
985			1.73		0.24	1.87		-0.30
1111			1.76		0.47	1.88		0.01
					-0.08			-0.08
			N6W		4.57	NW		
					-4.60			-4.52

LANDSLIDE II (cont.)

LII-3			LII-4			LII-5		
Easting (ft)	Northing (ft)	Elevation (ft)	Easting (ft)	Northing (ft)	Elevation (ft)	Easting (ft)	Northing (ft)	Elevation (ft)
41.04	65.78	1710.88	989.15	411.54	1720.14	629.47	485.58	1709.31
40.33	68.00	1710.62	988.64	413.25	1720.19	629.54	486.65	1709.58
39.16	69.74	1710.03	988.42	414.25	1720.09	629.72	488.00	1709.41
39.49	71.37	1709.63	987.86	414.08	1720.29	629.51	488.37	1709.61
39.30	72.20	1708.79	988.21	415.96	1719.33	629.59	487.09	1708.59
34.99	85.14	1698.71	987.28	414.34	1720.33	629.33	488.67	1709.41
Horiz. Dis.		Vert. Dis.	Horiz. Dis.		Vert. Dis.	Horiz. Dis.		Vert. Dis.
2.33		-0.26	1.78		0.05	1.07		-0.23
2.10		-0.59	1.02		-0.10	1.36		-0.17
1.66		-0.40	0.59		0.20	0.43		0.20
0.85		-0.84	NA		NA	NA		NA
13.64		-10.08	0.64		0.04	0.35		-0.20
Cum HD		Cum VD	Cum HD		Cum VD	Cum HD		Cum VD
2.33		-0.26	1.78		0.05	1.07		-0.23
4.38		-0.85	2.81		-0.05	2.43		-0.40
5.80		-1.25	2.85		0.15	2.79		-0.20
6.65		-2.09	NA		NA	NA		NA
20.28		-12.17	3.37		0.19	3.09		-0.40
HD Rate		VD Rate	HD Rate		VD Rate	HD Rate		VD Rate
2.42		-0.27	1.85		0.05	1.11		-0.24
2.35		-0.66	1.15		-0.11	1.52		-0.19
5.73		-1.38	2.02		0.69	1.46		0.69
1.55		-1.53	NA		NA	NA		NA
39.51		-29.20	0.71		0.04	0.39		-0.22
CHD Rate		CVD Rate	CHD Rate		CVD Rate	CHD Rate		CVD Rate
2.42		-0.27	1.85		0.05	1.11		-0.24
2.36		-0.46	1.51		-0.03	1.31		-0.22
2.70		-0.58	1.33		0.07	1.30		-0.09
2.46		-0.77	NA		NA	NA		NA
6.66		-4.00	1.11		0.06	1.02		-0.13
-0.31			-0.67			-0.05		
NW			NW			NW		
-17.35			33.80			2.86		
			-33.74			-2.59		

LANDSLIDE II (cont.)

LII-6			LII-7			LII-8		
Easting (ft)	Northing (ft)	Elevation (ft)	Easting (ft)	Northing (ft)	Elevation (ft)	Easting (ft)	Northing (ft)	Elevation (ft)
495.00	506.10	1730.22						
495.15	NA	1729.81	584.73	492.97	1718.31	755.59	492.62	1697.59
495.28	508.64	1729.42	584.01	493.89	1718.12	755.86	493.75	1697.35
495.25	509.30	1729.53	584.34	494.84	1718.25	755.75	493.80	1697.51
NM		NM	584.56	493.09	1716.99	755.76	493.46	1696.53
495.13	509.74	1729.50	584.24	495.16	1718.00	NM	NM	1697.44
Horiz. Dis.		Vert. Dis.	Horiz. Dis.		Vert. Dis.	Horiz. Dis.		Vert. Dis.
NA		-0.41	new		new	new		new
2.56		-0.39	1.17		-0.19	1.16		-0.24
0.66		0.11	1.01		0.13	0.12		0.16
NA		NA	NA		NA	NA		NA
0.46		-0.03	0.34		-0.25	NM		-0.07
Cum HD		Cum VD	Cum HD		Cum VD	Cum HD		Cum VD
NA		-0.41	new		new	new		new
2.56		-0.80	1.17		-0.19	1.16		-0.24
3.21		-0.69	1.91		-0.06	1.19		-0.08
NM		NM	NA		NA	NA		NA
3.64		-0.72	2.24		-0.31	NM		-0.15
HD Rate		VD Rate	HD Rate		VD Rate	HD Rate		VD Rate
NA		-0.43	new		new	new		new
2.86		-0.44	1.31		-0.21	1.30		-0.27
2.27		0.38	3.46		0.45	0.42		0.55
NA		NA	NA		NA	NA		NA
0.51		-0.03	0.37		-0.28	NM		-0.20
CHD Rate		CVD Rate	CHD Rate		CVD Rate	CHD Rate		CVD Rate
NA		-0.43	new		new	new		new
1.38		-0.43	0.63		-0.10	0.63		-0.13
1.49		-0.32	0.89		-0.03	0.55		-0.04
NM		NM	NA		NA	NA		NA
1.20		-0.24	0.74		-0.10	NM		-0.05
0.04			-0.22			0.14		
NE		2.29	NW		12.41	NE		11.31
2.05			-12.61			7.72		

LANDSLIDE II (cont.)

LII-9			LII-10			LII-11		
Easting (ft)	Northing (ft)	Elevation (ft)	Easting (ft)	Northing (ft)	Elevation (ft)	Easting (ft)	Northing (ft)	Elevation (ft)
mu								
7046.84	453.74	1713.70	217.94	469.62	1713.02	265.85	476.55	1712.89
7046.71	454.56	1712.73	218.13	470.01	1712.10	265.95	476.79	1712.70
7046.12	452.80	1713.79	218.11	470.71	1712.09	266.01	477.38	1711.79
			218.05	471.56	1712.61	265.94	478.01	1712.52
Horiz. Dis.		Vert. Dis.	Horiz. Dis.		Vert. Dis.	Horiz. Dis.		Vert. Dis.
new		new	new		new	new		new
mu		mu	0.43		-0.92	0.26		-0.19
0.83		-0.97	0.70		-0.01	0.59		-0.91
1.86		1.06	0.85		0.52	0.63		0.73
Cum HD		Cum VD	Cum HD		Cum VD	Cum HD		Cum VD
new		new	new		new	new		new
mu		mu	0.43		-0.92	0.26		-0.19
0.83		-0.97	1.10		-0.93	0.85		-1.10
1.18		0.09	1.94		-0.41	1.46		-0.37
HD Rate		VD Rate	HD Rate		VD Rate	HD Rate		VD Rate
new		new	new		new	new		new
mu		mu	1.49		-3.17	0.90		-0.65
1.51		-1.76	1.27		-0.02	1.08		-1.65
5.38		3.07	2.47		1.51	1.84		2.11
CHD Rate		CVD Rate	CHD Rate		CVD Rate	CHD Rate		CVD Rate
new		new	new		new	new		new
mu		mu	0.20		-0.43	0.12		-0.09
0.31		-0.36	0.41		-0.34	0.31		-0.41
0.39		0.03	0.64		-0.13	0.48		-0.12
		0.77			0.06			0.06
SW		37.60	NE			NE		
		37.45			3.25			3.53

LANDSLIDE III

Date	Jul.Day (day)	Time (days)	LIII-1			LIII-2		
			Easting (ft)	Northing (ft)	Elevation (ft)	Easting (ft)	Northing (ft)	Elevation (ft)
8/19/85	231	19	763.58	376.08	1723.71	647.55	397.86	1721.33
8/6/86	218	371	763.99	378.06	1723.38	648.34	401.10	1720.63
6/29/87	180	698	764.05	378.16	1723.47	647.73	400.74	1720.72
10/12/87	285	803	764.10	378.46	1723.49	648.17	400.15	1720.79
7/3/88	185	1068	764.24	379.05	1723.26	648.32	400.48	1720.70
10/10/88	284	1167			1722.98			1720.54

Horiz. Dis.		Vert. Dis.		Horiz. Dis.		Vert. Dis.	
NA		NA		NA		NA	
2.13		-0.24		2.89		-0.61	
0.30		0.02		0.74		0.07	
0.61		-0.23		0.36		-0.09	
0.14		-0.28		0.24		-0.16	

Cum HD		Cum VD		Cum HD		Cum VD	
NA		NA		NA		NA	
2.13		-0.24		2.89		-0.61	
2.44		-0.22		2.37		-0.54	
3.04		-0.45		2.73		-0.63	
3.18		-0.73		2.97		-0.79	

HD Rate		VD Rate		HD Rate		VD Rate	
NA		NA		NA		NA	
2.38		-0.27		3.22		-0.68	
1.06		0.07		2.56		0.24	
0.94		-0.32		0.50		-0.12	
0.52		-1.03		0.88		-0.59	

CHD Rate		CVD Rate		CHD Rate		CVD Rate	
NA		NA		NA		NA	
1.15		-0.13		1.55		-0.33	
1.13		-0.10		1.10		-0.25	
1.06		-0.16		0.95		-0.22	
1.01		-0.23		0.94		-0.25	

		0.22		0.29
beta1		12.52881		16.37770
beta2=gamma3		12.37080		49.08610
B		24.89961		32.70840
Hangle1-Ha gamma1 = C		0.04330		0.05555
hor dis (a)		75.40		133.54
A		155.0571		147.2360
c		0.14		0.24
gamma1				
sinC		0.00076		0.00097
sinA		0.42172	24.94	0.54118

LANDSLIDE III (cont.)

LIII-3			LIII-4			LIII-5		
Easting (ft)	Northing (ft)	Elevation (ft)	Easting (ft)	Northing (ft)	Elevation (ft)	Easting (ft)	Northing (ft)	Elevation (ft)
604.53	434.82	1715.19	446.92	429.75	1725.91	330.18	475.57	1721.78
605.40	435.93	1714.90	447.95	435.59	1725.08	331.73	482.30	1720.87
603.56	436.82	1714.94	447.53	430.20	1725.12	330.65	477.17	1721.11
604.83	437.24	1714.96	447.42	431.82	1724.51	330.70	477.27	1721.30
604.96	437.60	1714.78	447.58	431.89	1725.04	330.85	477.50	1721.22
	1714.70			1724.92			1720.92	

Horiz. Dis.		Vert. Dis.		Horiz. Dis.		Vert. Dis.		Horiz. Dis.		Vert. Dis.	
NA	NA	NA	NA	NA	NA	NA	NA	NA	NA	NA	NA
2.22	-0.25	0.76	-0.79	1.67	-0.67	2.44	-0.23	2.13	-1.40	1.78	-0.48
1.34	0.02	1.62	-0.61	0.11	0.19	2.81	-0.41	2.24	-0.87	2.04	-0.56
0.38	-0.18	0.17	0.53	0.27	-0.08	3.10	-0.49	2.55	-0.99	2.39	-0.86
0.29	-0.08	0.31	-0.12	0.35	-0.30						
Cum HD	Cum VD	Cum HD	Cum VD	Cum HD	Cum VD						
NA	NA	NA	NA	NA	NA						
2.22	-0.25	0.76	-0.79	1.67	-0.67						
2.44	-0.23	2.13	-1.40	1.78	-0.48						
2.81	-0.41	2.24	-0.87	2.04	-0.56						
3.10	-0.49	2.55	-0.99	2.39	-0.86						
HD Rate	VD Rate	HD Rate	VD Rate	HD Rate	VD Rate						
NA	NA	NA	NA	NA	NA						
2.48	-0.28	0.85	-0.88	1.86	-0.75						
4.65	0.07	5.64	-2.12	0.39	0.66						
0.53	-0.25	0.24	0.73	0.38	-0.11						
1.07	-0.29	1.14	-0.44	1.29	-1.11						
CHD Rate	CVD Rate	CHD Rate	CVD Rate	CHD Rate	CVD Rate						
NA	NA	NA	NA	NA	NA						
1.19	-0.13	0.41	-0.42	0.90	-0.36						
1.14	-0.11	0.99	-0.65	0.83	-0.22						
0.98	-0.14	0.78	-0.30	0.71	-0.19						
0.99	-0.16	0.81	-0.31	0.76	-0.27						

0.15	0.31	0.35
8.79262	17.14035	19.14446
67.08060	68.84860	75.83190
58.28798	51.70825	56.68744
0.03444	0.00139	0.02888
166.46	323.78	440.36
121.6276	128.2904	123.2837
0.29	0.01	0.27
0.00147	0.00002	0.00050
0.85	0.78	0.84

LANDSLIDE III (cont.)

LIII-6		
Easting (ft)	Northing (ft)	Elevation (ft)
293.73	523.10	1714.28
295.56	529.41	1713.63
293.96	523.77	1713.70
294.14	523.86	1713.72
294.25	524.06	1713.56
		1713.41

Horiz. Dis.	Vert. Dis.
NA	NA
0.71	-0.58
0.20	0.02
0.23	-0.16
0.54	-0.15

Cum HD	Cum VD
NA	NA
0.71	-0.58
0.86	-0.56
1.09	-0.72
1.63	-0.87

HD Rate	VD Rate
NA	NA
0.79	-0.65
0.70	0.07
0.31	-0.22
1.99	-0.55

CHD Rate	CVD Rate
NA	NA
0.38	-0.31
0.40	-0.26
0.38	-0.25
0.52	-0.28

0.54
 28.44293
 81.14310
 52.70017
 0.01917
 481.44
 127.2807
 0.20

 0.00033
 0.80

LANDSLIDE IV

Date	Jul.Day (day)	Time (days)	LIV-1			LIV-2		
			Easting (ft)	Northing (ft)	Elevation (ft)	Easting (ft)	Northing (ft)	Elevation (ft)
8/20/85	232	20	497.88	116.01	2324.79	557.10	191.32	2325.38
7/31/86	212	365	495.70	120.19	2323.93	505.06	275.84	2306.61
5/15/87	135	653	493.95	122.65	2323.79	495.38	291.95	2302.55
7/10/87	191	709	493.95	122.65	2323.79	495.38	291.95	2302.55
9/1/87	244	762	494.14	122.08	2323.50	NM		NM
10/13/87	286	804	494.06	122.44	2323.74	488.89	300.33	2300.57
4/4/88	95	978	494.06	122.20	2323.77	488.65	300.51	2300.51
5/2/88	123	1006	NM		NM	NM		NM
6/5/88	157	1040	NM		NM	NM		NM
9/1/88	245	1128	494.05	122.84	2323.84	462.56	334.81	2295.05
10/9/88	283	1166	493.80	122.10	2323.79	451.19	346.53	2292.41
			Horiz. Dis.		Vert. Dis.	Horiz. Dis.		Vert. Dis.
345			4.71	0.45	-0.86	99.26	0.53	-18.77
633			3.02	0.29	-0.14	18.79	0.10	-4.06
689			0.00	0.00	0.00	0.00	0.00	0.00
742			0.60	0.06	-0.29	NM	NM	NM
784			0.37	0.04	0.24	10.60	0.06	-1.98
958			0.24	0.02	0.03	0.30	0.00	-0.06
986			NM	NM	NM	NM	NM	NM
1020			NM	NM	NM	NM	NM	NM
1108			0.64	0.06	0.07	43.09	0.23	-5.46
1146			0.78	0.08	-0.05	16.33	0.09	-2.64
				1.00			1.00	
			Cum HD		Cum VD	Cum HD		Cum VD
345			4.71	0.64	-0.86	99.26	0.53	-18.77
633			7.72	0.41	-1.00	118.05	0.10	-22.83
689			7.72	0.00	-1.00	118.05	0.00	-22.83
742			7.13	-0.08	-1.29	NM	NM	NM
784			7.48	0.05	-1.05	128.59	0.05610	-24.81
958			7.27	-0.03	-1.02	128.87	0.00	-24.87
986			NM	NM	NM	NM	NM	NM
1020			NM	NM	NM	NM	NM	NM
1108			7.83	0.08	-0.95	171.83	0.23	-30.33
1146			7.33	-0.07	-1.00	187.90	0.09	-32.97
			2.23	1.00	-0.30	57.29	1.00	-10.05
			HD Rate		VD Rate	HD Rate		VD Rate
			4.99		-0.91	105.01		-19.86
			3.83		-0.18	23.82		-5.15
			0.00		0.00	0.00		0.00
			4.14		-2.00	NM		NM
			3.20		2.09	92.11		-17.21
			0.50		0.06	0.63		-0.13
			NM		NM	NM		NM
			NM		NM	NM		NM
			2.65		0.25	178.75		-22.65

	7.50	-0.48	156.84	-25.36
	CHD Rate	CVD Rate	CHD Rate	CVD Rate
345	4.99	-0.91	105.01	-19.86
633	4.45	-0.58	68.07	-13.16
689	4.09	-0.53	62.54	-12.09
742	3.51	-0.63	NM	NM
784	3.48	-0.49	59.87	-11.55
958	2.77	-0.39	49.10	-9.48
986	NM	NM	NM	NM
1020	NM	NM	NM	NM
1108	2.58	-0.31	56.61	-9.99
1146	2.33	-0.32	59.85	-10.50
	0.71	-0.10	18.25	-3.20
		-0.67		-0.68
		-33.82		-34.31

LANDSLIDE IV (cont.)

LIV-3			LIV-4			LIV-5		
Easting (ft)	Northing (ft)	Elevation (ft)	Easting (ft)	Northing (ft)	Elevation (ft)	Easting (ft)	Northing (ft)	Elevation (ft)
635.88	253.29	2325.27	438.79	402.52	2287.59	5077.75	695.39	2235.84
526.93	413.89	2292.50	330.02	487.55	2265.76	5035.53	726.17	2232.03
522.31	419.64	2292.31	328.48	488.45	2265.60	5034.98	726.10	2232.15
522.31	419.64	2292.31	328.48	488.45	2265.60	5034.98	726.10	2232.15
NM		NM	NM		NM	NM		NM
519.08	424.74	2292.44	327.78	488.70	2265.57	5034.90	726.13	2231.92
518.61	424.58	2292.41	NM		NM	NM		NM
NM		NM	NM		NM	NM		NM
NM		NM	NM		NM	5034.19	725.33	2231.53
504.50	448.87	2289.83	321.98	492.11	2265.12	5034.31	726.41	2232.01
503.26	449.49	2289.78	NM		NM	5032.94	724.85	2232.09
Horiz. Dis.		Vert. Dis.	Horiz. Dis.		Vert. Dis.	Horiz. Dis.		Vert. Dis.
194.07	0.82	-32.77	138.06	0.94	-21.83	52.25	0.91	-3.81
7.38	0.03	-0.19	1.78	0.01	-0.16	0.55	0.01	0.12
0.00	0.00	0.00	0.00	0.00	0.00	0.00	0.00	0.00
NM	NM	NM	NM	NM	NM	NM	NM	NM
6.04	0.03	0.13	0.74	0.01	-0.03	0.09	0.00	-0.23
0.50	0.00	-0.03	NM	NM	NM	NM	NM	NM
NM	NM	NM	NM	NM	NM	NM	NM	NM
NM	NM	NM	NM	NM	NM	1.07	0.02	-0.39
28.09	0.12	-2.58	6.73	0.05	-0.45	1.09	0.02	0.48
1.39	0.01	-0.05	NM	NM	NM	2.08	0.04	0.08
	1.00			1.00			1.00	
Cum HD		Cum VD	Cum HD		Cum VD	Cum HD		Cum VD
194.07	0.82	-32.77	138.06	0.94	-21.83	52.25	0.97	-3.81
201.42	0.03	-32.96	139.83	0.01	-21.99	52.65	0.01	-3.69
201.42	0.00	-32.96	139.83	0.00	-21.99	52.65	0.00	-3.69
NM	NM	NM	NM	NM	NM	NM	NM	NM
207.45	0.02561	-32.83	140.54	0.00480	-22.02	52.74	0.00154	-3.92
207.59	0.00	-32.86	NM	NM	NM	NM	NM	NM
NM	NM	NM	NM	NM	NM	NM	NM	NM
NM	NM	NM	NM	NM	NM	52.86	0.00226	-4.31
235.61	0.12	-35.44	147.21	0.05	-22.47	53.38	0.01	-3.83
236.82	0.01	-35.49	NM	NM	NM	53.63	0.00	-3.75
72.20	1.00	-10.82	44.88	1.00	-6.85	16.35	1.00	-1.14
HD Rate		VD Rate	HD Rate		VD Rate	HD Rate		VD Rate
205.32		-34.67	146.07		-23.10	55.28		-4.03
9.35		-0.24	2.26		-0.20	0.70		0.15
0.00		0.00	0.00		0.00	0.00		0.00
NM		NM	NM		NM	NM		NM
52.46		1.13	6.46		-0.26	0.74		-2.00
1.04		-0.06	NM		NM	NM		NM
NM		NM	NM		NM	NM		NM
NM		NM	NM		NM	11.48		-4.19
116.51		-10.70	27.91		-1.37	4.51		1.99

13.32	-0.48	NM	NM	19.94	0.77
CHD Rate	CVD Rate	CHD Rate	CVD Rate	CHD Rate	CVD Rate
205.32	-34.67	146.07	-23.10	55.28	-4.03
116.14	-19.01	80.63	-12.68	30.36	-2.13
106.70	-17.46	74.08	-11.65	27.89	-1.95
NM	NM	NM	NM	NM	NM
96.58	-15.28	65.43	-10.25	24.55	-1.83
79.09	-12.52	NM	NM	NM	NM
NM	NM	NM	NM	NM	NM
NM	NM	NM	NM	19.91	-1.54
77.62	-11.67	48.49	-7.40	17.58	-1.26
75.43	-11.30	NM	NM	17.08	-1.19
23.00	-3.45	14.78	-2.26	5.21	-0.36
	-0.68		-1.30		-1.52
	-34.06		-52.51		-56.68

LANDSLIDE IV (cont.)

LIV-6			LIV-7			LIV-8		
Easting (ft)	Northing (ft)	Elevation (ft)	Easting (ft)	Northing (ft)	Elevation (ft)	Easting (ft)	Northing (ft)	Elevation (ft)
5009.90	547.57	2234.02	837.30	596.80	2211.87	728.59	698.33	2203.86
4952.46	551.24	2228.4	809.93	595.93	2208.46	702.95	693.05	2197.00
4960.18	552.56	2228.77	807.25	597.11	2208.54	702.40	692.06	2197.61
4960.18	552.56	2228.77	807.25	597.11	2208.54	702.40	692.06	2197.61
NM		NM	NM		NM	NM		NM
4962.09	551.08	2228.49	807.72	592.20	2208.35	702.50	691.45	2197.49
4961.56	550.21	2228.55	809.06	594.52	2208.18	701.90	690.57	2197.53
NM		NM	NM		NM	NM		NM
NM		NM	NM		NM	NM		NM
4961.88	551.17	2228.73	809.24	595.58	2208.44	702.52	691.64	2197.64
4960.54	549.34	2228.62	808.17	593.58	2208.37	700.93	689.56	2197.50
Horiz. Dis.		Vert. Dis.	Horiz. Dis.		Vert. Dis.	Horiz. Dis.		Vert. Dis.
47.58	0.84	-5.62	27.38	0.66	-3.41	26.28	0.80	-6.86
2.63	0.05	0.37	2.91	0.07	0.08	1.13	0.03	0.61
0.00	0.00	0.00	0.00	0.00	0.00	0.00	0.00	0.00
NM	NM	NM	NM	NM	NM	NM	NM	NM
2.42	0.04	-0.28	4.93	0.12	-0.19	0.62	0.02	-0.12
1.02	0.02	0.06	2.68	0.06	-0.17	1.07	0.03	0.04
NM	NM	NM	NM	NM	NM	NM	NM	NM
NM	NM	NM	NM	NM	NM	NM	NM	NM
1.01	0.02	0.18	1.08	0.03	0.26	1.24	0.04	0.11
2.27	0.04	-0.11	2.27	0.05	-0.07	2.62	0.08	-0.14
	1.00			1.00			1.00	
Cum HD		Cum VD	Cum HD		Cum VD	Cum HD		Cum VD
47.58	0.96	-5.62	27.38	0.93	-3.41	26.28	0.90	-6.86
49.97	0.05	-5.25	30.05	0.09	-3.33	27.03	0.03	-6.25
49.97	0.00	-5.25	30.05	0.00	-3.33	27.03	0.00	-6.25
NM	NM	NM	NM	NM	NM	NM	NM	NM
47.94	-0.04112	-5.53	29.94	-0.00396	-3.52	27.08	0.00176	-6.37
48.41	0.01	-5.47	28.33	-0.05	-3.69	27.89	0.03	-6.33
NM	NM	NM	NM	NM	NM	NM	NM	NM
NM	NM	NM	NM	NM	NM	NM	NM	NM
48.15	-0.00521	-5.29	28.09	-0.00837	-3.43	27.01	-0.03022	-6.22
49.39	0.03	-5.40	29.31	0.04	-3.50	29.11	0.07	-6.36
15.06	1.00	-1.65	8.94	1.00	-1.07	8.88	1.00	-1.94
HD Rate		VD Rate	HD Rate		VD Rate	HD Rate		VD Rate
50.34		-5.95	28.97		-3.61	27.80		-7.26
3.34		0.47	3.69		0.10	1.44		0.77
0.00		0.00	0.00		0.00	0.00		0.00
NM		NM	NM		NM	NM		NM
21.00		-2.43	42.87		-1.65	5.37		-1.04
2.14		0.13	5.62		-0.36	2.23		0.08
NM		NM	NM		NM	NM		NM
NM		NM	NM		NM	NM		NM
4.20		0.75	4.46		1.08	5.13		0.46

21.79	-1.06	21.79	-0.67	25.15	-1.34
CHD Rate	CVD Rate	CHD Rate	CVD Rate	CHD Rate	CVD Rate
50.34	-5.95	28.97	-3.61	27.80	-7.26
28.81	-3.03	17.33	-1.92	15.58	-3.60
26.47	-2.78	15.92	-1.76	14.32	-3.31
NM	NM	NM	NM	NM	NM
22.32	-2.57	13.94	-1.64	12.61	-2.97
18.45	-2.08	10.79	-1.41	10.63	-2.41
NM	NM	NM	NM	NM	NM
NM	NM	NM	NM	NM	NM
15.86	-1.74	9.25	-1.13	8.90	-2.05
15.73	-1.72	9.33	-1.11	9.27	-2.03
4.80	-0.52	2.85	-0.34	2.83	-0.62
	-27.89		9.05		3.17
	-87.95		83.69		72.47

LANDSLIDE IV (cont.)

LIV-9			LIV-10			LV-11		
Easting (ft)	Northing (ft)	Elevation (ft)	Easting (ft)	Northing (ft)	Elevation (ft)	Easting (ft)	Northing (ft)	Elevation (ft)
508.20	251.41	2309.53	492.64	374.61	2294.26	336.31	461.6	2269.78
499.11	262.90	2308.26	484.15	385.21	2293.01	334.61	462.67	2269.41
499.11	262.90	2308.26	484.15	385.21	2293.01	334.61	462.67	2269.41
498.23	263.18	2307.91	483.37	385.41	2292.56	NM		NM
491.81	270.91	2307.52	479.68	390.39	2292.29	333.70	462.97	2269.16
491.63	270.84	2307.67	479.34	390.26	2292.47	333.34	462.54	2269.20
NM		NM	NM		NM	NM		NM
491.63	270.83	2307.35	NM		NM	333.31	462.48	2268.90
464.71	305.77	2301.38	461.12	411.91	2289.65	328.07	466.57	2268.49
454.15	317.79	2299.15	452.38	419.54	2288.37	322.98	468.35	2267.84
Horiz. Dis.		Vert. Dis.	Horiz. Dis.		Vert. Dis.	Horiz. Dis.		Vert. Dis.
new		new	new		new	new		new
14.65		-1.27	13.58		-1.25	2.01		-0.37
0.00		0.00	0.00		0.00	0.00		0.00
0.92		-0.35	0.91		-0.45	NM		NM
10.05		-0.39	6.20		-0.27	0.96		-0.25
0.19		0.15	0.36		0.18	0.56		0.04
NM		NM	NM		NM	NM		NM
0.01		-0.32	NM		NM	0.07		-0.30
44.11		-5.97	28.30		-2.82	6.65		-0.41
16.00		-2.23	11.60		-1.28	5.39		-0.55
Cum HD		Cum VD	Cum HD		Cum VD	Cum HD		Cum VD
new		new	new		new	new		new
14.65		-1.27	13.58		-1.25	2.01		-0.37
14.65		-1.27	13.58		-1.25	2.01		-0.37
15.43		-1.62	14.23		-1.70	NM		NM
25.47		-2.01	20.42		-1.97	2.95		-0.62
25.54		-1.86	20.54		-1.79	3.12		-0.58
NM		NM	NM		NM	NM		NM
25.53		-2.18	NM		NM	3.13		-0.88
69.62		-8.15	48.83		-4.61	9.62		-1.29
85.60		-10.38	60.33		-5.89	14.94		-1.94
26.10		-3.16	18.39		-1.80	4.56		-0.59
HD Rate		VD Rate	HD Rate		VD Rate	HD Rate		VD Rate
new		new	new		new	new		new
18.57		-1.61	17.21		-1.58	2.55		-0.47
0.00		0.00	0.00		0.00	0.00		0.00
6.36		-2.41	5.55		-3.10	NM		NM
87.32		-3.39	53.96		-2.35	8.33		-2.17
0.41		0.31	0.76		0.38	1.18		0.08
NM		NM	NM		NM	NM		NM
0.11		-3.44	NM		NM	0.72		-3.22
182.95		-24.76	117.37		-11.70	27.57		-1.70

153.68	-21.42	111.44	-12.29	51.79	-6.24
CHD Rate	CVD Rate	CHD Rate	CVD Rate	CHD Rate	CVD Rate
new	new	new	new	new	new
18.57	-1.61	17.21	-1.58	2.55	-0.47
15.55	-1.35	14.41	-1.33	2.13	-0.39
14.18	-1.49	13.09	-1.56	NM	NM
21.18	-1.67	16.98	-1.64	2.45	-0.52
15.20	-1.11	12.23	-1.07	1.85	-0.35
NM	NM	NM	NM	NM	NM
13.80	-1.18	NM	NM	1.69	-0.48
33.30	-3.90	23.36	-2.21	4.60	-0.62
39.01	-4.73	27.49	-2.68	6.81	-0.88
11.89	-1.44	8.38	-0.82	2.08	-0.27
	-0.81		-0.90		-1.97
	-39.15		-41.86		-63.14

LANDSLIDE IV (cont.)

LV-12			LV-13			LV-14		
Easting (ft)	Northing (ft)	Elevation (ft)	Easting (ft)	Northing (ft)	Elevation (ft)	Easting (ft)	Northing (ft)	Elevation (ft)
756.84	730.5	2208.15	820.88	844.31	2396.33	813.04	5941.40	2382.31
756.63	730.23	2208.20	794.87	868.48	2386.53	768.99	5981.64	2371.97
756.63	730.23	2208.20	794.87	868.48	2386.53	768.99	5981.64	2371.97
NM		NM	793.38	869.57	2385.78	767.29	5983.57	2371.33
756.33	729.82	2208.01	785.00	876.98	2384.11	756.58	5995.08	2368.98
755.75	728.97	2207.92	784.93	876.99	2384.24	756.51	5995.14	2369.15
NM		NM	785.08	877.24	2383.89	756.54	5995.07	2368.98
NM		NM	784.95	876.98	2383.83	NM		NM
756.13	730.15	2208.18	772.05	888.65	2381.08	725.76	6031.18	2361.25
754.73	727.98	2208.16	768.16	892.20	2380.23	714.64	6044.35	2358.54
Horiz. Dis.		Vert. Dis.	Horiz. Dis.		Vert. Dis.	Horiz. Dis.		Vert. Dis.
new		new	new		new	new		new
0.34		0.05	35.51		-9.80	59.66		-10.34
0.00		0.00	0.00		0.00	0.00		0.00
NM		NM	1.85		-0.75	2.57		-0.64
0.51		-0.19	11.19		-1.67	15.72		-2.35
1.03		-0.09	0.07		0.13	0.09		0.17
NM		NM	0.29		-0.35	0.08		-0.17
NM		NM	0.29		-0.06	NM		NM
1.24		0.26	17.40		-2.75	47.45		-7.73
2.58		-0.02	5.27		-0.85	17.24		-2.71
Cum HD		Cum VD	Cum HD		Cum VD	Cum HD		Cum VD
new		new	new		new	new		new
0.34		0.05	35.51		-9.80	59.66		-10.34
0.34		0.05	35.51		-9.80	59.66		-10.34
NM		NM	37.34		-10.55	62.22		-10.98
0.85		-0.14	48.53		-12.22	77.91		-13.33
1.88		-0.23	48.58		-12.09	78.00		-13.16
NM		NM	48.64		-12.44	77.93		-13.33
NM		NM	48.56		-12.50	NM		NM
0.79		0.03	65.96		-15.25	125.21		-21.06
3.29		0.01	71.22		-16.10	142.41		-23.77
1.00		0.0030	21.71		-4.91	43.42		-7.25
HD Rate		VD Rate	HD Rate		VD Rate	HD Rate		VD Rate
new		new	new		new	new		new
0.43		0.06	45.00		-12.42	75.61		-13.10
0.00		0.00	0.00		0.00	0.00		0.00
NM		NM	12.71		-5.17	17.71		-4.41
4.42		-1.65	97.21		-14.51	136.63		-20.42
2.16		-0.19	0.15		0.27	0.19		0.36
NM		NM	3.80		-4.56	0.99		-2.22
NM		NM	3.12		-0.64	NM		NM
5.14		1.08	72.15		-11.41	196.80		-32.06

24.80	-0.19	50.58	-8.16	165.56	-26.03
CHD Rate	CVD Rate	CHD Rate	CVD Rate	CHD Rate	CVD Rate
new	new	new	new	new	new
0.43	0.06	45.00	-12.42	75.61	-13.10
0.36	0.05	37.67	-10.40	63.31	-10.97
NM	NM	34.33	-9.70	57.21	-10.09
0.71	-0.12	40.35	-10.16	64.77	-11.08
1.12	-0.14	28.93	-7.20	46.44	-7.84
NM	NM	27.70	-7.08	44.37	-7.59
NM	NM	26.26	-6.76	NM	NM
0.38	0.01	31.55	-7.30	59.90	-10.07
1.50	0.00	32.46	-7.34	64.89	-10.83
0.46	0.00	9.89	-2.24	19.78	-3.30
	0.84		-1.10		-0.96
	39.94		-47.75		-43.71

LANDSLIDE IV (cont.)

LIV-15			LIV-16			LIV-17		
Easting (ft)	Northing (ft)	Elevation (ft)	Easting (ft)	Northing (ft)	Elevation (ft)	Easting (ft)	Northing (ft)	Elevation (ft)
787.79	6019.25	2371.61	704.58	121.26	2344.60	644.19	6061.93	2348.59
732.98	6074.77	2358.85	664.52	172.08	2332.22	615.62	6105.37	2338.68
732.98	6074.77	2358.85	664.52	172.08	2332.22	615.62	6105.37	2338.68
731.34	6077.88	2357.94	662.57	173.69	2331.23	614.28	6107.17	2337.94
719.06	6096.13	2355.41	650.32	187.38	2330.28	604.31	6122.35	2334.94
718.95	6096.21	2355.40	650.09	187.45	2330.74	604.17	6122.44	2335.06
718.91	6096.03	2355.25	NM		NM	604.22	6122.35	2334.96
718.92	6096.20	2355.19	650.15	187.45	2329.95	NM		NM
678.63	6151.27	2342.31	609.18	234.28	2321.50	568.51	6169.28	2325.55
665.88	6165.11	2338.10	595.87	248.45	2318.38	556.65	6183.49	2323.50
Horiz. Dis.		Vert. Dis.	Horiz. Dis.		Vert. Dis.	Horiz. Dis.		Vert. Dis.
new		new	new		new	new		new
78.02		-12.76	64.71		-12.38	51.99		-9.91
0.00		0.00	0.00		0.00	0.00		0.00
3.52		-0.91	2.53		-0.99	2.24		-0.74
22.00		-2.53	18.37		-0.95	18.16		-3.00
0.14		-0.01	0.24		0.46	0.17		0.12
0.18		-0.15	NM		NM	0.10		-0.10
0.17		-0.06	0.06		-0.79	NM		NM
68.23		-12.88	62.22		-8.45	58.97		-9.41
18.82		-4.21	19.44		-3.12	18.51		-2.05
Cum HD		Cum VD	Cum HD		Cum VD	Cum HD		Cum VD
new		new	new		new	new		new
78.02		-12.76	64.71		-12.38	51.99		-9.91
78.02		-12.76	64.71		-12.38	51.99		-9.91
81.39		-13.67	67.18		-13.37	54.23		-10.65
103.12		-16.20	85.53		-14.32	72.39		-13.65
103.26		-16.21	85.73		-13.86	72.55		-13.53
103.15		-16.36	NM		NM	72.44		-13.63
103.27		-16.42	85.70		-14.65	NM		NM
171.30		-29.30	147.90		-23.10	131.34		-23.04
190.10		-33.51	167.32		-26.22	149.80		-25.09
57.96		-10.22	51.01		-7.99	45.67		-7.65
HD Rate	VD Rate		HD Rate	VD Rate		HD Rate	VD Rate	
new		new	new		new	new		new
98.88		-16.17	82.01		-15.69	65.89		-12.56
0.00		0.00	0.00		0.00	0.00		0.00
24.21		-6.27	17.42		-6.82	15.45		-5.10
191.16		-21.99	159.65		-8.26	157.33		-26.07
0.29		-0.02	0.50		0.96	0.35		0.25
2.40		-1.96	NM		NM	1.34		-1.30
1.83		-0.64	0.64		-8.48	NM		NM
283.02		-53.42	258.08		-35.05	244.60		-39.03

180.75	-40.44	186.73	-29.97	177.78	-19.69
CHD Rate	CVD Rate	CHD Rate	CVD Rate	CHD Rate	CVD Rate
new	new	new	new	new	new
98.88	-16.17	82.01	-15.69	65.89	-12.56
82.78	-13.54	68.66	-13.14	55.17	-10.51
74.83	-12.57	61.77	-12.29	49.86	-9.79
85.74	-13.47	71.12	-11.91	60.19	-11.35
61.48	-9.65	51.05	-8.25	43.20	-8.06
58.74	-9.32	NM	NM	41.25	-7.76
55.84	-8.88	46.34	-7.92	NM	NM
81.95	-14.02	70.75	-11.05	62.83	-11.02
86.62	-15.27	76.24	-11.95	68.26	-11.43
26.41	-4.66	23.24	-3.64	20.81	-3.49
	-0.84		-0.85		-0.72
	-39.89		-40.52		-35.76

LANDSLIDE IV (cont.)

LIV-18			LIV-20			LIV-21		
Easting (ft)	Northing (ft)	Elevation (ft)	Easting (ft)	Northing (ft)	Elevation (ft)	Easting (ft)	Northing (ft)	Elevation (ft)
690.33	5960.91	2367.90						
650.95	6001.05	2358.41						
650.95	6001.05	2358.41						
649.29	6002.86	2357.72	5841.64	5977.66	2382.39	5853.38	5895.75	2391.81
638.57	6015.84	2354.26	5831.95	5986.12	2380.69	5842.88	5905.68	2390.11
638.83	6015.73	2354.54	5831.83	5986.20	2380.64	5842.80	5905.74	2390.14
638.68	6015.68	2354.17	5831.85	5986.08	2380.56	5842.84	5905.71	2389.89
NM		NM	5831.75	5986.24	HP	5842.60	5905.72	HP
619.52	6044.19	2348.26	5806.27	6010.11	2375.23	5818.89	5927.42	2384.49
611.34	6055.12	2345.50	5797.84	6017.38	2372.41	5811.96	5933.47	2382.99
Horiz. Dis.		Vert. Dis.	Horiz. Dis.		Vert. Dis.	Horiz. Dis.		Vert. Dis.
new		new						
56.23		-9.49						
0.00		0.00						
2.46		-0.69	new		new	new		new
16.83		-3.46	12.86		-1.70	14.45		-1.70
0.28		0.28	0.14		-0.05	0.10		0.03
0.16		-0.37	0.12		-0.08	0.05		-0.25
NM		NM	0.19		HP	0.20		HP
34.35		-5.91	34.91		-5.33	32.14		-5.40
13.65		-2.76	11.13		-2.82	9.20		-1.50
Cum HD		Cum VD	Cum HD		Cum VD	Cum HD		Cum VD
new		new						
56.23		-9.49						
56.23		-9.49						
58.69		-10.18	new		new	new		new
75.47		-13.64	12.86		-1.70	14.45		-1.70
75.22		-13.36	13.01		-1.75	14.55		-1.67
75.28		-13.73	12.91		-1.83	14.50		-1.92
NM		NM	13.09		HP	14.68		HP
109.31		-19.64	48.00		-7.16	46.82		-7.32
122.94		-22.40	59.13		-9.98	56.02		-8.82
37.48		-6.83	18.03		-3.04	17.08		-2.69
HD Rate		VD Rate	HD Rate		VD Rate	HD Rate		VD Rate
new		new						
71.27		-12.03						
0.00		0.00						
16.91		-4.75	new		new	new		new
146.30		-30.07	111.79		-14.77	125.59		-14.77
0.59		0.59	0.30		-0.10	0.21		0.06
2.06		-4.82	1.59		-1.04	0.65		-3.26
NM		NM	2.03			2.16		HP
142.47		-24.51	144.81		-22.11	133.31		-22.40

131.13	-26.51	106.92	-27.09	88.36	-14.41
CHD Rate	CVD Rate	CHD Rate	CVD Rate	CHD Rate	CVD Rate
new	new				
71.27	-12.03				
59.66	-10.07				
53.96	-9.36	new	new	new	new
62.75	-11.34	111.79	-14.77	125.59	-14.77
44.79	-7.95	21.98	-2.96	24.59	-2.82
42.87	-7.82	19.32	-2.74	21.69	-2.87
NM	NM	17.19	HP	19.28	HP
52.29	-9.40	47.87	-7.14	46.70	-7.30
56.02	-10.21	53.42	-9.02	50.61	-7.97
17.08	-3.11	16.29	-2.75	15.43	-2.43
	-0.84		-1.10		-1.10
	-39.98		-47.80		-47.68

LANDSLIDE IV (cont.)

LIV-23			LIV-24			LIV-26		
Easting (ft)	Northing (ft)	Elevation (ft)	Easting (ft)	Northing (ft)	Elevation (ft)	Easting (ft)	Northing (ft)	Elevation (ft)
5257.03	6374.27	2270.86	5240.75	6615.21	2258.10			
NM		NM	NM		NM			
NM		NM	NM		NM			
5257.09	6374.98	2271.11	NM		NM	5853.09	5945.47	2385.89
5256.57	6373.95	2271.17	5238.64	6615.13	2258.17	5846.45	5951.25	2384.41
Horiz. Dis.		Vert. Dis.	Horiz. Dis.		Vert. Dis.	Horiz. Dis.		Vert. Dis.
new		new	new		new			
NM		NM	NM		NM			
NM		NM	NM		NM			
0.71		0.25	NM		NM	new		new
1.15		0.06	2.11		0.07	8.80		-1.48
Cum HD		Cum VD	Cum HD		Cum VD	Cum HD		Cum VD
new		new	new		new			
NM		NM	NM		NM			
NM		NM	NM		NM			
0.71		0.25	NM		NM	new		new
0.56		0.31	2.11		0.07	8.80		-1.48
0.17		0.09	0.64		0.02	2.68		-0.45
HD Rate		VD Rate	HD Rate		VD Rate	HD Rate		VD Rate
new		new	new		new			
NM		NM	NM		NM			
NM		NM	NM		NM			
2.96		1.04	NM		NM	new		new

11.08	0.58	20.28	0.67	84.56	-14.22
CHD Rate	CVD Rate	CHD Rate	CVD Rate	CHD Rate	CVD Rate
new	new	new	new		
NM	NM	NM	NM		
NM	NM	NM	NM		
1.73	0.61	NM	NM	new	new
1.09	0.60	4.10	0.14	84.56	-14.22
0.33	0.18	1.25	0.04	25.78	-4.33
	1.44		26.38		-1.15
	55.18		87.83		-48.96

LANDSLIDE V

Date	Jul.Day (day)	Time (days)	LV-1			LV-2		
			Easting (ft)	Northing (ft)	Elevation (ft)	Easting (ft)	Northing (ft)	Elevation (ft)
8/21/85	233	21	673.16	6997.76	1616.16	619.06	6975.74	1620.53
7/17/86	198	351	672.71	7000.71	1618.80	618.79	6979.19	1619.15
5/13/87	133	651	671.83	7000.84	1615.58	618.34	6979.21	1618.37
10/13/87	286	804	671.83	7000.84	1615.58	618.42	6979.22	1618.78
9/2/88	246	1129	671.77	7000.66	1615.27	618.51	6979.16	1618.88

Horiz. Dis.			Vert. Dis.			Horiz. Dis.			Vert. Dis.		
2.98	0.73	2.64	3.46	0.84	-1.38	0.89	0.22	-3.22	0.45	0.11	-0.28
0.00	0.00	0.00	0.08	0.02	-0.09	0.19	0.05	-0.31	0.11	0.03	0.10

Cum HD			Cum VD			Cum HD			Cum VD		
2.98	0.73	2.64	3.46	0.84	-1.38	3.35	0.22	-0.58	3.54	0.11	-1.66
3.35	0.22	-0.58	3.54	0.11	-1.75	3.22	0.05	-0.89	3.46	0.03	-1.65

HD Rate			VD Rate			HD Rate			VD Rate		
3.30	1.08	0.00	2.92	-3.92	0.00	3.83	0.55	0.19	-1.53	-0.34	-0.21
0.21	0.00	-0.35	0.12	0.11	0.11	0.12	0.11	0.11	0.11	0.11	0.11

	CHD Rate		CVD Rate			CHD Rate		CVD Rate		
	330	630	783	1108		330	630	783	1108	
	3.30	1.94	1.56	1.06		3.83	2.05	1.65	1.14	
	2.92	-0.34	-0.27	-0.29		-1.53	-0.96	-0.82	-0.54	

		-2.09						-6.22		
	25.6	-64.40				9.1		-80.9		
NW					NW					

LANDSLIDE V (cont.)

LV-3			LV-4			LV-5		
Easting (ft)	Northing (ft)	Elevation (ft)	Easting (ft)	Northing (ft)	Elevation (ft)	Easting (ft)	Northing (ft)	Elevation (ft)
590.32	6985.34	1619.83	708.03	6808.16	1681.77	730.43	6747.17	1701.01
589.68	6987.09	1619.04	707.7	6813.98	1679.1	729.82	6750.82	1699.6
589.47	6987.34	1618.64	707.2	6814.14	1678.56	729.51	6750.96	1699.02
589.46	6987.46	1618.54	707.32	6814.22	1678.5	729.53	6750.69	1699.08
589.48	6987.43	1618.73	707.37	6814.22	1678.52	729.57	6750.68	1699.22

Horiz. Dis.		Vert. Dis.	Horiz. Dis.		Vert. Dis.	Horiz. Dis.		Vert. Dis.
1.86	0.79	-0.79	5.83	0.89	-2.67	3.70	0.85	-1.41
0.33	0.14	-0.40	0.52	0.08	-0.54	0.34	0.08	-0.58
0.12	0.05	-0.10	0.14	0.02	-0.06	0.27	0.06	0.06
0.04	0.02	0.19	0.05	0.01	0.02	0.04	0.01	0.14
Cum HD		Cum VD	Cum HD		Cum VD	Cum HD		Cum VD
1.86		-0.79	5.83		-2.67	3.70		-1.41
2.17		-1.19	6.04		-3.21	3.90		-1.99
2.29		-1.29	6.10		-3.27	3.63		-1.93
2.25		-1.10	6.10		-3.25	3.61		-1.79

HD Rate		VD Rate	HD Rate		VD Rate	HD Rate		VD Rate
2.06		-0.87	6.45		-2.95	4.09		-1.56
0.40		-0.49	0.64		-0.66	0.41		-0.71
0.29		-0.24	0.34		-0.14	0.65		0.14
0.04		0.21	0.06		0.02	0.05		0.16

CHD Rate		CVD Rate	CHD Rate		CVD Rate	CHD Rate		CVD Rate
2.06		-0.87	6.45		-2.95	4.09		-1.56
1.26		-0.69	3.50		-1.86	2.26		-1.15
1.07		-0.60	2.84		-1.52	1.69		-0.90
0.74		-0.36	2.01		-1.07	1.19		-0.59

	-2.49		-9.18		-4.08
21.9	-68.1	6.22	-83.78	13.8	-76.2
NW		NW		NW	

LANDSLIDE VI

Date	Jul. Day (day)	Time (days)	LVI-1			LVI-2		
			Easting (ft)	Northing (ft)	Elevation (ft)	Easting (ft)	Northing (ft)	Elevation (ft)
8/28/85	240	28	235.82	708.71	2335.79	301.27	651.88	2332.66
8/7/86	219	372	234.41	708.59	2335.26	300.26	651.24	2332.47
9/1/87	244	762	233.76	708.29	2334.48	299.47	650.74	2331.70
6/19/88	171	1054	233.80	708.21	2334.55	299.34	650.49	2331.65

Horiz. Dis.		Vert. Dis.		Horiz. Dis.		Vert. Dis.	
1.42		-0.53		1.20		-0.19	
0.72		-0.73		0.93		-0.77	
0.09		0.07		0.28		-0.05	

Cum HD		Cum VD		Cum HD		Cum VD	
1.42		-0.53		1.20		-0.19	
2.10		-1.31		2.13		-0.96	
2.08		-1.24		2.38		-1.01	

HD Rate		VD Rate		HD Rate		VD Rate	
1.50		-0.56		1.27		-0.20	
0.67		-0.73		0.88		-0.72	
0.11		0.09		0.35		-0.06	

CHD Rate		CVD Rate		CHD Rate		CVD Rate	
344	1.50	-0.56		1.27	-0.20		
734	1.05	-0.65		1.06	-0.48		
1026	0.74	-0.44		0.85	-0.36		

		0.25				0.72	
SW		14.00		SW		35.80	

LANDSLIDE VI (cont.)

LVI-3			LVI-4			LVI-5		
Easting (ft)	Northing (ft)	Elevation (ft)	Easting (ft)	Northing (ft)	Elevation (ft)	Easting (ft)	Northing (ft)	Elevation (ft)
352.24	582.12	2333.46	346.20	399.94	2331.14	382.44	203.99	2343.17
350.98	581.67	2333.19	341.64	403.31	2328.16	382.61	203.00	2343.03
350.06	580.86	2332.77	340.44	403.91	2327.17	382.73	202.33	2342.32
349.97	580.69	2332.80	340.30	403.92	2327.18	386.15	205.49	2341.90

Horiz. Dis.		Vert. Dis.	Horiz. Dis.		Vert. Dis.	Horiz. Dis.		Vert. Dis.
1.34		-0.27	5.67		-2.98	1.00		-0.14
1.23		-0.42	1.34		-0.99	0.68		-0.71
0.19		0.03	0.14		0.01	4.66		-0.42
Cum HD		Cum VD	Cum HD		Cum VD	Cum HD		Cum VD
1.34		-0.27	5.67		-2.98	1.00		-0.14
2.52		-0.69	7.00		-3.97	1.69		-0.85
2.68		-0.66	7.12		-3.96	4.00		-1.27

HD Rate		VD Rate	HD Rate		VD Rate	HD Rate		VD Rate
1.42		-0.29	6.02		-3.16	1.07		-0.15
1.15		-0.39	1.26		-0.93	0.64		-0.66
0.24		0.04	0.18		0.01	5.82		-0.53

CHD Rate		CVD Rate	CHD Rate		CVD Rate	CHD Rate		CVD Rate
1.42		-0.29	6.02		-3.16	1.07		-0.15
1.25		-0.34	3.48		-1.97	0.84		-0.42
0.95		-0.23	2.53		-1.41	1.42		-0.45

SW		0.63	NW		-0.67	NE		0.40
32.20			-33.80			21.80		

LANDSLIDE VI (cont.)

LVI-6		
Easting	Northing	Elevation
(ft)	(ft)	(ft)
525.33	44.42	2335.36
525.24	44.50	2335.52
525.20	44.24	2334.94
525.19	44.10	2335.00

Horiz. Dis.	Vert. Dis.
0.12	0.16
0.26	-0.58
0.14	0.06
Cum HD	Cum VD
0.12	0.16
0.22	-0.42
0.35	-0.36

HD Rate	VD Rate
0.13	0.17
0.25	-0.54
0.18	0.07

CHD Rate	CVD Rate
0.13	0.17
0.11	-0.21
0.12	-0.13

2.29
 SW 66.40
 S24W

LANDSLIDE VII

Date	Jul.Day (day)	Time (days)	LVII-1			LVII-2		
			Easting (ft)	Northing (ft)	Elevation (ft)	Easting (ft)	Northing (ft)	Elevation (ft)
8/28/85	240	0	84.58	201.83	2056.53	53.31	202.83	2108.91
8/7/86	219	344	81.90	199.62	2055.40	42.5	198.18	2082.9
9/1/87	244	734	80.26	198.71	2054.48	40.29	196.55	2080.46
9/2/88	246	1101	79.66	198.09	2054.28	39.22	196.04	2079.81

Horiz. Dis.		Vert. Dis.		Horiz. Dis.		Vert. Dis.	
3.47		-1.13		11.77		-26.01	
1.88		-0.92		2.75		-2.44	
0.86		-0.20		1.19		-0.65	

Cum HD		Cum VD		Cum HD		Cum VD	
3.47		-1.13		11.77		-26.01	
5.33		-2.05		14.46		-28.45	
6.18		-2.25		15.64		-29.10	
1.88		-0.69		4.77		-8.87	

HD Rate		VD Rate		HD Rate		VD Rate	
3.69		-1.20		12.49		-27.60	
1.76		-0.86		2.57		-2.28	
0.86		-0.20		1.18		-0.65	

CHD Rate		CVD Rate		CHD Rate		CVD Rate	
344	3.69	-1.20	12.49	-27.60			
734	2.65	-1.02	7.19	-14.15			
1101	2.05	-0.75	5.19	-9.65			
	0.62	-0.23	1.58	-2.94			

LANDSLIDE VII (cont.)

LVII-3			LVII-4			LVII-5		
Easting (ft)	Northing (ft)	Elevation (ft)	Easting (ft)	Northing (ft)	Elevation (ft)	Easting (ft)	Northing (ft)	Elevation (ft)
59.86	261.33	2094.63	62.17	241.91	2096.12	24.89	187.61	2106.56
52.12	244.06	2087.94	54.51	243.71	2097.86	16.51	189.43	2104.44
49.65	240.64	2086.93	52.01	244.32	2096.79	13.56	190.22	2103.4
48.98	239.91	2086.79	51.34	244.21	2096.9	12.93	190.07	2103.3

Horiz. Dis.		Vert. Dis.	Horiz. Dis.		Vert. Dis.	Horiz. Dis.		Vert. Dis.
18.93		-6.69	7.87		1.74	8.58		-2.12
4.22		-1.01	2.57		-1.07	3.05		-1.04
0.99		-0.14	0.68		0.11	0.65		-0.10
Cum HD		Cum VD	Cum HD		Cum VD	Cum HD		Cum VD
18.93		-6.69	7.87		1.74	8.58		-2.12
23.07		-7.70	10.44		0.67	11.63		-3.16
24.02		-7.84	11.07		0.78	12.21		-3.26
7.32		-2.39	3.38		0.24	3.72		-0.99
HD Rate		VD Rate	HD Rate		VD Rate	HD Rate		VD Rate
20.08		-7.10	8.35		1.85	9.10		-2.25
3.95		-0.95	2.41		-1.00	2.86		-0.97
0.99		-0.14	0.68		0.11	0.64		-0.10
CHD Rate		CVD Rate	CHD Rate		CVD Rate	CHD Rate		CVD Rate
20.08		-7.10	8.35		1.85	9.10		-2.25
11.47		-3.83	5.19		0.33	5.78		-1.57
7.96		-2.60	3.67		0.26	4.05		-1.08
2.43		-0.79	1.12		0.08	1.23		-0.33

APPENDIX C

STREAMFLOW/SEDIMENT DATA

1N Terrace Creek		
Date	Q (cfs)	Ts (g/l)
7/24/86	0.48	0.261
7/26/86	0.45	0.157
6/14/87	0.30	0.200
7/8/87	0.28	0.190
7/14/87	0.90	0.551
7/20/87	0.35	0.213
7/30/87	0.43	0.166
5/1/88	1.42	0.306
5/13/88	0.38	0.244
5/30/88	4.52	17.820
6/3/88	4.20	0.537
6/25/88	0.24	0.174
8/16/88	0.23	0.180
8/29/88	0.24	0.179
9/5/88	0.25	0.184
9/29/88	0.23	0.180

2N Badlands		
Date	Q (cfs)	Ts (g/l)
7/24/86	0.37	1.136
7/26/86	0.42	0.544
7/14/87	1.50	44.060
7/20/87	0.31	4.382
7/19/87	0.34	1.337
7/30/87	0.51	8.129
5/13/88	0.93	14.650
6/3/88	3.60	105.900
6/18/88	8.00	823.000
6/25/88	0.27	0.244
7/8/88	1.20	949.000
8/16/88	0.13	0.160
9/5/88	0.28	0.831
9/29/88	0.10	0.177

3N Two Bull Creek		
Date	Q (cfs)	Ts (g/l)
7/27/86	0.280	3.732
7/26/86	0.340	3.870
5/13/88	0.805	16.430
6/3/88	3.700	30.620
6/18/88	0.150	2.417
6/18/88	4.800	327.000
6/25/88	0.175	1.132
7/8/88	0.270	21.640
7/11/88	1.500	158.800
7/21/88	0.410	16.131
8/16/88	0.084	0.465
8/29/88	0.100	0.249
9/5/88	0.123	0.327
9/29/88	0.074	0.208

9N Slide Creek		
Date	Q (cfs)	Ts (g/l)
8/2/86	2.45	1.038
8/8/86	1.94	0.784
9/6/86	1.56	0.946
6/15/87	1.79	2.560
6/29/87	1.43	1.164
7/10/87	1.14	0.718
7/15/87	1.32	0.444
7/20/87	2.26	2.990
7/30/87	5.91	9.349
5/13/88	2.91	4.358
5/31/88	28.34	28.880
6/26/88	2.19	1.797
7/8/88	1.57	0.514
7/22/88	3.64	3.082
8/21/88	1.33	0.364
9/5/88	1.76	0.584
9/29/88	2.41	1.868

4N Frances Creek		
Date	Q (cfs)	Ts (g/l)
7/24/86	0.77	1.416
7/26/86	1.11	7.671
9/17/86	0.18	0.330
6/23/87	0.11	2.250
7/14/87	0.13	11.757
7/19/87	0.11	1.697
7/30/87	0.51	3.034
5/1/88	0.50	7.224
5/13/88	0.65	15.900
5/26/88	0.19	1.530
5/31/88	4.25	43.400
6/2/88	0.45	2.071
6/3/88	1.31	12.496
6/6/88	0.29	1.226
6/18/88	0.15	1.592
6/25/88	0.14	0.672
6/28/88	0.29	0.983
7/8/88	0.24	6.977
7/10/88	0.24	4.990
7/11/88	1.33	19.858
7/17/88	0.10	0.482
7/22/88	0.94	6.080
7/22/88	1.03	21.130
7/25/88	0.16	0.433
8/16/88	0.09	0.441
8/29/88	0.05	0.498
9/5/88	0.11	0.461
9/15/88	0.05	0.489
9/29/88	0.07	0.505
10/7/88	0.07	0.699

7N Popovitch Creek		
Date	Q (cfs)	Ts (g/l)
7/24/86	0.38	0.454
7/26/86	5.56	12.594
8/13/86	1.23	0.751
8/22/86	5.20	23.541
6/23/87	0.38	0.160
7/14/87	0.28	0.134
7/19/87	0.33	0.141
7/30/87	0.62	0.823
5/2/88	1.83	1.929
5/13/88	1.62	4.347
5/30/88	1.54	7.589
5/31/88	1.63	7.560
5/23/88	0.49	1.120
5/26/88	0.61	0.600
6/2/88	0.82	0.361
6/3/88	0.89	0.857
6/6/88	0.68	0.159
6/18/88	0.43	0.208
6/26/88	0.33	0.163
7/8/88	0.38	0.241
7/10/88	0.54	1.419
7/10/88	1.24	1.236
7/22/88	0.93	25.521
8/14/88	0.46	0.165
8/21/88	0.55	0.154
8/29/88	0.49	0.149
9/5/88	0.65	0.245
9/13/88	0.58	0.133
9/29/88	0.33	0.152
10/7/88	0.43	0.178

5N Louise Creek		
Date	Q (cfs)	Ts (g/l)
7/24/86	0.310	2.713
7/26/86	1.890	18.175
9/17/86	0.120	0.446
6/14/87	0.050	0.560
7/6/87	0.050	0.576
7/8/87	0.030	0.570
7/20/87	0.140	0.888
7/30/87	0.300	2.738
7/30/87	0.460	9.450
8/18/87	0.560	20.550
5/1/88	0.616	2.225
5/13/88	0.220	1.804
5/31/88	2.630	72.510
6/2/88	0.390	2.815
6/3/88	0.460	18.700
6/18/88	0.090	0.578
6/25/88	0.077	0.510
7/8/88	0.252	20.140
7/10/88	0.224	35.594
7/22/88	1.624	140.700
9/5/88	0.081	0.955
9/29/88	0.027	0.462

UH Upper Hoseanna Creek		
Date	Q (cfs)	Ts (g/l)
8/2/86	12.28	0.373
8/7/86	7.14	0.187
8/8/86	7.20	0.180
6/15/87	7.53	0.660
7/8/87	4.41	0.428
7/10/87	5.71	1.483
7/15/87	14.98	2.685
5/13/88	14.94	3.533
5/26/88	7.21	1.175
5/31/88	154.00	16.070
6/2/88	16.00	1.154
6/19/88	12.73	1.927
6/26/88	13.97	0.760
7/17/88	6.31	0.764
7/22/88	27.50	2.701
8/21/88	7.46	0.173
9/3/88	6.19	0.143
9/5/88	9.65	1.156
9/29/88	5.83	0.490

10N North Hoseanna		
Date	Q (cfs)	Ts (g/l)
8/2/86	2.950	2.834
8/8/86	2.130	1.376
8/13/86	5.800	5.702
9/11/86	2.960	2.570
5/13/88	6.400	3.384
6/2/88	4.700	2.475
6/3/88	10.700	6.542
7/9/88	5.090	4.669
7/10/88	3.850	1.834
7/25/88	3.100	0.713
8/14/88	2.800	0.456
8/21/88	2.380	0.327
9/5/88	3.320	0.728
9/29/88	3.360	0.257

2S Slime Creek		
Date	Q (cfs)	Ts (g/l)
7/24/86	0.52	0.743
7/26/86	2.17	2.636
6/14/87	0.64	3.350
7/8/87	0.17	1.707
8/19/87	2.28	0.427
5/1/88	1.38	0.771
5/13/88	1.51	2.357
5/31/88	21.27	14.347
6/2/88	2.80	2.013
6/25/88	0.52	0.366
8/16/88	0.46	0.300
9/5/88	0.59	0.323
9/29/88	0.36	0.338

3S Pipe Creek		
Date	Q (cfs)	Ts (g/l)
7/24/86	0.61	0.432
7/26/86	8.46	13.526
6/14/87	0.78	1.290
7/8/87	0.10	0.807
7/30/87	11.54	7.103
8/19/87	4.14	0.481
5/1/88	1.13	1.016
5/13/88	1.21	3.588
5/31/88	33.59	19.971
6/2/88	3.80	1.268
6/18/88	0.19	0.466
6/25/88	0.47	0.369
8/21/88	0.26	0.373
9/5/88	0.31	0.353
9/29/88	0.39	0.350

5S Iron Creek		
Date	Q (cfs)	Ts (g/l)
7/24/86	1.930	0.300
7/26/86	14.640	0.437
9/11/86	1.670	0.265
9/13/86	1.670	0.295
9/27/86	1.670	0.292
6/14/87	1.860	0.390
7/6/87	1.400	0.564
7/8/87	1.370	0.562
7/15/87	0.420	0.574
7/20/87	1.050	0.834
7/30/87	7.650	2.080
5/13/88	3.300	0.706
5/31/88	34.390	4.079
6/2/88	5.700	0.252
7/2/88	1.580	0.382
7/10/88	4.770	3.915
8/21/88	1.420	0.314
9/2/88	1.160	0.354
9/29/88	1.650	0.480

CS Clear Creek		
Date	Q (cfs)	Ts (g/l)
7/24/86	0.74	0.107
7/26/86	8.50	0.763
6/14/87	0.50	0.470
7/8/87	0.10	0.134
7/20/87	0.20	0.162
5/14/88	1.00	0.245
7/2/88	0.37	0.129
7/10/88	1.69	2.076
8/21/88	0.26	0.126
9/2/88	0.22	0.139
9/29/88	0.19	0.136

4S Schist Creek		
Date	Q (cfs)	Ts (g/l)
7/24/86	0.67	0.471
7/26/86	7.94	1.071
5/13/88	1.17	0.676
7/2/88	0.29	0.456
7/9/88	1.08	0.332
9/5/88	0.52	0.449
9/29/88	0.33	0.192

6S Sixth South Creek		
Date	Q (cfs)	Ts (g/l)
8/8/86	0.50	0.963
6/15/87	0.66	2.810
7/8/87	0.31	1.489
7/15/87	0.30	1.413
7/20/87	0.68	5.043
5/13/88	1.44	2.506
6/3/88	9.00	5.349
6/18/88	0.61	4.742
7/9/88	0.72	1.823
8/21/88	0.56	1.431
9/5/88	0.78	1.350
9/29/88	0.76	1.212

7S Mosquito Creek		
Date	Q (cfs)	Ts (g/l)
8/2/86	0.900	0.710
8/8/86	0.550	0.601
7/10/87	0.350	0.714
7/15/87	0.390	0.793
7/20/87	0.520	1.290
8/19/87	1.200	0.707
5/13/88	1.120	5.372
7/22/88	1.110	6.887
8/21/88	0.710	0.689
9/5/88	0.520	1.041
9/29/88	0.580	0.731

9S Clinker Creek		
Date	Q (cfs)	Ts (g/l)
8/2/86	1.43	0.193
8/8/86	0.96	0.190
6/15/87	0.49	0.780
7/8/87	0.27	0.347
5/13/88	1.36	2.232
5/31/88	32.05	13.540
6/2/88	3.40	0.484
6/26/88	1.72	0.308
7/17/88	0.76	0.221
7/22/88	3.78	4.187
7/23/88	20.00	6.285
8/21/88	1.02	0.208
9/5/88	1.54	0.476
9/29/88	1.06	0.320

10Sa Sanderson above mining		
Date	Q (cfs)	Ts (g/l)
8/13/86	5.13	0.480
9/11/86	5.17	0.570
7/15/87	16.44	1.001
7/17/88	3.77	0.604
7/25/88		0.512
8/21/88	3.12	0.679
9/3/88	2.58	0.793
9/29/88	1.92	0.740

10Sb Sanderson below mining		
Date	Q (cfs)	Ts (g/l)
8/2/86	4.32	0.731
8/7/86	3.36	0.802
8/8/86	2.31	0.765
6/15/87	2.71	0.850
7/8/87	0.98	1.052
7/15/87	10.75	2.651
5/13/88	18.69	9.071
5/31/88	144.41	13.507
6/2/88	30.00	6.263
6/26/88	12.79	3.458
7/17/88	6.20	0.769
7/22/88	27.16	6.921
8/21/88	5.10	0.847
9/3/88	4.22	1.000
9/29/88	3.10	0.999

Poker Creek		
Date	Q (cfs)	Ts (g/l)
8/8/86	3.82	0.096
6/14/87	3.13	0.113
7/8/87	4.29	0.120
7/15/87	5.20	0.110
5/13/88	2.69	0.125
5/30/88	8.82	2.222
5/31/88	17.50	0.598
5/31/88	16.60	0.788
6/18/88	4.00	0.113
6/18/88	4.43	0.218
6/25/88	3.80	0.106
7/8/88	3.80	0.129
7/22/88	4.06	0.196
8/23/88	1.61	0.117
9/3/88	3.44	0.118
9/29/88	2.94	0.127

1M Hoseanna Creek Bridge 1		
Date	Q (cfs)	Ts (g/l)
7/19/86	380.0	29.920
7/19/86	490.0	47.830
7/19/86	930.0	39.400
7/19/86	1264.0	38.760
7/20/86	504.0	8.240
7/21/86	330.0	4.740
7/21/86	455.0	9.260
7/21/86	480.0	6.220
7/23/86	56.0	1.340
8/1/86	32.0	1.143
8/11/86	25.4	0.540
8/13/86	41.0	2.540
8/22/86	480.0	8.780
8/22/86	76.0	3.891
8/26/86	96.0	1.765
9/10/86	66.0	1.385
6/14/87	30.7	1.340
6/16/87	24.6	1.480
6/17/87	23.6	1.540
6/19/87	20.2	1.170
6/20/87	19.2	1.000
6/23/87	18.4	1.050
6/24/87	18.2	1.010
6/26/87	18.1	0.850
6/27/87	18.0	0.993
6/29/87	15.7	0.856
6/30/87	14.9	0.818
7/3/87	15.7	0.784
7/5/87	15.3	0.782
7/6/87	14.9	0.737
7/8/87	15.7	0.723
7/10/87	15.7	0.941
7/12/87	15.8	0.952
7/14/87	19.2	1.550
7/15/87	83.0	13.920
7/15/87	71.0	9.649
7/15/87	57.0	5.316
7/15/87	40.0	3.294
7/16/87	22.8	0.852
7/19/87	25.9	0.593
7/20/87	30.0	1.767
7/20/87	37.0	2.742
7/21/87	38.0	1.831
7/23/87	25.7	0.998
7/23/87	33.5	1.494
7/24/87	40.0	3.112
7/24/87	42.0	2.590

7/24/87	92.0	15.437
7/24/87	93.0	12.270
7/24/87	62.0	7.138
7/25/87	74.0	4.973
7/26/87	31.0	1.154
7/30/87	168.0	16.534
7/30/87	281.0	16.564
7/30/87	232.0	8.377
7/31/87	56.0	1.894
8/3/87	30.0	0.581
8/5/87	23.0	0.489
8/10/87	21.0	0.484
8/13/87	21.0	0.476
8/17/87	22.0	0.561
8/18/87	106.0	14.370
8/19/87	190.0	12.800
8/19/87	254.0	14.710
8/19/87	267.0	14.000
8/19/87	186.0	7.440
8/20/87	79.0	2.338
8/21/87	45.0	0.834
8/23/87	27.0	0.810
8/28/87	18.0	0.610
9/22/87	19.0	0.900
5/22/88	86.0	2.720
5/23/88	57.0	1.596
5/23/88	35.0	0.967
5/24/88	210.0	7.857
5/26/88	60.0	1.500
5/30/88	460.0	28.173
5/31/88	642.0	25.403
5/31/88	440.0	14.170
5/31/88	364.0	13.021
6/2/88	105.0	2.356
6/3/88	230.0	10.323
6/3/88	242.0	16.356
6/6/88	54.0	2.340
6/9/88	54.0	1.859
6/13/88	62.0	3.071
6/18/88	54.0	2.556
6/18/88	90.0	17.837
6/25/88	48.0	2.011
6/26/88	40.0	1.451
6/26/88	51.0	2.676
6/28/88	148.0	11.367
7/2/88	28.0	0.562
7/3/88	26.0	0.640
7/4/88	27.0	0.541
7/8/88	25.0	0.805

7/8/88	35.0	6.338
7/9/88	44.0	4.962
7/9/88	54.0	4.564
7/9/88	71.0	7.212
7/9/88	74.0	7.164
7/9/88	62.0	4.018
7/10/88	71.0	3.242
7/10/88	73.0	4.540
7/10/88	75.0	5.683
7/10/88	73.0	5.801
7/11/88	44.0	1.136
7/11/88	57.0	2.972
7/16/88	19.5	0.656
7/17/88	19.5	0.573
7/18/88	18.0	0.423
7/21/88	36.0	2.609
7/21/88	76.0	5.956
7/21/88	82.0	6.825
7/22/88	58.0	2.722
7/22/88	86.0	6.343
7/22/88	156.0	14.522
7/22/88	410.0	35.743
7/22/88	470.0	28.890
7/23/88	520.0	27.553
7/23/88	525.0	27.397
7/23/88	205.0	10.868
7/23/88	115.0	4.858
7/23/88	72.0	2.366
7/24/88	66.0	1.127
7/25/88	67.0	0.834
7/28/88	34.0	0.616
8/2/88	34.0	0.770
8/5/88	22.0	0.583
8/9/88	32.0	0.785
8/12/88	54.0	1.667
8/12/88	75.0	4.142
8/12/88	125.0	12.349
8/12/88	178.0	16.647
8/14/88	47.0	0.593
8/16/88	38.0	0.505
8/20/88	34.0	0.463
8/21/88	34.0	0.450
8/22/88	35.0	0.420
8/23/88	31.0	0.382
8/26/88	33.0	0.446
8/27/88	31.0	0.404
8/29/88	27.0	0.414
9/1/88	28.0	0.482
9/5/88	29.0	0.538

9/5/88	47.0	1.125
9/11/88	31.0	0.497
9/12/88	28.0	0.435
9/13/88	26.0	0.427
9/20/88	27.0	0.445

PLEASE NOTE:

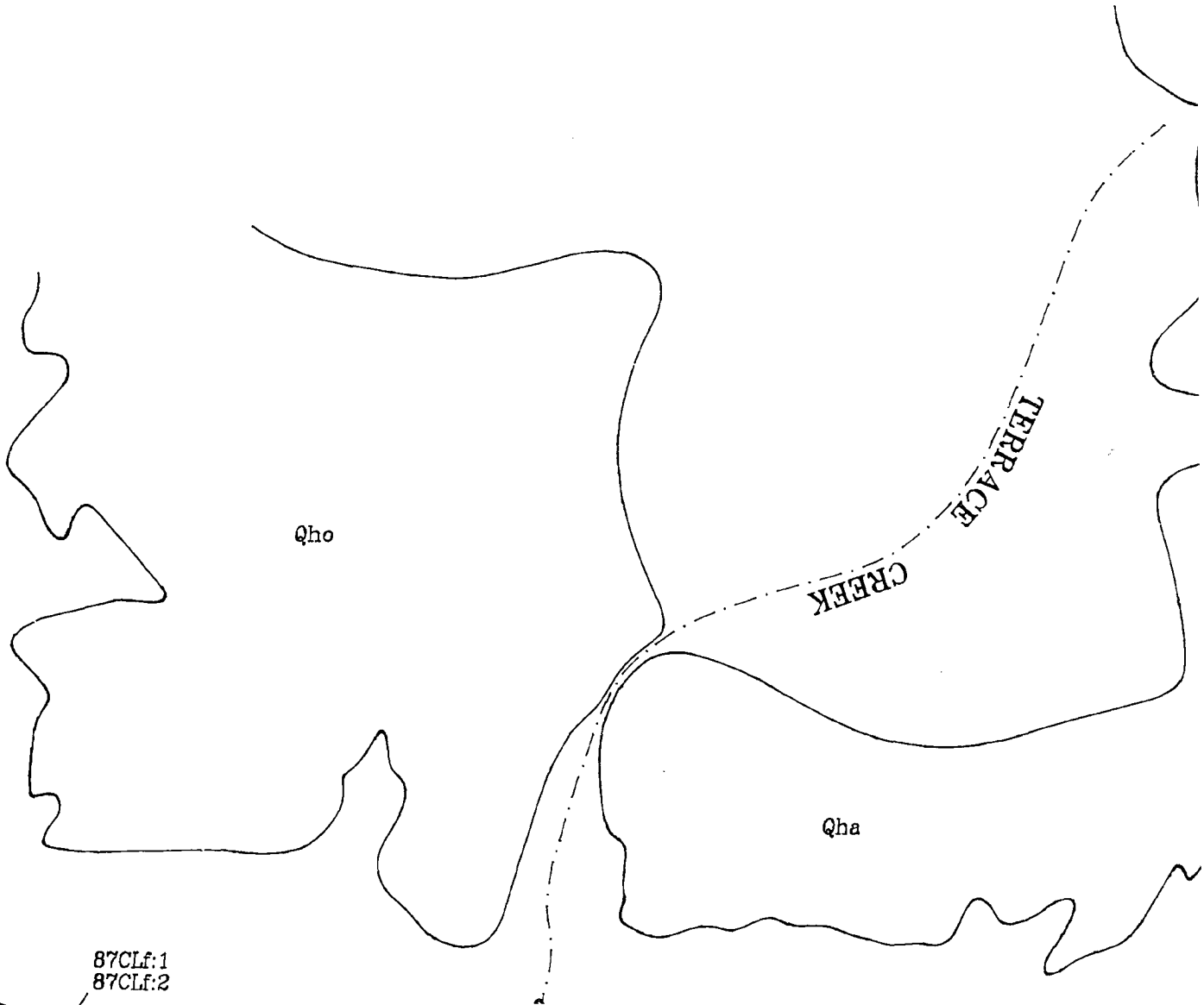
Oversize maps and charts are filmed in sections in the following manner:

LEFT TO RIGHT, TOP TO BOTTOM, WITH SMALL OVERLAPS

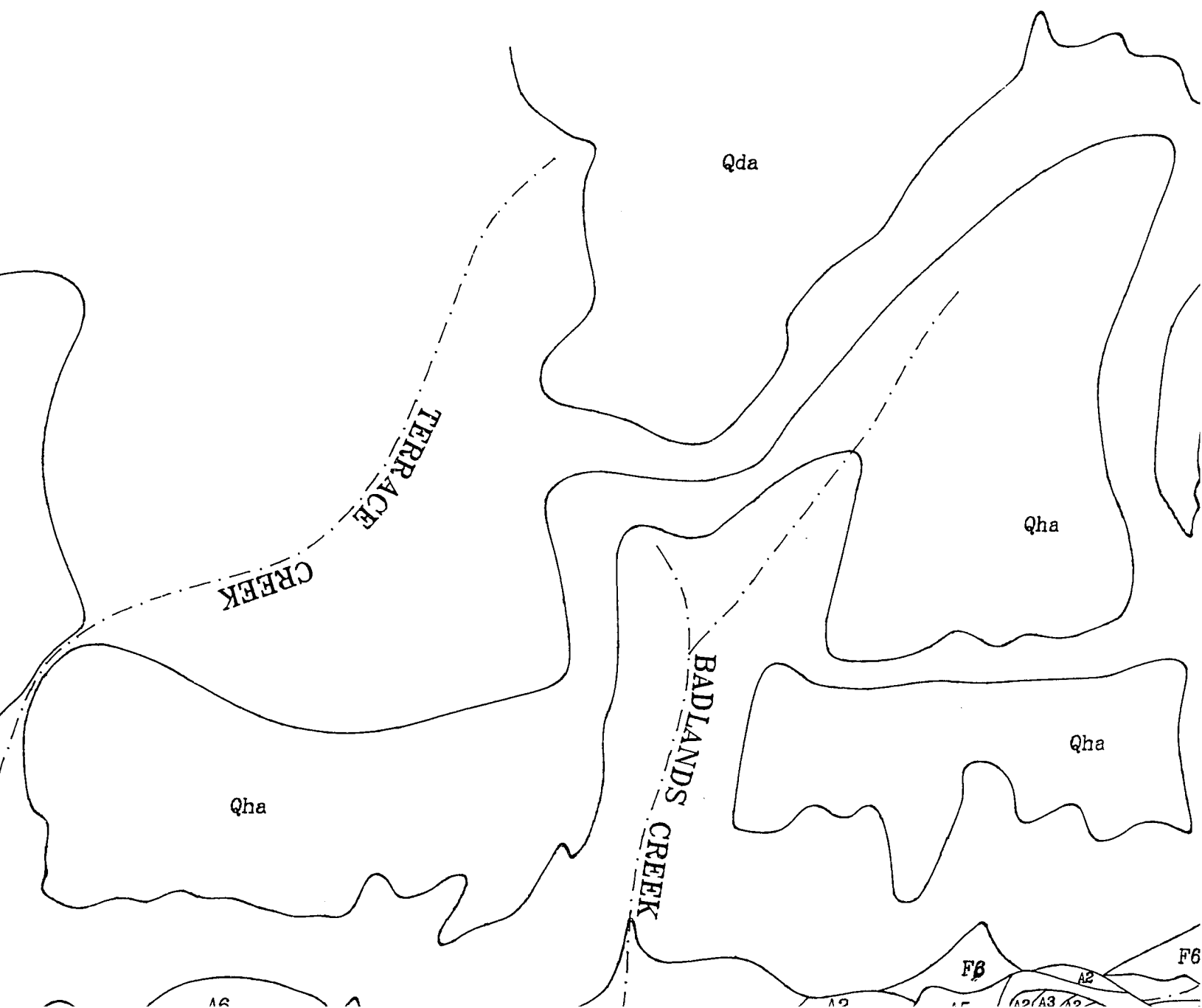
The following map or chart has been refilmed in its entirety at the end of this dissertation (not available on microfiche). A xerographic reproduction has been provided for paper copies and is inserted into the inside of the back cover.

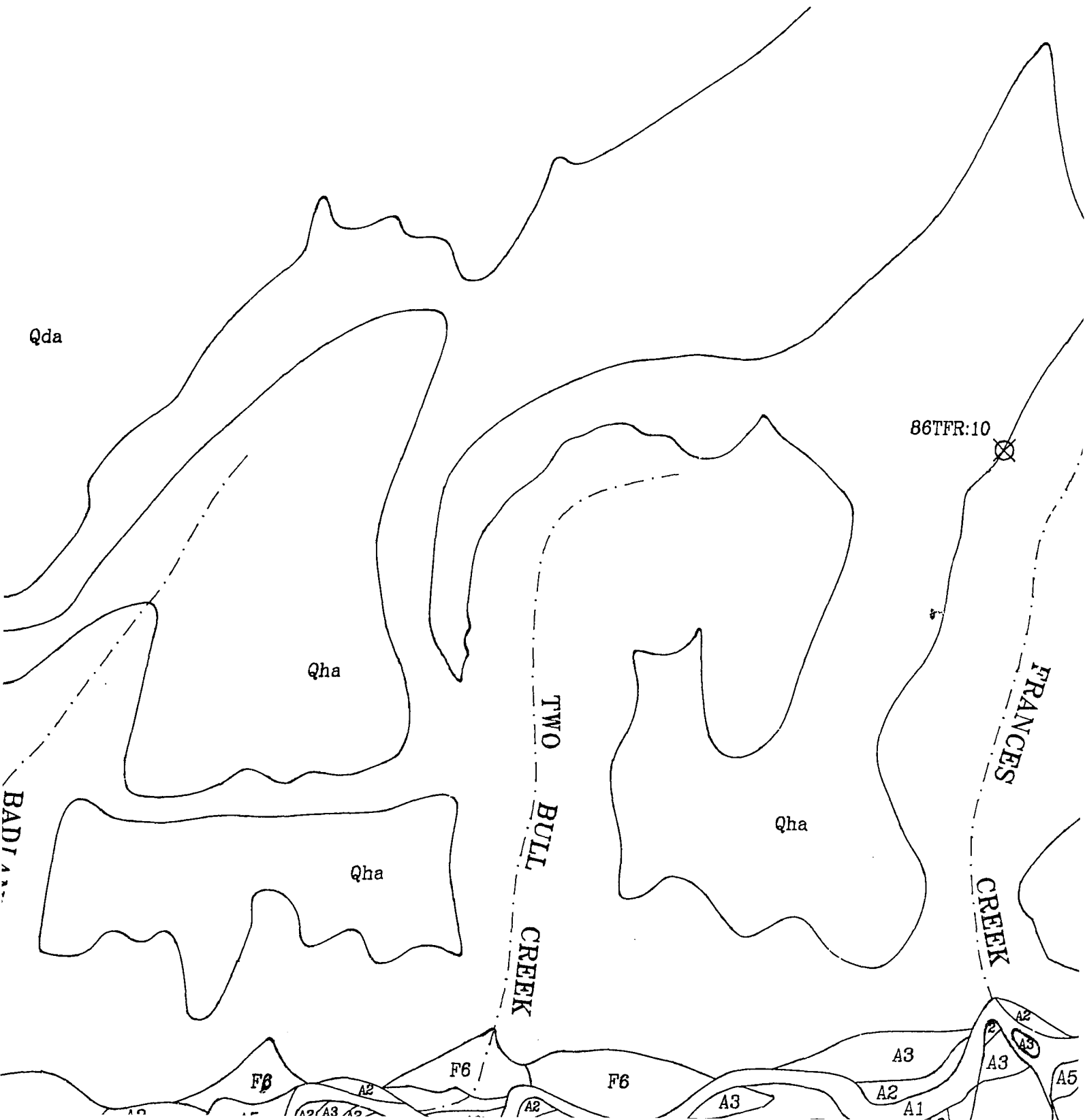
Black and white photographic prints (17" x 23") are available for an additional charge.

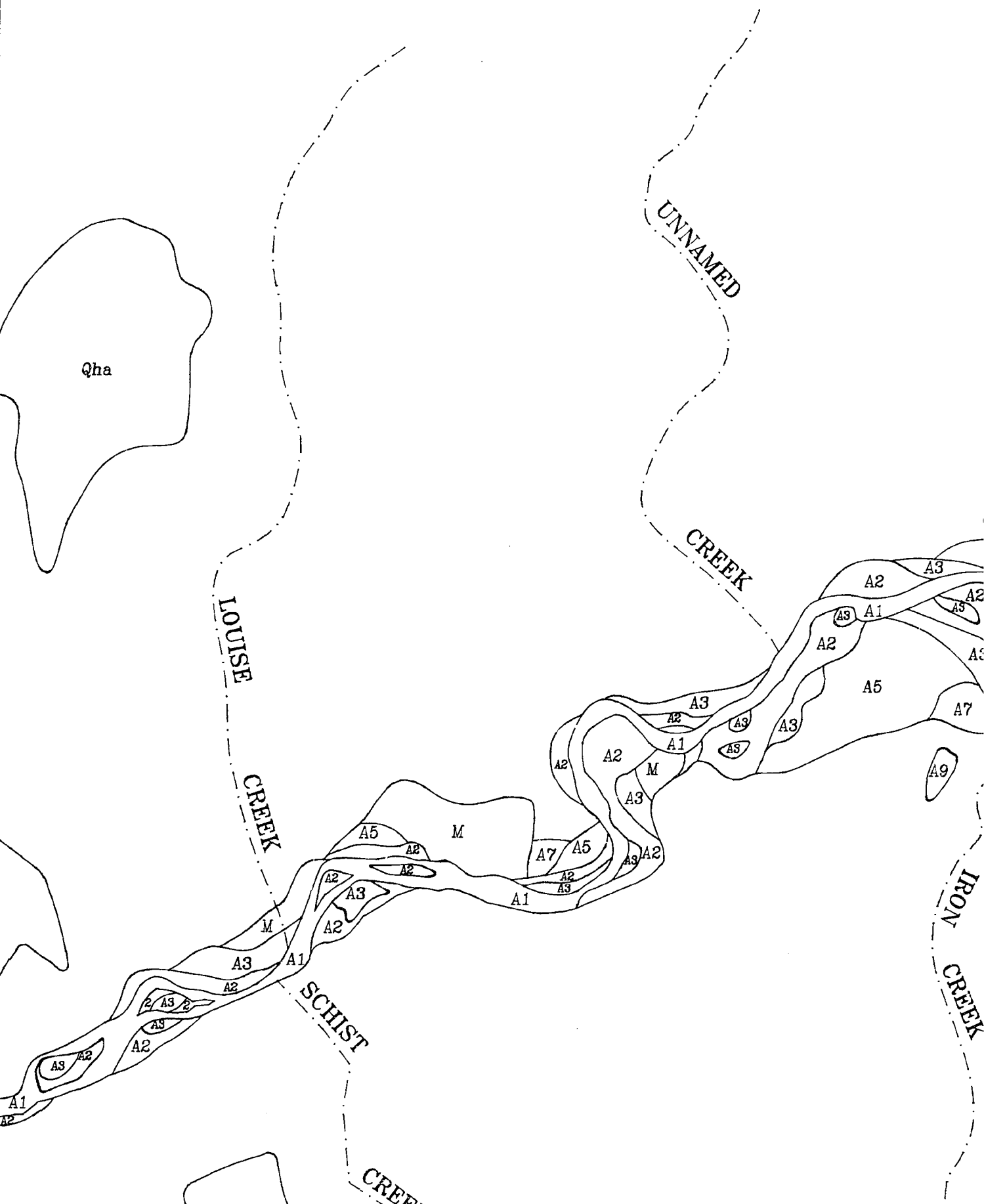
University Microfilms International



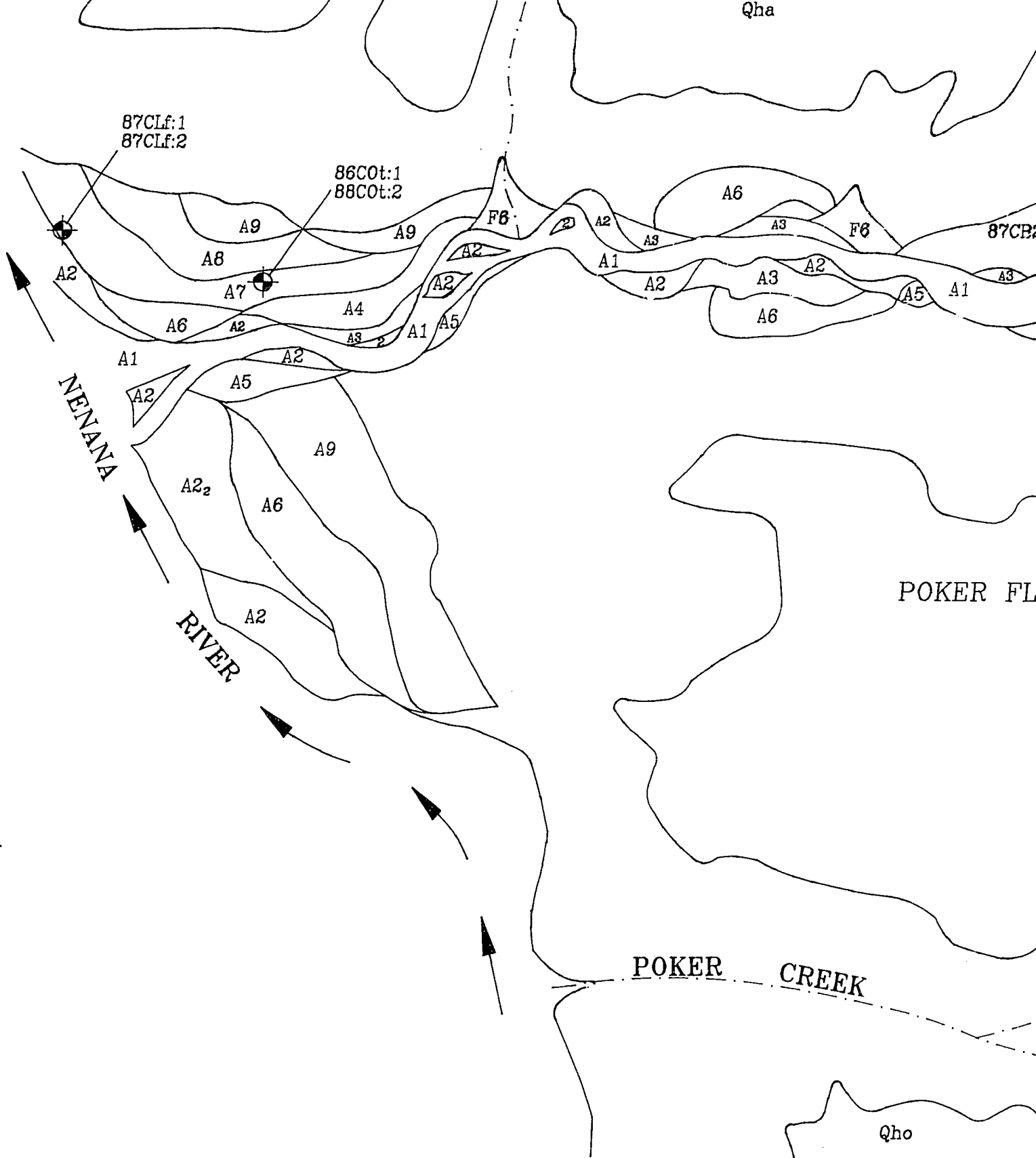
87CLF:1
87CLF:2

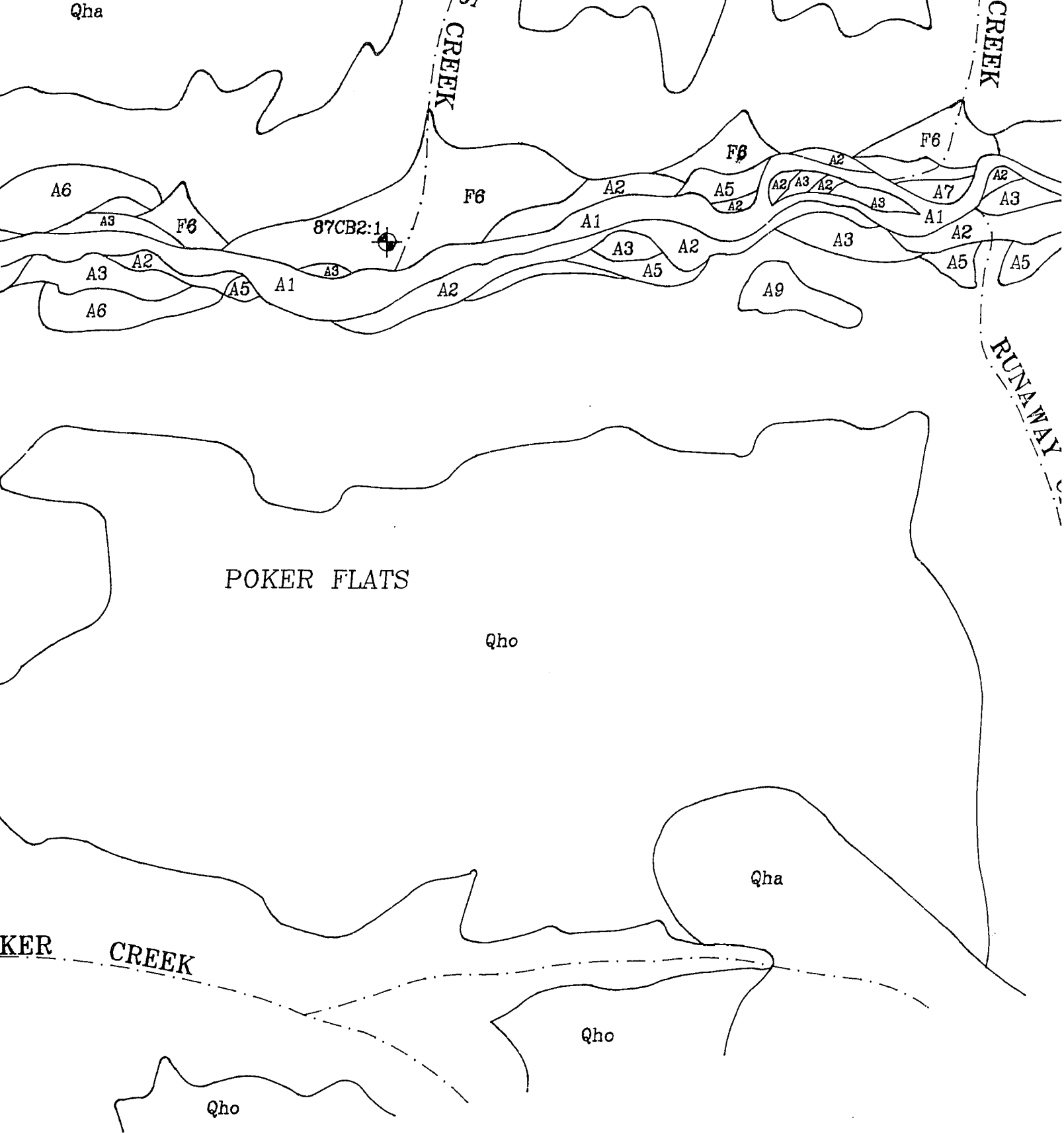


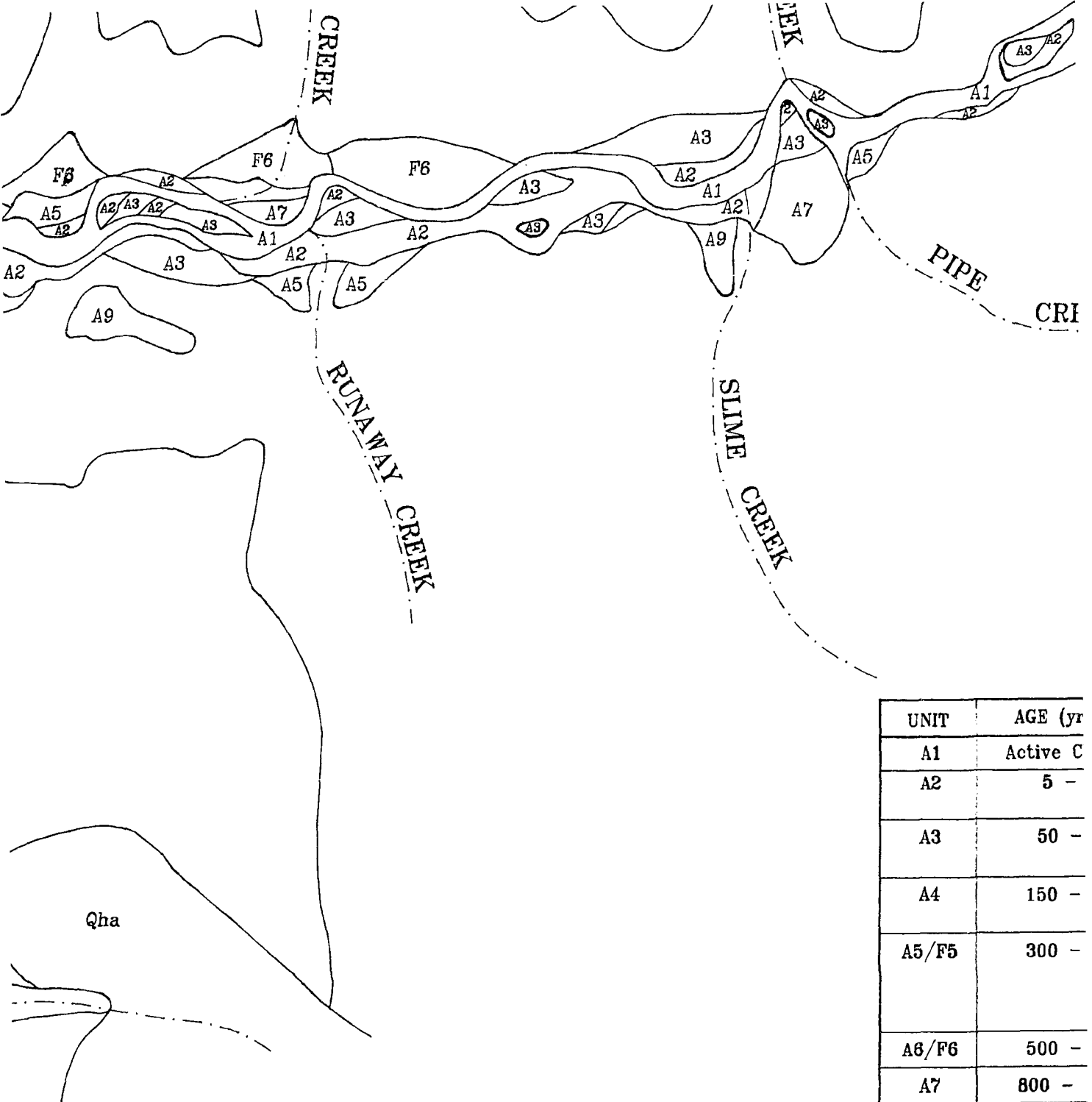




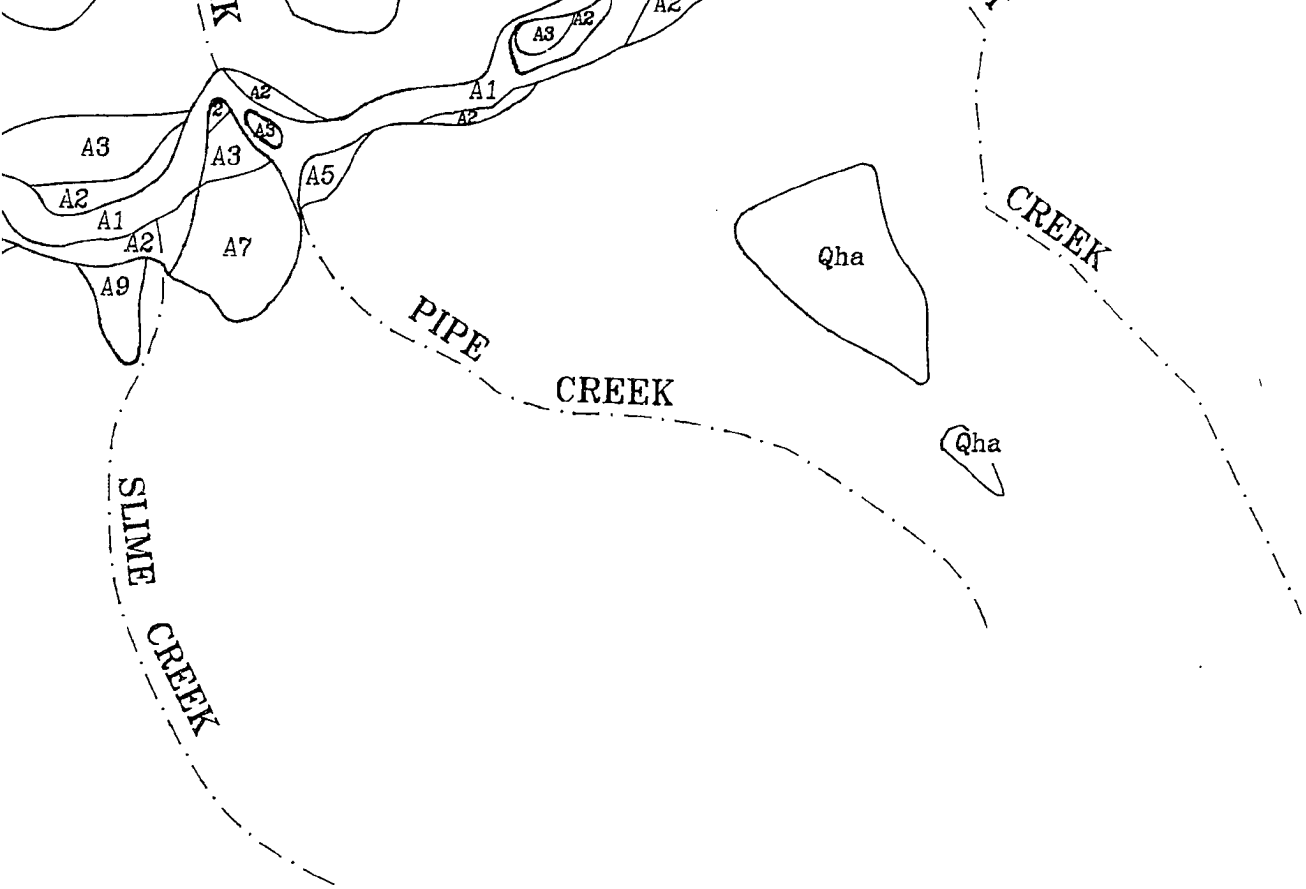




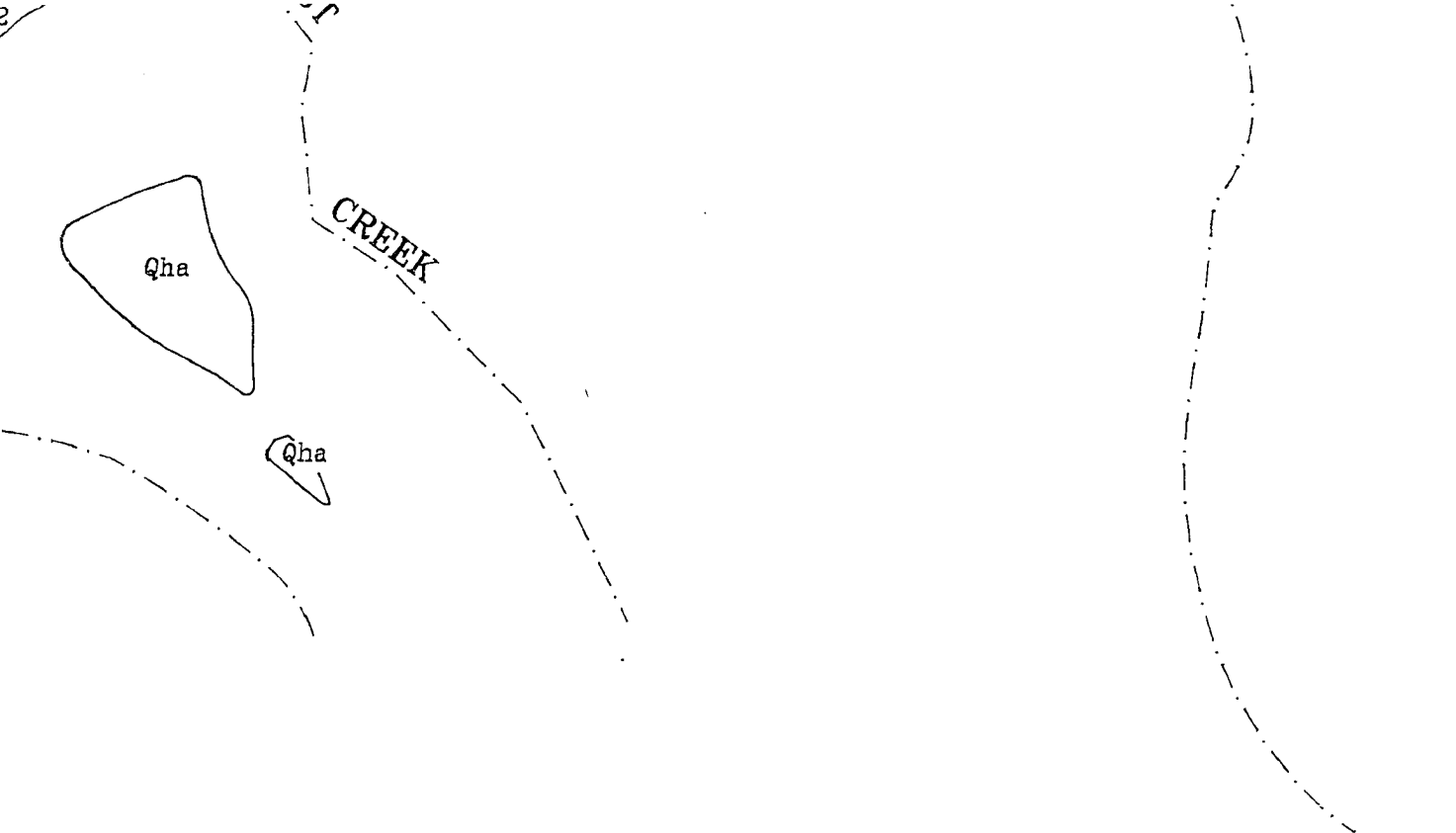




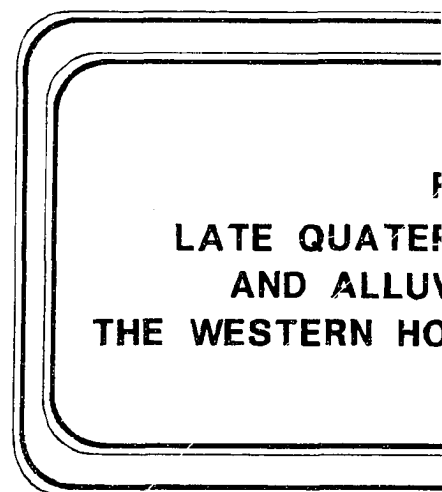
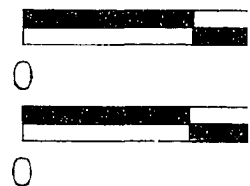
UNIT	AGE (yr)
A1	Active C
A2	5 -
A3	50 -
A4	150 -
A5/F5	300 -
A6/F6	500 -
A7	800 -
A8	1,400 -
A9	>2,200, and
Qra	9,500 -
Qha/Qho	54,000 -
Qda	>230,0
M	Mining ac
⊕	Radiocarb
⊗	Thermolu



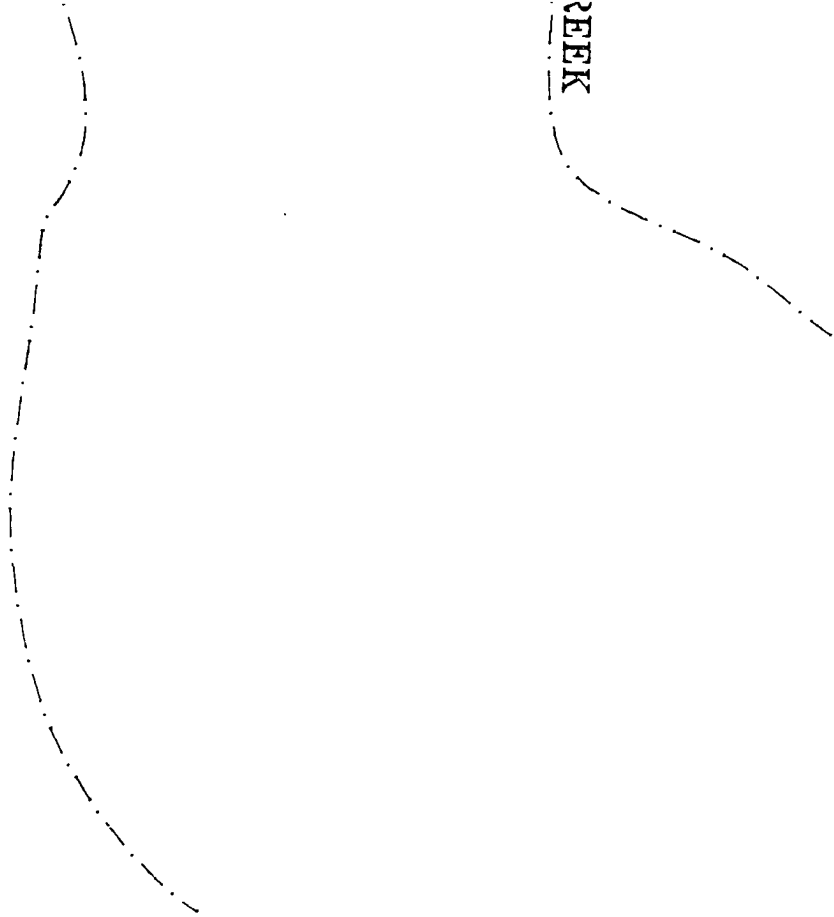
UNIT	AGE (yrs BP)	DESCRIPTION
A1	Active Channel	Units A1 - A9 based on 1974 air photos
A2	5 - 50	Covered by alders, willows, grasses, and shrubs; may be covered by aufeis during the winter
A3	50 - 150	Covered by young mixed deciduous forest (pre-dominantly large poplars) and young white spruce
A4	150 - 300	Covered by mixed deciduous and coniferous forest with thick understory
A5/F5	300 - 500	Covered by mature white spruce forest or mature mixed forest (birch and white spruce); or when in permafrost covered by black spruce forest and sphagnum tundra
A6/F6	500 - 800	Covered by tall mature forests with thin understory and thick forest litter; ages distinguished on the basis of morphostratigraphic position, elevation, and radiocarbon dated samples of correlated horizon
A7	800 - 1,400	
A8	1,400 - 2,200	
A9	>2,200, and <9,500	
Qra	9,500 - 25,000	Riley Creek Glaciation alluvium
Qha/Qho	54,000 - 230,000	Healy Glaciation alluvium (Qha) and outwash (Qho)
Qda	>230,000	Dry Creek Glaciation alluvium
M	Mining activity	
⊙	Radiocarbon sample locations	
⊗	Thermoluminescence sample locations	



	DESCRIPTION
el	Units A1 - A9 based on 1974 air photos
	Covered by alders, willows, grasses, and shrubs; may be covered by aufeis during the winter
	Covered by young mixed deciduous forest (pre-dominantly large poplars) and young white spruce
	Covered by mixed deciduous and coniferous forest with thick understory
	Covered by mature white spruce forest or mature mixed forest (birch and white spruce); or when in permafrost covered by black spruce forest and sphagnum tundra
0	Covered by tall mature forests with thin understory and thick forest litter; ages distinguished on the basis of morphostratigraphic position, elevation, and radiocarbon dated samples of correlated horizons.
500	
10	Riley Creek Glaciation alluvium
000	Healy Glaciation alluvium (Qha) and outwash (Qho)
	Dry Creek Glaciation alluvium
y	
sample locations	
science sample locations	



ice
est
ire
nd
erstory
the
n,
orizons.
ho)



SCALE

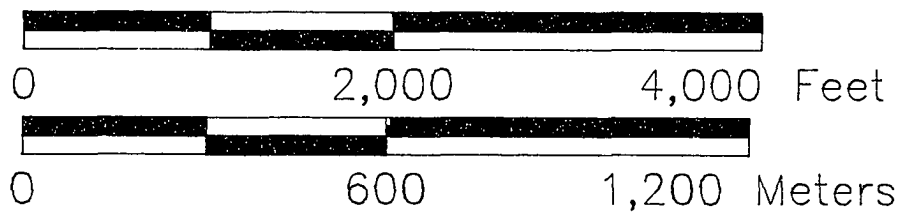


FIGURE 2.3-3
LATE QUATERNARY STREAM TERRACE
AND ALLUVIAL FAN DEPOSITS IN
THE WESTERN HOSEANNA CREEK WATERSHED

Mapped by S. Wilbur/Drafted by B. Bates